JOURNAL OF
GEOPHYSICAL RESEARCH

The continuation of

ESTRIAL MAGNETISM AND ATMOSPHERIC ELECTRICITY
(1896-1948)

An International Quarterly

UME 56 December, 1951 NUMBER 4

CONTENTS

(Contents concluded on outside back cover)

Part one of two parts

PUBLISHED BY
THE WILLIAM BYRD PRESS, INC.
P. O. Box 2-W—Sherwood Ave. and Durham St., Richmond 5, Virginia
FOR THE JOHNS HOPKINS PRESS, BALTIMORE 18, MARYLAND

EDITORIAL OFFICE:
5241 Broad Branch Road, Northwest, Washington 15, D.C., U.S.A.

HREE DOLLARS AND FIFTY CENTS A YEAR SINGLE NUMBERS, ONE DOLLAR

JOURNAL OF GEOPHYSICAL RESEARCH

The continuation of

Terrestrial Magnetism and Atmospheric Electricity

(1896-1948)

An International Quarterly

Founded 1896 by L. A. BAUER *Continued 1928–1948 by* J. A. FLEMING

Fields of Interest

Terrestrial Magnetism
Atmospheric Electricity
The Ionosphere
Solar and Terrestrial Relationships
Aurora, Night Sky, and Zodiacal Light
The Ozone Layer
Meteorology of Highest Atmospheric Levels
The Constitution and Physical States of th Upper Atmosphere
Special Investigations of the Earth's Cru and Interior, including experimental seism waves, physics of the deep ocean and ocea bottom, physics in geology
And similar topics

This Journal serves the interests of investigators concerned with terrestrial magnetism and ele tricity, the upper atmosphere, the earth's crust and interior by presenting papers of new analys and interpretation or new experimental or observational approach, and contributions to inte national collaboration. It is not in a position to print, primarily for archive purposes, extensi tables of data from observatories or surveys, the significance of which has not been analyzed.

Forward *manuscripts* to the editorial office of the Journal at 5241 Broad Branch Road, Northwes Washington 15, D. C., U.S.A., or to one of the Associate Editors. It is preferred that manuscrip be submitted in English, but communications in French, German, Italian, or Spanish are al acceptable. A brief abstract, preferably in English, must accompany each manuscript. A *public tion charge* of $4 per page will be billed by the Editor to the institution which sponsors the work any author; private individuals are not assessed page charges. Manuscripts from outside t United States are invited, and should not be withheld or delayed because of currency restrictio or other special difficulties relating to page charges. Costs of publication are roughly twice t total income from page charges and subscriptions, and are met by subsidies from the Carne Institution of Washington and international and private sources.

Back issues and *reprints* are handled by the Editorial Office, 5241 Broad Branch Road, N.W Washington 15, D.C., U.S.A.

Subscriptions are handled by The Johns Hopkins Press, Baltimore 18, Maryland, U.S.A.

THE JOHNS HOPKINS PRESS

Baltimore 18, Maryland

Entered as second-class matter at the Post Office at Richmond, Virginia, under the act of March 3, 1879.

Journal of

GEOPHYSICAL RESEARCH

The continuation of

errestrial Magnetism and Atmospheric Electricity

UME 56 DECEMBER, 1951 No. 4

A QUICK METHOD FOR ANALYSING IONOSPHERIC RECORDS

BY J. A. RATCLIFFE

Cavendish Laboratory, Cambridge, England

(Received October 6, 1951)

ABSTRACT

A method is described by which routine $(h' - f)$ records can be analysed quickly to give information about the vertical distribution of electron density in the ionosphere. The method is approximate but is simple and quick to use, and is therefore convenient for making analyses of the type required for testing theories of the ionosphere. It consists in assuming, after Appleton, that the electron distribution is parabolic and then in constructing a series of curves, similar to those of Booker and Seaton, on a transparent scale, in such a way that they can be matched directly to the photographic records. The important parameters can then be read directly from the scale. Retardation in the $F1$ layer can be allowed for when the $F2$ layer is being analysed. Scales based on other electron distributions are also described and are useful in the analysis of unusual records of the type sometimes encountered at Huancayo. An account is given of the calculation of the total number of electrons in a unit column of the $F2$ layer below the level of the maximum. The calculations are made on the assumption that the earth's magnetic field is zero, and the effect of removing this limitation is discussed.

1—INTRODUCTION

Iuch information about the ionosphere has been accumulated over several s at observatories situated in different parts of the world. The most usual of information exists in the form of photographically-recorded $(h' - f)$ traces

in which the equivalent height (h') of reflection of a pulse of frequency f is recor as a function of the frequency. It is well known that the critical frequencies wh can be read from records of this type provide useful information about the mi mum electron densities (N_m) in the different ionospheric layers.

It is also well known that these ($h' - f$) records contain most of the infor tion necessary for deducing the electron density at different heights in the io sphere, so that the "shape" of the electron layer can be deduced from them 1, 2, and 3 of "References" at end of paper]. A knowledge of the shape, and particular the thickness and height, of the layer is important for ionosph theory, and it might be wondered why so little use has been made of this asp of the available information. The reason undoubtedly is that the deduction the exact electron distribution from the observed ($h' - f$) record involve numerical integration which is tedious even in its simplest form. The method h therefore, only been used in the analysis of some special isolated examples [and has not been used to investigate what happens to the ionosphere at differ places at different seasons, and at different parts of the sunspot cycle.

A knowledge of the vertical distribution of the electrons is, however, so v important for ionospheric theory that it is worth while developing a much precise method, which will give an approximate measure of this distribution a in particular, the thickness and height of the layer, provided the method can used quickly. It is the purpose of this paper to describe a method of this kind

A simple mathematical form is assumed for the distribution of electrons the layer, and the ($h' - f$) curve which would result is calculated. By compar the observed ($h' - f$) curve with the calculated, it is then possible to de whether the actual distribution approximates to that assumed, and, if it does is an easy matter to determine the fundamental parameters (for example, hei and thickness of layer) which characterise the distribution. In a large propor of the observed cases it turns out that the assumption of a parabolic distribu of ionisation, as first suggested by Appleton [4], agrees well with the results, sometimes it is necessary to assume a linear distribution given by $N = \alpha(h -$ for $h > h_0$ (Fig. 5), or a distribution given by $N = \beta(h - h_0)^2$ (Fig. 8).

A series of calculated ($h' - f$) curves, for layers of different thicknesses, drawn on a transparent scale in such a way that when the scale is placed over photographic record the curve giving the best fit can be found. The group reta tion produced by an $F1$ layer below the $F2$ layer can be allowed for.

The rapidity with which the method can be used may be illustrated by sta that the analysis required for the results of the companion paper in this s issue [9] on "Some regularities in the $F2$ layer of the ionosphere" (here ca Paper 2) was performed by one person in about three weeks.

2—CONSTRUCTION OF THE SCALES

(*a*) *A parabolic layer*—Booker and Seaton [6], following Appleton [4], h considered a layer in which the electron density (N) varies with the height as given by

$$\frac{N_m - N}{N_m} = \left\{\frac{h_m - h}{T}\right\}^2 \dots\dots\dots\dots\dots\dots\dots$$

s expression, h_m represents the height of maximum electron density, T repre- the semi-thickness of the layer, and N_m represents the maximum electron y, which is related to the critical penetration frequency (f_c) by the well- n relation $N_m = 1.24 \times 10^{-8} f_c^2$. The distribution is illustrated in Figure 1.

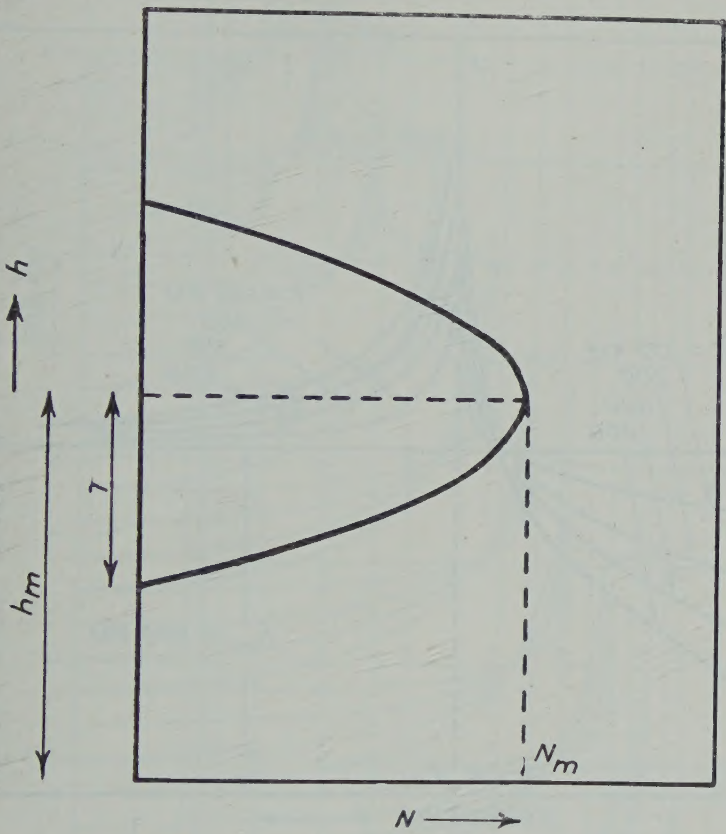

FIG. 1—A parabolic distribution of electron density (N).

calculate virtual heights, Booker and Seaton used a function

$$\phi\left(\frac{f}{f_c}\right) = \frac{1}{2}\left(\frac{f}{f_c}\right) \log_e \left| \frac{f_c + f}{f_c - f} \right| - 1 \qquad (2)$$

owed that the virtual height of reflection of a pulse of frequency $f(<f_c)$ ne layer is given by

$$h' = h_m + T\phi\left(\frac{f}{f_c}\right) \quad (f < f_c) \qquad (3)$$

lse of frequency $f(> f_c)$ penetrates the layer and is reflected from another tuated at the level h_m, then the equivalent height of reflection is increased unt of group retardation in the half parabola below h_m. We shall call this e of the equivalent height the group retardation $\Delta h'$; it is given by

$$\Delta h' = T\phi\left(\frac{f}{f_c}\right) \qquad (f > f_c)\ldots\ldots\ldots\ldots\ldots\ldots$$

The function $T\phi(f/f_c)$ is plotted in Figure 2 for values of T equal to 100, 200, 400 km.

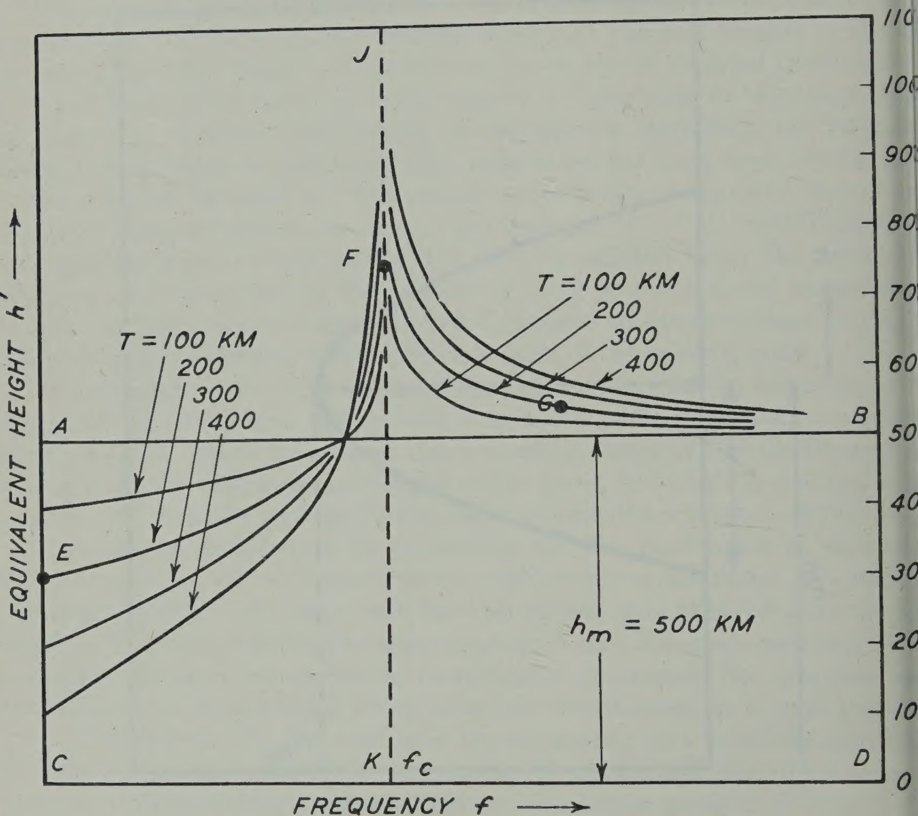

Fig. 2—Curves for parabolic regions of different semi-thickness (T) having the same penet frequency (f_c) and with their maxima at the same height (h_m). The distances between CD an curves to the left of the line JK represent the equivalent heights h' for frequencies (less th which are reflected from the layer. The distances between AB and the curves to the right represent the group retardations $\Delta h'$ produced by half of the parabolic layer in waves ref from an upper layer for frequencies greater than the penetration frequency f_c.

We can now use the curves of Figure 2 in conjunction with equation (3) i following way to represent h' for any parabolic layer at any height. Cho base-line such as CD which is a distance h_m below AB (here taken as 500 Choose the curve appropriate to the semi-thickness T of the parabola; fo ample, the curve EF corresponding to T = 200 km. Then the distance o from the base-line CD represents h' as a function of f.

We can also use the curves in conjunction with equation (4) to represen group retardation $\Delta h'$ produced in an echo which penetrates the lower h the parabola. Equation (4) shows that $\Delta h'$ is represented by the distance be

FIG. 3—A reduced copy of the scale used in the analysis of parabolic records. Each set of curves represents "Booker-Seaton" curves for layers of semi-thickness 100, 200, 300, 400 km. The two sets of curves in the top left-hand corner also contain curves for half thicknesses of 50 km. Where only one curve is shown on the right-hand side, it is for a semi-thickness of 100 km. The frequency scale is that appropriate to the records of the Carnegie Institution of Washington and is labeled in terms of 1/10 (f^2), with f in Mc/sec.

the zero line AB and the appropriate curve (for example, FG for a layer of se thickness 200 km).

Let us now suppose that we had a series of ionospheric $(h' - f)$ records, ma with a linear frequency scale, on occasions when there was a single layer in wh the distribution of electron density was parabolic as given by equation (1). I us also suppose that the critical penetration frequencies all had the same va f_c . Then, if a transparent copy of Figure 2, with the scales of h' and f the sa as those on the record, were fitted to the trace, it would be a quick and easy mat to determine (possibly by interpolation) the value of T which gave the best agr ment, and also to read off the height (h_m) of the maximum of ionisation. If critical penetration frequencies differed from one record to another, a series families of curves like those of Figure 2 could be prepared, corresponding different penetration frequencies, and that series having penetration freque nearest to the observed value could be used without much error.

In the actual records, the frequency scale depends on the nature of the cording apparatus and is not usually linear. The transparent scale contain families of curves corresponding to Figure 2 can then be made so that each fam has the scale appropriate to one penetration frequency and it will be sufficien accurate for penetration frequencies which are not far removed from the for which it is constructed.

Figure 3 shows a reduced copy of a scale of this type used in the analysis records made with the apparatus designed by workers at the Carnegie Institut of Washington [7]. The frequency scale for these records is shown in Figure

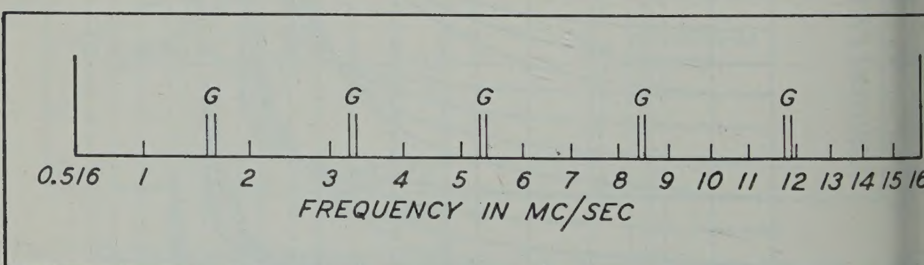

FIG. 4—A reduced copy of the frequency scale used on the records made by the Carnegie Institu of Washington. The marks at the points G denote gaps in the scale corresponding to the chan of coils in the equipment.

and it will be noticed that there are gaps marked G corresponding to the times w the coils were changed in the recording apparatus. These gaps are small, howe and of standard size, so that for the purpose of constructing the curves of Figu the frequency scale has been distorted slightly so as to run smoothly and cont ously through them. The resulting error is small.

The set of curves shown in Figure 3 was made simply by drawing curve represent the function $T\phi(f/f_c)$ with the appropriate frequency scale, and t reproducing the drawing full-size on a photographic plate. In Figure 3, the quency scale has been labeled in terms of $1/10(f^2)$, where f is in Mc/sec. quantity is proportional to N_m and it is often the most convenient quantity

ifying the penetration frequency. "Booker-Seaton" curves are plotted for a s of different penetration frequencies in each case for layer thicknesses of 200, 300, 400 km. For the two top sets of curves, a layer of semi-thickness 50 km so included, since this is sometimes useful in measurements of the E_2 layer. pt in the top left-hand corner of the scale, the right-hand part of the "Booker-on" curve is shown only for a layer 100 km thick, since this is generally icable to the $F1$ layer. At the higher frequencies, where no $F1$ layer is likely e present, this part is omitted completely.

The detailed method of using these curves will be described in Section 3.

b) *A linear distribution of electrons*—It sometimes happens, particularly in the rds made at Huancayo, that the $F1$ and $F2$ traces merge together to produce gle trace which cannot be fitted, even approximately, to the curves of Figure or the analysis of these records, it is sometimes better to assume other vertical

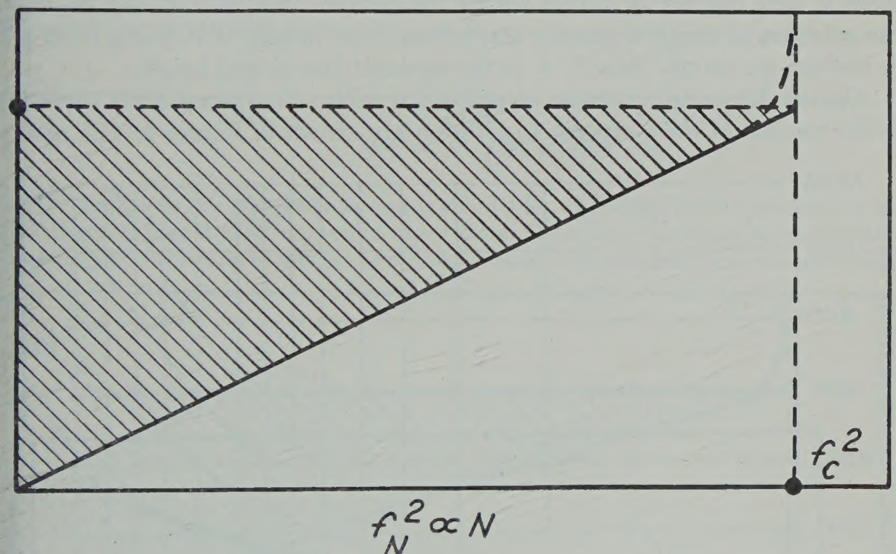

5—A linear distribution of electron density (N). In practice, a distribution of this kind would probably have a shape like that shown dotted near the level y_c.

ibutions for the electrons, and in this Section we consider a linear distribution. We shall express the electron density N in terms of the wave frequency f_N which N would be the critical density, so that

$$1.24 \times 10^{-8} f_N^2 = N$$

known that when the earth's magnetic field is neglected

$$\mu^2 = 1 - \frac{f_N^2}{f^2}$$

sider now a linear gradient of electron density, as given by

$$f_N^2 = ay$$

where y is the height (Fig. 5). Then

$$\mu^2 = 1 - \left(\frac{a}{f^2}\right)y$$

Appleton [5] has considered this variation of refractive index and has shown (I equation 28) that a group of frequency f would be reflected from a virtual heig h' given by

$$h' = \frac{P'}{2} = \frac{2f^2}{a} \ldots\ldots\ldots\ldots\ldots\ldots\ldots$$

This expression enables us to plot curves of h' against f, with the scales of h and suitably adjusted to match the records, for different values of the parameter It will be noticed that, since a critical frequency does not enter into this mod there is only one set of curves for all frequencies. We have so far assumed th the gradient of electron density starts from zero height; if it starts from a heig h_0 instead, we simply take $h_0 + h'$ to represent the virtual height.

Curves drawn to represent equation (5) with a frequency scale correspondi to the records of the Carnegie Institution are shown in Figure 6. The heavy lin

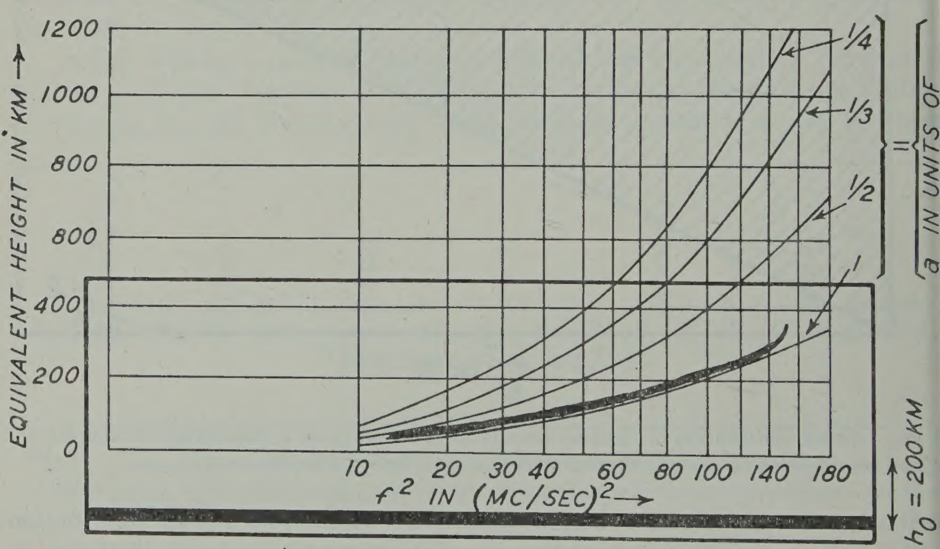

FIG. 6—Curves to represent the expression $h' = 2f^2/a$, corresponding to a linear distributio electrons. The scales are those appropriate to the records of the Carnegie Institution of Washingt The two thick lines represent the traces of the ground wave and the F echo, recorded at Huanc at $08^h\ 00^m$, November 24, 1938.

represent the ground wave and the F-region traces as recorded at Huanca at $08^h\ 00^m$ on November 24, 1938, and the F-region trace is seen to coinc fairly well with the curve representing a layer with $h_0 = 200$ km a $a = 1(\text{Mc/sec})^2\ \text{km}^{-1}$. This distribution of electrons is shown by the continu line in Figure 7.

It is of interest to compare the distribution obtained on the assumption t

$f_N^2 = ay$ with the distribution which is calculated by the accurate methods of numerical integration. S. E. Forbush kindly made an accurate calculation of this kind from the same record and obtained the electron distribution shown by the

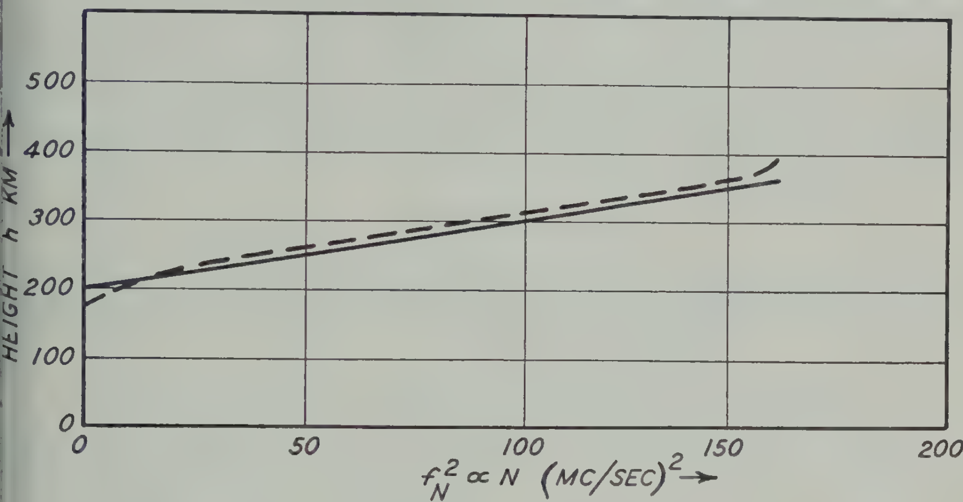

FIG. 7—The continuous line represents the linear distribution of electron density deduced, by the method of Figure 6, from the $(h' - f)$ record shown there. The broken line represents the distribution determined from the same record by the method of numerical integration [see references 1,2,3].

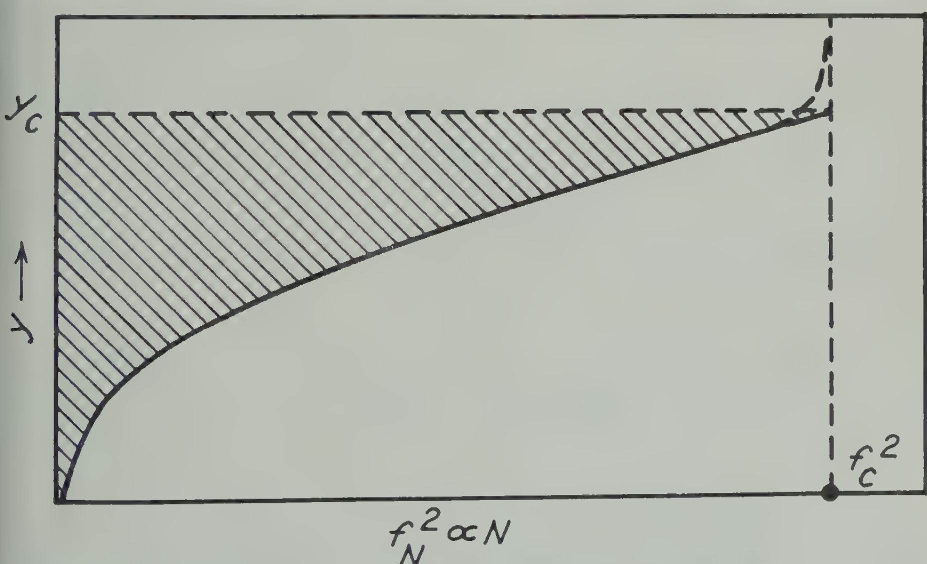

FIG. 8—A distribution of electrons given by $f_N{}^2 = b^2y^2$. In practice, a distribution of this kind would more probably have a shape like that shown by the broken line near the level y_c.

broken line in Figure 7. The agreement with our curve is good enough to show (a) that our deduction of a linear gradient on this occasion is sound, and (b) that the value determined for its slope is accurate enough for most purposes.

(c) *A distribution of electron density given by* $N = \beta(h - h_0)^2$—We now co sider a distribution of electron density given by $N = \beta(h - h_0)^2$. This can co veniently be represented, as in Figure 8, in terms of a layer which has a low boundary at $y = 0$ and in which

$$f_N^2 = b^2y^2 \quad \ldots\ldots\ldots\ldots\ldots\ldots\ldots\ldots$$

so that $\mu^2 = 1 - (b^2/f^2)y^2$. Appleton [5] shows in his equation (23) that virtual height of reflection h' of a group of frequency f from this distribution electrons is given by

$$h' = \frac{P'}{2} = \left(\frac{\pi}{2b}\right)f$$

Curves drawn to represent this linear relationship between h' and f, on the sc of the records from the Carnegie Institution, are shown in Figure 9 for differe

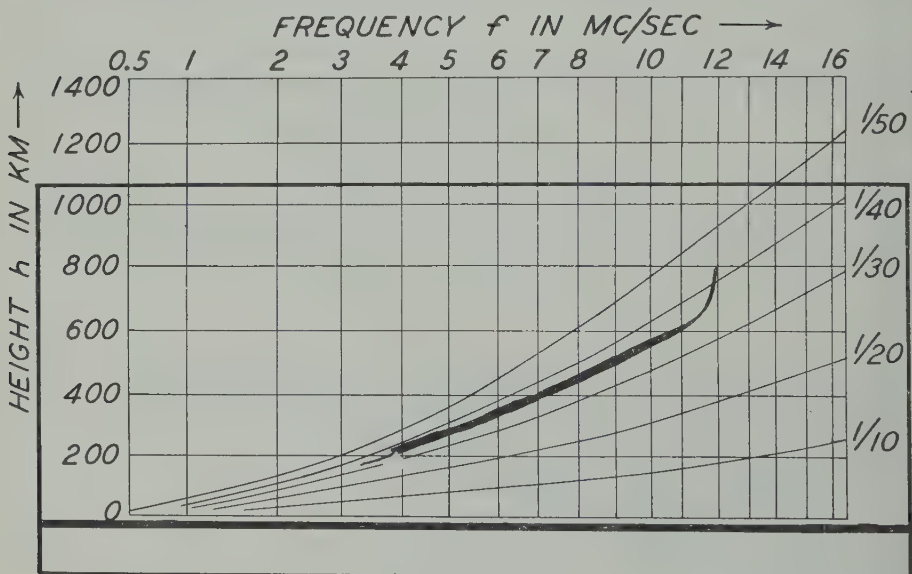

FIG. 9—Curves to represent the expression $h' = (\pi/2b)f$, corresponding to a distribution of e trons given by equation (6) and shown in Figure 8. The scales are those appropriate to the rec of the Carnegie Institution of Washington. The two thick lines represent the traces of the gro wave and the F echo, recorded at Huancayo at $15^h\ 45^m$, November 24, 1938.

values of b. These curves can be used to represent a layer starting at a heigh by moving them bodily upwards through a distance h_0. The heavy lines repres the ground wave and the F-region echo recorded at Huancayo at $15^h\ 45^m$ November 24, 1938, and they are seen to agree approximately with the cu for $h_0 = 25$ km, $b = 1/35\ \text{km}^{-1}$ (Mc/sec). The corresponding distributio electron density is shown in the continuous line in Figure 10. The distribu calculated from the original ($h' - f$) curve by S. E. Forbush, using the met of numerical integration, is shown by the broken line in Figure 10. The agreem is fairly good and justifies the use of the scale for rapid analyses.

(*d*) *The effect of the earth's magnetic field*—The construction of the curves described above depends on the relation $\mu^2 = 1 - (f_N^2/f^2)$, which gives the refractive index (μ) of a medium in terms of the wave frequency f, and a quantity f_N^2 which is related to the electron density of the medium by the expression $N = 1.24 \times 10^{-8} f_N^2$. In this expression for μ, the effect of the earth's magnetic field is not taken into account. When it is included, the expression takes a more complicated form, which for "quasi-longitudinal" conditions is $\mu^2 = 1 - \{f_N^2/(f^2 \pm f f_L)\}$,

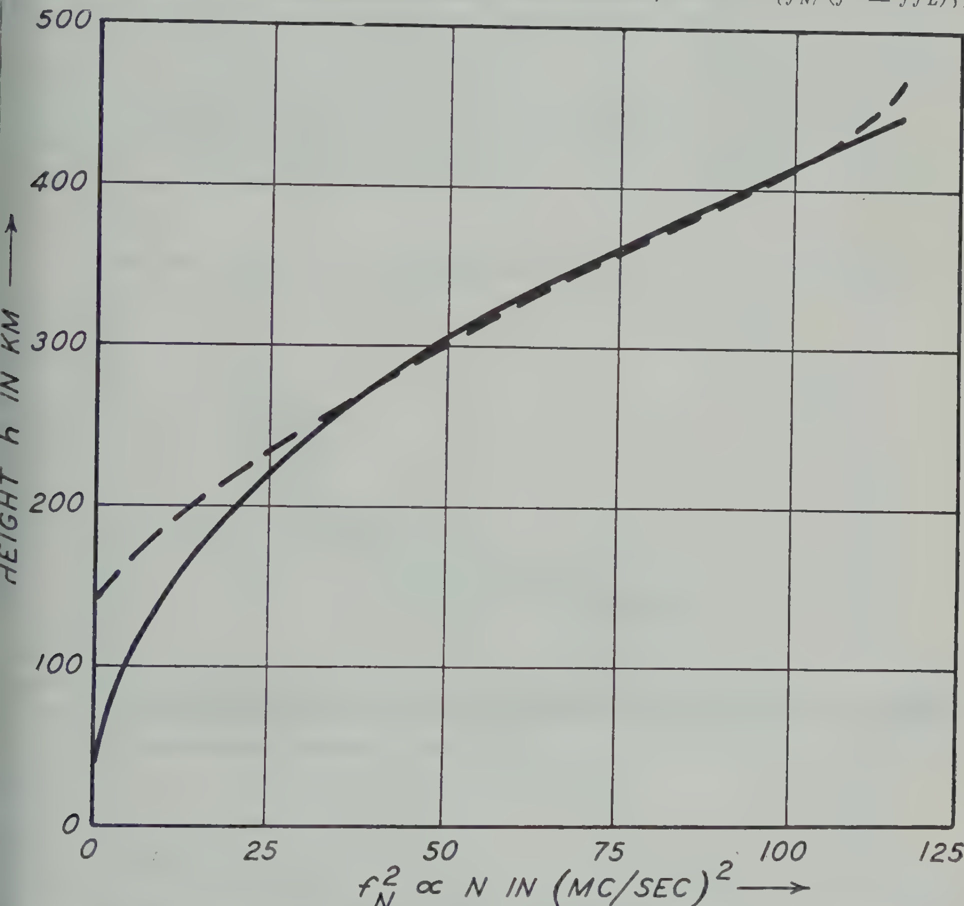

FIG. 10—The solid line represents the distribution of electron density deduced, by the method of Figure 9, from the $(h' - f)$ trace shown there. The broken line represents the distribution determined from the same record by the method of numerical analysis.

where f_L is the frequency at which electrons naturally gyrate round the longitudinal component of the magnetic field. The expression is, in general, more complicated than this.

Whale and Shinn [8] have recently calculated the group velocity for both the ordinary and the extraordinary waves in the presence of the earth's magnetic field, and have applied their calculations to the case of a parabolic distribution of electron density. They have shown that, if a method such as that of Booker and

Seaton is used to deduce the thickness of an ionospheric layer from the $(h' -$ trace for the ordinary wave, then the calculated thickness may be in error by much as 20 or 30 per cent. The error depends on the strength and direction the magnetic field in the layer concerned, and also on the range of frequenci used in the analysis. It seems probable that this recent work contains data fro which corrected curves of the Booker-Seaton type could be plotted, for differe parts of the world. Curves of this type would be an improvement on those show in this paper. It should also be possible to plot corrected curves relating to electr distributions of the types shown in Figures 5 and 8.

Until curves based on the work of Whale and Shinn are available, considerab use can be made of the uncorrected curves discussed here. Although the absolu magnitude of the semi-thickness T of a parabolic layer deduced from these curv

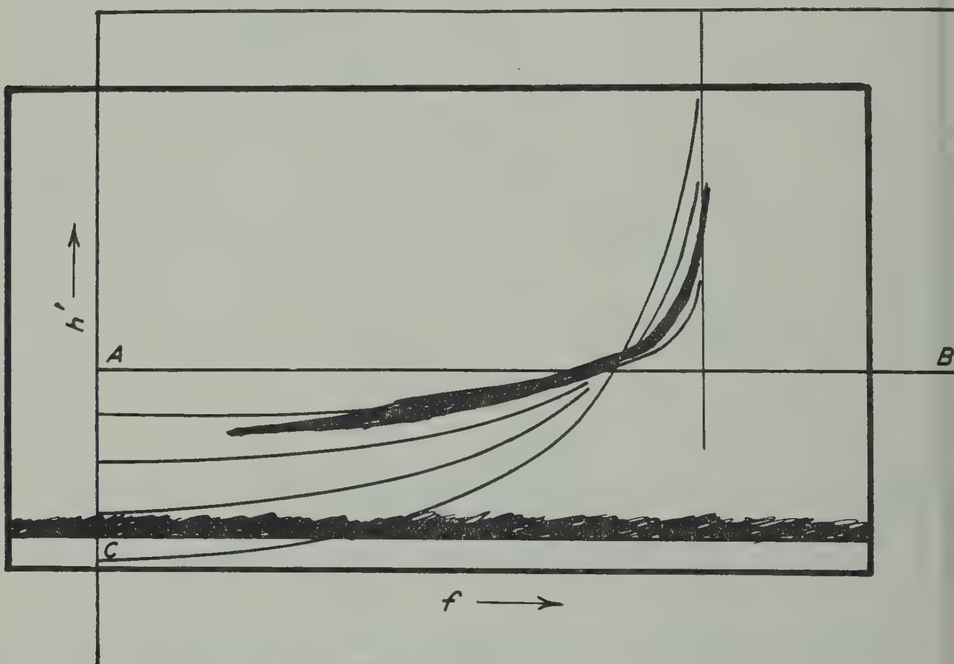

Fig. 11—To illustrate the analysis of a simple layer which approximates to a parabola. T explanation is given in the text.

may be in error, the *changes* in the calculated thickness are similar, whether not the magnetic field is included. It appears that analyses in which the field neglected will be useful in exposing some of the major changes in the vertic distribution of electrons in the ionosphere, but that for detailed analyses correct curves will have to be used.

3—METHOD OF ANALYSIS

(*a*) *Single layers, approximately parabolic*—It often happens that the $F2$ lay exists alone, without the $F1$ layer, and that the $(h' - f)$ curve can be fitted qu

closely to one of the curves of Figure 3 corresponding to a parabolic distribution of electron density. When this is the case, the analysis proceeds as follows.

The scale of Figure 3 is placed on the $(h' - f)$ curve with its frequency scale properly aligned with the frequency scale of the record. The set of curves on the scale having their penetration frequency nearest to the recorded penetration frequency is then selected and the scale is moved sideways to make the two penetration frequencies coincide. The scale is now moved vertically until the recorded $(h' - f)$ curve coincides as nearly as possible with one of the curves on the scale, or with an interpolated curve as judged by eye.* Figure 11 represents the situation at this stage and the important parameters can be read straight off the scale. The "semi-thickness" (T) is simply the label on the appropriate curve of the series, or on the interpolated curve; thus, in the Figure, $T = 150$ km. The "height of maximum" (h_m) is the distance AC and is easily read directly on the left-hand side of the scale by reading downwards from the line AB; in the Figure, $h_m = 350$ km.

Sometimes the layer is very thin and it is difficult to decide just where it fits inside the curve for $T = 100$ km. On these occasions, use may often be made of multiple reflections.** Thus, if a trace is used which corresponds to a wave reflected n times from the layer, simple considerations show that the values of T and h_m obtained by fitting a curve to the trace are n times the magnitude of T and h_m for the actual layer. The penetration frequency is not always clearly visible on the trace formed by a multiple echo and, when the method of multiples is used, it is important that the scale should be aligned with the correct penetration frequency as observed on the trace of the first reflection.

(b) *Double layers, separated and approximately parabolic*—A common type of $(h' - f)$ curve, in the daytime, is illustrated by the heavy line in Figure 12 (a, b, c, d) and corresponds to a case where an $F1$ layer is present below an $F2$ layer. Similar cases occur when an intermediate, or $E2$, layer occurs below an F layer. Booker and Seaton [6] have described the analysis of curves of this type by their method, and the procedure is as follows when the scale is used.

We first estimate the retardation which the $F1$ layer produces in the trace ABC (Fig. 12a), which corresponds to the $F2$ layer. For this purpose, the set of curves with critical frequency nearest to A is selected and the one which fits DA most nearly is chosen. An example is shown in which the portion DA is fitted by the curve corresponding to a "half thickness" of 100 km. We now require to know what retardation $\Delta h'$ the lower half of this $F1$ layer will produce in the trace ABC, and we must subtract this retardation before making measurements on ABC.

For this purpose, we use the right-hand side of the Booker-Seaton curves which relates $\Delta h'$ to f. Select the right-hand curve corresponding to that which fits the $F1$ layer and slide the scale up until this curve at some point, G, coincides with the bottom of trace ABC, as in Figure 12b. The point G, where the curves cross, is retarded by an amount GH, so that if the $F1$ layer were not present the

*In making an interpolation, it is useful to remember that, on all the curves, the distance from the line AB of Figure 2 is proportional to the semi-thickness T of the assumed layer.

**It is fortunate that thin layers usually occur at night, when multiple reflections are more common.

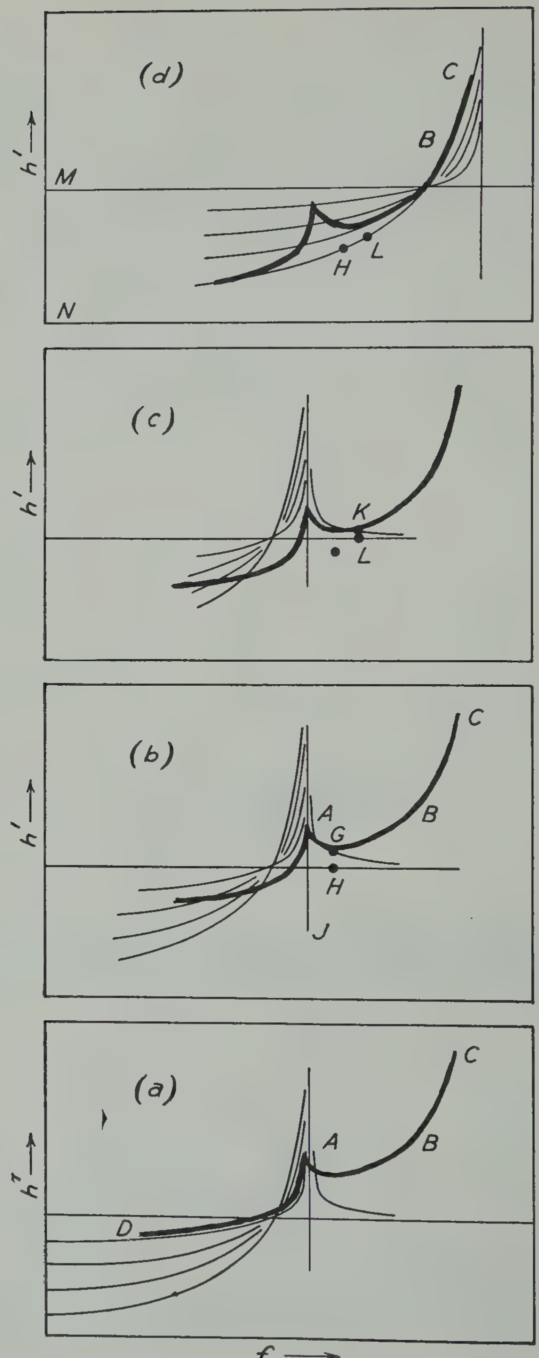

Fig. 12—To illustrate the analysis of a $(h' - f)$ curve, of the type shown by heavy lines, resulting from separated $F1$ and $F2$ layers, both having parabolic distributions of electron density. The explanation is given in the text.

2 trace would pass through H. A point is put at H to represent the corrected $F2$ ace. This point can be inserted in pencil, but after a little practice it is visualised n the mind's eye" to be at some characteristic position on the record. The scale ust be moved vertically during this process so that the line AJ slides along its wn length.

Next we find, and subtract, the $F1$ retardation at another frequency. This is one by sliding the scale up a little further till another point K on the right-hand

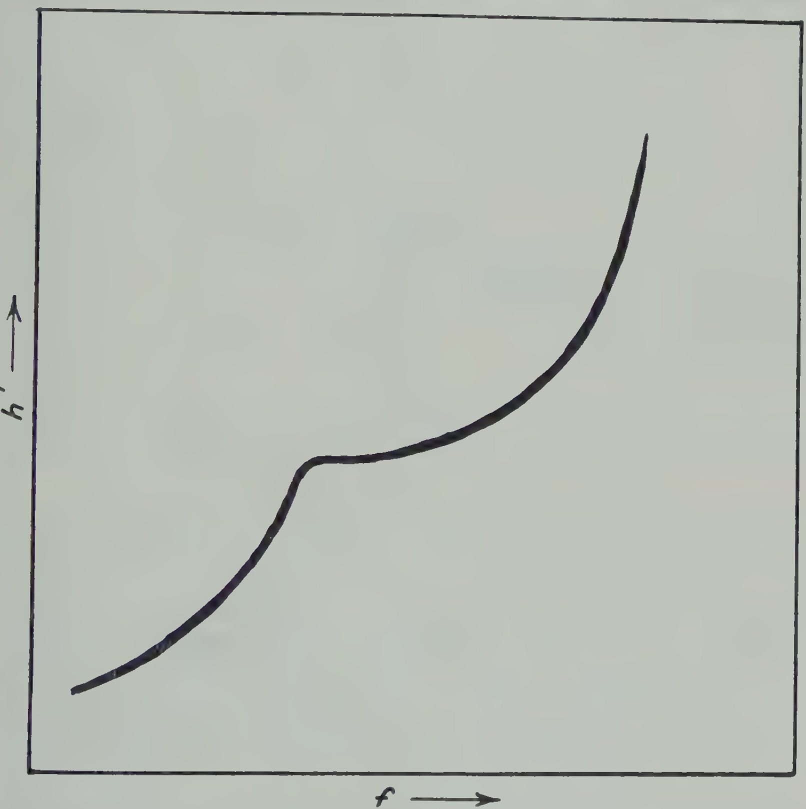

FIG. 13—Type of $(h' - f)$ curve which results from a distribution of electron density which is represented by two overlapping parabolae, as shown in Figure 14.

rve coincides with the record (Fig. 12*c*). Again a dot L is made (in pencil or imagination) to show where the corrected trace would fall.

It is now necessary to find the parameters appropriate to a layer which would oduce the corrected $F2$ trace $CBLH$ (Fig. 12*d*). For this purpose, we select e set of curves with penetration frequency nearest to that of the point C and ake one of them coincide as nearly as possible with $CBLH$. In the example own, the interpolated curve corresponding to a semi-thickness of 400 km is ken as the best fit and the corresponding parabolic layer would have its maxi-um at a height (MN) of 500 km.

(*c*) *Double layers, partially merged, approximately parabolic*—The $(h' - f)$ rves of the type shown in Figure 13 are not uncommon. They correspond to

electron distributions which can be represented approximately by two parab which intersect below the maximum of the lower parabola, as shown in Figure The group retardation produced by the shaded portion ABC of the lower lay calculated in the Appendix, and is shown to depend both on the semi-thickne the lower parabola DEC and also on the position on it of the point B. From expression derived in the Appendix, the curves of Figure 15 can be drawn.

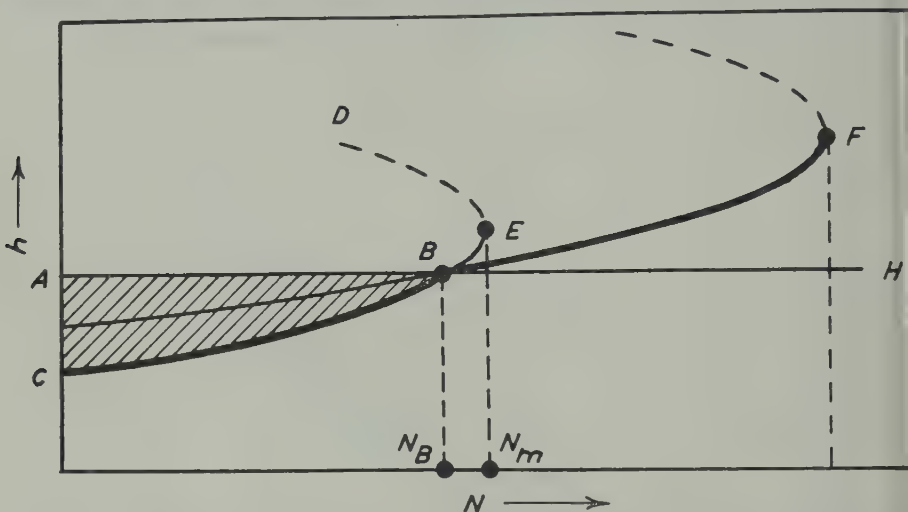

FIG. 14—To illustrate a case where the vertical distribution of electron density, shown by curve CBF, is made up of two overlapping parabolas.

We will describe these curves by reference to the one labeled ABC. The por AB represents the $(h' - f)$ curve for an echo reflected from the lower paral for which the frequency f_c would be the penetration frequency if its maxir were not obscured by the higher region. The distance between the portion and its asymptote DC represents the retardation $(\Delta h')$ suffered by a puls passing through the ionisation represented by the shaded region in Figure The other curves of the series correspond to other positions of the point B w the two parabolae intersect (Fig. 14). The frequency f_B , of the cusp in Figur is related to the electron density (N_B) at the point B in Figure 14 through expression $N_B = 1.24 \times 10^{-8} f_B^2$.

It would make the scale very confused if it were necessary to include cu like those of Figure 15 for several different semi-thicknesses of the lower para Fortunately, the $(h' - f)$ curve of the $F1$ layer can nearly always be fitted accurately by a curve appropriate to a semi-thickness of 100 km, and so sufficient to plot curves like those of Figure 15 for this semi-thickness alone.

The analysis of a curve like that shown by the heavy line in Figure 16* proceeds as follows. A calculated curve such as AB in Figure 15 is chose

*The thick line which represents the $(h' - f)$ curve in Figure 16 is plotted with a linea of f, and its appearance is therefore different from those in other Figures which are plotted frequency scale appropriate to the measuring equipment.

it, with least sideways movement of the scale, it coincides with the recorded $-f$) curve over the first ($F1$) part of its course. The position will now be as istrated in Figure 16 and the parameters appropriate to the $F1$ layer may be d off as follows: The semi-thickness is that appropriate to the curve which s best (usually found to be 100 km), and the height of the (obscured) maximum ionisation in the lower parabola (E in Fig. 14) is given by the distance GK of

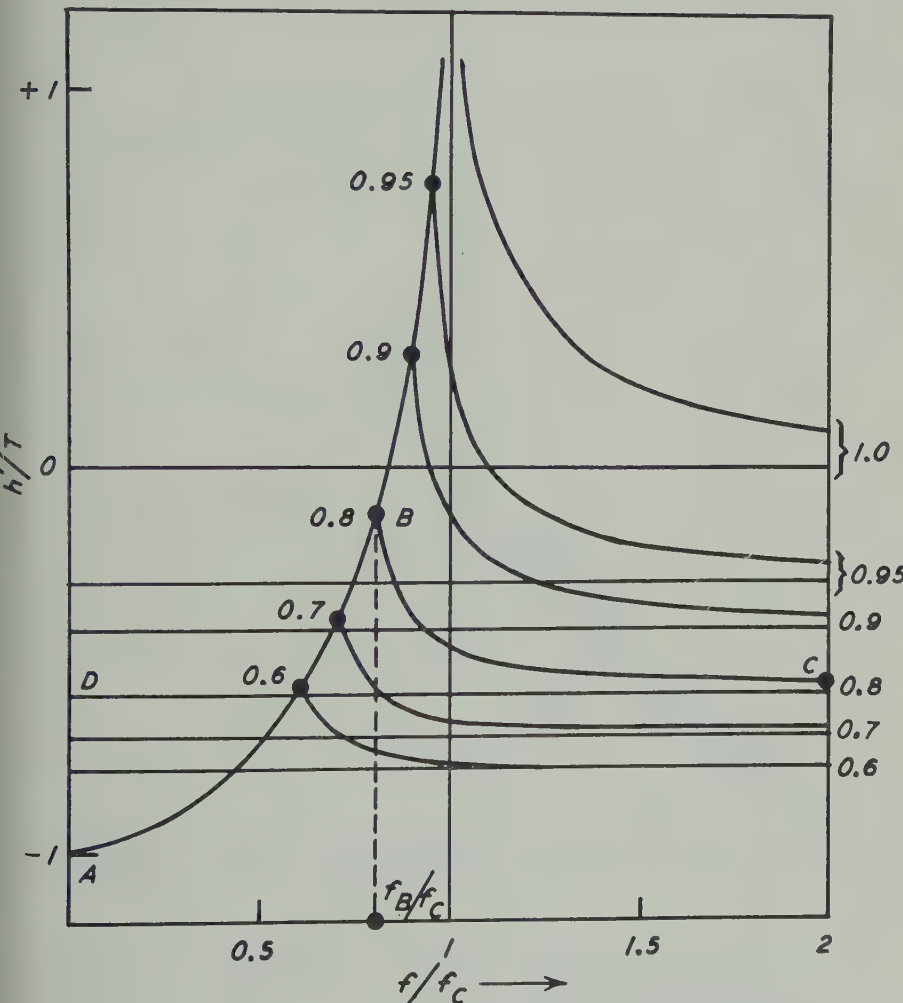

FIG. 15—Normalised ($h' - f$) curves for electron distributions such as that of Figure 14. These curves are calculated in the Appendix.

H above the base line (easily read from the left-hand side of the scale). The oup retardation $\Delta h'$ to be subtracted from the equivalent height of the echo om the $F2$ layer is represented at the different frequencies by the distance been the lines BC and DC, and in particular the group retardation at the point is equal to BJ, so that J is a point on the corrected ($h' - f$) curve for the $F2$

layer.* If one of the "retardation" curves, such as BC, does not pass through point B, where the $(h' - f)$ record leaves the theoretical curve AB, it is nece to insert an interpolated curve vertically between two of those drawn on the s It is usually sufficient to determine the one point J and to extrapolate the $(h'$

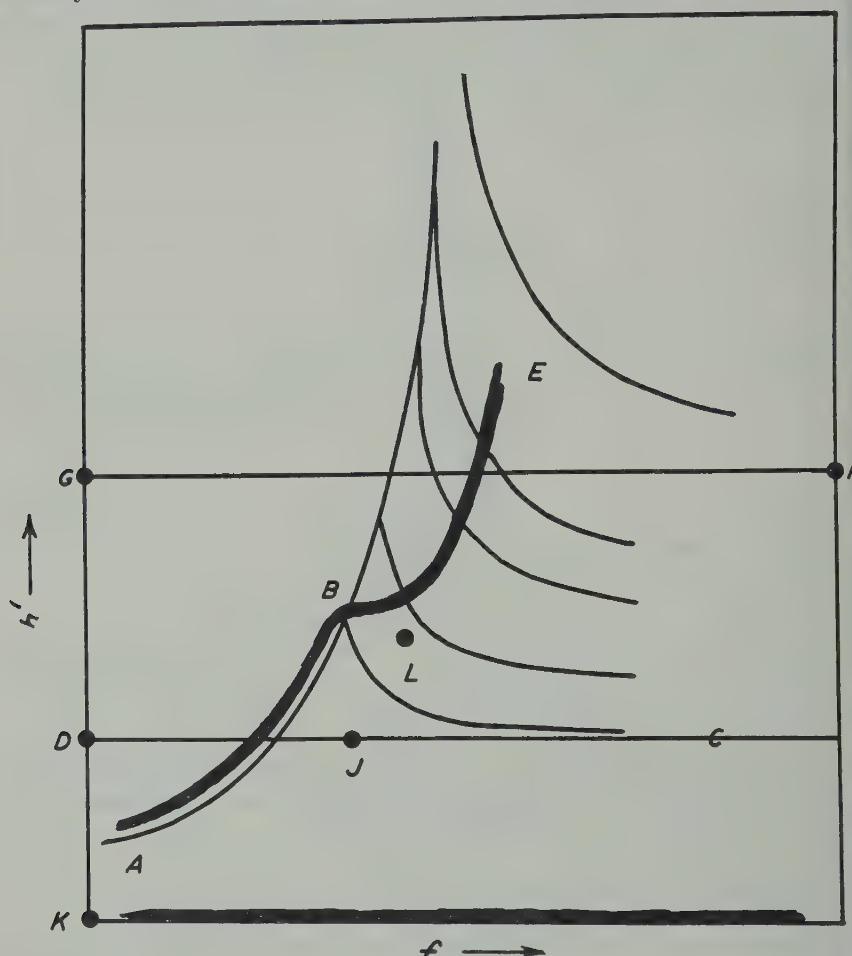

FIG. 16—To illustrate the analysis of a $(h' - f)$ curve having the form of the thick line ABE. The procedure is explained in the text. It should be noted that the frequency scale on this Figure is linear, so that the $(h' - f)$ curve differs from those in other Figures where the frequency scale is that appropriate to the experimental equipment.

curve for the $F2$ layer through it before fitting it to the scale. If, however, points, such as that shown at L, are required on the "corrected" curve for th layer, they can be obtained by using the curve BC in a way similar to tha scribed in connection with Figures 12*b* and 12*c*.

(*d*) *Layers in which* $N = \alpha(h - h_0)$ *and* $\beta(h - h_0)^2$—If the record does n approximately to the curves representing a parabolic layer, the curves approp

*The point J represents the actual height at which the upper and lower parabolae int

the other types of layer can be tried. The method of using them has been suffi-
ently explained in (*b*) and (*c*) of Section 2. It has always been found that there
a reasonably good agreement between the experimental record and one of the
pes of curve here discussed.

—THE CALCULATION OF THE TOTAL ELECTRON CONTENT IN UNIT COLUMN OF THE LAYER UP TO THE LEVEL OF MAXIMUM IONISATION

Special interest attaches to the quantity (n) which measures the number of
ectrons in unit column of the $F2$ layer up to the level of the maximum of the
yer. Paper 2 [9] gives an account of an extensive series of determinations of this
antity. In this Section we shall show how it can be calculated.

If the records fit curves of the type appropriate to a parabolic layer, the
ethods of Section 3 can be used to find the semi-thickness T. The number of
ectrons per unit column up to the level where the electron density has its maxi-
um value (N_m) is then given by

$$n = \tfrac{2}{3}TN_m$$

, if we substitute $N_m = Bf_c^2$, where f_c is the critical frequency in cycles per
cond and $B = 1.24 \times 10^{-8}$, we have

$$n = \tfrac{2}{3}BTf_c^2 \qquad \text{(7)}$$

ost of the results for Paper 2 are calculated in this way, and n is expressed in
umber of electrons per cm^2 column."

If the records fit curves appropriate to a linear gradient of electron density as
ven by $f_N^2 = ay$, and if the critical penetration frequency is f_c, then n represents
e number of electrons per cm^2 column corresponding to the shaded area in
gure 5, so that

$$n = \tfrac{1}{2}By_cf_c^2 = \frac{\tfrac{1}{2}Bf_c^4}{a} \qquad \text{(8)}$$

ne magnitude of n can be calculated directly from this expression.

When a large amount of data are being dealt with, it is often convenient to
press all the results in terms of an equivalent parabolic layer which would
ntain the same number of electrons. If T_{eq} represents the thickness of the
uivalent parabolic layer, so that

$$n = \tfrac{2}{3}T_{eq}Bf_c^2 \qquad \text{(8a)}$$

mparison of equations (8) and (8*a*) shows that

$$T_{eq} = \frac{3}{4}\left(\frac{f_c^2}{a}\right) \qquad \text{(9)}$$

If the records fit curves appropriate to a distribution of electrons given by
$= b^2y^2$, and if the critical penetration frequency is f_c, then n represents the
mber of electrons per cm^2 column, corresponding to the shaded area in Figure 8.
is gives

$$n = \frac{B}{3}\frac{1}{b}f_c^3 \qquad \text{(10)}$$

which can be written

$$n = \tfrac{2}{3}BT_{eq}f_c^2$$

with

$$T_{eq} = \frac{f_c}{2b} \dots\dots\dots\dots\dots\dots\dots\dots$$

Expression (10) gives n directly, or if it is desired to work in terms of the equiva semi-thickness of a parabolic layer, expression (11) may be used.

The electron distributions which can be analysed in terms of the approxi tions sketched in Figures 5 and 8 are, of course, not likely to terminate sha at the upper end, as shown by the shaded areas. It is more likely that they have an upper part as indicated by the dotted lines. This would produce a r termination on the $(h' - f)$ curve; a sharp termination to the $(h' - f)$ c will correspond to an even-sharper termination to the $(N - h)$ curve. The served terminations are usually so sharp that it is a reasonable approxima to assume that it is completely sudden. Figures 7 and 10 show the difference tween the $(N - h)$ curves (continuous lines) deduced by the present met with the assumption of a sudden termination and the curves (broken lines) ded by a full calculation from the complete $(h' - f)$ curve.

When a large number of $(h' - f)$ curves is to be used to determine n, often convenient to deal with the straight type of curve sometimes obtaine Huancayo by fitting one of the curves of Figure 3, deduced for a parabolic la so that it lies evenly about the $(h' - f)$ record, although the shapes of the cu are not at all similar. The value of n is calculated in the usual way from the c which is fitted. This is equivalent to fitting a parabola evenly about the parabolic $(N - h)$ curve and then using the parabola to deduce the value A comparison of this method and that in which the curves of Figures 6 and 9 used has been made on several occasions and has shown that the results for n reasonably correct if the curves for the parabola are used.

5—CONCLUSIONS

The scales described in this paper provide a quick method of making ar proximate analysis of $(h' - f)$ records so as to determine the vertical distribu of electron density in the atmosphere. The scales are easy to construct and to For most purposes, the one set of scales, based on parabolic distribution, wi found sufficient, but under special conditions (for example, for several of records from Huancayo) the other types of scales described in (b) and (Section 2 may be necessary. Although no very great accuracy can be obta with this method of analysis, it seems probable that some interesting results be obtained if the method were applied to some of the extensive series of re now in existence. One such application, to a series of records obtained by Carnegie Institution of Washington at Watheroo, Huancayo, and Alaska i scribed in a companion paper [9]. The neglect of the effect of the earth's mag field on the scales described may lead to an appreciable error in the absolute

the thickness deduced for the layers, but it is not likely to affect seriously deductions made about changes of these thicknesses.

6—ACKNOWLEDGMENTS

The opportunity to do this work arose through the generosity of the Carnegie Institution of Washington, who invited me to work at their Department of Terrestrial Magnetism as a guest investigator. An examination of the beautiful series of records which they had made at Watheroo, Huancayo, and Alaska over a period of several years stimulated me to devise a quick method of analysis. In devising and using the method, I benefited very considerably from discussions with workers in the Department, in particular with Messrs. Wells, Vestine, Forbush, and Berko. The method in (*c*) of Section 3 for the analysis of curves of the type shown in Figure 13 arose out of discussions with them. I am much indebted to S. E. Forbush for performing the numerical integrations which led to the broken-line curves of Figures 7 and 10. Mr. Hendrix gave most valuable help with the construction of the scales. My thanks are due to these individuals, to the Carnegie Institution of Washington, and to Cambridge University who granted me leave of absence to work in Washington.

APPENDIX

The $(h' - f)$ curve for part of a parabolic region—Assume that the electron density (N) is distributed with height (y), as shown by the shaded region in Figure

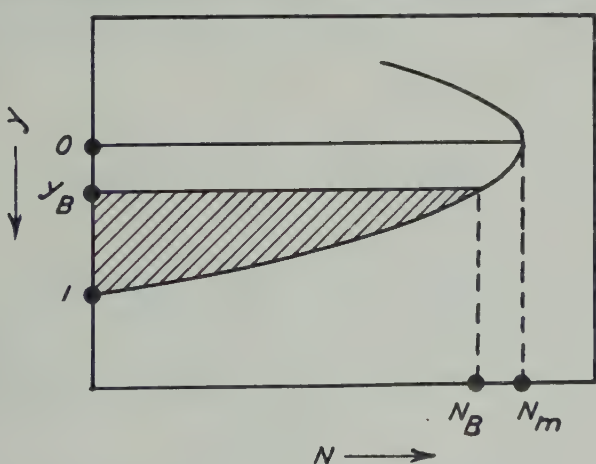

FIG. 17—A portion of a parabolic distribution of electron density, to illustrate the calculation of the retardation produced by the shaded part.

17. This shaded region is part of the parabolic distribution given by

$$N = N_m(1 - y^2) \quad \ldots\ldots(12)$$

included between the levels $y = 1$ and $y = y_B$. The refractive index (μ) at any level (y) for a radio wave of frequency (f) is given, if we neglect the effect of the earth's magnetic field, by

$$\mu^2 = 1 - \left(\frac{e^2}{\pi\epsilon_0 m}\right)\frac{N}{f^2}$$

$$\mu^2 = 1 - \left(\frac{e^2}{\pi\epsilon_0 m}\right)\left(\frac{N_m}{f^2}\right)(1 - y^2)$$

$$\mu^2 = 1 - \left(\frac{f_c}{f}\right)^2(1 - y^2) \;\ldots\ldots\ldots\ldots\ldots\ldots\ldots\ldots$$

if we write $(e^2N_m/\pi\epsilon_0 m) = f_c^2$ to relate the value of N_m to the frequency (f_c) whi would be critical for that electron density. We can rewrite equation (13) thus:

$$\mu = \left(\frac{f_c}{f}\right)\left\{y^2 + \left(\frac{f}{f_c}\right)^2 - 1\right\}^{1/2} \ldots\ldots\ldots\ldots\ldots\ldots$$

Now consider a wave-group of frequency (f) sufficiently great to penetra the densest part of the shaded region so that $f^2 > (e^2/\pi\epsilon_0 m)N_B$. While the gro is traversing the actual thickness $(1 - y_B)$ of the shaded portion, it is retard so that the "group path" is given by

$$\Delta h' = \int_{y=1}^{y=y_B}\left(\frac{c}{U}\right)\mathrm{d}y \;\ldots\ldots\ldots\ldots\ldots\ldots\ldots$$

where U is the group velocity. Now $c/U = 1/\mu$ if the earth's magnetic field neglected [10], so that

$$\Delta h' = \int_{y=1}^{y=y_B}\frac{\mathrm{d}y}{\mu}$$

$$\Delta h' = \left(\frac{f}{f_c}\right)\int_{y=1}^{y=y_B}\left\{y^2 + \left(\frac{f}{f_c}\right)^2 - 1\right\}^{-1/2}\mathrm{d}y \;\ldots\ldots\text{from (}$$

$$\Delta h' = \left(\frac{f}{f_c}\right)\log_e\left\{\frac{1 + f/f_c}{y_B + \sqrt{y_B^2 + (f/f_c)^2 - 1}}\right\} \ldots\ldots\ldots\ldots$$

Now we write f_B for the frequency which just penetrates the shaded layer Figure 17, so that $\mu = 0$ for this frequency at the level y_B and therefore

$$0 = 1 - \left(\frac{f_c}{f_B}\right)^2(1 - y_B^2)$$

or

$$y_B^2 = 1 - \frac{f_B^2}{f_c^2} \ldots\ldots\ldots\ldots\ldots\ldots\ldots\ldots\ldots\ldots$$

so that Equation (16) becomes

$$\Delta h' = \left(\frac{f}{f_c}\right)\log_e\left\{\frac{1 + f/f_c}{\sqrt{1 - (f_B/f_c)^2} + \sqrt{(f/f_c)^2 - (f_B/f_c)^2}}\right\} \ldots\ldots$$

Equation (18) gives the magnitude of $\Delta h'$ for $f > f_B$, while for $f < f_B$ reflect

from the parabolic part of the shaded region in Figure 17 and the magnitude f h' is given by Appleton's expression

$$h' = \frac{1}{2}\left(\frac{f}{f_c}\right)\log\left(\frac{1 + f/f_c}{1 - f/f_c}\right) \qquad (19)$$

hich is the same as $1 + \phi(f/f_c)$ of Booker and Seaton. From equations (18) and 9), it is possible to plot a series of curves showing h' and $\Delta h'$ as a function of f r different values of the parameter f_B/f_c. These are the curves shown in Figure 15.

The calculation given above was performed on the assumption that the half-ickness of the complete parabola of Figure 17 was unity. If its thickness is T, is easy to see that the curves of Figure 15 are still applicable if the scale of h' multiplied by T.

References

[1] C. L. Pekeris, Terr. Mag., **42**, 205 (1940).
[2] O. Rydbeck, Phil. Mag., **30**, 282 (1940).
[3] O. Rydbeck, Phil. Mag., **34**, 130 (1943).
[4] E. V. Appleton, Proc. R. Soc., **162**, 451 (1937).
[5] E. V. Appleton, Proc. Phys. Soc., **41**, 43 (1928).
[6] H. G. Booker and S. L. Seaton, Phys. Rev., **57**, 87 (1940).
[7] L. V. Berkner, H. W. Wells, and S. L. Seaton, Trans. Edinburgh Meeting, 1936; Internat. Union Geod. Geophys., Assoc. Terr. Mag. Electr., Bull. 10, 340–357 (1937).
[8] H. A. Whale and D. H. Shinn, J. Atmos. Terr. Phys., in preparation.
[9] J. A. Ratcliffe (Paper 2), J. Geophys. Res., **56**, 487–507 (1951).
[10] G. Breit and M. A. Tuve, Phys. Rev., **28**, 571 (1926).

SOME REGULARITIES IN THE $F2$ REGION OF THE IONOSPHERE

By J. A. RATCLIFFE

Cavendish Laboratory, Cambridge, England

(Received October 6, 1951)

ABSTRACT

A quick and approximate method was used to analyse $(h' - f)$ records of radio waves reflected from the ionosphere so as to give the total number (n) of electrons below the level of maximum electron density in a column of unit cross-section in the $F2$ region. The analysis was carried out on records obtained at Watheroo (Australia), Huancayo (Peru), and College (Alaska) for two magnetically quiet days per month in a year of sunspot maximum and a year of sunspot minimum. It was found that the quantity n was closely related to the zenith angle (χ) of the sun's rays, whereas it is well known that the maximum electron density N_m in the $F2$ layer is not simply related to this angle. The well-known anomalies which are apparent when N_m is studied as a function of time of day, time of the year, and geographical position, all seemed to disappear when the quantity n was studied instead. A new kind of anomaly which was observed at Huancayo in years of sunspot minimum is described and discussed. A relation between the thickness and the height of the $F2$ layer is established and the possibility of using it in ionospheric forecasting and theory is discussed. Since the deductions of this paper are made on data from only three stations, it is suggested that a similar analysis should be made for other stations. This is all the more necessary because two other sets of workers have reported results in disagreement with those obtained in this paper.

1—INTRODUCTION

Much of the information about the ionospheric layers rests on a knowledge the way in which the maximum electron density (N_m) in the layers varies with ne and place. It is well known that the behaviour of the E and $F1$ layers seems be fairly simple when expressed in terms of N_m , but that the $F2$ layer shows ch little sign of regular behaviour that it is often said to be "abnormal." From e earliest days of ionospheric investigation, it has been suggested [see 1 and 2 "References" at end of paper] that some, if not all, of these irregularities might removed if attention were directed, not to variations of N_m , but to variations

of the total electron content of a unit column of the layer. It is the purpos this paper to describe an analysis of this total electron content and to show in the $F2$ layer this quantity varies in a much more regular manner than quantity N_m .

The analysis made here depends on the use of a quick method for estima the thickness of the $F2$ layer. This method, which is described in a compa paper, here referred to as Paper 1 [3], is a simple adaptation of methods previo suggested. The accuracy of the results is probably not better than 25 per c but it will be seen from what follows that this is sufficient for our purpose.

The data used were of limited extent; they are described in Section 3. It w be of great interest to see the results of similar analyses applied to records m at other times and places.

2—THE CALCULATION OF THE TOTAL ELECTRON CONTENT PER UNIT COLU

The methods of analysis are fully described in Paper 1, in which it is sh how it is usually possible to represent the distributions of electron densit the $F2$ layer, and in the $F1$ layer if present, by approximating parabolae as i cated in Figure 1. The total number (n) of electrons in unit column of the

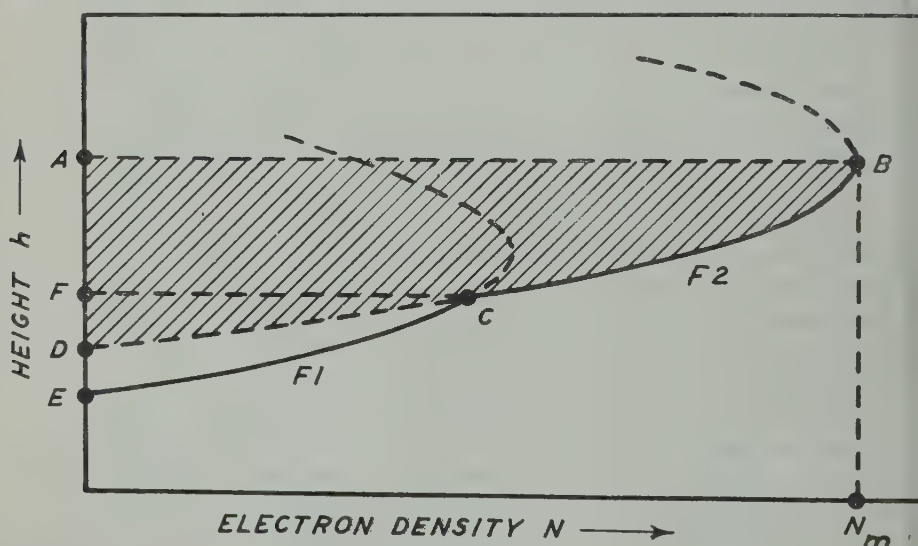

Fig. 1—To illustrate the approximation to the distribution of electron density by means o parabolas.

layer, below the maximum of the layer, is taken to be

$$n = \frac{2}{3} TN_m$$

where T is the measured "semi-thickness" AD of the parabola representing $F2$ layer. This number is proportional to the shaded area in the Figure. Meas ments were made on the $F1$ layer only for the purpose of estimating its retar effect on echoes from the $F2$ layer. The number of electrons in the $F1$ layer is

cluded in the results, but usually it is small compared with the number in $F2$ d its inclusion would make little difference. It might be thought that the electron ntent of the $F2$ layer would be better represented by taking FCB as the lower undary of the layer, but the difference would usually be small.

On some occasions, the $F1$ and $F2$ layers are distorted in such a way as to oduce a composite layer in which the relation between electron density and ight is not even approximately parabolic. The analysis of records of this type discussed in Paper 1 and it is shown how it can be carried out in terms of dis-butions represented by $N = \alpha(h - h_0)$ and $N = \beta(h - h_0)^2$, and also by assuming parabolic distribution which approaches most closely to that observed.

In considering the significance of the measurements to be discussed in this per, the following points should be noted:

(*a*) The nature of the $(h' - f)$ record depends on the distribution of electrons low the maximum of the $F2$ layer, and it cannot give information about the ectron content above that maximum.

(*b*) The part of the $(h' - f)$ record appropriate to the $F2$ layer can give in-rmation only about that part of the layer in which the electron density is greater an in lower layers.

(*c*) The effect of the earth's magnetic field has been neglected. This neglect is scussed in Paper 1, where it is shown that it is not likely to invalidate deductions out *changes* of n, but the absolute values of n may be in error by 20 to 30 per nt.

3—THE RECORDS USED IN THE ANALYSIS

The selection of data for analysis was determined by the fact that the author d access to a long series of $(h' - f)$ records of ionospheric reflections, made by e Carnegie Institution of Washington at Watheroo (Australia), Huancayo eru), and College (Alaska). It was planned to use these records to make a pre-iinary survey of the total electron content per unit column of the $F2$ layer in ch a way as to demonstrate its variation with time and place. In order to make e survey possible in a limited time, it was decided to select records in the fol-ving way to show up the variations expected with time of day and season, phase the sunspot cycle, and position on the earth.

(*a*) The results for a year of sunspot maximum and a year of sunspot minimum were analysed for each of the three places.

(*b*) In each of the years investigated, two days were analysed in each month.

(*c*) The days were chosen from the five "magnetically quietest" days per month, as determined from international measurements.

(*d*) At two of the places (Watheroo and Huancayo), the months of December and June were analysed for intermediate years to show up variations through the sunspot cycle.

Figure 2*A* shows this selection as planned. For various reasons, records were t available from all three stations at all the times required and the complete

scheme of analysis could not be carried out. The analyses actually made are sho in Figure 2B. The most important difference between the scheme as plan

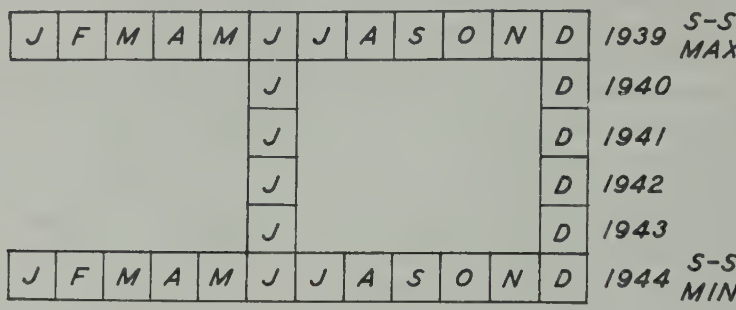

FIG. 2A

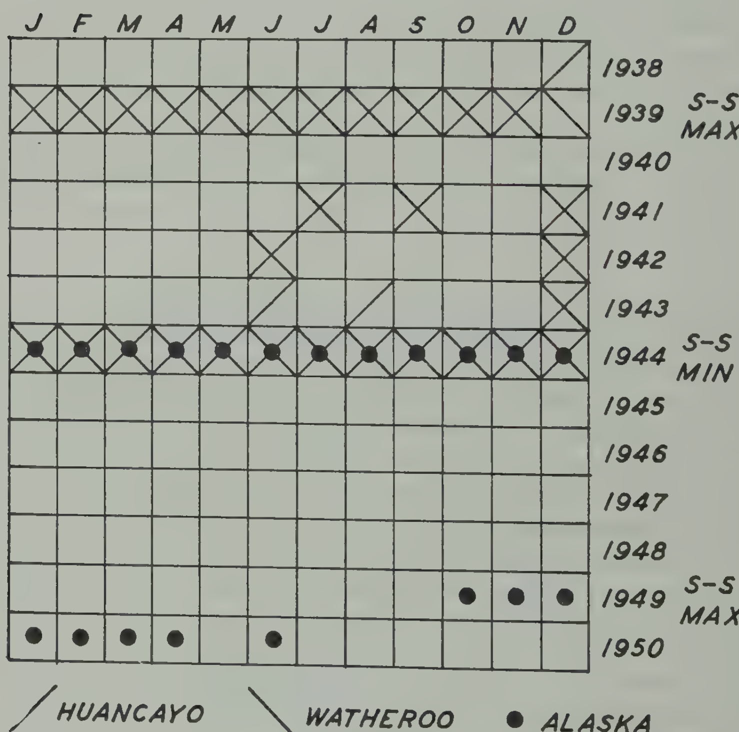

FIG. 2B

Fig. 2—To illustrate the dates of the records which were analysed. Records were chosen from two magnetically quiet days in each of the months indicated. Shows (*A*) the investigation as planned, and (*B*) as actually carried out.

and as carried out is that records were not available from Alaska for the y 1939 of maximum sunspots, and therefore records were used for the year 1949 of maximum sunspots in the next solar cycle.

—THE MAJOR "ANOMALIES" IN THE QUIET-DAY BEHAVIOUR OF THE *F*2 LAYER

In this Section, we shall deal in turn with the major types of "anomaly" of ıe *F*2 layer which are noticeable even on days which are ionospherically and ıagnetically quiet. For each type, we shall first describe and illustrate the anomaly" as exhibited by a study of the maximum electron density N_m , and e shall then show that the behaviour appears more normal when studied in erms of n, the total electron content per unit column.

Before we consider the obvious anomalies, however, it is desirable to discuss ıe day-to-day consistency of the results for magnetically quiet days.

(*a*) *Day-to-day variations*—Use was made of a short series of records made at Vashington, D. C., to examine the day-to-day consistency over a short period. n Washington, in winter, the diurnal variation of N_m is simple and reaches a maxi-ıum near midday. It might therefore be thought that this maximum would behave ı a regular manner. It was found, however, that, even during a period which was omparatively quiet magnetically, the midday maximum values of N_m varied quite onsiderably from day to day. This phenomenon is illustrated in Figure 3*A*, which ıows the midday portion of the $(N_m - t)$ curve for a succession of 13 days. The ıagnetic character figure is included for reference. It is clear that N_m had unusual alues at times of magnetic disturbance, but it is also noticeable that the midday ıaximum of N_m varied from day to day even when the magnetic character figure as small. Figure 3*B* shows the diurnal variation of n on the same days, and it clear that on days which were magnetically quiet the midday maximum values n were approximately the same from day to day, even though there were con-derable variations in the midday maximum values of N_m . It was also found ıroughout the whole of the analysis that the values of n determined from two ıagnetically quiet days in the same month were always closely similar. These ıcts suggest that results of significance can be obtained by measuring values of for only two magnetically quiet days in each month.

If we compare the magnetically quiet days with the disturbed days, we notice ıat the value of n was approximately the same on all occasions, whereas the ılue of N_m assumed unusual values on some disturbed days. Although we have ot, so far, paid much attention to magnetically disturbed occasions, the little e have done seems to support the view that the total electron content is not uch altered during the disturbance, although the distribution of the electrons sometimes profoundly modified.

(*b*) *The diurnal anomaly*—Frequently the variation of N_m throughout the day oes not seem to be related in any simple way to the sun's zenith distance. This fect has been noticed most strikingly at Huancayo, and typical examples are ıown for the first six months of 1939 in Figure 4*A*. Some of these show clearly e well-known minimum near midday, which has sometimes been referred to as e "bite-out." Figure 4*B* shows the variation of n on the same days, and it is ear that the "anomaly" is no longer apparent. It is always found that curves n against time of day show a much more normal behaviour than curves of N_m . ırther examples will be found in later Figures.

(*c*) *The seasonal anomaly*—At places where the diurnal "anomaly" is not

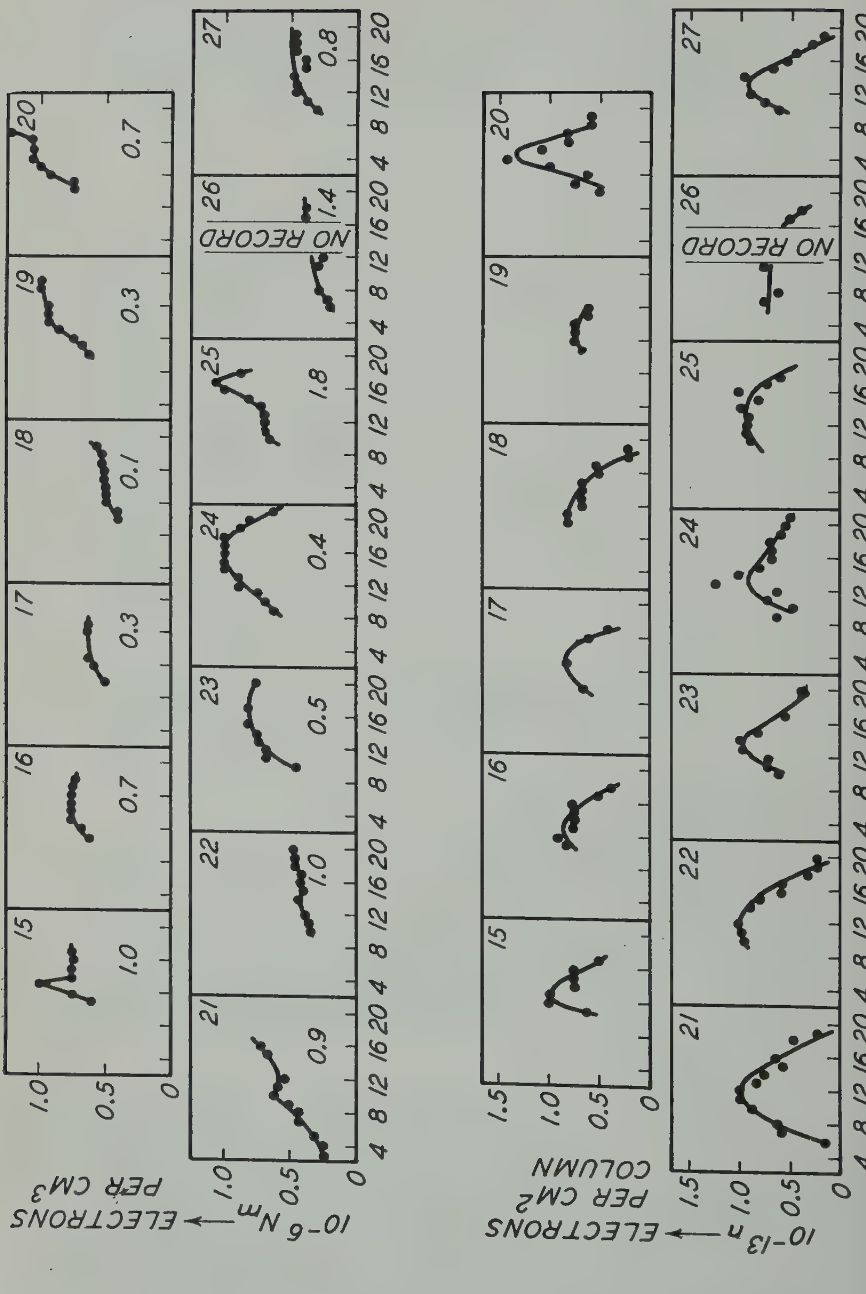

FIG. 3—Diurnal variations of N_m and n deduced from records made at Washington, D.C., on a succession of days in April 1940.

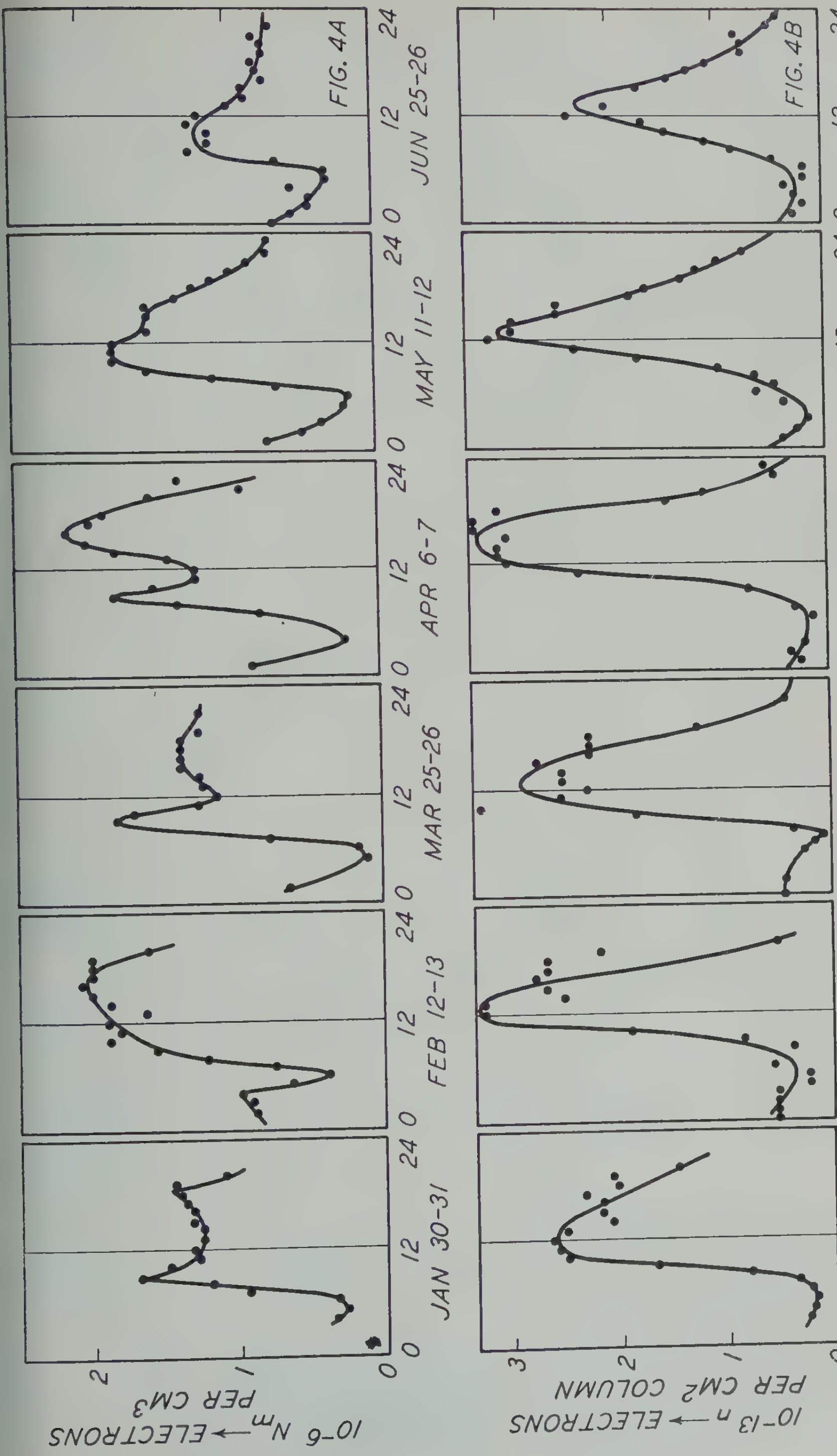

FIG. 4—Diurnal variations of N_m and n deduced from records made at Huancayo in 1939. Each curve corresponds to a record which started at $09^h\,00^m$ on the first date given and ended at $09^h\,00^m$ on the second date. The abscissas represent local time.

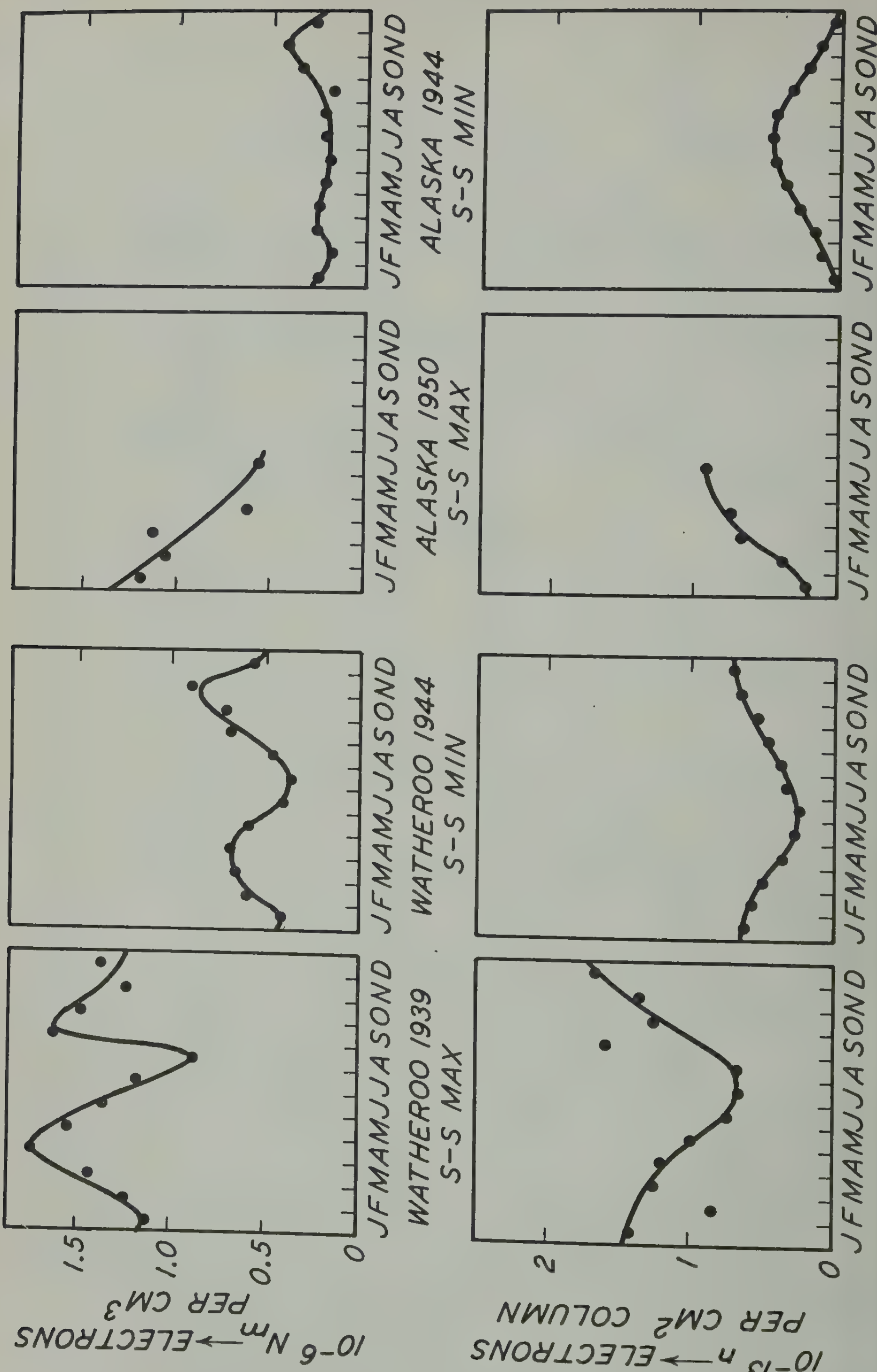

Fig. 5—Midday maximum values of N_m and n deduced from records made at Watheroo and College (Alaska) in

arked, so that N_m has a maximum near midday, it might be expected that this aximum would follow the seasons and be greater in summer than in winter. he observation that the variation of N_m is often not of this type has led to the ecognition of a "seasonal anomaly." This is illustrated in the upper part of igure 5, which shows how the midday maximum value of N_m varied throughout he year at Watheroo and at College (Alaska). The curve for N_m for Alaska in he year 1950 (sunspot maximum) shows the "seasonal anomaly" in a very violent orm, since the magnitude of N_m in January (when the sun barely rose above he horizon) was twice as great as in June (when the sun's zenith angle was 46°). he curve for N_m at Alaska in the year 1944 (sunspot minimum) was also abnormal, ut not in such a striking way. At Watheroo, the curve for N_m shows a double eriodicity both in the years of sunspot maximum and minimum, although the un there is almost overhead in December and the zenith angle increases steadily p to 53° in June.

The annual variation of the midday maximum value of n deduced from the ame set of observations is shown in the lower part of Figure 5. It is seen at once hat the anomalies are removed and the variations are in the expected sense, so hat the smaller the sun's zenith angle, the greater is the number of electrons per nit column.

At Huancayo, the sun's zenith angle does not change very much through the ear and has two maximum values, so that the phenomena are not so striking. hey are best studied later, in Section 5, when we discuss the relation between n nd the sun's zenith angle (χ).

—RELATION BETWEEN TOTAL ELECTRON CONTENT PER UNIT COLUMN (n) AND THE SUN'S ZENITH ANGLE (χ)

Since the total electron content per unit column (n) appears to vary with the un's zenith angle (χ) in a reasonable manner, it is of interest to enquire how early the midday maximum value of n is a single valued function of χ. The value f χ at midday varies from season to season and from place to place, and by taking ll seasons at Watheroo, Huancayo, and Alaska we have available data correponding to all values of χ. In Figure 6, the midday maximum values of n are lotted against χ for these three stations. All the data indicated in Figure 5 are sed in plotting the curves. The results for Huancayo, for the year (1939) of sunpot maximum, are dealt with in the same way, but those for this station in 1944 sunspot minimum) are treated differently, as described in Section 6, and are ndicated by the broken line.

It is clear from Figure 6 that, for places so differently situated as Watheroo nd Alaska, the midday maximum value of n is approximately a single-valued unction of χ, as represented by the straight lines drawn through the points. his relationship is apparent for the years both of maximum and minimum sunpots. It is almost certain that the greater scatter of the points for Watheroo in he year (1939) of sunspot maximum arises because of the difficulty of analysing ome of the records made during that year. The difficult records were of the type escribed in Section 3(c) of Paper 1, and when the analysis was made the best ethod of carrying it out had not been understood.

The results for Huancayo in 1939 also show considerable scatter, again pr ably attributable to the difficulty of analysing some of the curves obtained th If a line is tentatively drawn through the scattered points, it appears to be sim to that for Watheroo and Alaska, and to correspond to values of n appro mately twice as large.

From Figure 6, it is tempting to draw the conclusion that the midday maxim values of n depend mainly on the value of χ, for all places on the earth, but

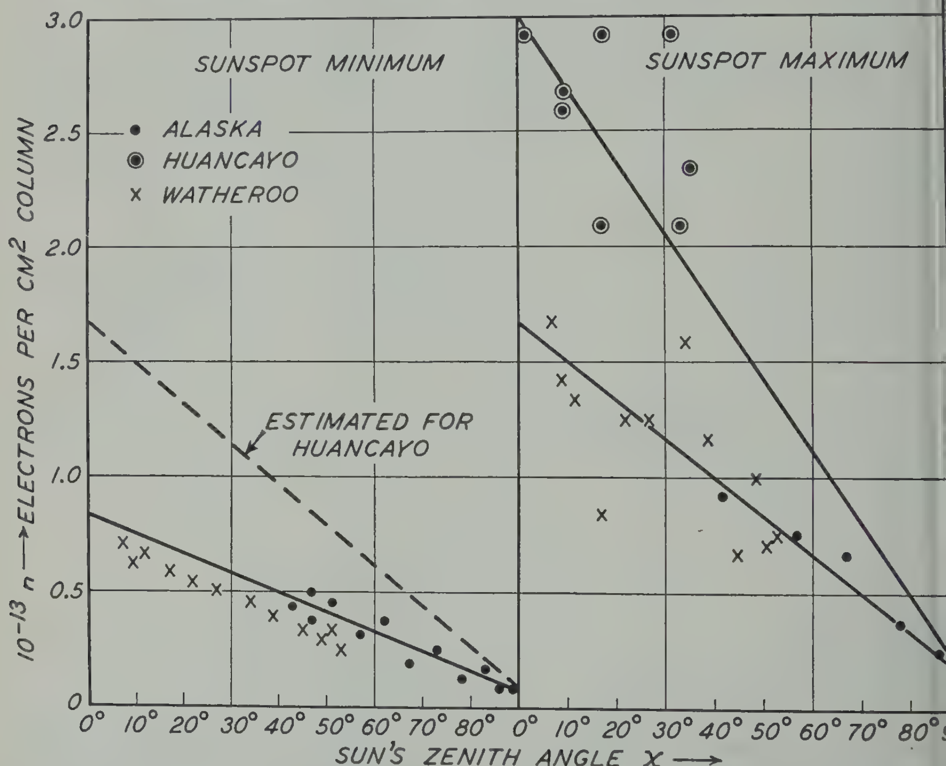

Fig. 6—Midday maximum values of n plotted as a function of χ for three stations in years maximum and minimum sunspots. The significance of the broken line on the left-hand part of Figure is explained in Section 6.

course before this conclusion can properly be drawn it will be necessary to anal results from several other observing stations. In case further analyses should sh agreement with these results, it is of interest to consider them in more detail.

First, we note that the total rate at which electrons are produced, in a u column of the atmosphere, by radiation absorbed according to a mass-absorpt law, is proportional to cos χ even if the scale height (H) of the atmosphere chan with height; see Chapman [4]. The ratio of the number of electrons produced ab and below the level of maximum production depends on how H changes w height.

The number of electrons (n) existing at any one time in a unit column up the height of the maximum depends not only on the rate of production but a

n the rate of disappearance by attachment or recombination, and the coefficient etermining this rate may be different in different parts of the world and at different eights. Hence, even though the rate of production of electrons per unit column ould be expected to depend only on χ, we would not necessarily expect the relation etween χ and n to be simple. In particular, it might be different if we consider rst one place at different seasons, and next different places at the same season. he results shown in Figure 6 show however that n, as observed at Alaska and Vatheroo, is determined uniquely by the value of χ; it therefore appears that the omplicating factors mentioned above are of secondary importance when these wo places are compared. The fact that the values for Huancayo are about twice oo great could be simply explained in terms of one or more of the complications ientioned.

The curves of Figure 6 indicate that under similar conditions the total number n) per unit column up to the height of the maximum changes by a factor of two rough the sunspot cycle. If there were no complicating factors, this would imply iat during the sunspot cycle the rate of production (q) of electrons, and hence ie intensity of the ionising radiation, varied by a factor of two if an attachment iw ($q = \beta N$ at the midday maximum) were appropriate at each level, and by a ictor of four if a recombination law ($q = \alpha N^2$) were appropriate. It may be emarked that, from measurements of N_m, the radiation responsible for the ionisa- on of the E and $F1$ layers is thought [5] to change by a factor of 2.3.

6—THE ANOMALIES AT HUANCAYO

It is well known that the ionosphere above Huancayo is anomalous in several espects. It has here been shown that, by considering the quantity n instead of N_m, it is possible to remove most of these anomalies in the year (1939) of sunspot aximum. When, however, the year (1944) of sunspot minimum is considered, an iteresting phenomenon is encountered. During the morning hours, the high- equency end of the $(h' - f)$ record shows a "spur" which moves to higher fre- uencies and finally, sometime before noon, disappears at the top of the trace nd is no longer seen. The sequence of events is sketched in Figure 7. Although iis "spur" is properly allowed for in the calculation of n, the diurnal curves iowing the variation of n are found to have an irregular form, of the type shown Figure 8. This Figure presents results for the first six months of 1944 and, on ome of the curves, the time at which the "spur" disappeared is marked with an rrow. A comparison of the diurnal variations of Figure 8 (for 1944) with those Figure 4B (for 1939) suggests that the curves for 1944 would have followed omething like the dotted lines but that, at the time marked by the arrow, some- iing happened which altered the run of events. It is as though, after the "spur" ad disappeared from the record, there were too few electrons below the level of aximum electron density. The rising "spur" represents a subsidiary layer of ectrons which moved up during the morning hours, and an obvious suggestion that, after the "spur" had disappeared from view, the electrons which had reviously been produced in this subsidiary layer were produced at levels above e maximum of the main layer, so that they could not be detected, with the sult that the measured number of electrons was too small.

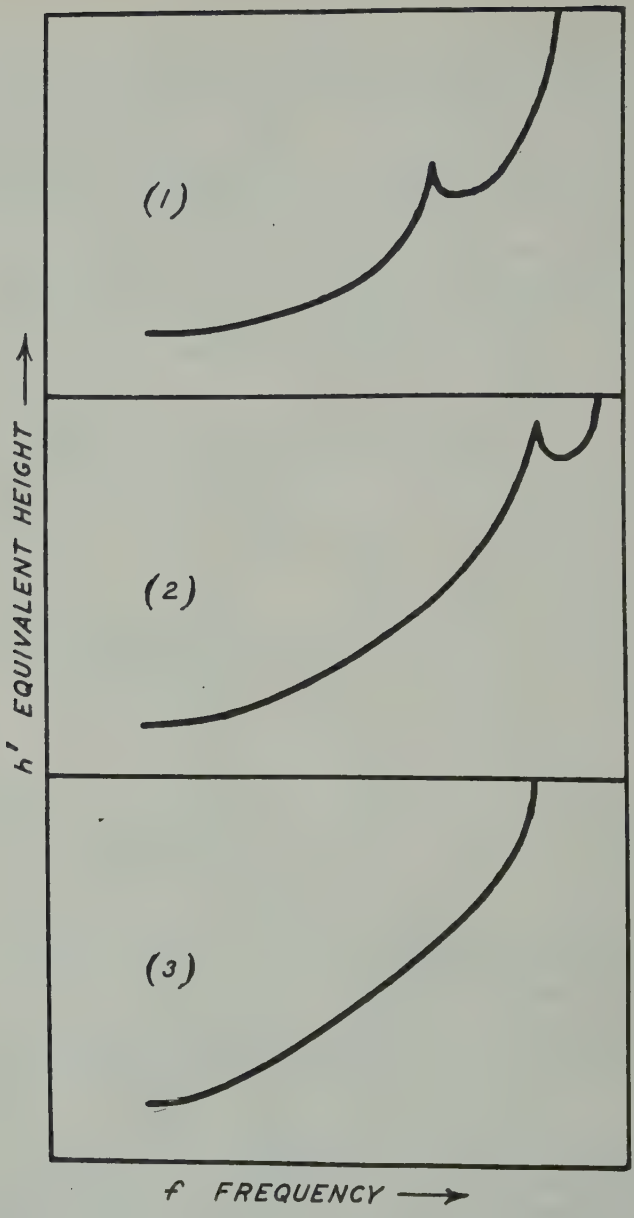

Fig. 7—Figures 1, 2, and 3 are sketches of the successive forms assumed by the $(h' - f)$ curves in the mornings in a year of minimum sunspots at Huancayo.

It is interesting to notice that, although the diurnal curves for N_m sho midday "bite-out" at all epochs of the sunspot cycle, yet when n is plotted "bite-out" is removed in the year of sunspot maximum, but is not remove the year of sunspot minimum. The suggestion here made is that the "bite-o is always caused by changes in the distribution of the electrons; in the year

sunspot maximum this distribution is such that the "bite-out" is not evident if the total electron content (n) below the level of the maximum is considered, but in years of sunspot minimum it occurs even in curves of n, because of a radical redistribution of the proportion of electrons above and below the maximum. It is suggested that in curves showing the total number of electrons from top to bottom of the ionosphere there would never be any "bite-out." Of course, such curves cannot be plotted from ordinary ionospheric data.

The records from Huancayo for the year 1944 all show the phenomenon illustrated in Figures 7 and 8. The time of day at which the results departed from the

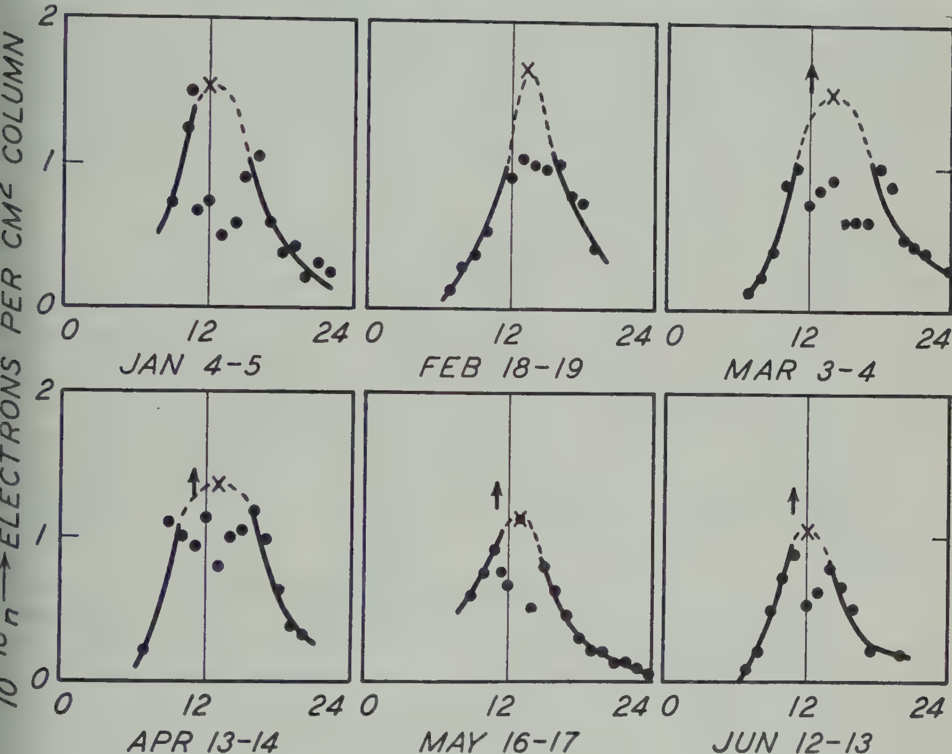

FIG. 8—The quantity $10^{-13}n$, plotted against local time from six months of results at Huancayo in the year 1944 of sunspot minimum. The dotted parts of the curves have been sketched so as to pass through their maxima at the points marked by the crosses which have been inserted to correspond to the broken line of Figure 6, as explained in the text. Each curve corresponds to a record which started at $09^h\ 00^m$ on the first date given and ended at $09^h\ 00^m$ on the second date.

smoothly rising part of the curve (Fig. 8) always coincided with the time at which the "spur" (Fig. 7) disappeared in the morning, but in the afternoon there was no noticeable change in the $(h' - f)$ curve when the n curve started to fall smoothly. In 1939, no diurnal curves of the type shown in Figure 8 were encountered. As the sunspot cycle was followed for the month of December from 1939 to 1944, the "abnormal" behaviour was found to occur first in 1943.

The $(h' - f)$ curves of Figure 7 are similar to those described for 1939 by McNish [6], who found that the phenomenon of the "spur" was related to lunar

time and represented an upward-moving layer. The relation between his c servations and ours is not clear and needs further investigation. For instance, contradistinction to his observations, the phenomenon which we have noticed c not occur in 1939, and in 1944 occurred only in the morning.

It is interesting to follow up the suggestion that, even in 1944, the total numb of electrons per unit column reached a maximum near midday, and that tl maximum behaved like the one in 1939, but that some of the electrons were r observed around midday because they were then above the maximum of the lay On this assumption, the broken line is drawn in Figure 6 to represent the midd maximum value of n which would be expected for different values of χ if the curv for 1944 were similar to those for 1939 but with the scale of n halved. The a propriate values are taken from this curve and inserted as the midday value the dotted curves of Figure 8, and they appear to fit reasonably on to the extr

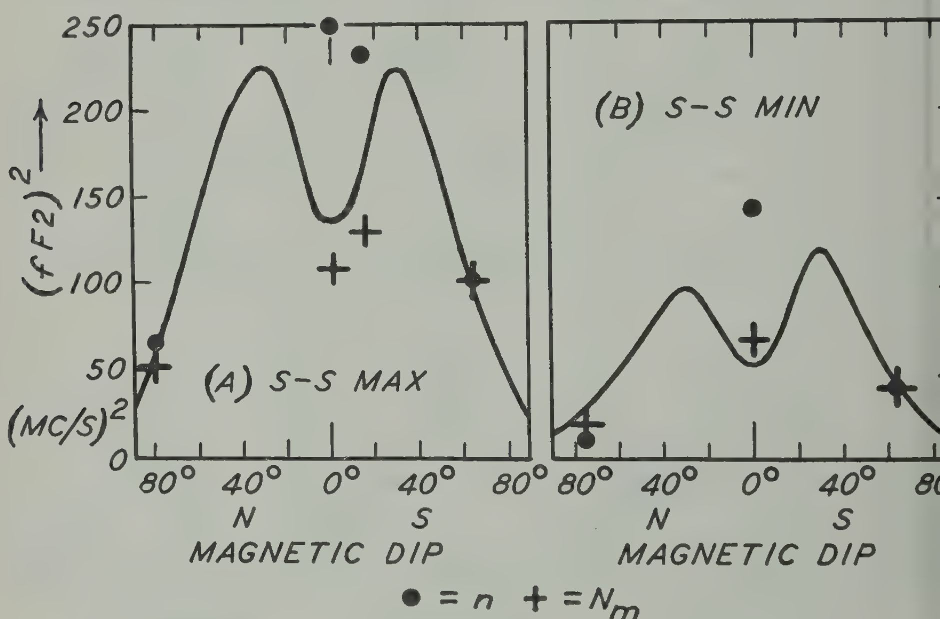

Fig. 9—To illustrate the "geomagnetic" anomaly. The curves are taken from Figures 5 and (Appleton's paper [7] with the ordinates squared. The crosses (N_m) and the dots (n) represent magnitudes which we have found at Watheroo (dip 64° S), Huancayo (dip 4° N), and Ala (dip 80° N) in the equinoxial month of March. The scales have been adjusted so that the points Watheroo fall on the curves.

polated parts of the smooth morning and afternoon curves. A similar fit v obtained with the curves for the other days in 1944.

It is well known that, if midday values of N_m are plotted against magne dip at the equinox, the curve shows a minimum near the magnetic equat Appleton [7] has summarised present-day knowledge of this phenomenon in cur (his Figs. 5 and 6) which show the midday maximum values of $F2$ measured the equinoxes plotted against the magnetic dip. The curves of our Figures and 9B are copies from his curves, with the ordinates squared so as to be p

ortional to N_m . The magnitudes of N_m and n, determined from our records nade at the three stations in the month of March, are superimposed on the curves, he scale having been adjusted so that the points for Watheroo lie on the curves. t is at once clear that the crosses representing N_m fit well on to Appleton's curves vhich show the geomagnetic anomaly, but that the dots, representing n, look as hough they might fit on to a curve with a single maximum, and without any nomaly. Of course, this question cannot be settled by considering observations rom only three places and it would be of the greatest interest to plot a curve for determined at several other locations. Since it would be necessary to consider nly two or three magnetically quiet days, in March, in two years, the work would ot be onerous. If it proved that a curve of n against magnetic dip had no minimum ear the equator, the "geomagnetic anomaly" would have to be explained in erms of some anomaly in the height distribution of the electrons near the geo-agnetic equator. In considering this matter, it must be remembered that the oints representing n for sunspot-maximum years in Figure 9 are derived directly rom the measured height-distributions, but those for sunspot-minimum years volve a guess, supported only by indirect evidence, that an undue proportion f the electrons are situated above the maximum of the layer at noon in those years.

Note added in proof (October 1951): Through the kind offices of the Director of adio Research, D.S.I.R., London (Dr. Smith-Rose), the ionospheric records ade in 1950 at Singapore have been made available. Two magnetically quiet ays in March were chosen and the values of N_m and n deduced for midday. The oints are shown in Figure 9*A*, along with those of other observatories for years f sunspot maximum. It appears that these results support the conclusions men-oned in the paper. I am grateful to Dr. Smith-Rose for allowing me to quote ese results.

7—THE DIURNAL VARIATION OF n

The curves of Figure 4*B* indicate the diurnal variation of n at Huancayo in e year (1939) of sunspot maximum. Figure 10 shows similar curves for four fferent months at Watheroo and Alaska in years of sunspot maximum and nspot minimum. All curves showing the diurnal variations were of this type, cept those for Huancayo in the year 1944 of sunspot minimum, which have ready been discussed. Since it is quite clear that the shapes of the curves are nsiderably affected by contraction and expansion of the layer, it does not appear ofitable to use them to investigate processes of the production and loss of ectrons. The full data from which the curves are derived should, however, con-in enough information for these processes to be investigated at each level in e atmosphere, and that investigation is in hand.

8—THE DISTRIBUTION OF THE ELECTRONS IN THE *F*2 LAYER

Although the main purpose of this paper is to suggest that the total electron ntent per unit column of the *F*2 layer behaves in a regular and normal manner t least for the stations considered), the analysis undertaken has shown up some teresting facts about the way in which these electrons are distributed in the

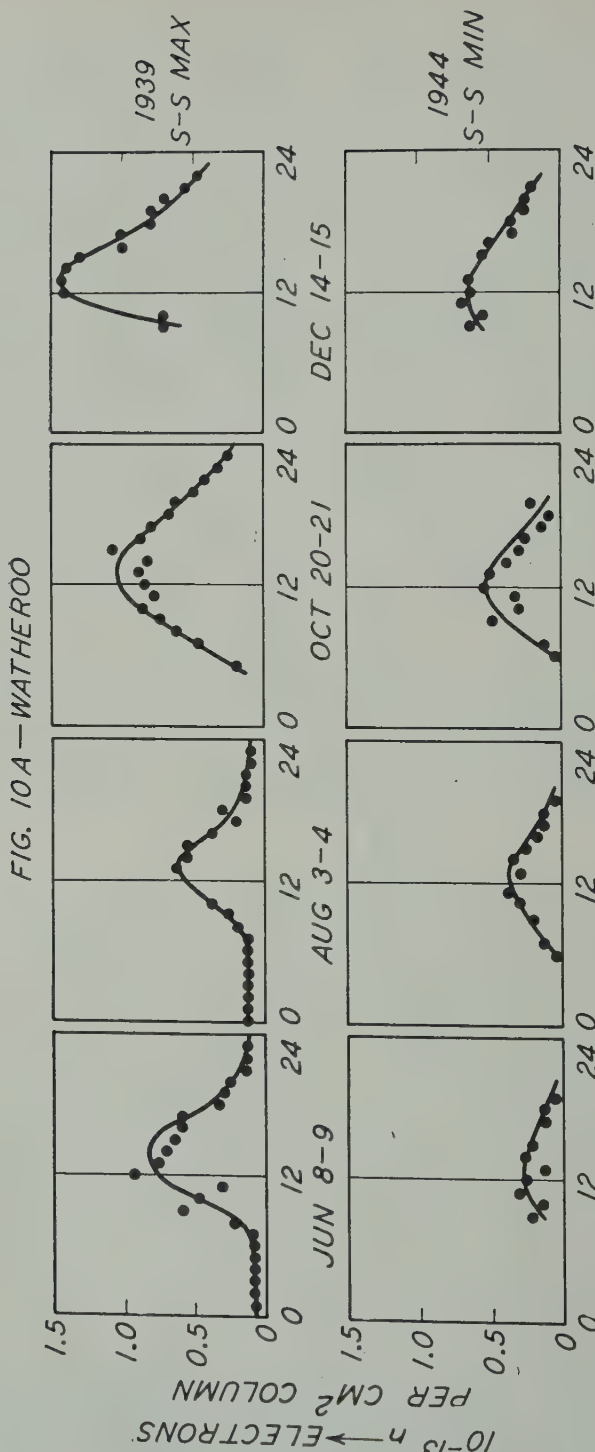

FIG. 10A—WATHEROO

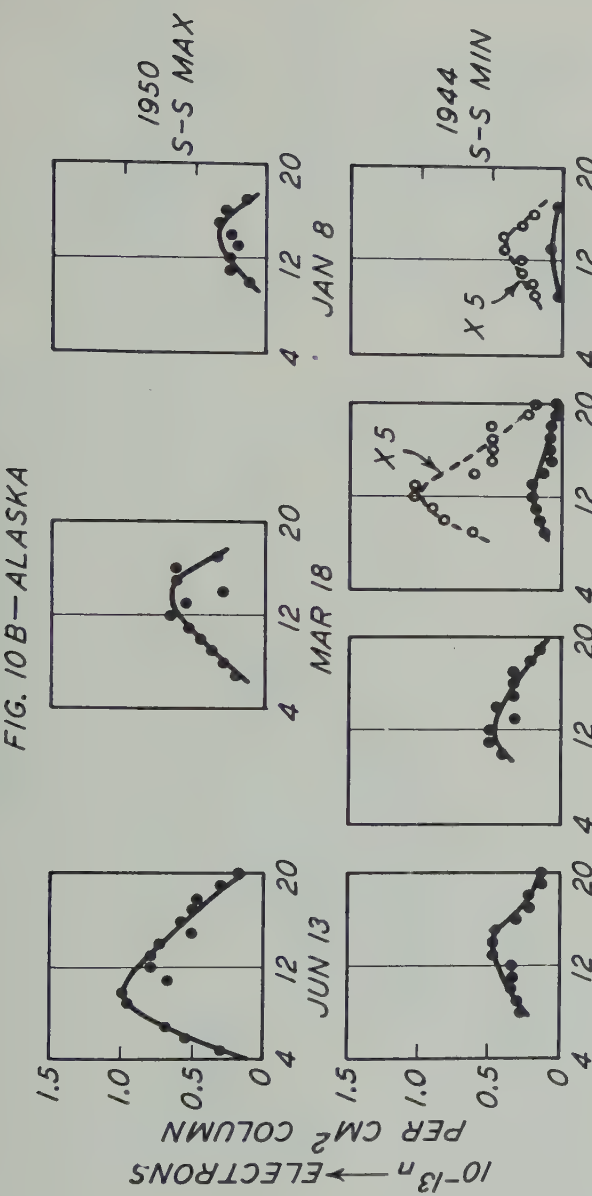

Fig. 10—To illustrate the type of curve obtained when n is plotted against local time at Watheroo and Alaska in years of sunspot maximum and minimum. The results for Alaska in October and December 1944 are also shown on a scale enlarged five times.

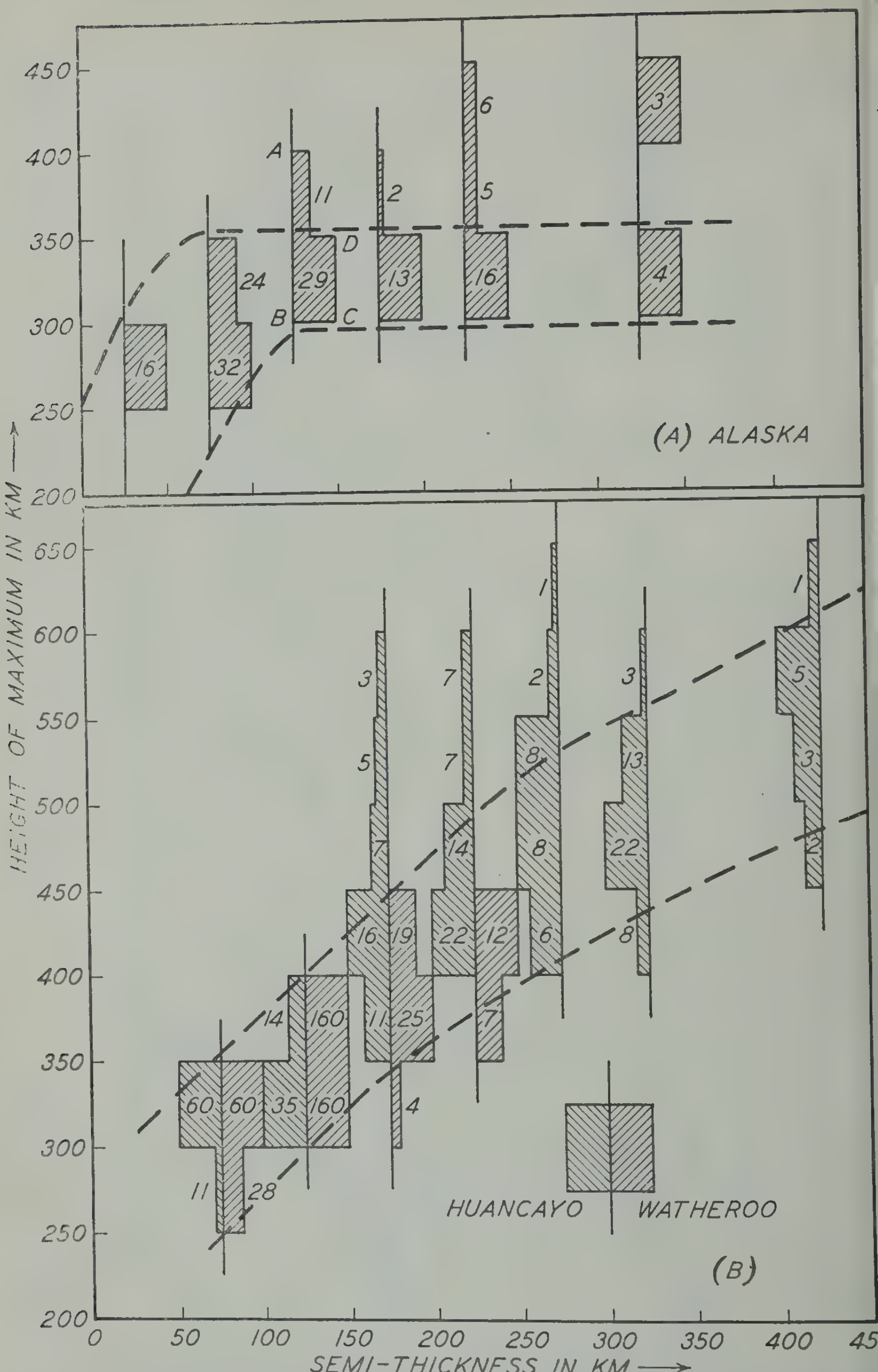

FIG. 11—Histograms to show the statistical relation between the semi-thickness of the $F2$ layer and the height of its maximum. The semi-thickness corresponds to the distance AD in Figure 1.

atmosphere. Some of these facts are noted shortly below; it is hoped to consider them in more detail on another occasion.

(*i*) The $(N - h)$ curve relating electron density (N) to height (h) in the $F1$ layer is always close to a parabola, with a semi-thickness of about 100 km and with its maximum at a height of about 200 km. The upper part of the parabola may be obscured by the $F2$ layer.

(*ii*) Except at Huancayo, the $(N - h)$ curve for the $F2$ layer is close to a parabola.

(*iii*) However distorted the $(N - h)$ curve may have been during the day, it rapidly assumes an accurately parabolic form near sunset and thereafter during the night. This phenomenon must have some important significance.

It is interesting to enquire whether there is any simple relation between the thickness of the $F2$ layer and the height at which the maximum electron density occurs. The results for Alaska are shown in Figure 11*A*. In this Figure, for each interval of semi-thickness (T), a histogram is constructed to show the number of occasions when the height of the maximum fell within a given range of heights. For example, for semi-thicknesses between 100 and 150 km, the histogram $ABCD$ indicates, when viewed on its side with AB as the base line, that the height of the maximum fell between 300 and 350 km on a number of occasions represented by BC, and between 350 and 400 km on a number of occasions represented by AD. All the histograms are normalised, so that the heights of their maximum portions (for example, BC) are equal. The number of readings contributing to each part of each histogram is indicated by a figure. It is seen that the majority of the observations lie between the two broken lines.

A similar set of histograms has been drawn for the observations at Watheroo and Huancayo, and they are shown together in Figure 11*B*. The results for these two stations agree in showing that most observations lie between the two broken lines, and that the thicker layers have their maxima higher. It might be thought that this result is inevitable if the lower edge of the layer is to lie above the ground, but it should be remembered that the parabola only represents the electron distribution which is "visible" past the penetration frequency of the $F1$, or E, layer.

A comparison of Figures 11*A* and 11*B* seems to show a difference between the behaviour at Alaska and that at Watheroo and Huancayo.

If we accept the curves of Figures 6 and 11 as summarising the results of this paper, we notice that a determination of the midday maximum value of N_m alone can be used to deduce the vertical electron distribution in the ionosphere at that time to a first order of approximation. Thus, Figure 6 tells us the value of n for the (known) value of χ at the time; the relation $n = 2/3(N_m T)$ then gives us the semi-thickness (T) and the graphs of Figure 11 then provide an approximate value for the height h_m of the maximum. Once these quantities N_m, T, and h_m are known, it is possible to calculate maximum usable frequencies. It is possible that the relations here mentioned might be useful in ionospheric forecasting.

Until such time as more analyses of the type here described have been made, it might be profitable to estimate the distribution of T and h_m over the earth on

the present hypothesis and use these estimates to test theories of the ionosphe
such as those proposed by Martyn [8].

9—COMPARISON WITH OTHER RESULTS

Although the results of this paper seem to lead to some simple and clear-c conclusions, they are unfortunately in conflict with the results of at least two otl sets of workers. White and Wachtel [9], of the National Bureau of Standar computed electron densities for Washington for the summer, winter, and equin of 1945 at noon and midnight by the method of Booker and Seaton, which equivalent to what has been done in this paper. They found that the total numb of electrons in the regions E, $F1$, and $F2$ per unit column below the maximum $F2$ was approximately the same in the three seasons, although χ varied fro 16° to 62°. Reference to our Figure 6 shows that we should have expected t number to vary by a factor of two. If the contribution of the E and $F1$ layers subtracted from the results of White and Wachtel, in an attempt to compa with our results for the $F2$ layer alone, the agreement with us is even worse.

Alpert [10] calculated the thickness of the layer by performing a numeri integration of the type discussed by Rydbeck [11]. He analysed results from Russian station for June and July and November and December 1945, and ca to the conclusion that the seasonal anomaly was not removed when the to electron content was considered.

It is difficult to explain these two cases of clear disagreement with our co clusions. The existence of the disagreement makes it all the more important th analyses should be made for other places and by other workers.

10—CONCLUSIONS AND INDICATION OF FURTHER DESIRABLE INVESTIGATIO

For the three stations considered (Watheroo, Huancayo, and College, Alask it is concluded that the number of electrons per unit column in the $F2$ layer bel the maximum of the layer behaves in a fairly regular manner, related to the su zenith angle as shown in Figure 6. The results for Huancayo are anomalou small in the year of sunspot minimum and the anomaly is related to peculiarit in the $(h' - f)$ curve, which suggests that the missing electrons are produc above the maximum of the layer where they would not be observable. If th deductions, made from three stations well separated on the earth, are confirm by the analysis of results from other stations, the known peculiar behaviour of $F2$ layer can be referred to peculiarities in the upper atmosphere which cause electrons to be distributed in layers of different thickness at different times a places, as has often been suggested, first by Appleton and Hulburt [1,2]. T methods of analysis which have been used here, although somewhat crude, sufficiently good to enable these peculiarities of the upper atmosphere to be vestigated in considerable detail. It seems important, at the present stage of knowledge, to have approximate data from several places and at several tim rather than to have more accurate data for only a few times and a few places.

It is to be hoped that methods like the ones described here will be used (a) make a similar analysis for other stations, to find whether the generalisati

tentatively made in this paper are valid for a greater number of stations; and (*b*) to make analyses about the way in which the electron distribution varies with time and place, so that theories of the ionosphere such as those recently advanced by Martyn [8] can be extended in the light of more data.

11—ACKNOWLEDGMENTS

This work was done while the author was working at the Department of Terrestrial Magnetism of the Carnegie Institution of Washington as a guest investigator. He wishes to thank the Institution for their kindness and generosity in making his visit possible and also in putting all their records at his disposal. The records existing at the Department provide a valuable series of most beautiful records, all to the same scale, and are ideal for analysis of the kind discussed here. All ionospheric workers are indebted to those who planned the taking of these long runs of records, made the apparatus, and supervised its working, and amongst these the present author was particularly fortunate in having the help and advice of L. V. Berkner and H. W. Wells, to whom he is much indebted. He is also indebted to the University of Cambridge for granting him leave of absence to go to America.

References

[1] E. V. Appleton and R. Naismith, Proc. R. Soc., **150**, 685 (1935); and E. V. Appleton, Phys. Rev., **47**, 89 (1935).
[2] E. O. Hulburt, Phys. Rev., **46**, 822 (1934).
[3] J. A. Ratcliffe, J. Geophys. Res., **56**, 463–485 (1951). [Here called Paper 1.]
[4] S. Chapman, Proc. Phys. Soc. (London), **43**, 26 (1931).
[5] E. V. Appleton and R. Naismith, Phil. Mag., **27**, 144 (1939).
[6] A. G. McNish, Proc. Conf. Ionospheric Physics, Pennsylvania State College, p. 10CC (1950).
[7] E. V. Appleton, J. Atmos. Terr. Phys., **1**, 106 (1950).
[8] D. F. Martyn, Proc. R. Soc., **189**, 241 (1947); **190**, 273 (1947); **194**, 429 (1948); and **194**, 445 (1948).
[9] G. R. White and I. S. Wachtel, J. Geophys. Res., **54**, 239 (1949).
[10] Ya. L. Alpert, J. Exp. Theor. Phys., USSR, **18**, 995 (1948).
[11] O. E. H. Rydbeck, Trans. Chalmers Univ., Gothenburg, No. 3 (1942); and Phil. Mag., **30**, 282 (1940).

Journal of Geophysical Research Volume 56, No. 4 December, 1951

THE MEASUREMENT OF STRATOSPHERIC DENSITY DISTRIBUTION WITH THE SEARCHLIGHT TECHNIQUE

By Louis Elterman

Geophysics Research Division,
Air Force Cambridge Research Center,
Cambridge, Massachusetts

(Received June 25, 1951)

ABSTRACT

An investigation of light scattering from a beam projected into the atmosphere over New Mexico has been made by means of the searchlight technique. The beam intensity is modulated by a shutter mechanism fronting the searchlight in order to differentiate the scattered light from the light of the night sky. A 60-inch parabolic mirror and photo-multiplier tube mounted at its focus comprise the sensing device. A narrow-band tunable amplifier then selects the desired signal component from the photo-multiplier output. Absolute values of atmospheric densities were obtained by assuming Rayleigh scattering and matching the measured response at 15 km with the densities obtained from radiosonde measurements at that height. Eight vertical density-distributions to 61.8 km were so determined. They are in good agreement with the Rand distribution for a model atmosphere. A seasonal trend for densities at high altitudes is evident.

1—INTRODUCTION

The measurement of the light scattered from a searchlight beam provides a convenient method for studying some of the properties of the upper atmosphere. The amount of scattered light, as described by Rayleigh, essentially is a function of the molecular density in the region above the tropopause. Therefore, information concerning the density distribution can be derived with the use of this technique. Historically, this searchlight probing technique was conceived on an ambitious scale in 1930 by E. H. Synge [see 1 of "References" at end of paper], who proposed concentrating several hundred high-intensity beams on a region in the atmosphere so that the intensity of the volume of intersection would exceed the intensity of the light of the night sky at great altitudes. This proposal was never undertaken, probably due to the difficulties associated with so vast an enterprise. In 1935, M. A. Tuve and others [2] described a method of attaining great heights

by modulating the searchlight beam, thus permitting frequency discrimination the scattered light from that of the night sky. This requires a photo-tube f detection, and a resonant amplifier for selecting the modulating frequency.

The experiment performed by Hulbert [3] in 1937 is significant, and is the fir instance of light-scattering measurement from a beam in the region beyond th tropopause. The method used was that of photographing the beam, rather tha the modulating technique just mentioned. The theoretical brightness of the bea was calculated and compared to the measured brightness for various altitudes u to 22 km. The results are expressed as a ratio of particle scattering as compare to that due to pure air. Non-Rayleigh scattering was evidenced below 11 km.

In 1939, Johnson [4] and his co-workers, following the proposal of M. A. Tuv modulated the beam with a shutter rotating at 10 cycles per second. Scatterin to a height of 25 km was measured with good agreement between theory and ex periment above 8 km. The discrepancies below 8 km were attributed to non Rayleigh scattering.

The light-scattering measurements to be described were conducted in th vicinity of Albuquerque, New Mexico. The use of a 60-inch light-collecting mirro a wide-angle photo-multiplier tube, a 20.5-km base-line between sights, a selectiv amplifier having a 0.6-cycle band-width are some factors which permitted measure ments to an altitude of 61.8 km. The high altitude of the sites and the dry a mosphere of New Mexico are further contributing factors.*

2—THEORETICAL CONSIDERATIONS

(2.1) *Rayleigh scattering from a searchlight beam*—Figure 1 has been drawn present the searchlight geometry. The transmitting mirror T has a divergence and its position is fixed at ϕ_T in elevation. The beam is in line with the receivir mirror R which varies through the angle ϕ_R as the beam is scanned. Both mirro are identical. The scattering volume is determined by the intersection of th beam and the field. Since the divergence is small, the opposing extremities of th scattering volume are very nearly equal, both angularly and in length. The sca tered light from an element of the beam will be accepted through the cone or sol angle (steradians). If the beam length which is being scanned is L and the a ceptance angle ω, then according to Rayleigh the amount of light received angle β is

$$I_{S\lambda} = I_{O\lambda} \frac{2\pi^2(\mu - 1)^2(1 + \cos^2 \beta)}{N\lambda^4} L\omega \ldots\ldots\ldots\ldots\ldots\ldots (\ $$

where

$I_{O\lambda}$ = total energy at a given wave-length incident on a plane normal to the axis of the beam

μ = index of refraction of the medium

*For a full discussion of instrumentation, as well as other phases of this experiment, refer Geophysical Research Paper No. 9, "Measurement of stratospheric density distribution with t searchlight technique," scheduled for publication January 1952 by Geophysics Research Divisio Air Force Cambridge Research Center, Cambridge, Massachusetts.

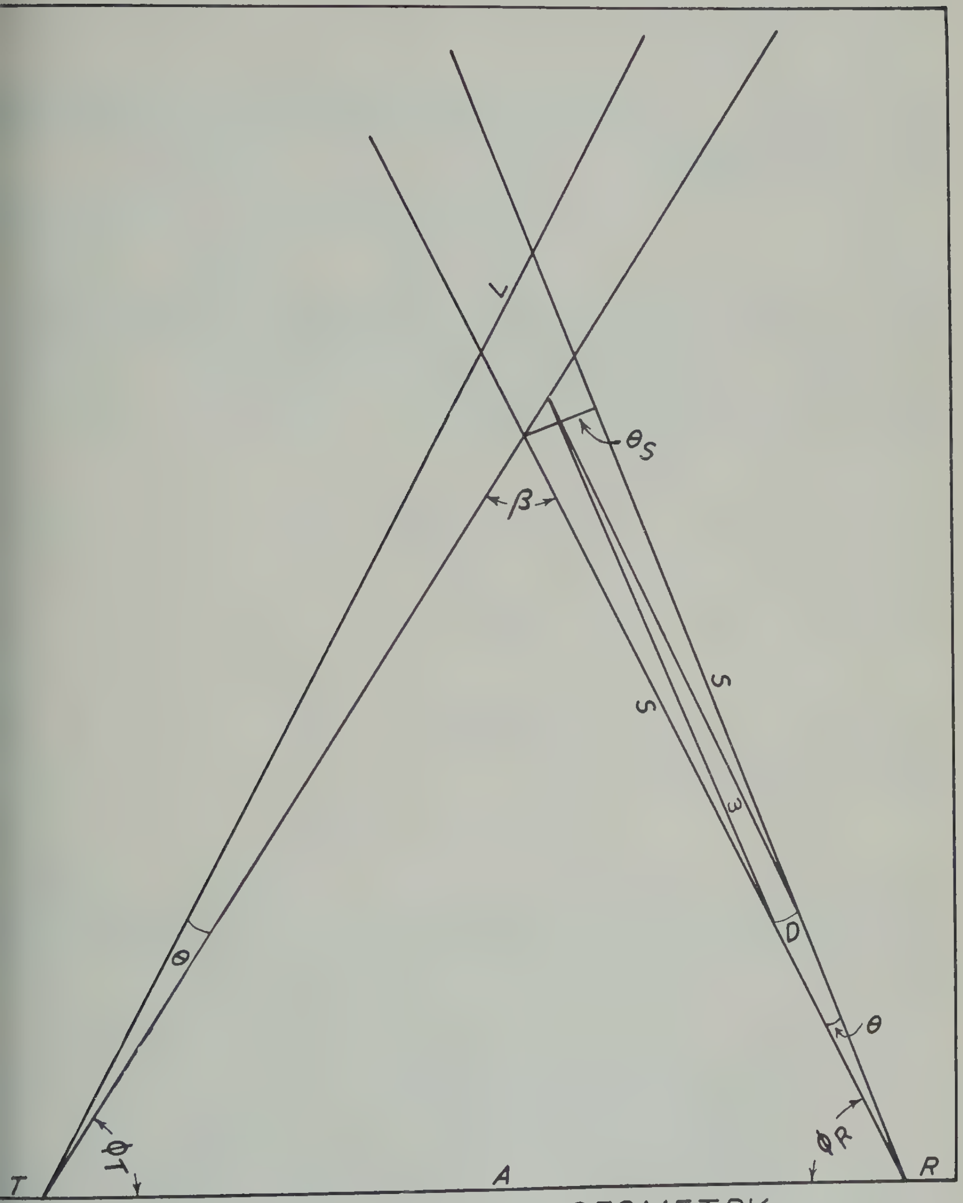

FIG. 1—SEARCHLIGHT GEOMETRY

β = angle of scatter
N = molecular density 1/cm^3
λ = wave-length of light in cm

Applying Cabannes correction for depolarization, for air, $\mu - 1 = \alpha N$, where
is very nearly constant between 3000 and 7000 Å and has the value 1.08 $\times$ 10^{-}
then equation (1) becomes

$$I_{s\lambda} = I_{o\lambda} \frac{2\pi^2\alpha^2 N(1 + \cos^2 \beta)}{\lambda^4} L\omega \ldots\ldots\ldots\ldots\ldots\ldots (\,$$

It should be noted that as the various portions of the beam are scanned, th
product $L\omega$ remains constant. This is evident from Figure 1, where θ and D a
the divergence and diameter, respectively, of the receiving mirror, and S is th
distance between R and the scattering volume (as determined by the intersectio
of the optical axis of the mirrors). Neglecting the curvature of R, and with A
the base-line between the sites

$$L\omega = \frac{\theta S}{\sin \beta} \cdot \frac{\pi D^2}{4S^2} \ldots\ldots\ldots\ldots\ldots\ldots\ldots\ldots (\,$$

$$\sin \beta = \frac{A}{S} \sin \phi_T$$

$$\therefore L\omega = \frac{\pi D^2 \theta}{4A \sin \phi_T} = \text{constant} \ldots\ldots\ldots\ldots\ldots\ldots (\,$$

Equation (2) then can take the form

$$I_{s\lambda} = K_1 I_{o\lambda} N \frac{(1 + \cos^2 \beta)}{\lambda^4} \ldots\ldots\ldots\ldots\ldots\ldots (\,$$

It has been shown by Sinclair [5] that Rayleigh was in error when developing t
theory from plane polarized to unpolarized light, so that the Rayleigh formu
for the angular distribution of scattered light gives results which are too great
a factor of two. This correction is absorbed in K_1 of equation (5).

(2.2) *Transmission losses*—In this application, transmission losses refer to t
attenuation of energy in the beam, along the path from the source to the volu
in the atmosphere from which the scattered light is measured. There are thr
effects which contribute to this attenuation. The upper atmosphere is responsi
for losses due to molecular scattering only. In the lower atmosphere, the loss
are caused by molecular scattering, scattering by particles larger than one-ten
the wave-length of light, and by absorption. The transmission losses (for a giv
wave-length) of a beam passing through a layer in the atmosphere is, to a fi
approximation

$$\text{Percentage loss} = 100\sigma\Delta h \ldots\ldots\ldots\ldots\ldots\ldots$$

where

$$\sigma = \frac{32\pi^3\alpha^2 N}{3\lambda^4} \ldots\ldots\ldots\ldots\ldots\ldots$$

is the scattering coefficient. The layer thickness is Δh and N is taken at the midpoint of the layer.

It is difficult to calculate the losses in the lower atmosphere, since in this region the transmission characteristics are affected by such factors as industrial haze, dust, and moisture, and these factors in turn vary with geographical location, season of the year, and altitude. Near industrial areas, diurnal transmission-changes may be expected. General Electric Company searchlight engineers [6] estimate the losses to be about 5 per cent per kilometer for a very clear atmosphere. Measurements conducted in England during the war showed that a transmission

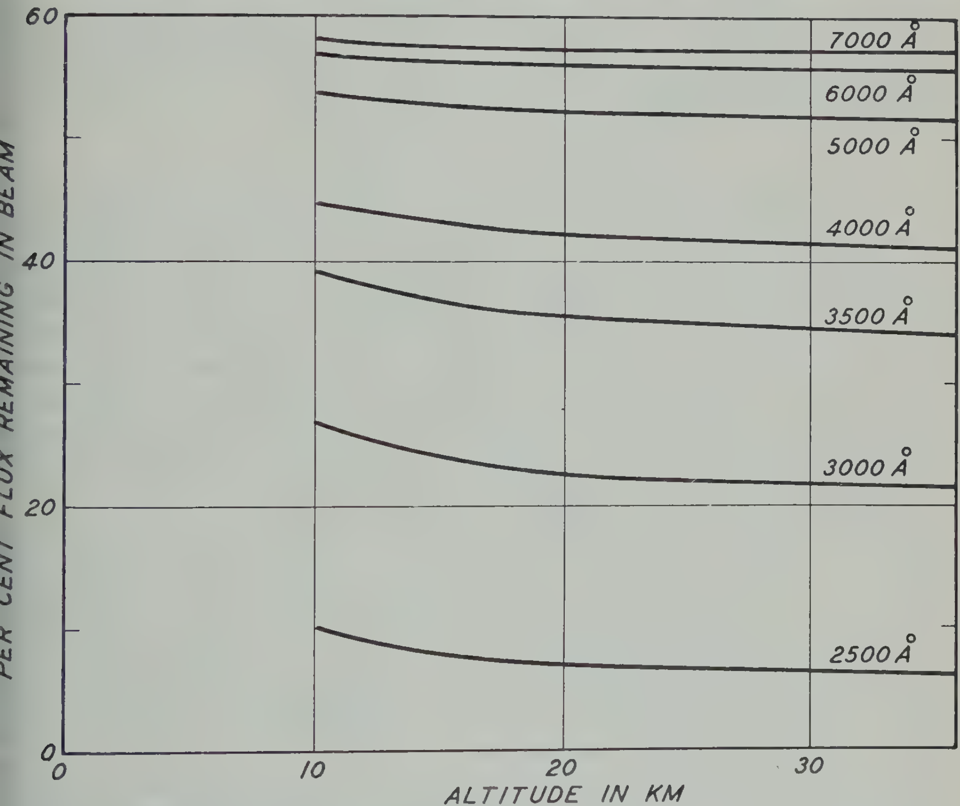

FIG. 2—ENERGY IN BEAM AFTER PARTICLE AND MOLECULAR TRANSMISSION LOSSES

loss of 10 per cent per kilometer can be expected in clear air to an altitude of 10 km. Since the measurements to be described were conducted in the dry atmosphere of New Mexico, away from industrial areas, and since the searchlight was located at an altitude of 7,700 feet, a clear atmosphere can be assumed. A reasonable estimate for particle losses would be an additional 5 per cent per kilometer to that for molecular losses.

Assuming a beam projected vertically into the atmosphere, the combined molecular and particle losses were calculated for the first 10 km and the calculations were then continued for altitudes above 10 km, employing molecular losses only.

Figure 2 presents the results of these calculations. The curves indicate the amoun of energy incident on the scattering volume for a given altitude after accountin for both particle and molecular attenuation. It is important to note that abov 10 km, the region with which these measurements are concerned, the losses ar small. Thus, the spectral content, as well as the intensity of each wave-length (i the spectral range of the instrumentation) incident on the scattering volum undergoes insignificant attenuation from 10 km to great heights. This permi the factors $I_{O\lambda}/\lambda^4$ in equation (5) to be very nearly constant and the equatic takes the form

$$I_S = K_2 N(1 + \cos^2 \beta) \ldots\ldots\ldots\ldots\ldots\ldots\ldots\ldots (8$$

where I_S is the integrated spectral energy emerging from the scattering volum at an angle β to the beam.

3—TECHNICAL DETAILS

(3.1) *Searchlight*—The optical features of the United States Army 60-inc searchlight include a paraboloidal-shaped mirror with a focal length of 25.5 inche and a divergence angle of 1.25 degrees. The surface of the mirror is electroforme with rhodium. This metallic surface permits good reflection of the ultra-violet a compared with a glass surface. The carbon arcs, which strike and feed automati ally, normally operate at 78 volts and 150 amperes. The normal beam-intensit was increased by cutting out the ballast in the arc circuit and adjusting the ar current regulator. This made it possible to operate the carbons at 86 volts an 180 amperes, an increase of about 2 kilowatts. Tests conducted over a period four hours disclosed the beam stability to be satisfactory.

The modulating shutter was bolted to the front of the searchlight after tl glass was removed. The shutter comprises a series of vanes of the Venetian-blin type. The vanes are geared to a 1/2 horsepower motor, which is activated by a electronic speed-control (General Radio Type 1700 AL) having good speed-regul tion [7]. This arrangement permits the shutter vanes to be rotated continuous from 0 to 15 cycles per second, the upper limit being set by the mechanical limit tions of the shutter. With this arrangement, the intensity of the beam was mac to vary sinusoidally at 6 cycles per second.

(3.2) *Photo-multiplier and instrumentation*—The photo-multipliers general available (the 931A, 1P21, 1P22, and 1P28), although their thermionic properti are admirably suited for this application, have constructional features whic present some serious difficulties when used in conjunction with the 60-inch par bolic mirror. Since the light reflected from the mirror converges to the focus an angle of 120°, some light will be lost because it approaches the photo-multipli at grazing incidence. Further, the recessed position of the photo-cathode effective prevents utilization of the entire area of the mirror surface. A photo-multipli with a more suitable tube geometry was developed recently by RCA [8]. T Type C7140 is designed for head-on reception of light flux. The semi-transpare photo-cathode has a diameter of 1.5 inches and is located on the inner glass surfa of the face end of the bulb. This design permits the wide-angle acceptance of fl from the 60-inch mirror.

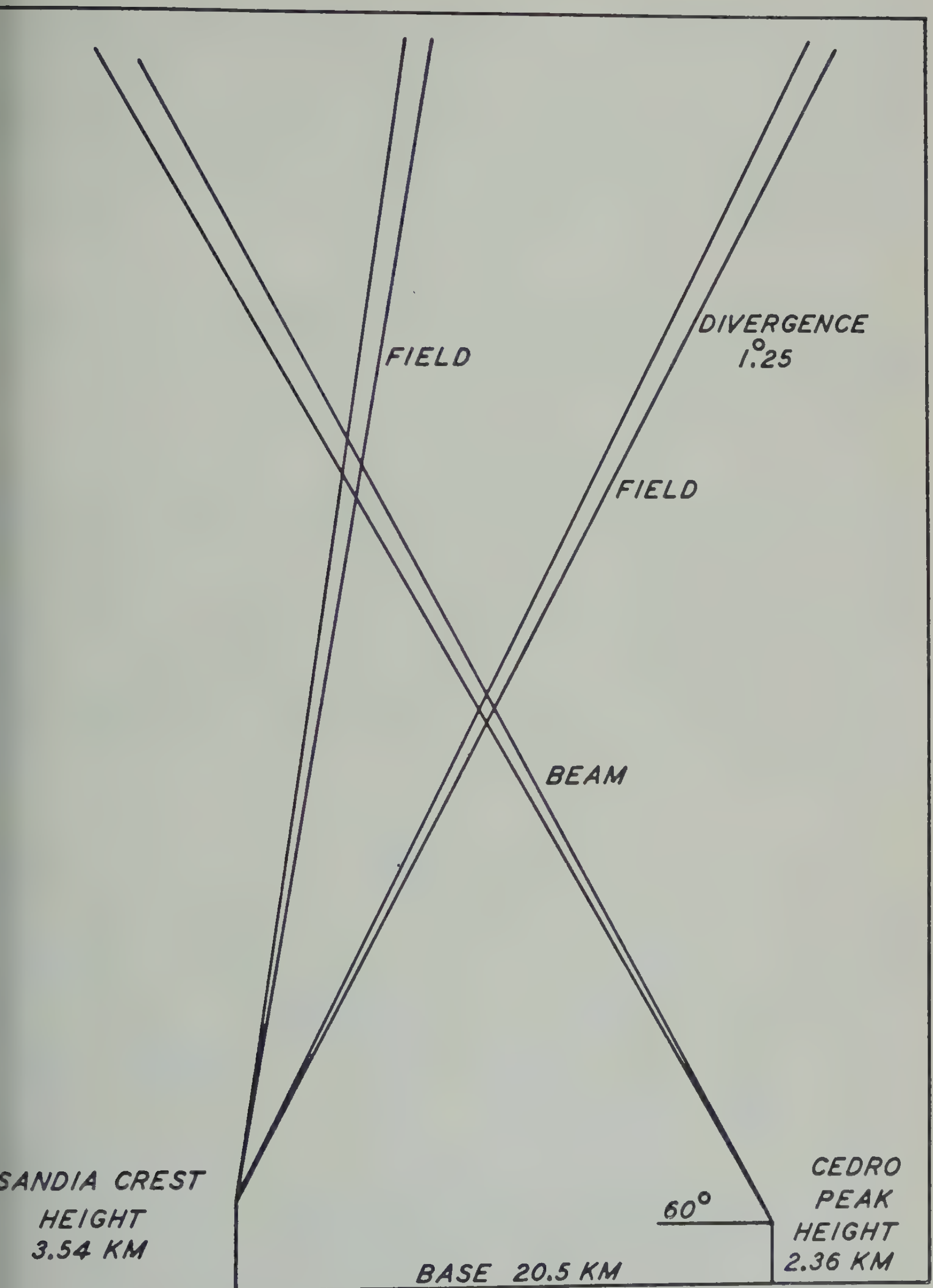

FIG. 3—SEARCHLIGHT SCENE

The selective amplifier used was operated at a frequency of 6 cycles per secon and band-width of 0.6 cycle. Shutter operation, amplifier characteristics, and nois considerations determined the choice of frequency and band-width. During opera tion, the shutter-frequency component passes from the photo-multiplier anode t an impedance match of 200 megohms and thence to the selective amplifier. Th instrumentation response is linear throughout the entire range of voltages measured so that the output-signal voltage E_o is proportional to the light intensity I_S inci dent on the photo-multiplier, and from equation (8)

$$E_o = CN(1 + \cos^2 \beta) \qquad \text{(9}$$

The search light scene representing actual field conditions is shown in Figure 3 The 20.5-km distance between sites permits good resolution of the scatterin volume at high altitudes.

4—DETERMINING DENSITY DISTRIBUTION

Equation (9) is the basic expression used to derive density distribution, in tha it provides a direct relationship between the density and the output response E of the instrumentation. The value of β in the factor $(1 + \cos^2\beta)$ is derived fron the searchlight scene geometry.

The constant C was determined by the following procedure. The response E for a given altitude, say 15 km, is given by equation (9); namely, $E_o = CN$ $(1 + \cos^2 \beta)$. E_o is measured as the voltage output of the instrumentation $(1 + \cos^2 \beta)$ is determined from the searchlight geometry for this particular alti tude, and the value N at 15 km can be calculated independently from radiosond data by means of the formula

$$N = 7.29 \times 10^{18} \frac{P}{T} \qquad \text{(10}$$

where P is the pressure in millibars and T is the temperature in °K. Thus, th constant $C = E_o/N(1 + \cos^2 \beta)$ was calculated for each night from the 15-kn sounding made at Albuquerque (release time 8 p.m., Mountain Standard Time)

During August and November 1950, eight density distributions were determine with the searchlight technique, all in good agreement with the Rand densities [9] fo a model atmosphere. Table 1 shows the altitudes (h_s) at which the measurement were made and the output voltages (E_o) measured at these altitudes. The nois level and radiosonde data for each night also are submitted. The density value N_c were calculated after the noise voltage was deducted from the output voltag (E_o). Figure 4 presents three representative density distributions of the eigh derived from the searchlight data. The density distribution for a model atmosphe at 45° latitude (Rand report) is submitted for comparison. A very definite tren is indicated in these distributions. In August 1950, the densities are larger tha the Rand values. In October 1950, the densities in the region from 20 to 50 kı fall below the Rand values; and in November 1950, the measured densities dro markedly below the Rand distribution in that region. The lowering of the densit distribution can readily be associated with seasonal change.

TABLE 1—*Scattering data and calculations*

h_s	8/19—8/20/50		9/7—9/8/50		9/9—9/10/50		9/12—9/13/50		9/13—9/14/50		10/11—10/12/50		10/13—10/14/50		11/15—11/16/50	
	E_o	N_c	E_o	N_c	E_o	N_c	E_o	N_c	E_o	N_c	E_o	N_c	E_o	N_c	E_o	N_c
km	*Volts*	*mol/cm*^{3}	*Volts*	*mol/cm*^{3}	*Volts*	*mol/cm*^{3}	*Volts*	*mol/cm*^{3}	*Volts*	*mol/cm*^{3}	*Volts*	*mol/cm*^{3}	*Volts*	*mol/cm*^{3}	*Volts*	*mol/cm*^{3}
9.3	4.6	9.6×10^{18}	4.35	9.2×10^{18}	4.2	9.7×10^{18}	5.75	1.1×10^{19}	5.5	1.1×10^{19}	5.2	9.9×10^{18}	5.4	9.9×10^{18}	5.5	8.3×10^{18}
10.7	3.6	7.7 "	3.8	8.2 "	3.55	8.4 "	5.0	9.5×10^{18}	4.65	9.2 "	4.15	8.1 "	4.5	8.4 "	4.7	7.3 "
11.9	3.1	6.6 "	3.3	7.2 "	3.05	7.2 "	4.25	8.2 "	3.85	7.7 "	3.55	7.0 "	3.9	7.4 "	4.2	6.6 "
13.3	2.7	5.7 "	2.8	6.0 "	2.65	6.2 "	3.6	6.8 "	3.15	6.2 "	3.0	5.9 "	3.2	6.0 "	3.55	5.5 "
14.6	2.3	4.8 "	2.5	5.3 "	2.40	5.5 "	3.0	5.6 "	2.65	5.1 "	2.6	5.0 "	2.7	4.9 "	3.0	4.5 "
15.9	2.0	4.0 "	2.1	4.3 "	1.95	4.3 "	2.6	4.7 "	2.3	4.3 "	2.3	4.2 "	2.25	4.0 "	2.5	3.7 "
17.4	1.7	3.3 "	1.8	3.5 "	1.55	3.3 "	1.95	3.3 "	1.85	3.3 "	1.85	3.3 "	1.8	3.0 "	1.95	2.7 "
18.8	1.5	2.7 "	1.5	2.7 "	1.3	2.6 "	1.5	2.4 "	1.6	2.7 "	1.45	2.4 "	1.55	2.5 "	1.55	2.0 "
20.5	1.2	2.0 "	1.2	2.1 "	1.05	2.0 "	1.2	1.8 "	1.35	2.1 "	1.2	1.9 "	1.15	1.7 "	1.2	1.5 "
22.3	0.97	1.6 "	0.85	1.4 "	0.82	1.4 "	0.90	1.3 "	1.05	1.6 "	0.94	1.4 "	0.90	1.3 "	0.95	1.1 "
24.4	0.72	1.1 "	0.65	9.8×10^{17}	0.635	1.1 "	0.70	9.4×10^{17}	0.77	1.1 "	0.68	9.3×10^{17}	0.645	8.5×10^{17}	0.69	7.6×10^{17}
27.4	0.50	6.9×10^{17}	0.44	6.1 "	0.425	6.5×10^{17}	0.45	5.6 "	0.52	6.7×10^{17}	0.43	5.5 "	0.40	4.9 "	0.39	3.9 "
29.7	0.35	4.6 "	0.31	4.1 "	0.34	4.9 "	0.32	3.7 "	0.36	4.4 "	0.31	3.7 "	0.285	3.3 "	0.26	2.5 "
31.9	0.27	3.4 "	0.23	2.9 "	0.225	3.1 "	0.25	2.8 "	0.27	3.2 "	0.215	2.5 "	0.205	2.3 "	0.19	1.8 "
34.1	0.20	2.4 "	0.17	2.1 "	0.16	2.1 "	0.17	1.8 "	0.19	2.1 "	0.15	1.6 "	0.15	1.6 "	0.14	1.2 "
37.9	0.11	1.2 "	0.11	1.2 "	0.093	1.1 "	0.11	1.1 "	0.12	1.2 "	0.096	9.7×10^{16}	0.084	8.0×10^{16}	0.091	7.6×10^{16}
41.5	0.073	7.4×10^{16}	0.075	7.8×10^{16}	0.067	7.4×10^{16}	0.066	5.9×10^{16}	0.080	7.7×10^{16}	0.068	6.4 "	0.060	5.3 "	0.065	5.1 "
45.9	0.048	4.3 "	0.046	4.2 "	0.045	4.4 "	0.040	3.0 "	0.049	4.2 "	0.045	3.8 "	0.042	3.3 "	0.043	3.1 "
51.0	0.030	2.2 "	0.030	2.2 "	0.031	2.5 "	0.028	1.7 "	0.030	2.0 "	0.030	2.1 "	0.030	2.0 "	0.030	2.0 "
56.0	0.023	1.4 "	0.023	1.4 "	0.023	1.5 "	0.020	9.1×10^{15}	....	......	0.022	1.2 "	0.023	−1.3 "	0.0205	1.2 "
58.6	0.020	1.0 "	0.020	1.0 "	0.020	1.1 "	0.018	7.1 "	0.020	9.5×10^{15}	0.019	9.3×10^{15}	0.020	10.0×10^{15}	0.0155	7.6×10^{15}
61.8	.....	......	0.017	6.8×10^{15}	0.017	7.5×10^{15}	0.016	5.0 "	0.017	6.3 "	0.016	6.2 "	0.017	6.9 "	0.012	4.7 "
Noise level, volts	0.011		0.011		0.011		0.011		0.011		0.010		0.010		0.0062	
Radio-sonde data	At 14.6 km P = 138 mb T = 209°.4K $C = 4.65\times10^{-19}$		At 14.9 km P = 142 mb T = 207°K $C = 4.6\times10^{-19}$		At 15.0 km P = 140 mb T = 212°K $C = 4.2\times10^{-19}$		At 16.65 km P = 124 mb T = 206°K $C = 5.2\times10^{-19}$		At 15.9 km P = 120 mb T = 204°K $C = 5.0\times10^{-19}$		At 14.6 km P = 142 mb T = 205°K $C = 5.07\times10^{-19}$		At 14.6 km P = 138 mb T = 202°.2K $C = 5.28\times10^{-19}$		At 14.6 km P = 128 mb T = 204°.6K $C = 6.4\times10^{-19}$	

E_o = output volts; N_c = calculated density; T = Temperature °K; P = Pressure; and C = Constant for calculating densities.

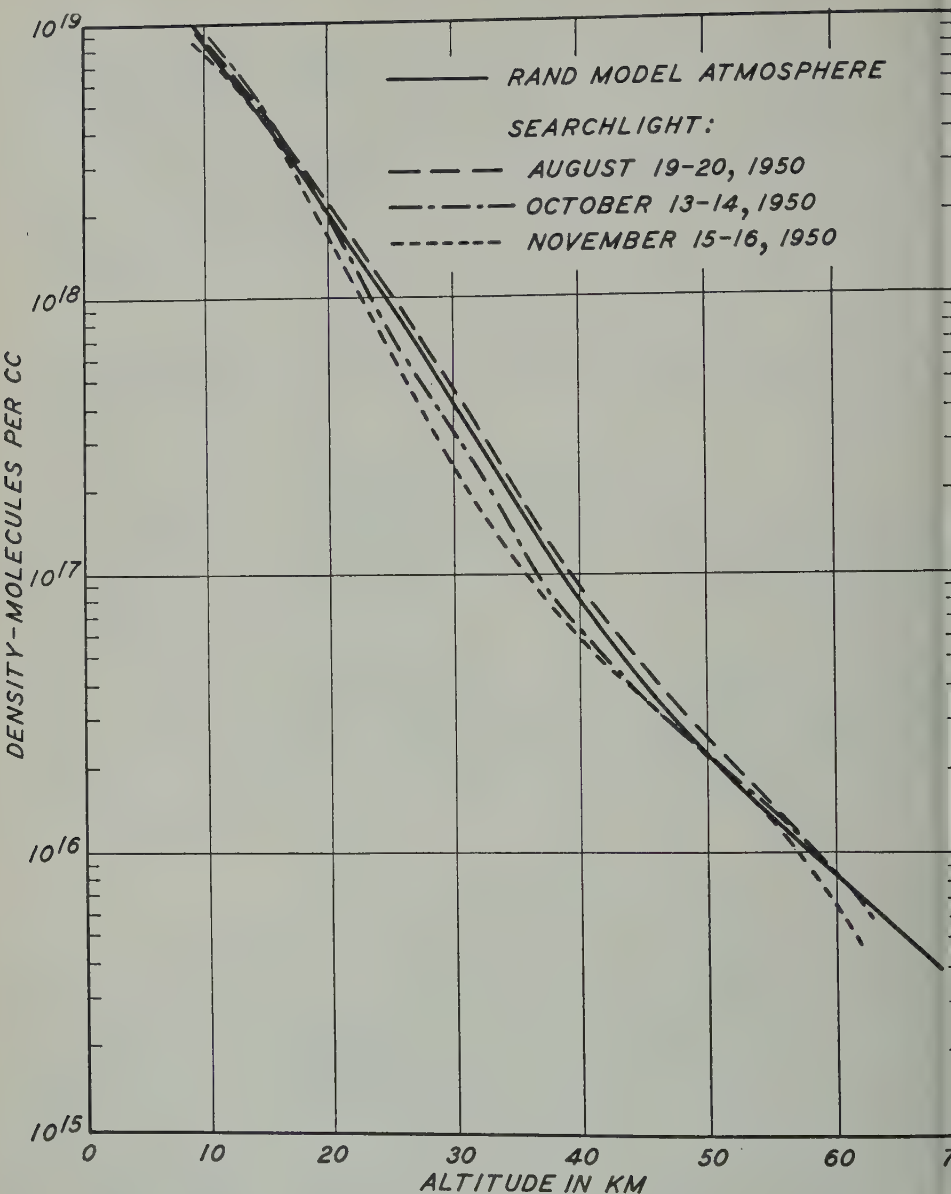

FIG. 4—DENSITY DISTRIBUTION FROM SEARCH-LIGHT DATA

5—ERROR CONSIDERATIONS

The carbon electrodes of the arc are fed automatically and, except for occa-sional transients, provide a constant intensity beam. As demonstrated in paragrap 2.2, the spectral content of the beam undergoes selective attenuation in the regio 0 to 10 km, but this does not bear on the results, since final data are concerne

ith altitudes above 10 km. The distance between the transmitter and receiver ites is 20.5 km and is accurate within 0.3 km. The error due to setting and reading f elevation scales for the mirrors is within 3 minutes of arc. Linearity of amplifier ould result in error well within 1 per cent. The accuracy of the vacuum-tube oltmeter is within 5 per cent of full scale-reading, including changes due to tube ging, battery-voltage changes, and calibration error. The measurements were latched to radiosonde data at 15 km, and at that altitude the error in pressure about 6 mb; the radiosonde temperature-error, in the absence of solar radiation, within 0°.5 C.

6—CONCLUSIONS

The usefulness of the searchlight method of probing the atmosphere has been emonstrated by the derived density distributions, which are in satisfactory agreement with Rand densities. The potentialities are good for further extension of esults. Heights greater than 61.8 km can be attained by utilization of a recently-eveloped carbon lamp, which provides three times the intensity of the lamp used this experiment. The mercury-arc lamp, as an intense light source, also presents teresting possibilities, in that it can provide a highly-regulated modulated beam ithout requiring the use of a shutter. Greater accuracy can be realized with rther improvement of electronic instrumentation.

It would appear that the searchlight method has sufficient versatility for its pplication to the study of other important problems. The results described in is paper establish the method as suitable for investigating the middle and upper tmospheric regions inaccessible to direct observation.

7—ACKNOWLEDGMENTS

Acknowledgment is due to the personnel of Kirtland Air Force Base, New Iexico, for supplying operating headquarters, base services, and supplies, and, enerally, for the excellent cooperation which made this experiment possible; to Ir. Arthur L. Hartman, of the Air Force Cambridge Research Center, for his illed operation of the searchlight equipment; to Dr. Victor H. Regener, Chairman the Physics Department of the University of New Mexico, for his generous advice nd for extending the facilities of his laboratory; and to Dr. Rudolf Penndorf, of the eophysics Research Division, for the many helpful discussions.

References

[1] E. H. Synge, A method of investigating the higher atmosphere, Phil. Mag., **9**, 1014–1020 (1930).

[2] M. A. Tuve, E. A. Johnson, and O. R. Wulf, A new experimental method for study of the upper atmosphere, Terr. Mag., **40**, 452–454 (1935).

[3] E. O. Hulburt, Observations of a searchlight beam to an altitude of 28 kilometers, J. Optical Soc. Amer., **27**, 377–382 (1937).

[4] E. A. Johnson, R. C. Meyer, R. E. Hopkins, and W. H. Mock, The measurement of light scattered by the upper atmosphere from a searchlight beam, J. Optical Soc. Amer., **29**, 512–517 (1939).

[5] D. Sinclair, Light scattering by spherical particles, J. Optical Soc. Amer., **37**, 475–586 (1947).

[6] General Electric Company, Operator's manual: Searchlight and control station for 60-in antiaircraft searchlight, Model 1942, 154 pp. (U. S. War Department, Operating instru tions manual TM 5–7045).
[7] The General Radio Experimenter, Variac motor speed controls, **23**, 8 pp. (April 1949).
[8] RCA Victor Division, Preliminary and tentative data, RCA developmental tube ty C-7140 (Sept. 14, 1949).
[9] G. Grimminger, Analysis of temperature, pressure and density of the atmosphere extendi to extreme altitudes, Rand Corporation, R-105, 149 pp. (Nov. 1948).

URNAL OF GEOPHYSICAL RESEARCH VOLUME 56, No. 4 DECEMBER, 1951

SYSTEMATIC IONOSPHERIC WINDS

By C. D. SALZBERG AND R. GREENSTONE

Central Radio Propagation Laboratory, National Bureau of Standards, Washington 25, D. C.

(Received June 29, 1951)

ABSTRACT

A study of fading patterns of pulsed radio waves reflected by the ionosphere has led to the determination of horizontal drifts in the ionosphere. Equipment has been operated at 2.3 Mc at the National Bureau of Standards since March 1949. The wind may blow from any direction over a period of time. It exhibits diurnal characteristics which change with the seasons. Apparent wind speeds may range up to 300 m/sec, but are predominantly in the range from 50 to 100 m/sec. Marked changes in the character of the winds are associated with the transition from E- to F-region reflections. Good agreement is found between wind directions and speeds observed at Washington, D. C., and those observed at Cambridge, England.

1—INTRODUCTION

For more than two centuries the subject of atmospheric oscillations and the ssociated wind systems in the upper atmosphere has been intensely studied. urrent theory indicates a wind system which is world-wide in character and is used primarily by solar tidal (gravitational and thermal) forces which are agnified many fold by resonance effects. An excellent presentation of work in is subject is given by M. V. Wilkes [see 1 of "References" at end of paper]. he existence of such a wind system in the upper atmosphere also offers a satis- ctory explanation for the quiet-day variation of terrestrial magnetic forces. alfour Stewart in his dynamo theory showed that the diurnal magnetic variation uld be produced by a system of currents induced by motion of the conducting rtions of the upper atmosphere across the earth's magnetic field.

From time-to-time, evidence of the presence of motion in the upper atmosphere s been reported. Primarily, this evidence is based on visual observations of minous phenomena in the night sky, such as noctilucent clouds and long en- ring meteor trails [2,3,4,5,6]. From these observations, horizontal motions oc- rring at heights of 80 to 100 km with speeds ranging up to 177 m/sec were duced. In addition to the visual methods, several experimenters have used radio ethods of tracking ionospheric anomalies in order to measure ionospheric winds.

Munro [7] found effects indicating a horizontal motion in the F region with a spee of about 100 m/sec. His method involved examination of the echoes received a single site, from three transmitters spaced several kilometers apart at the vertic of a right triangle. Mimno [8] reported that clouds of intense ionization in th E region, as observed at receivers situated 60 km apart, appeared to move wit a velocity of 1,000 m/sec. Beynon [9] observed that irregularities in the $F2$ regio appeared to travel a distance of 500 km with a speed of about 120 m/sec. Mo recently, Manning, Villard, and Peterson [10] developed a method for measurin the velocity of winds in the 90- to 110-km height region, using the Doppler shi imparted to CW reflections from drifting meteoric ionization. Average wind spee of 40 m/sec were reported. Gerson [11] and Ferrell [12] have reported winds wit speeds between 30 and 50 m/sec deduced from reports by radio amateurs sporadic-E reflections at 50 Mc. Mitra [13], Krautkrämer [14], and the prese authors have used a radio fading method in which horizontal motions in the ion sphere are deduced from motions of the diffraction pattern of the reflected wa produced by ionospheric irregularities. Of these methods, only the latter and th of Manning, Villard, and Peterson seem to be suitable for both regular and reliab observations of ionospheric winds.

In this paper we discuss briefly the theory associated with the radio fadin method for measuring ionospheric winds, describe the equipment used at th National Bureau of Standards, indicate the method of data reduction, prese the results of six months' systematic accumulation of data, examine these da for diurnal and seasonal trends, and finally compare the results with those obtain by others.

2—THEORY

Pawsey [15] in 1935 conducted a study of fading patterns of radio waves r flected by the ionosphere. He found on several occasions that the patterns obtain from receivers spaced several wave-lengths apart were very similar, but displac in time. Behavior of this sort can be explained by assuming the ionosphere to made up of patches of ionization of different intensities. Reflection from such irregular region produces a complex diffraction pattern on the ground. If the were no motion or changes of the layer, the diffraction pattern on the grou would be fixed and no fading would occur. If there were a motion of the lay and the irregularities did not rapidly change shape or relative position, then t diffraction pattern would sweep over the ground and the resultant fading patter observed by means of spaced receivers would be similar but displaced in time. should be noted that phase interference effects between magneto-ionic co ponents or multiple-hop echoes can also produce motions of the diffraction patte Therefore, it is necessary to work with a single mode to observe the ionosphe wind velocity. If there were turbulence in the region and the patches of ionizati changed shape and relative position, then there would be fading at each receivi site, but the fading patterns from receivers spaced sufficiently far apart would dissimilar. What actually occurs in the ionosphere is a combination of all the phenomena in varying proportions.

It should be possible then to use three receivers placed at the vertices of a rig

triangle to obtain the speed and direction of the drift of the diffraction pattern on the ground. Briggs, Phillips, and Shinn [16] have shown how to deduce from the three fading records a value of steady drift velocity and a measure of the random internal changes in the pattern. (The wind speed in the ionosphere is of course half the value of the drift speed of the ground pattern.)

When the fading patterns at the three receivers are very similar, turbulence is at a minimum, and the time displacements between the three records can be used as a measure of the steady wind speed.

In Figure 1, the receivers A_1, A_2, and A_3 are shown spaced a distance d apart.

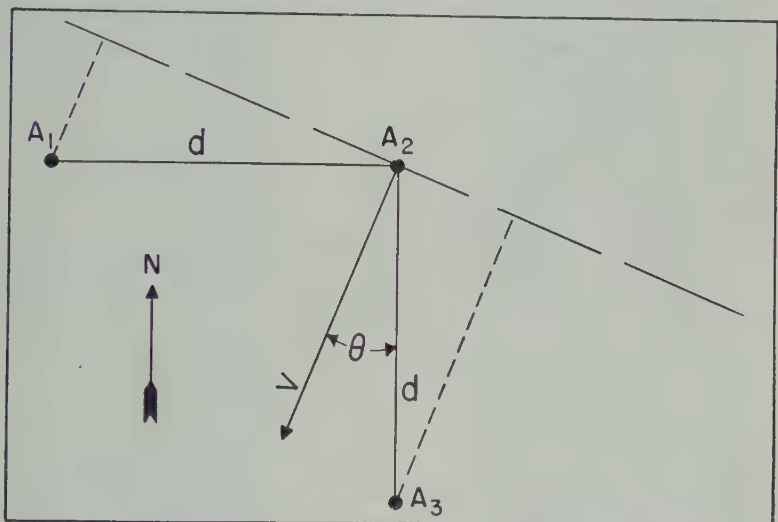

FIG. 1—Geometry of the wind velocity problem. The three receiving antennas are indicated by points A_1, A_2, A_3. The motion of the diffraction pattern is indicated by the arrow with speed V making an angle θ with the line A_2A_3.

The diffraction pattern represented as a wave front (broken line) is moving at speed V and making angle θ with respect to the line A_2A_3. From the geometry, the relations between the velocity and the time delays τ_{21}, τ_{23} can be obtained as follows:

$$V = \frac{d \cos \theta}{\tau_{23}} = \frac{d \sin \theta}{\tau_{21}}$$

$$\tan \theta = \frac{\tau_{21}}{\tau_{23}}$$

(τ_{21} is defined as the time required for the wave front to move from A_2 to A_1 and τ_{23} is the time for the wave front to move from A_2 to A_3.) The values of τ are deduced from the records.

3—EQUIPMENT

The discussion in the preceding section is applicable if the diffraction pattern is not complicated by phase interference effects between magneto-ionic com-

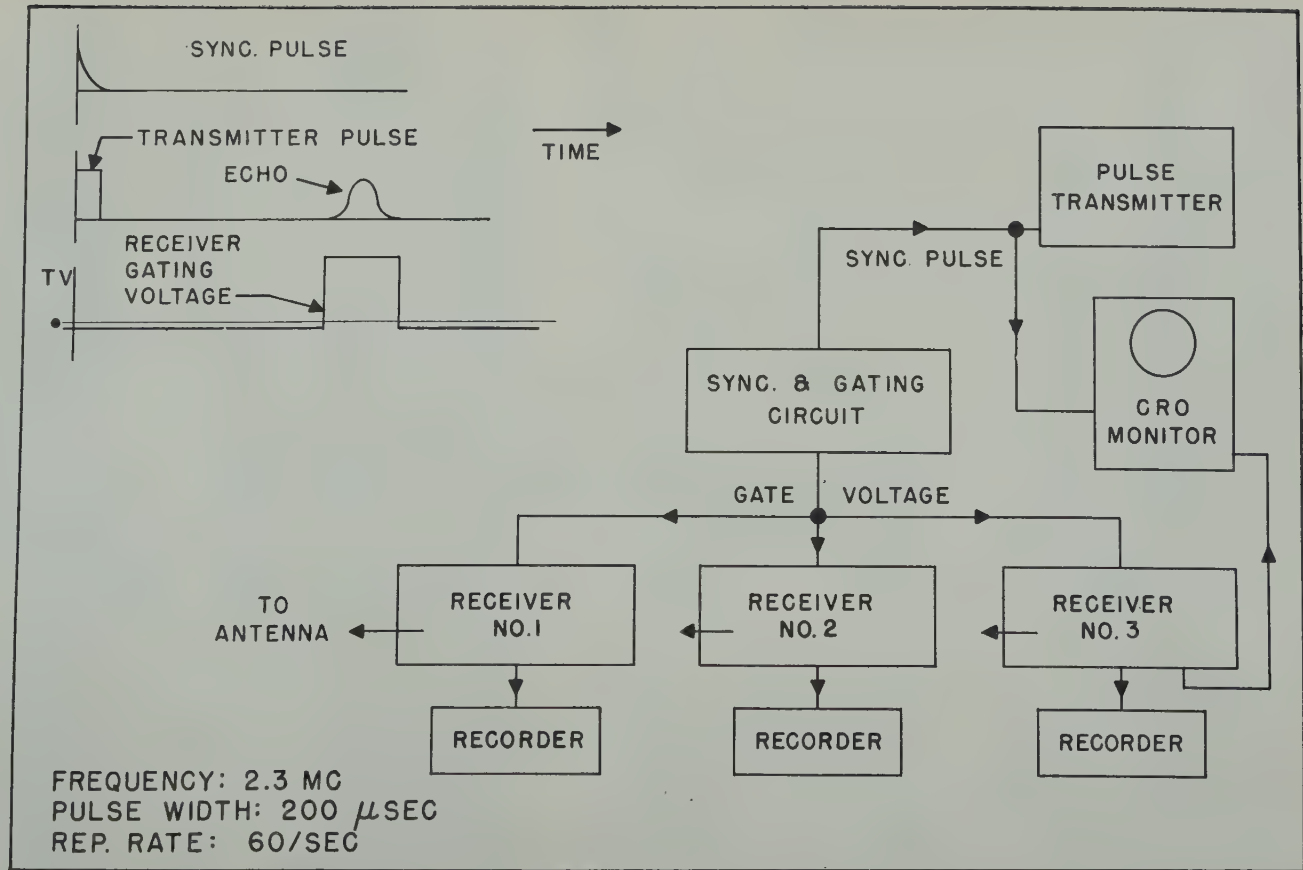

Fig. 2—Block diagram of transmitting and receiving equipment. The synchronizer keys the transmitter 60 times per second and also keys the variable width-variable delay gates to the receivers.

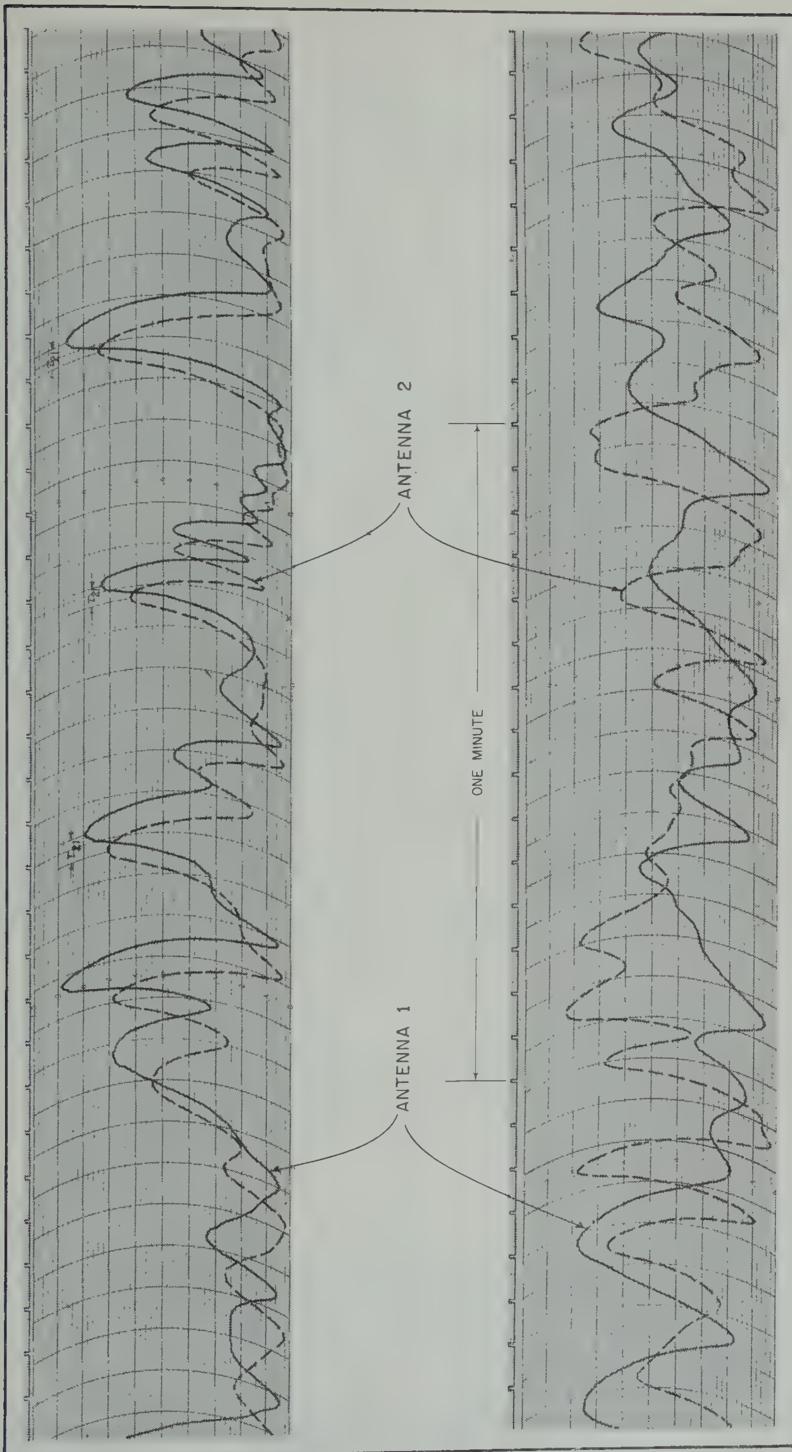

FIG. 3—Typical fading records. The output voltages from receivers 1 and 2 are shown superposed. The upper set of records shows good similarity in fading pattern. τ_{21} equals (−2) seconds. The lower set of records shows poor similarity. No attempt was made to analyze this sort of record.

ponents or by multiple-hop echoes. Consequently, the equipment must be abl to isolate a single downcoming wave.

The equipment used in the experiment consists of the following: A pulse trans mitter working at 2.3 Mc, 10-kw peak power, 200-μ sec pulse width, 60/sec repe tition rate; a synchronizing and gating circuit; three conventional receivers con verted for pulse reception; dc amplifiers and paper tape recorders. Figure 2 is block diagram showing the arrangement of equipment. Average rectified puls amplitude is recorded. The over-all time constant for the system is establishe by the recorder pen response-time and is of the order of 1/10 sec. In Figure 3 records from two receivers have been superposed to illustrate the extremes i pattern similarity obtained. Time coincidence between the records can be ac curately established by means of the time markers, placed at four-second interval on the paper margin, with time increasing from right to left. The upper set o records illustrates a case of excellent similarity between fading patterns. It i obvious that the diffraction pattern was intercepted first by antenna number one and about two seconds later by antenna number two. Therefore, τ_{21} would b assigned a value of (-2) sec. The lower set of records shows no similarity, indi cating extreme turbulence in the diffracting layer, which completely obscure any regular drift which may have existed at the time. No attempt is made t analyze this sort of record. A monitor oscilloscope provided with a time bas enables the operator to set the variable-width variable-delay receiver gating cir cuits so that only the desired echo will be received, thus eliminating multiho transmissions and the initial transmitter pulse. Elimination of either of the mag neto-ionic components is accomplished by transmitting a circularly polarized wav obtained from crossed half-wave dipoles fed 90° out of phase. (At the latitude o Washington, D. C. a circularly polarized wave is reflected as essentially a pur mode.) The receiving antennas are folded half-wave dipoles, oriented in an east west direction, and placed 200 meters apart at the vertices of an isosceles right triangle, as in Figure 1. The transmitter is located near the center of the triangle

4—DATA REDUCTION

The most desirable method of obtaining the time shift between a pair of fadin records is to compute the cross correlation function

$$\phi(\tau) = \frac{\frac{1}{N}\sum x_i y_{i\pm\tau} - \bar{x}\bar{y}}{\sigma_x \sigma_y}$$

for a sufficient number of values of τ. Several such computations were performe and a typical pair of correlograms is shown in Figure 4. The time difference be tween records is determined by the point of maximum correlation. Also the valu of the correlation function at the maximum is a qualitative indication of th degree of similarity between the records.

The actual computation of the desired cross correlation functions is, howeve an extremely laborious task. The systematic schedule we have adopted provid us with 120 sets of records each month, and complete correlation analysis of suc

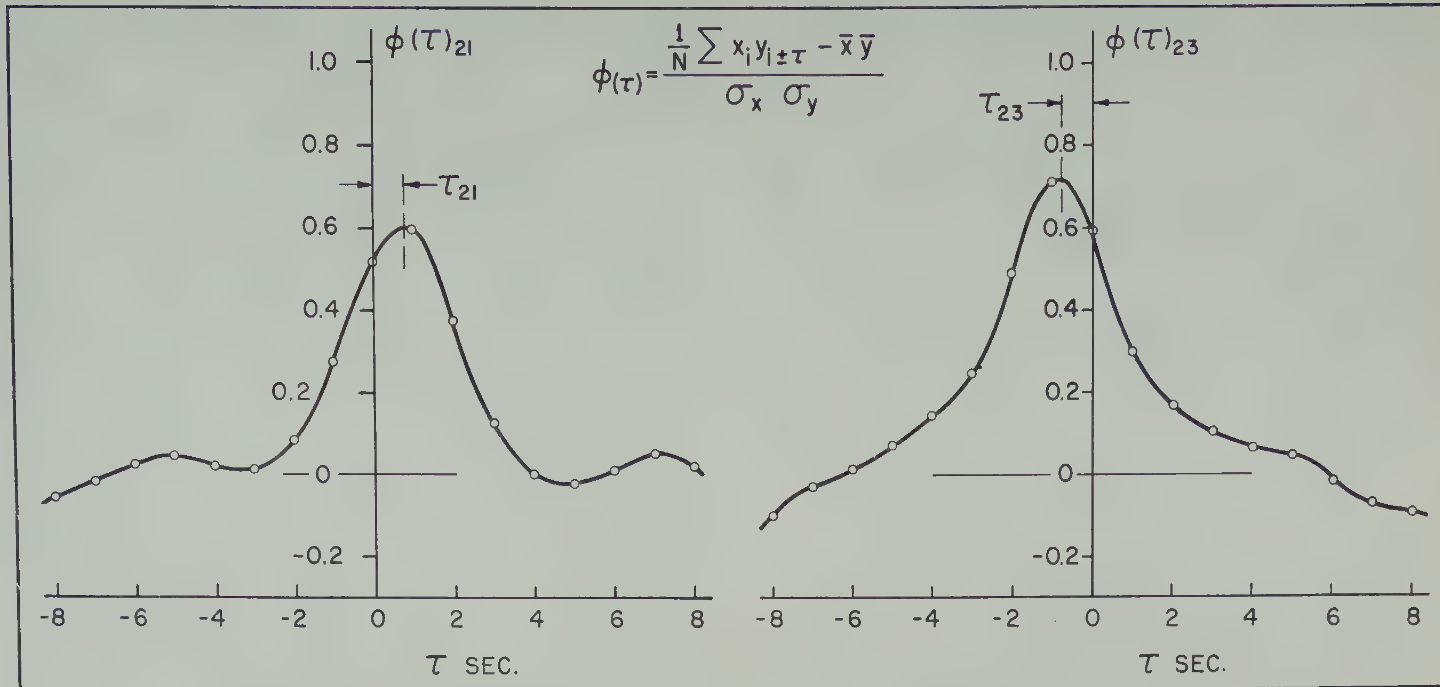

FIG. 4—Typical correlograms: The cross correlation coefficient between records $\varphi(\tau)$, is plotted against relative time delay, τ, for a typical wind run. The value of τ that maximizes $\varphi(\tau)$ is taken to be the correct time difference between records. Thus, in this example, record 2 leads record 1 by one second, while record 2 lags record 3 by one second.

a large amount of data is impractical, even using punched card techniques. An analog type computer, designed specifically to perform this work, would appear to be the answer to the problem. Until such time as a suitable device can be prepared, we have adopted a visual method of analysis which consists of averaging the obvious time shifts on a set of superposed records, as illustrated in Figure 3. For those records on which both the correlation and visual analysis have been performed, the time shifts obtained are in good agreement.

A more extended discussion of the treatment of information available from correlation analysis, and its implications, is given by Briggs, Phillips, and Shinn [16]. They show that the velocity deduced from the time shifts between records is only an apparent drift velocity. In order to determine the correct drift velocity, one must take into account the amount of random change which is occurring in the diffraction pattern due to turbulent motion in the ionosphere. However, if analysis is restricted to only those records which are obviously similar (a prerequisite for our visual analysis), then turbulence is at a minimum and the apparent drift velocity differs but little from the correct velocity [16].

Only about 10 per cent of the data taken during the period on which we are reporting was rejected for not satisfying the requirement of sufficient similarity or because the speeds obtained were greater than the upper limit of reliability of the method (about 300 m/sec).

5—RESULTS

5.1—*Azimuths*

Figure 5 shows the azimuths of the wind vectors (that is, vectors in the direction of wind flow) for winds that were obtained on three-day runs in each of the six months from July to December, 1950. Salient features are as follows:

(*a*) *A sunrise-sunset effect*—At times of transition from E- to F-region reflections, there is a marked shift in azimuth accompanied by increased scatter in the data. (Transition times are indicated by hatching on the diagram.) This effect is most clear in the July and August data, but can also be observed in the other months.

(*b*) *Seasonal effect*—In the summer months there is a prevailing easterly azimuth for daylight hours and a prevailing westerly azimuth for night hours.

For the month of December, our data are somewhat incomplete due to equipment failure. The available data show a prevailing south to west azimuth during day and night. Until our January and February data have been analyzed, we will not be able to draw any conclusions concerning a possible winter trend.

For the fall months, September, October, and November, there is an indication of a semidiurnal rotation in a clockwise sense. In October, the semidiurnal rotation is especially striking.

It should be added that data collected in the spring, March, April, and May, 1950, when preliminary runs were made, also exhibited a semidiurnal rotation. Figure 6 shows points representing the average of measurements obtained on approximately seven different days in these months.

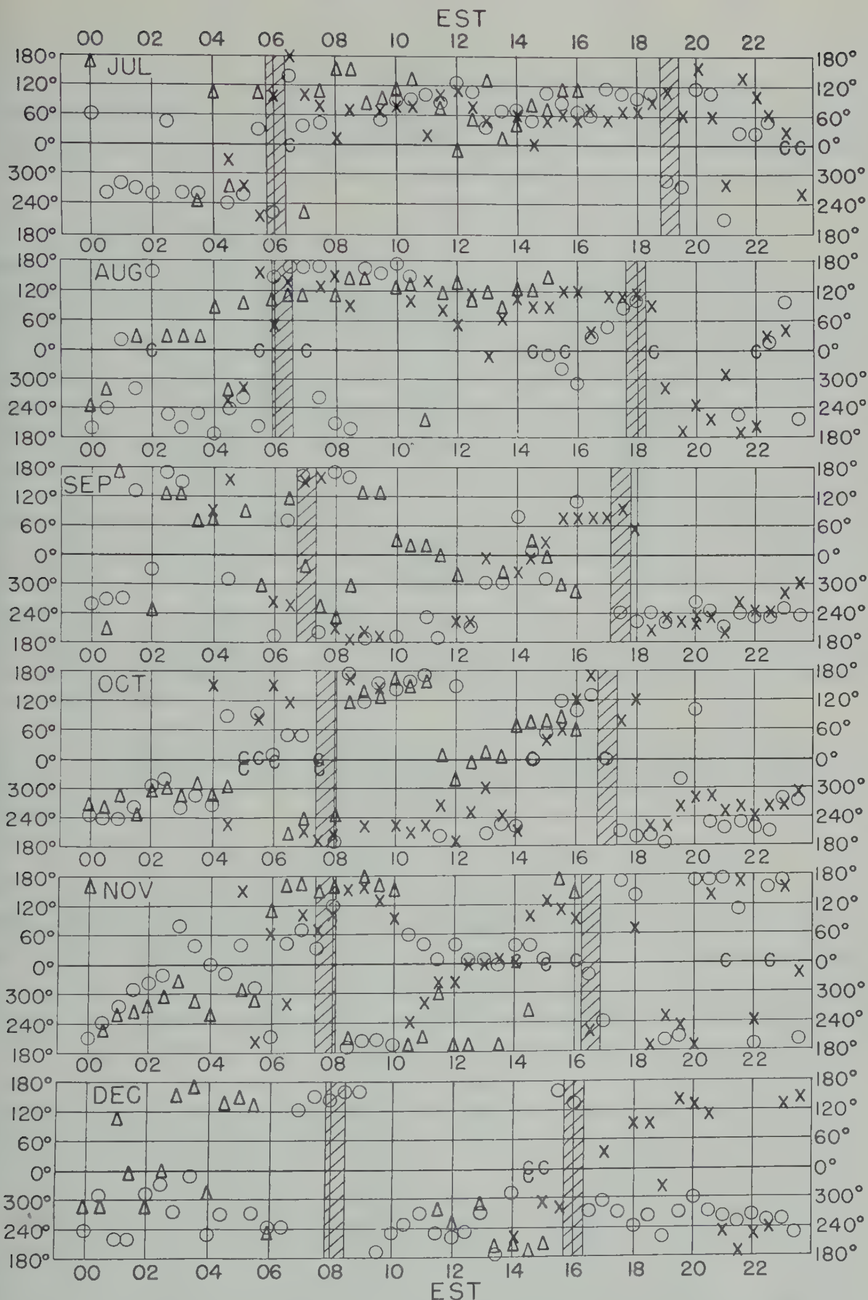

FIG. 5—Wind azimuths for three-day runs—July to December, 1950. Wind azimuths are shown for five-minute observations made at half-hour intervals. The hatched areas indicate approximate transition times between E- and F-region reflections. The symbols X, O, and Δ indicate first, second, and third days, respectively. C means zero speed.

5.2—*Speeds*

Figure 7 shows the relative distributions of speeds for the months March through December 1950. It appears that 70 m/sec is a representative speed for the greater part of the year. In November and December, however, speeds increased and were more on the order of 100 m/sec.

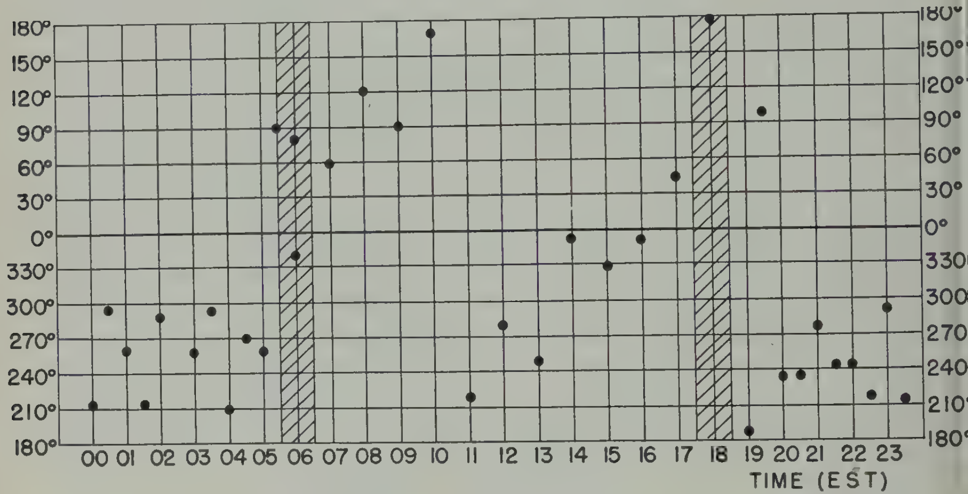

Fig. 6—Average azimuths observed in March, April, and May 1950. The hatched areas indicate approximate transition times between *E*- and *F*-region reflections.

5.3—*Other data*

(*a*) G. J. Phillips, Cavendish Laboratory, Cambridge, England, has been con tinuing the work on ionospheric winds first reported by Mitra [13]. We have founc good agreement between his results and ours. Prevailing directions are the sam for the same local time. Times of transitions from one direction to another generall agree to the nearest hour. His speeds are in the same range as ours and show th same tendency to increase in the winter months.

(*b*) Recently, Krautkrämer [14] has reported on ionospheric wind measure ments made in Germany from August 14 to October 14, 1942. He determine the winds in the same manner as Mitra [13] and the present authors. He doe not give the hour-by-hour variation of azimuths, but does give a predominan azimuth for *E*-region reflections as between 180° and 210°. For *F* reflections, th predominant azimuth is between 0° and 40°. There appears to be no agreemen between Krautkrämer's azimuth data for 1942 and the data obtained in 194 and 1950. His speeds, however, are of the order of 100 m/sec, which is in agreemen with the more recent data.

(*c*) Manning, Villard, and Peterson [10] have measured winds at Stanfor University, California, using reflections from meteor trails in the 90- to 100-k region of the upper atmosphere. They report azimuths which are predominantl between north and northeast, and speeds of the order of 35 m/sec. These resul

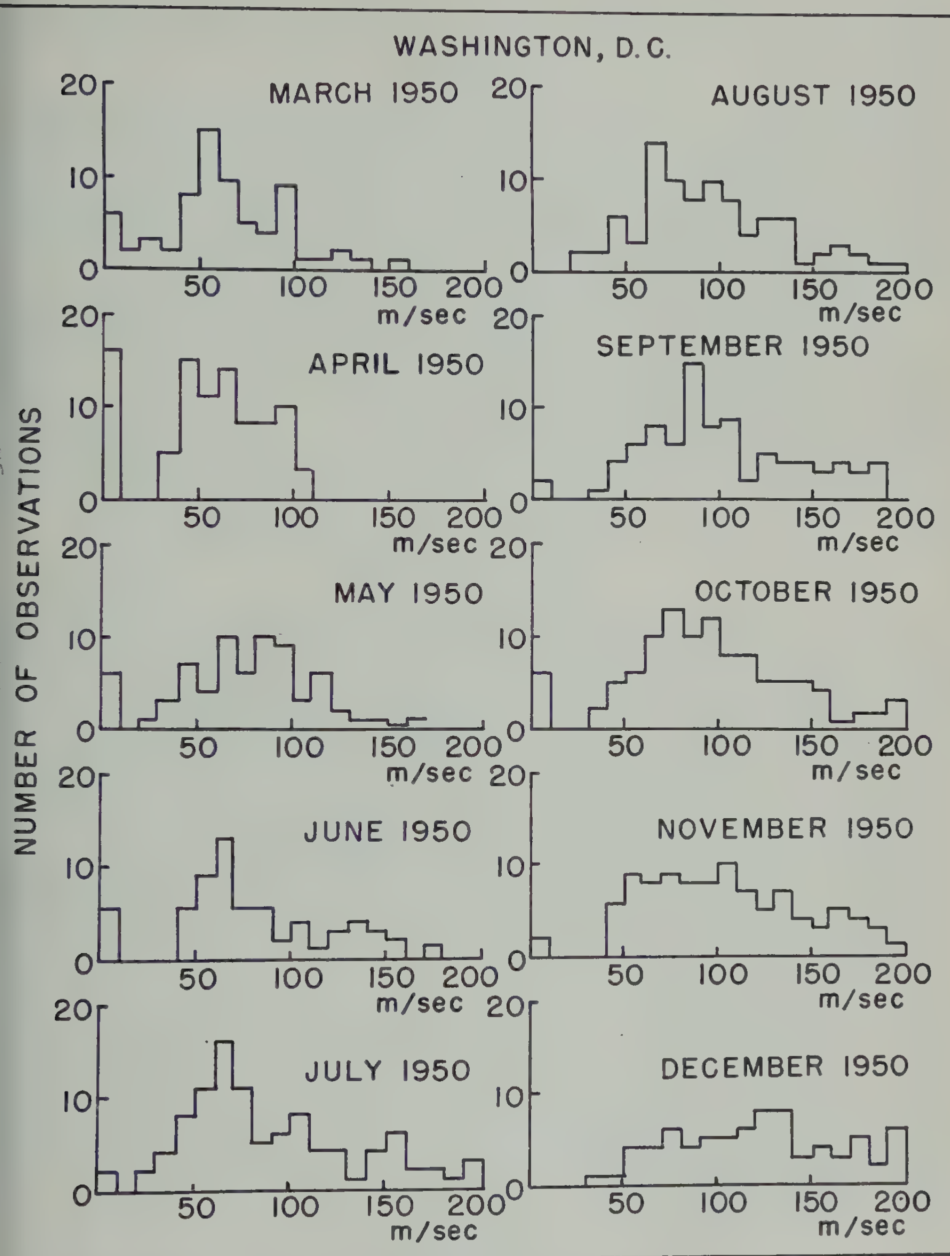

FIG. 7—The distributions of observed wind speeds for the months March through December, 1950. Speeds greater than 200 m/sec were rarely observed and have been omitted.

are based on observations made between 2 a.m. and 4 a.m., local time, durin the summer of 1949. They may be compared with Figures 4 and 6, which sho that for the hours between 2 a.m. and 4 a.m., local time, in the months fro March to August 1950, the wind azimuths observed at Washington, D. C., a predominantly between south and west. Phillips has also pointed out a significa trend toward directions between south and southwest in the small hours of th morning in the 1949 and 1950 data for Cambridge. Thus, the azimuths observe at Cambridge and Washington are mutually consistent, but are oppositely directe to those observed at Stanford. The speeds reported by the Stanford group a only half as great as those observed at Cambridge and Washington.

(*d*) It should be noted, in comparing the results of the early observers [2,3,4,5, with the present data, that the number of observations was usually small an that the observations were restricted to night hours. It was not possible, therefor to observe any diurnal trends. The movements reported were generally toward th south and west. The visual observations, despite their limited nature, are in goo agreement with the current regular observations using radio methods an strengthen the concept of a world wind pattern at ionospheric levels.

5.4—*Location of winds*

During the daytime, when reflections are from the E region, it is clear th the motions observed must take place in the E region at some point below th level of reflection. But at night there is some ambiguity. Although the reflectio are from the F region, the region responsible for the moving diffraction patte on the ground may be either the E or F. It may be that the residual ionization the E region is sufficient to give the effect of a moving transmission grating. (the E region may be too weak and the F region predominant in producing th moving diffraction pattern on the ground. The method of measuring winds fro variations in the ground diffraction pattern does not allow us to distinguish b tween the two levels. There is some independent evidence, however, which sugges that the winds observed at night are indeed in the E region. Winds deduced fro visual observations of the motions of noctilucent clouds [2,3,4,5] agree with tho deduced by the radio reflection method. It is known that these noctilucent clou are at approximately 80 km. Also Mitra [13] has reported instances where r flections have been taken alternately from E-sporadic and from F. The win deduced were much the same in each case. We have confirmed this effect at Was ington. Simultaneous measurements using the radio fading technique at fr quencies above and below the E-layer critical frequency would provide mo direct evidence on this point.

6—CONCLUSION

It is possible to make systematic studies of motions in the ionosphere by usi radio reflections. These wind motions probably take place in the 80- to 100-k height region of the ionosphere. There is no one prevailing wind azimuth, b rather there are systematic diurnal and seasonal changes. Finally, these wi motions appear to be part of a world-wide circulation system.

Further work is contemplated to determine the level of the winds and to present a more complete picture of winds throughout the year.

7—CREDITS

The authors wish to thank Mr. Jose Martinez, of the Instituto de Electrotecnica, Montevideo, Uruguay, and Mr. A. Epstein, of this Laboratory, for their assistance in developing the experimental equipment used in this study. Miss Isabelle Arsham, Miss Dorothy A. Bryan, and Mrs. Phyllis Underwood have carried out the laborious reduction of the data. Messrs. R. Anderson, T. N. Gautier, R. W. Knecht, R. S. Lawrence, D. R. Paquette, W. Taylor, and B. Wieder have all participated in the round-the-clock observations.

References

[1] M. V. Wilkes, Oscillations of the earth's atmosphere, London, Cambridge University Press (1949).
[2] R. Surung, Naturwiss., **23**, 555 (1935).
[3] C. Störmer, Astroph. Norvegica, **1**, No. 3 (1935).
[4] E. H. Vestine, J. R. Astr. Soc. Can., **28**, 249 (1934).
[5] C. Störmer, Geofys. Pub., Oslo, **9**, No. 6 (1932).
[6] C. P. Olivier, Proc. Amer. Phil. Soc., **72**, 215 (1933).
[7] G. H. Munro, Nature, **162**, 886 (1948).
[8] H. R. Mimno, Rev. Mod. Phys., **9**, 1 (1937).
[9] W. J. G. Beynon, Nature, **162**, 887 (1948).
[10] L. A. Manning, O. G. Villard, and A. M. Peterson, Proc. Inst. Radio Eng., **38**, 887 (1950).
[11] N. C. Gerson, Nature, **166**, 316 (1950).
[12] O. P. Ferrell, Proc. Inst. Radio Eng., **37**, 879 (1948).
[13] S. N. Mitra, Proc. Inst. Elec. Eng., **96**, Pt. 3, 441 (1949).
[14] J. Krautkrämer, Archiv. Elektr. Uebertrag., **4**, Heft 4, 133 (1950).
[15] J. L. Pawsey, Proc. Cambridge Phil. Soc., **31**, 125 (1935).
[16] B. H. Briggs, G. J. Phillips, and D. H. Shinn, Proc. Phys. Soc., B, **63**, 106 (1950).

URNAL OF GEOPHYSICAL RESEARCH VOLUME 56, No. 4 DECEMBER, 1951

WAVE PACKETS, THE POYNTING VECTOR, AND ENERGY FLOW: PART IV—POYNTING AND MACDONALD VELOCITIES IN DISSIPATIVE ANISOTROPIC MEDIA (CONCLUSION)

By C. O. HINES*

Radio Physics Laboratory, Defence Research Board, Ottawa, Canada

(Received July 9, 1951)

ABSTRACT

This paper is the last in a series designed to determine the path of electromagnetic energy flow in media of complex natures. In it, the common method of using the Poynting vector is extended to dissipative media. It is found preferable to replace Poynting's vector by Macdonald's to obtain physically suitable results, but even then the direction obtained for the energy flow shows a discrepancy with that found by packet methods. No conclusive decision can be reached, but argument appears to favour the packet as giving the observable energy flow.

1—*Introduction and summary*

Two methods for finding the direction of energy flow in electromagnetic pro-agation are in common use, the one employing wave packets and the other in-olving the Poynting vector. However, there appear to have been few attempts correlate the results. The need for an investigation of this field became apparent hen Booker [see 1 of "References" at end of paper] using the packet and Scott ,3] using the Poynting vector obtained discrepant results for an absorbing nosphere.

In Part I of this series [4] it was shown that the two methods agree on the rection of energy flow in an anisotropic medium so long as it is non-absorbing. was therefore felt that the discrepancy might have been introduced by im-oper generalizations of one or both methods when absorbing media were to be eated; both seemed questionable. In Parts II and III [5,6] the packet concept as generalized for absorbing media, and an expression for the packet velocity as found. In the present paper, the Poynting vector method is generalized. It found that the results are physically acceptable only if a constant of integration added to the usually accepted expression for the energy density, but that even en the motion of the energy is very peculiar. This peculiarity is removed if

*Present address: 41A Burleigh Street, Cambridge, England.

Macdonald's theorem is accepted in place of Poynting's. This gives as the direction of energy flow the direction of the mean Poynting vector, so Scott's formulae (if not their bases) are justified even for the absorbing case. However, there still appears a discrepancy between the directions obtained by the two methods. While nothing conclusive can be determined by the present arguments, it appears more likely that the packet method should give the better description of the observable results.

2—*General formulae*

In a medium having effective permittivity matrix ϵ_{pq}, plane waves having complex field vectors proportional to $\exp i\varphi \equiv \exp ik(nz - ct)$ can be derived as in Part I. The equations for the complex refractive index $n \equiv n_1 + in_2 \equiv N\epsilon^{i2\nu}$ and electric amplitude components E_p are

$$(\epsilon_{11} - n^2)E_1 + \epsilon_{12}E_2 + \epsilon_{13}E_3 = 0 \qquad (1)$$

$$\epsilon_{21}E_1 + (\epsilon_{22} - n^2)E_2 + \epsilon_{23}E_3 = 0 \qquad (2)$$

$$\epsilon_{31}E_1 + \epsilon_{32}E_2 + \epsilon_{33}E_3 = 0 \qquad (3)$$

[cf. equations (11) to (13) of Part I, setting $\lambda = \mu = 1 - \nu = 0$ and replacing h_{pq} by the more general ϵ_{pq} applicable here].

Multiplying (1) by E_1, (2) by E_2, (3) by E_3, and adding, we obtain

$$E_p\epsilon_{pq}E_q = n^2(E_1^2 + E_2^2) \qquad (4)$$

and similarly

$$\tilde{E}_p\epsilon_{pq}E_q = n^2(E_1\tilde{E}_1 + E_2\tilde{E}_2) \qquad (5)$$

where summations are to be taken over the repeated subscripts p and q, and ~ denotes the complex conjugate.

Poynting's equation in Heaviside-Lorentz units may be written, for non-magnetic media, as

$$-c\int_S \mathbf{E} \times \mathbf{H} \cdot \mathbf{ds} = \int_V \left(\mathbf{E} \cdot \frac{\partial}{\partial t}\mathbf{D}_{eff} + \mathbf{H} \cdot \frac{\partial}{\partial t}\mathbf{H}\right) dv \qquad (6)$$

[cf. equation (6), Part I, but now taking **E**, **H**, and $\mathbf{D}_{eff}$ as real vectors, the electric, magnetic, and effective displacement fields]. The left side is usually taken as the flow of energy into V and the right side as the rate of increase of energy in V. The integrand on the right may be broken into two parts, involving the Hermitian and anti-Hermitian components (h_{pq} and a_{pq}) of ϵ_{pq} separately, and the complex field components. These parts are the rate of increase in density of the flowing electromagnetic energy,

$$\frac{\partial}{\partial t}\mathcal{E}_F = \frac{1}{4}\Big[(E_p\epsilon^{i\varphi} + \tilde{E}_p\epsilon^{-i\tilde{\varphi}})\frac{\partial}{\partial t}(h_{pq}E_q\epsilon^{i\varphi} + \tilde{h}_{pq}\tilde{E}_q\epsilon^{-i\tilde{\varphi}})$$

$$+ (H_p\epsilon^{i\varphi} + \tilde{H}_q\epsilon^{-i\tilde{\varphi}})\frac{\partial}{\partial t}(H_p\epsilon^{i\varphi} + \tilde{H}_p\epsilon^{-i\tilde{\varphi}})\Big] \qquad (7)$$

and the rate at which heat energy is being developed,

$$\frac{1}{4}(E_p\epsilon^{i\varphi} + \tilde{E}_p\epsilon^{-i\tilde{\varphi}})\frac{\partial}{\partial t}(a_{pq}E_q\epsilon^{i\varphi} + \tilde{a}_{pq}\tilde{E}_q\epsilon^{-i\tilde{\varphi}})$$

The mathematical distinction is that the first contains all the terms having zero mean value, while the second contains all those having non-zero means.

Poynting's vector is $\mathbf{S} = c\mathbf{E} \times \mathbf{H}$, having components given in terms of the complex components, by

$$S_1 = -\frac{c}{2}\epsilon^{-2kn_2z}[N\mathfrak{X}\cos 2(\varphi_1 + \xi + \nu) + X] \quad \text{.............(8)}$$

$$S_2 = -\frac{c}{2}\epsilon^{-2kn_2z}[N\mathfrak{Y}\cos 2(\varphi_1 + \eta + \nu) + Y] \quad \text{.............(9)}$$

$$S_3 = \frac{c}{2}\epsilon^{-2kn_2z}[N\mathfrak{Z}\cos 2(\varphi_1 + \zeta + \nu) + Z] \quad \text{...........(10)}$$

where

$$\varphi_1 = k(n_1z - ct) = \text{real part of } \varphi$$

$$\mathfrak{X}\epsilon^{i2\xi} = E_1E_3 \qquad X = \tfrac{1}{2}[nE_1\tilde{E}_3 + \tilde{n}\tilde{E}_1E_3]$$

$$\mathfrak{Y}\epsilon^{i2\eta} = E_2E_3 \qquad Y = \tfrac{1}{2}[nE_2\tilde{E}_3 + \tilde{n}\tilde{E}_2E_3]$$

$$\mathfrak{Z}\epsilon^{i2\zeta} = E_1^2 + E_2^2 \qquad Z = n_1[E_1\tilde{E}_1 + E_2\tilde{E}_2]$$

These equations come directly from substituting the complex components $H_1 = -nE_2$, $H_2 = nE_1$, and $H_3 = 0$, derived from $c \operatorname{curl} \mathbf{E} = -\partial\mathbf{H}/\partial t$, in the corresponding formula for $\mathbf{S}$.

The density of the flowing energy is

$$\mathcal{E}_F = \tfrac{1}{8}\epsilon^{-2k_2z}[(E_p\epsilon^{i\varphi_1} + \tilde{E}_p\epsilon^{-i\varphi_1})(h_{pq}E_q\epsilon^{i\varphi_1} + \tilde{h}_{pq}\tilde{E}_q\epsilon^{-i\varphi_1})$$
$$+ (H_p\epsilon^{i\varphi_1} + \tilde{H}_p\epsilon^{-i\varphi_1})(H_p\epsilon^{i\varphi_1} + \tilde{H}_p\epsilon^{-i\varphi_1}) + 4J] \text{....(11)}$$

where J is independent of t (and usually taken $= 0$). It may be readily verified that the time derivative of (11) is (7). On setting $h_{pq} = \epsilon_{pq} - a_{pq}$ in (11), using (4), (5), and their conjugates, and substituting for the H_p's, (11) becomes

$$\mathcal{E}_F = \tfrac{1}{2}\epsilon^{-2kn_2z}[N^2\mathfrak{Z}\cos 2(\varphi_1 + \zeta + 2\nu) - \mathfrak{A}\cos 2(\varphi_1 + \alpha) + n_1Z + J] \text{....(12)}$$

where $\mathfrak{A}\epsilon^{i2\alpha} = \frac{1}{2}E_pa_{pq}E_q$ and J is an arbitrary function of x, y, and z.

3—*Poynting motion*

In all classical discussions of energy flow as a physical process, one has in mind essentially a fluid analogy; without this, $\mathcal{E}_F$ and $\mathbf{S}$ have only analytical meaning, no physical implications. We shall, therefore, associate with the energy

an "energy fluid" having, according to Poynting's theorem, density $\mathcal{E}_F$ and flux $\mathbf{S}$. Assuming that all the "flowing energy" present in any region will be flowing with the same velocity, this will be the "Poynting velocity" $\mathbf{S}/\mathcal{E}_F$. The validity of this fluid analogy is not under question here; it appears to be the only basis for using $\mathbf{S}/\mathcal{E}_F$ in simple media, and so will be used as the basis for the present generalizations. The density of heat energy is not added to $\mathcal{E}_F$, as it does not take part in the ordered flow described by $\mathbf{S}$.

If in a non-absorbing medium ($N = n_1 = n$, $\mathcal{A} = 0$, $\varphi_1 = \varphi$) we take $J = 0$, we obtain immediately $S_3/\mathcal{E}_F = c/n$; that is, all bits of energy have the same z-speed, and it is equal to the phase speed. Each bit of energy then moves with constant φ and hence with constant direction. In an anisotropic medium the directions taken by successive bits are not the same; bits of energy which start near one another, therefore, move well apart in the course of time. This is the first of several peculiarities we shall find resulting from our assumptions.

In general, the instantaneous z-speed is $(dz/dt) \equiv V_3 \equiv (S_3/\mathcal{E}_F)$, which can be obtained as a function of φ_1 from (10) and (12). Except in the particular case just treated, we must introduce this function into $(d\varphi_1/dt) = k[n_1(dz/dt) - c]$ and assume J a constant before integration can be carried out. Setting

$$N^2\mathfrak{Z} \sin 2\nu \sin 2(\zeta + \nu) + \mathcal{A} \cos \alpha = \mathcal{W} \sin 2\omega$$

$$N^2\mathfrak{Z} \sin 2\nu \cos 2(\zeta + \nu) - \mathcal{A} \sin \alpha = \mathcal{W} \cos 2\omega$$

$$N^2\mathfrak{Z} \cos 2\nu \cos 2(\omega - \zeta - \nu) = \mathcal{W} L_z$$

$$N^2\mathfrak{Z} \cos 2\nu \sin 2(\omega - \zeta - \nu) = \mathcal{W} M_z$$

$$NZ \cos 2\nu = \mathcal{W} N_z \qquad J = \mathcal{W} K$$

$$\gamma = \varphi_1 + \omega \qquad \gamma_0 = \gamma(t = 0)$$

we obtain the result

$$2kct = 2(M_z - 1)(\gamma - \gamma_0) + L_z(F - F_0) + (M_z K + N_z)(G - G_0) \quad \ldots (13)$$

where

$$F = \log | K - \sin 2\gamma |$$

$$G = \log | \tan \gamma | \qquad \text{if } K = 0$$

$$= \frac{1}{\sqrt{1 - K^2}} \log \left| \frac{K \tan \gamma - 1 + \sqrt{1 - K^2}}{K \tan \gamma - 1 - \sqrt{1 - K^2}} \right| \qquad \text{if } 0 < K^2 < 1$$

$$= -\tan\left(\frac{\pi}{4} \pm \gamma\right) \qquad \text{if } K = \pm 1$$

$$= -\frac{2}{\sqrt{K^2 - 1}} \tan^{-1} \frac{K \tan \gamma - 1}{\sqrt{K^2 - 1}} \qquad \text{if } K^2 > 1$$

$$F_0 = F(t = 0) \qquad G_0 = G(t = 0)$$

Similarly, using $(d\varphi_1/dx) = k[n_1(dz/dx) - c(dt/dx)] = k(n_1 S_3 - c\mathcal{E}_F)/S_1$ and setting

$$N^2\mathfrak{X} \cos 2\nu \cos 2(\omega - \xi - \nu) = \mathfrak{W} L_x$$

$$N^2\mathfrak{X} \cos 2\nu \sin 2(\omega - \xi - \nu) = \mathfrak{W} M_x$$

$$NX \cos 2\nu = \mathfrak{W} N_x$$

we can integrate to obtain

$$-2kn_1(x - x_0) = 2M_x(\gamma - \gamma_0) + L_x(F - F_0) + (M_x K + N_x)(G - G_0) \quad \ldots (14)$$

where $x_0 = x(t = 0)$. Equations (13), (14), and a similar one for y, are the equations of motion of the various bits of energy. Let us see what sort of motion is depicted.

First consider the case $K^2 < 1$. We observe that energy in special planes having $\sin 2\gamma_0 = K$ will have $\gamma = \gamma_0$ for all finite time. All other energy (having $\sin 2\gamma_0 \neq K$) will have $\sin 2\gamma \neq K$ for all finite time, thus bounding $\gamma - \gamma_0$ to values less than π. These conditions are deduced from the fact that infinities appear on the right of (13), in the $(F - F_0)$ and $(G - G_0)$ terms, if they are not satisfied. Although the infinities could cancel if $|M_z K + N_z| = |L_z| \sqrt{1 - K^2}$, it will be shown that this condition is physically inadmissible.

As $t \to \pm\infty$, infinities must be introduced on the right of (13), and this can only be done if $\sin 2\gamma \to K$ then. When this occurs, $F \to -\infty$ only, whereas $G \to \pm\infty$ depending on which root of $\gamma = (\sin^{-1} K)/2$ is approached. In order that t may approach either $+$ or $-\infty$ (taking γ as the independent variable), the G term must outweigh the F term. Investigation shows that this requires $|M_z K + N_z| > |L_z| \sqrt{1 - K^2}$.

As t becomes infinite in one or other direction, $x - x_0$ becomes infinite with a factor $-L_x \pm (M_x K + N_x)(1 - K^2)^{-1/2}$, the sign being different in the two cases. Except when $L_x = 0$, this indicates that the energy approaches x_0 in one direction and leaves in a different one. A similar situation exists, of course, with the y-coordinate.

The complete picture is somewhat like this, then: There are a number of special planes of energy (having $\sin 2\gamma = K$) moving the constant z-speed. All the energy between a particular pair of these planes (at finite t) came originally from very near one of them and is going to end up very near the other one. In spite of this, the main bulk of the energy will always lie between special planes, as is obvious from the form of $\mathcal{E}_F$.

Moreover, the energy comes from one general direction and leaves in another which is not opposite. The whole picture, it must be admitted, is most peculiar.

More reasonable results are found when we turn to the case $K^2 > 1$. Now F simply oscillates and G varies in an orderly (if not simple) manner as γ increases or decreases, hence $\gamma - \gamma_0$ is no longer bounded. The corresponding motion of the energy is likewise orderly, though by no means simple, and all bits go through the same motions in the course of a cycle. Nevertheless, because of the varying velocity, there is some bunching of the bits of energy. This is not reflected in the over-all density $\mathcal{E}_F$, however. This implies that the amount of energy contained

in a "bit" varies over the cycle, some of it being absorbed at one time and regenerated at a later time. The picture has been improved, but it still seems unsatisfactory, at least to the present author.

4—*Mean Poynting velocity*

To compare results of this investigation with experiments or with the packet velocity, an appropriate mean value of the energy velocity must be found. One mean is found by taking a weighted average of the velocities of the bits of energy successively passing through one particular point as they are passing through it. This leads to a mean velocity given by dividing the mean density of flowing energy into the mean Poynting vector. Such an averaging method is inappropriate, however; it is of academic interest only, since no experiment can measure it. In practice, and in packet methods, we consider a flow of energy between two quite separated points. The velocity which would be obtained should therefore correspond to the mean velocity of the energy as it travels along its path, averaged over all bits of energy if need be.

If we take $J = 0$ in non-absorbing media, we obtain the constant c/n as the z-speed. Both methods of averaging this will, of course, give the same result, c/n. The same is true of the average direction of flow, though in the second method of averaging there is some question as to the physical meaning of the result when anisotropic media are considered.

If we take $J \neq 0$ in non-absorbing media, we obtain

$$\frac{\mathrm{d}\varphi}{\mathrm{d}t} = k\left(n\,\frac{\mathrm{d}z}{\mathrm{d}t} - c\right) = \frac{k(nS_3 - c\mathcal{E}_F)}{\mathcal{E}_F} = -\,\frac{kcJ}{\mathcal{E}_F} \qquad (15)$$

and the mean velocity as determined by the second method of averaging is given by

$$\overline{V}_1 = \int \frac{\mathrm{d}x}{\mathrm{d}t}\,\mathrm{d}t \Big/ \int \mathrm{d}t$$

$$= \int \frac{S_1}{\mathcal{E}_F}\,\frac{\mathcal{E}_F}{(-kcJ)}\,\mathrm{d}\varphi \Big/ \int \frac{\mathcal{E}_F}{(-kcJ)}\,\mathrm{d}\varphi$$

$$= \overline{S}_1/\overline{\mathcal{E}}_F \qquad (16)$$

$$\overline{V}_2 = \overline{S}_2/\overline{\mathcal{E}}_F \qquad (17)$$

$$\overline{V}_3 = \overline{S}_3/\overline{\mathcal{E}}_F \qquad (18)$$

where the integrals extend over long periods of time and $\overline{S}_{1,2,3}$ and $\overline{\mathcal{E}}_F$ are the usual averages over φ. Thus we again obtain the result: mean velocity = mean Poynting vector / mean energy density, the means on the right being the usual ones. Hence the two methods of averaging the velocity again give the same result. By proper choice of J, this mean velocity can be made equal to the packet velocity.

This is no longer true when we turn to absorbing media; equation (15) no longer holds and so the averaging method used in (16) breaks down. We obtain two general results for these media, depending on the magnitude of K.

If $K^2 < 1$, the bits of energy remain between the same two special planes always, and so over a very long time must have average z-speed equal to the phase speed c/n. From the discussion in section 3, it can be seen that the mean x- and y-speeds will depend on what ranges of t are used ($-\infty \to +\infty$, $-\infty \to 0$, $0 \to +\infty$, etc.), and so are of little use. A further complication arises in taking a weighted average over all bits of energy: those that are important at one time are of little importance at another. Further investigation of this case seems of little use, however.

If $K^2 > 1$, we obtain the following: when γ increases by π, t increases by $\pi/k(n_1\overline{V}_3 - c)$, F shows no net increase, G increases by $\mp 2\pi(K^2 - 1)^{-1/2}$ (according as $K = \pm |K|$), and x increases by $\overline{V}_1\pi/(n_1\overline{V}_3 - c)$. Introducing these into (13) and (14), and a similar equation for y, we obtain the mean velocity

$$\overline{\mathbf{V}} = \frac{[-M_x\mathcal{K} - N_x, -M_y\mathcal{K} - N_y, M_z\mathcal{K} + N_z]}{[(M_z - 1)\mathcal{K} + N_z + K]} \cdot \frac{c}{n_1} \quad \ldots\ldots.(19)$$

where $\mathcal{K} = K \mp (K^2 - 1)^{1/2}$, according as $K = \pm |K|$. Whether or not a suitable value of J can be found which will make this velocity equal to the packet velocity will be left an open question; the analytical difficulties in finding an answer are overwhelming. It can be shown, however, that J would have to be a discontinuous function of k for this to be true, and this itself seems physically unacceptable.

5—*Macdonald velocity*

Macdonald [7] has championed an alternative to Poynting's theorem: that the equation of energy is not (6) but rather

$$-c \int_S \left[\mathbf{E} \times \mathbf{H} + \frac{1}{2c}\frac{\partial}{\partial t}(\mathbf{A} \times \mathbf{H})\right] \cdot \mathbf{ds}$$

$$= \int_V \left[\mathbf{E} \cdot \frac{\partial}{\partial t}\mathbf{D}_{eff} + \frac{1}{2c}\frac{\partial}{\partial t}\left(\mathbf{A} \cdot \frac{\partial}{\partial t}\mathbf{D}_{eff}\right)\right] dv \ldots.(20)$$

where $\mathbf{A}$ is the vector potential chosen so $\mathbf{H} = \operatorname{curl} \mathbf{A}$. The merits of Macdonald's theorem (and a modified form of it) will not be discussed here; they are treated in a separate paper [8]. We shall, however, find the consequences of accepting Macdonald's view in the present problem.

If we take the scalar potential as zero, we obtain $c\mathbf{E} = -(\partial/\partial t)\mathbf{A}$. The rate of increase of energy density is then a constant, $(ikc/2)\, E_p\tilde{a}_{pq}\tilde{E}_q$, as may be readily derived. Macdonald, then, obtains a constant rate of conversion to heat energy (equal to Poynting's mean rate) and a constant value for the density of the flowing energy, say

$$\mathfrak{D}_F = \tfrac{1}{2}\epsilon^{-2kn_2z}[n_1Z + J] \ldots\ldots\ldots\ldots\ldots\ldots\ldots(21)$$

where J is independent of t. It may also be shown that Macdonald's flux is the constant vector

$$\mathbf{R} = \frac{c}{2}\epsilon^{-2kn_2z}[-X, -Y, +Z] \ldots\ldots\ldots\ldots\ldots\ldots(22)$$

equal to the mean Poynting vector. Macdonald's velocity, $\mathbf{R}/\mathfrak{D}_F$, is then a constant—the same for every bit of energy at all times. The mean velocity, no matter how calculated, is this same value. The motion is absolutely uniform, no peculiarities being encountered.

Since the direction of this vector is that of the mean Poynting vector as usually calculated, Scott's formulae for the direction of energy flow are vindicated on the present basis. This direction was shown [4] to be that of a wave packet in non-absorbing media, and the arbitrary J allows for correlation of the speeds given by the two methods. When the medium absorbs, J can still be used for correlation—and it is here a continuous function of k. The discrepancy in the directions obtained by the two methods reappears, however, as may be shown by a return to the problem which led to the present investigation—that of the westward deflection of energy vertically incident on the ionosphere.

6—*General summary and conclusion*

The ultimate aim of this investigation is to determine the physically observable velocity with which a signal is propagated. This, in itself, has no exact meaning, for a signal changes shape as it travels; the best we can hope for is a velocity which represents closely the motion of the signal as a whole.

Two methods, both designed to yield such a velocity, are in common use, one based on wave packets and the other on the fluid analogy. In non-absorbing media, the two results can be made to agree completely, a fact which leads to a certain amount of complacency in accepting them. When generalized for absorbing media, as they have been in the present series, their results are found to be discrepant. This leads us to consider their bases in an effort to decide which of them, if either, gives the desired velocity.

In the packet method, we build a very broad signal and follow, as best we can, the position of the maximum. This process requires approximations, so the result cannot be considered an accurate one. Nevertheless, it at least *tries* to obtain the desired velocity, its only failing being its lack of accuracy. Even this cannot be considered too great a fault, since no single result can be accurate for all signals.

It might be thought preferable to follow the "centre of mass" of the packet, rather than its maximum. This was not done in Part III, but it may be readily seen that the same result would have been obtained. This is because the packet envelope is parabolic in the relevant coordinates—t, x, y in equation (4), and x, y, z or t in equation (33) of Part III—so long as the approximations used are valid.

The alternative method, based on the fluid analogy and either Poynting's or Macdonald's theorem, does not even try to obtain the desired velocity. Instead, it finds the velocity of bits of energy in infinite waves, although there is no reason to expect that this will give the velocity of a signal.

If we wish to use the fluid analogy to find the velocity of a signal, we should logically find the velocity of the energy in just such a signal. This may be done by the same method as was used in deriving the packet velocity. We may find the energy density, flux, and velocity as series in three parameters, K, L, and M, from the expressions for the fields as given in [6]. On letting K, L, $M \rightarrow 0$ as we

did there, we find that the expression for energy velocity approaches that given for infinite plane waves. It is only now that we have any cause at all for expecting this latter expression to give the velocity of a signal. Such an expectation need not be fulfilled, however, as may be made clear by a further analogy.

Consider a stream of identical cars moving along a highway. They are evenly spaced, for the most part, but there is a bunching in one region. If all the cars in the stream (or at least, in the bunch) move with the same speed, then the region of bunching will also move with this speed. However, the cars could be moving somewhat faster than this region—cars from behind slowing down as they approach it, moving slowly through it, and then speeding up as they reach the front of it. The cars obviously correspond to bits of energy and the region of bunching to the region of the signal.

Bits of energy *can*, then, move at a different speed than the signal as a whole. To obtain such a situation, it is only necessary to have different velocities for bits in different regions. Although such a variation was not obtained above, it may be introduced by the following consideration. The approximations made on letting $K, L, M \to 0$ are only valid so long as the coefficients in the series are not too large. This is a condition that does not obtain in the distant portions of the field, so the expression obtained for energy velocity need not apply in these regions.

Thus the fluid analogy need not break down even at this stage (although some authors reject it as soon as they encounter dispersive media of the simplest kind). The only failing of the velocity derived from this analogy is that it need not be the velocity of a signal. Apparently it *is* the signal velocity in the non-absorbing case and is *not* if absorption occurs.

From all this it seems that the best approximation we can make for the velocity of a signal, at least at the present level of investigation, is the packet velocity. For homogeneous waves this is

$$\mathbf{V}_{hom} = \frac{c}{(\mathrm{R.P.}kn)_k}\left[-\frac{(\mathrm{R.P.}n^2)_\lambda}{2\mathrm{R.P.}n^2}, -\frac{(\mathrm{R.P.}n^2)_\mu}{2\mathrm{R.P.}n^2}, 1\right] \quad\ldots\ldots\ldots(23)$$

and for inhomogeneous waves of the type considered in [6] it is

$$\mathbf{V}_{inhom} = \frac{c}{(\mathrm{R.P.}kn)_k}\left[-\mathrm{R.P.}\frac{n_\lambda}{n}, -\mathrm{R.P.}\frac{n_\mu}{n}, 1\right]\ldots\ldots\ldots\ldots\ldots(24)$$

Here R.P. denotes the real part, λ and μ are direction cosines, and subscripts k, λ, μ indicate partial derivatives.

Of course, this is known to break down near absorption bands, as is discussed by Stratton [9]. A more delicate treatment, such as that of Sommerfeld [10] and Brillouin [11], must then be undertaken. As this is on an entirely different level of endeavour than the present investigation, the matter will now be dropped.

This investigation was initiated and supervised by J. C. W. Scott, to whom the author is indebted for many fruitful discussions of the subject. This work was carried out at the Radio Physics Laboratory, Defence Research Board, Ottawa.

References

[1] H. G. Booker, Phil. Trans. R. Soc., A, **237**, 411 (1938).
[2] J. C. W. Scott, Proc. Inst. Radio Eng., **38**, 1057 (1950).
[3] J. C. W. Scott, J. Geophys. Res., **55**, 65 (1950).
[4] C. O. Hines, J. Geophys. Res., **56**, 63 (1951).
[5] C. O. Hines, J. Geophys. Res., **56**, 197 (1951).
[6] C. O. Hines, J. Geophys. Res., **56**, 207 (1951).
[7] H. M. Macdonald, Electric waves, Cambridge University Press (1902).
[8] C. O. Hines, in press, Can. J. Phys.
[9] J. A. Stratton, Electromagnetic theory, McGraw-Hill Book Co., Inc., New York (1941)
[10] A. Sommerfeld, Ann. Physik, **44**, 177 (1914).
[11] L. Brillouin, Ann. Physik, **44**, 203 (1914).

ADDENDA AND CORRIGENDA, PARTS I AND II

Part I (*J. Geophys. Res.*, **56**, 63-72, 1951):

Page 64, section 2, eighth line, replace "network" by "net work."

Part II (*J. Geophys. Res.*, **56**, 197–206, 1951):

Page 199, equation (9), replace cosh $[2Kk\dot{n}_{2z}]$ by cosh $[2Kk\dot{n}_2 z]$.

Page 199, equation (10), replace kn_1 in the numerator by $k\dot{n}_1$.

Page 203, equation (26), replace $4\mathcal{R}(k)E_1$ by $4\mathcal{R}(k)E_1^+$. (Here, $\mathcal{R}(k)$ is not, of course, a reflection coefficient; $4\mathcal{R}(k)$ is actually the amplitude transmission coefficient. The notation was unfortunate.)

Page 204, second last line, replace "we have reverted to kn" by "we have reverted to $k\dot{n}$."

Page 205, equation (37), replace $(k\dot{n} + k\dot{n})$ by $(k\dot{n} + k\dot{\tilde{n}})$.

ELECTRICAL CONDUCTIVITY OF AIR IN THE TROPOSPHERE

By Rita C. Callahan, S. C. Coroniti, A. J. Parziale, and R. Patten

Geophysics Research Division, Air Force Cambridge Research Center, Cambridge 39, Mass.

(Received August 16, 1951)

ABSTRACT

Extensive aircraft measurements of the electrical conductivity of the atmosphere in fair weather were carried out over widely separated areas in the United States between February and November, 1950. Instrumentation of the plane is briefly discussed. The positive and negative conductivities were found to be equal throughout the altitude range of 35,000 feet investigated. The results are compared with those obtained earlier by other investigators. An expression for the electrical conductivity is derived on the basis of Thomson's theory of volume recombination of oppositely charged small ions, making use of Sayers' experimental results for air. This expression, taking into consideration the dependence of ionic mobility on temperature and pressure, together with the assumption that the small-ion production above the first few kilometers is due entirely to cosmic rays, gives values in excellent agreement with those observed on the B-17 and the B-29 aircraft.

An accurate determination of the electrical conductivity of the air in fair weather is important to the interpretation of ionization balance and the mechanism of electrical conduction in the lower atmosphere. The most commonly accepted values for the variation of conductivity with altitude are the results of a single flight of the balloon *Explorer II* in 1935 [see 1 of "References" at end of paper].

This laboratory has recently conducted more extensive measurements with improved apparatus using B-17 and B-29 type aircraft in order to determine more exactly the variation of electrical conductivity with altitude and time of day over widely separated areas. It was also decided to further investigate, both experimentally and theoretically, the dependence of electrical conduction on temperature, pressure, and ion production in the atmosphere. The conductivity due to the presence of both positive and negative small ions has been measured.

The apparatus consists of a cylindrical condenser system, of the Gerdien type [2] through which air flows, and a current measuring device. The current due to the charge arriving at the central electrode is passed through a high resistance,

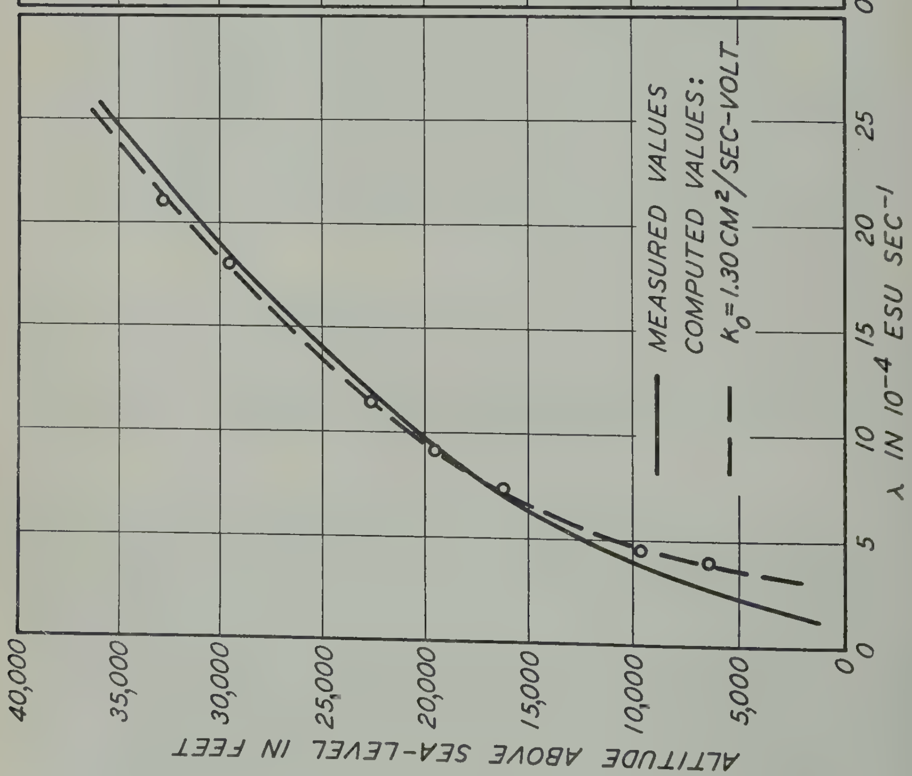

FIG. 1—ALTITUDE VS POSITIVE CONDUCTIVITY

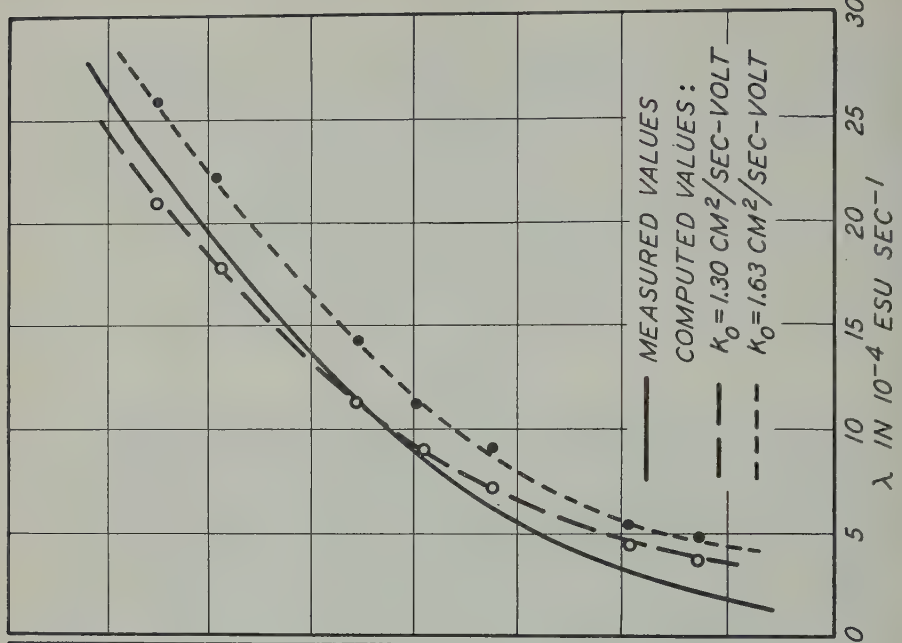

FIG. 2—ALTITUDE VS NEGATIVE CONDUCTIVITY

approximately 10^{10} ohms. The resulting iR drop is measured with a vibrating reed electrometer [3] and recorded with a Brown electronic recorder. Swann [4] has shown that, if the air-flow through the condenser is great enough, the voltage V' measured with the electrometer is given by the equation $V' = 4\pi RCV\lambda$, where C is the measured capacity of the condenser, V is the voltage applied to the condenser (90 volts in these experiments), R is the high resistance in series with the central electrode, and λ is the polar conductivity of the air.

On the B-17 aircraft, this apparatus was located in the nose of the aircraft. Air entered the chamber through a pipe which extended three feet in front of the plane and after passing through the conductivity chamber was exhausted through a hole in the side of the aircraft. The conductivity chamber on the B-29 aircraft was located in the front bomb-bay, and the recording apparatus was mounted in an adjacent radio compartment.

Discussion of results

The results of positive and negative small-ion conductivity measurements obtained on 33 flights are shown in Figures 1 and 2. These flights were conducted between March and October 1950, over areas in Florida, California, and the Northeast, throughout the daylight hours. The arithmetic mean of all observations at each altitude is indicated by the solid line. The maximum conductivity variation at a given altitude is shown in Table 1. It is surprising that such small variations occur when the measurements were obtained under such varied conditions. This variation includes any seasonal change and also any daily variation between 9 a.m. and 5 p.m. local time.

TABLE 1

Altitude	Positive conductivity		Negative conductivity	
	Mean	Limits of variation	Mean	Limits of variation
feet	*(sec^{-1})esu*		*(sec^{-1})esu*	
5,000	2.4×10^{-4}	$(1.7 - 3.2) \times 10^{-4}$	1.8×10^{-4}	$(0.72 - 2.6) \times 10^{-4}$
10,000	4.0×10^{-4}	$(3.4 - 4.4) \times 10^{-4}$	3.3×10^{-4}	$(1.6 - 4.6) \times 10^{-4}$
15,000	6.2×10^{-4}	$(5.2 - 7.1) \times 10^{-4}$	5.5×10^{-4}	$(3.6 - 7.7) \times 10^{-4}$
20,000	10.1×10^{-4}	$(9.4 - 10.8) \times 10^{-4}$	8.9×10^{-4}	$(8.1 - 10.7) \times 10^{-4}$
25,000	14.1×10^{-4}	$(13.7 - 14.4) \times 10^{-4}$	13.6×10^{-4}	$(12.7 - 14.1) \times 10^{-4}$
30,000	19.5×10^{-4}	$(19.0 - 21.1) \times 10^{-4}$	19.0×10^{-4}	$(18.4 - 19.3) \times 10^{-4}$
35,000	24.5×10^{-4}	$(22.9 - 26.1) \times 10^{-4}$	26.0×10^{-4}	

In general, the variations at a given altitude from one area to another were no greater than the day to day variations over the same area. The fluctuations in positive conductivity, shown in Table 1, are smaller than that for negative conductivity. This is due to the manner in which the observations were made. Approximately 90 per cent of the positive-ion data were obtained over the same area in Florida within an interval of about two weeks. The smaller variation in negative

conductivity above 20,000 feet is due to a greatly reduced number of observations at these altitudes.

Only measurements obtained on days which could be described as slightly hazy to clear were included in these results. It was found that dense haze definitely decreased the conductivity values. A comparison of the average values obtained on hazy and clear days is shown in Table 2.

Table 2

Altitude	Negative conductivity (mean)	
	Clear days	Hazy days
feet	$(sec^{-1})esu$	$(sec^{-1})esu$
5,000	1.8×10^{-4}	0.7×10^{-4}
10,000	3.3×10^{-4}	2.3×10^{-4}
15,000	5.5×10^{-4}	4.3×10^{-4}
20,000	8.9×10^{-4}	7.5×10^{-4}
25,000	13.6×10^{-4}	13.3×10^{-4}
30,000	19.0×10^{-4}	18.2×10^{-4}

The positive conductivity, λ_+, was found equal to that of the negative, λ_-, in the altitude range included in these experiments. This was determined by changing the polarity of the conductivity chamber in flight while maintaining constant altitude. The fact that the average value of λ_+ is slightly greater than λ_-, as indicated in Table 1, is not significant. This is explained by the fact that 90 per cent of the positive-ion data were obtained in Florida in March, where temperatures were relatively high and the weather clear. The negative-ion data, on the other hand, include many flights in the Northeast, where the temperatures were lower and slight haze was often present in the atmosphere which tended to decrease the conductivity values. The mean values of the positive and negative conductivity measurements obtained in Florida are equal.

The variation with altitude of the electrical conductivity, due to positive ions, measured in the present tests, as shown in Table 3, is in agreement with the results of the *Explorer II* flight of 1935. Very little negative conductivity data were obtained below 35,000 feet on the balloon flight. The values obtained by extrapolation are, however, consistently higher than those obtained from measurements on the B-17 flights.

A significant difference is found in the value of the ratio of the conductivities. At all altitudes where the *Explorer II* measurements were considered reliable, the negative conductivity was found to be greater than the positive. The ratio was approximately constant at all altitudes and equal to about 1.3. On the other hand, at all altitudes investigated in the present measurements, the positive conductivity was found equal to the negative. The ratio of the two conductivities determined by Gish and Wait [5] in connection with their thunderstorm investigations was also very close to unity.

It is of interest to compare computed and measured values of conductivity at

various altitudes. The computation involves a knowledge of how the mobility and concentration of small ions and the rate at which they combine depend on temperature, pressure, and the rate of small-ion production, since the conductivity, λ, is defined by the equation

$$\lambda = nek \qquad (1)$$

where k and n are the mobility of the small ion and the number of small ions per cc, and e is the charge per ion. The mobility varies inversely with gas density; therefore, $k = k_0(TP_0/T_0P)$, where T_0, P_0, and k_0 are the values of temperature, pressure, and mobility, respectively, at N.T.P. Assuming that volume recombina-

TABLE 3

Altitude	Positive conductivity	
	Average	Explorer II
feet	*(sec⁻¹)esu*	*(sec⁻¹)esu*
5,000	2.4×10^{-4}	1.8×10^{-4}
10,000	4.0×10^{-4}	3.2×10^{-4}
15,000	6.2×10^{-4}	6.0×10^{-4}
20,000	10.1×10^{-4}	11.1×10^{-4}
25,000	14.1×10^{-4}	15.0×10^{-4}
30,000	19.5×10^{-4}	21.0×10^{-4}
35,000	24.5×10^{-4}	27.0×10^{-4}

tion is the most important source of ion loss in the lower atmosphere and that $n_+ = n_-$, then the small-ion concentration is given by the relation $n = \sqrt{q/\alpha}$. If cosmic radiation is considered the only source of ionization, then q, the rate of production of ions, is proportional to the cosmic-ray intensity reduced to standard temperature and pressure and to the air density; that is, $q = I_0(PT_0/P_0T)$, where I_0 is the ionization intensity reduced to N.T.P. Thomson's [6] theoretical results for the variation of the recombination coefficient α with temperature and pressure, together with Sayers' [7] experimental results verifying this theory for temperature $T = 273$ degrees absolute, give the following expression

$$\alpha = \alpha_{T=273}\left(\frac{T}{T_0}\right)^{-3/2} \frac{\omega}{\omega_{T=273}}$$

ω is a probability function, which is the chance that a positive or negative ion should make a collision with a neutral molecule when the separation of the two is less than or equal to a certain specified distance. The expression for the recombination coefficient α is considerably simplified by substituting the expression $(T_0/T)^2$ for the expression $\omega/\omega_{T=273}$, which was shown to be approximately true by expanding in series the exponential terms in the equation for the ratio of the probability functions $\omega/\omega_{T=273}$. Upon factoring out the term $(T_0/T)^2$, errors in first-order terms are eliminated. A maximum error of six per cent in the value of α is introduced by

this approximation up to an altitude of 45 km. Substituting the resulting expression for n and k in equation (1), one obtains

$$\lambda = ek_0 \sqrt{\frac{I_0}{\alpha_{T=273}}} \left(\frac{P_0}{P}\right)^{1/2} \left(\frac{T}{T_0}\right)^{9/4} \qquad (2)$$

This equation was applied in the computation of values of λ, the results being plotted as dashed lines in Figures 1 and 2. Millikan's cosmic-ray data for geomagnetic latitude 48° were used in the computations. Good agreement is obtained with the measured values of positive conductivity, which indicates that the nature of electrical conduction in the lower atmosphere during fair weather is well understood. Below 10,000 feet, only fair agreement is obtained. This is to be expected, since below this altitude the presence of large ions and nuclei becomes important in determining the small-ion content. This was not taken into account in deriving the expression for λ.

The variation of negative conductivity with altitude was computed for two different mobility values. When the negative-ion mobility is chosen equal to that for the positive ion, $k_0 = 1.3$, good agreement, as is shown in Figure 2, is obtained between the theoretical and observed values of negative conductivity. This also results in good agreement between the computed and measured ratios of the polar conductivities, that is, λ_+/λ_- equal to unity.

Mobility measurements in the laboratory and in the atmosphere, however, have shown that, in general, k_- is greater than k_+ . Both the absolute value and the ratio of the mobilities were found to vary with water content, impurities, the age of ions, etc. The reported values of the ratio k_-/k_+ for atmospheric ions range from 1.04 to about 1.4. For this reason, the negative conductivity was also calculated using a negative-ion mobility value greater than that for the positive ion; $k_{0-} = 1.63$ or $k_-/k_+ = 1.24$. The results of these computations, shown in Figure 2, indicate only fair agreement with the measured values. This also leads to poor agreement between the measured and computed ratio λ_+/λ_- . The ion mobility is the only factor which differs in equation (2) when computing the negative and positive conductivity. Therefore, the calculated ratio of the conductivities will be equal to the ratio of the mobility values used.

The assumption that the positive small-ion content is equal to the negative small-ion content, used in deriving equation (2) was reexamined. This is an approximation, since a positive space-charge is known to exist in the free atmosphere. It has a maximum value at the surface, and decreases rapidly with altitude. Computations of the variation of positive space-charge with altitude, however, show that the excess of positive ions above one kilometer is extremely small, so that the assumption $n_+ = n_-$ is valid.

The use of a value of negative-ion mobility equal to that for the positive ion results in good agreement between the theoretical and observed values of negative conductivity. Therefore, these experimental results also indicate that within the accuracy of the measurements the mobility of the negative small ions in the free atmosphere at N.T.P. is equal to the mobility of positive ions.

Since this result is contrary to previous laboratory measurements, it appears

hat direct measurements of the mobilities of positive and negative atmospheric ons are desirable.

Summary of results in fair weather

1. There exists no important daily variation in the electrical conductivity of he atmosphere, above a few kilometers, throughout the daylight hours.
2. No significant seasonal variation in λ was found.
3. Above a few kilometers, the absolute value of the conductivity at any given ltitude was the same throughout the United States.
4. The positive conductivity was found equal to the negative up to an altitude of 35,000 feet.
5. The deduced mobility of the positive and negative ions is equal.
6. The electrical conductivity decreased in haze.
7. Very good agreement was obtained between the theoretical and observed values of conductivity. This is an indirect verification of

   (*a*) Thomson's recombination theory for the dependence of α on T and P
   (*b*) The dependence of mobility on temperature and pressure
   (*c*) The assumption that cosmic radiation is the only important source of small-ion production in the atmosphere, above a few kilometers.

The authors wish to acknowledge the cooperation of the personnel of the 3171st Squadron at Griffiss Air Force Base at Rome, New York, who flew and maintained the aircraft. We would also like to express thanks to the Air Force personnel who took part in some of these experiments.

References

[1] J. A. Fleming (editor), Terrestrial magnetism and electricity, New York, Dover Publications, Inc., p. 205 (1949).
[2] H. Gerdien, Terr. Mag., **10**, 65–79 (1905).
[3] H. Palevsky, R. K. Swank, and R. Grenchik, Rev. Sci. Instr., **18**, 298–314 (1947).
[4] W. F. G. Swann, Terr. Mag., **19**, 81–92 (1914).
[5] O. H. Gish and G. R. Wait, J. Geophys. Res., **55**, 473–484 (1950).
[6] L. B. Loeb, Fundamental processes of electrical discharge in gases, New York, John Wiley and Sons, Inc., p. 112 (1947).
[7] J. Sayers, Proc. R. Soc., **169**, 83–101 (1938).

OURNAL OF GEOPHYSICAL RESEARCH VOLUME 56, No. 4 DECEMBER, 1951

FURTHER DETERMINATIONS OF THE CONCENTRATION OF CONDENSATION NUCLEI IN THE AIR OVER THE NORTH ATLANTIC

BY VICTOR F. HESS

Fordham University, New York 58, New York

(Received September 10, 1951)

ABSTRACT

On account of the relative scarcity of data on nuclei over the oceans, the author repeated his earlier observations (1948) in July and August 1951 on the S.S. *America* from New York to Le Havre and back.

The average number of nuclei found per cubic centimeter for the western half of the Atlantic was 1,512 on the eastward trip and 1,229 on the westbound trip. On the eastern half of the Atlantic, the respective figures were 462 and 887. The mean (total) was 956 in July and 1,019 in August. Both figures are somewhat higher than in 1948.

Three years ago, I carried out a series of counts of Aitken nuclei during a oyage of the S.S. *America* (United States Lines) from New York to Le Havre France) and back (in June and August), the results of which were published in *errestrial Magnetism and Atmospheric Electricity* [see 1 of "References" at end f paper]. This year (1951), I had an opportunity to repeat this series of nucleus ounts on a journey from July 3 to July 9 (eastbound) and August 17 to 23 (westound) on the same boat; the same instrument (Aitken pocket dust counter, odified model after G. Luedeling) was used which had been recalibrated acording to the findings of V. F. Hess and C. O'Brolchain [2].

Since the number of nuclei over sea seldom exceeds 2,000 per cm^3, the "1/5 lution mark" was used throughout for sampling, so that with lower concentraons the number of droplets falling on 2, 4, or even 9 squares of the counting age could easily be observed. In all cases, the number of droplets falling after e second and third expansion was added to the number observed after the first roke of the piston. Ordinarily, this added about 10 per cent to the number of oplets noted after the first stroke.

The samples were taken aft on the upper deck of the *America*, always on the ndward side, at a spot where smoke from the funnels was not likely to produce y disturbance. This spot was about 20 feet above the water level.

In each case, about 20 individual counts were made; the average values of

each of these series of 20 are listed in the following Tables, No. 1 (eastbound trip) and No. 2 (westbound trip). On each day, about three to four such series were taken at different times of the day (morning, noon, and evening). Altogether the figures reported amount to a total number of about 800 individual counts for both trips, and the average should be fairly representative for the weather conditions of each trip. Both trips were quite different in this respect. The eastbound trip (July 3 to 10) was smooth, with fair weather prevailing during the first three days and overcast skies later, while the westbound trip was very rough for the first three days, with fair weather only on the last day.

The meteorological data were taken from the ship's log (courtesy of Mr. D. L. Lefman, Navigator and Second Officer of the *America*).

Table 1—*Nucleus content of air*
(Eastbound voyage 81 of S.S. *America*, July 3–9, 1951, from New York to Le Havre)

Date	Local time	Cloudiness	Wind	Sea	Visibility scale No.	No. nuclei N, per cm^3	Average distance from American Continent	Long. (west)	Lat. (north)	Air temp.
1951	*h m*						(*nautical miles*)	°	°	°F
July 3	20 15	Clear	SW 1	Smooth	6	1,700	46	70	41	75
July 4	09 30	Clear	SE 2	Smooth	6	2,170	356	65	41	76
	16 00	Clear	SE 3	Smooth	7	3,100	506	63	41	75
	19 45	Partly cloudy	SE 1	Smooth	7	1,600	597	61	42	74
July 5	07 30	Partly cloudy	ESE 2	Calm	6	1,920	837	55	42	74
	11 30	Hazy	ESE 3	Slight	6	1,220	929	53	42	74
	16 15	Overcast	ESE 4	Moderate	5	850	1,033	49	43	69
July 6	07 45	Cloudy	S 2	Moderate	7	585	1,382	45	44	64
	10 00	Partly cloudy	S 2	Slight	7	650	1,439	43	45	64
	13 30	Overcast	SW 3	Moderate	7	513	1,509	42	45	63
	17 00	Overcast	SW 4	Moderate	7	745	1,591	40	46	66
July 7	07 45	Cloudy	S 3	Moderate	6	625	1,912	34	47	63
	11 00	Cloudy	S 3	Moderate	6	475	1,981	31	48	63
	14 30	Rain	S 3	Slight	6	425	2,061	30	49	61
	17 15	Overcast	S 4	Moderate	6	575	2,131	28	49	63
July 8	09 45	Rain	SW 3	Slight	6	338	2,498	20	50	60
	13 45	Rain	SW 4	Slight	5	282	2,590	17	51	61
	17 30	Drizzle	SW 4	Slight	6	182	2,657	12	51	57
July 9	07 00	Fog	S	Calm	3	4.150	Off Cobh (Eire)			55
	19 00	Overcast	SW 5	Moderate to rough	6	325	Near Lands End			57
		Ship arrived at Le Havre L.V. 1:22 a.m., July 10, 1951								

Discussion of the results—According to a review of nucleus count observations over the oceans by H. Landsberg [3], the mean values of the number of nuclei obtained on the high seas range from $N = 490$ to 950 per cm^3. Similar values were reported from the cruises of the *Carnegie* over the other oceans at locations far from continents, and by J. Clay and his coworkers [4] during their journeys from Europe to the Dutch Indies (excluding the measurements in the vicinity of the African and Asiatic continents).

The values found by V. F. Hess in 1948 were $N = 575$ (June) and 813 (August) for the western part of the Atlantic, $N = 478$ (June) and 504 (August) for the eastern part of the Atlantic, while in 1951 the figures were somewhat higher, as follows:

	Western half	*Eastern half*	*Mean (total)*
Voyage in July	1512	462	956
Voyage in August	1229	887	1019

Thus, it is definitely established that the air in the western half of the Atlantic contains more nuclei than the eastern half. This is understandable, since the general circulation of the atmosphere from west to east tends to carry a great number of the nuclei generated over the American continent far out over the Atlantic.

TABLE 2—*Nucleus content of air*
(Westbound voyage 83 of S.S. *America*, August 17–23, 1951, from Le Havre to New York)

Date	Local time	Cloudiness	Wind	Sea	Visibility scale No.	No. nuclei, N, per cm^3	Average distance from Ireland	Long. (west)	Lat. (north)	Air temp.
1951	*h m*						(*nautical miles*)	°	°	°*F*
Aug. 17	16 00	Overcast	W 2	Smooth	6	4,100	Off Le Havre	0	49	65
	18 00	Clear	W 4	Moderate	7	14,000	In Eng. Channel 80 miles from Le Havre	1	50	63
Aug. 18	07 30	Cloudy	SSW 4	Rough	7	394	Nearing Cobh	8	52	61
	12 00	Cloudy	SW 6 gale	Rough	7	188	Off Cobh, in gale	8	52	62
	16 00	Cloudy; rain	SW 7 gale	Very rough	6	463	42	9	51	60
Aug. 19	07 30	Overcast	WNW 6	Very rough	7	1,205	378	18	51	58
	10 30	Overcast	WNW 7	Very rough	6	1,380	441	20	51	60
	14 30	Overcast	WNW 7	Rough	7	430	529	22	50	59
	17 00	Overcast	NW 6	Rough	7	2,000	617	24	50	61
Aug. 20	09 30	Fog	WSW 4	Rough	3	365	1,005	33	49	64
	Noon	Mist	WSW 5	Rough	4	1,190	1,050	34	48	62
	15 30	Overcast	W 4	Moderate	7	1,590	1,140	37	48	63
	17 45	Overcast	WNW 5	Moderate	7	550	1,185	37	47	63
Aug. 21	07 00	Clear	SW 1	Moderate	7	500	1,521	45	45	57
	10 00	Clear	SW 1	Smooth	6	1,730	1,616	47	44	62
	16 30	Overcast	SW 2	Moderate	6	615	1,758	50	43	65
Aug. 22	07 45	Overcast	SW 3	Moderate	7	525	2,141	58	42	69
	11 45	Partly cloudy	SW 4	Moderate	6	675	2,237	60	42	64
	17 00	Partly cloudy	SSW 5	Moderate	7	605	2,381	64	41	79
Aug. 23	07 45	Partly cloudy	NNW 3	Slight	7	4,000	About 115 miles from Ambrose L.V. (2,725 miles from Daunt L.V.)	71	40	67

There is no question, however, that a certain percentage of nuclei must be of oceanic origin and must be due to hygroscopic salt particles formed by evapora-

tion of sea-water spray, as predicted by Landsberg [3]. This will account for 10 to 500 of nuclei per cm^3 in parts of the Atlantic at 2,000 or more miles from th American continent. The smallest figures (around 180 to 200 per cm^3) were foun in the Irish Sea, with winds from the southwest. In fog or mist, the nucleus conten is not very different. Very rough sea (August 18-20) tends to increase the nucleu content (spray evaporation). On the westbound voyage, with southerly wind low values of N = 500 to 600 (August 22) prevailed even at distances of 500 mile from the American coast, while at a point 115 miles off Ambrose Light Vessel count of 4,000 was found (August 23). On the eastbound trip (July 3-5), highe nucleus content was noticeable up to about 800 miles from the American coas although the (slight) surface winds were from the southeast.

If we accept a mean value of N = 800 for the total concentration of nucle over the North Atlantic and assume according to J. J. and P. J. Nolan, A. R Hogg, F. Schachl, and others that the ratio of the number of uncharged nuclei t the number of charged ones of either sign (Langevin ions) is 2.2, we can conclud that the Langevin ions amount to about 120 of either sign, per cm^3.

The number of small ions of each sign over the sea, according to Clay [4] an his associates, is only about 200 to 300; the observations aboard the *Carnegie* gav a value of 500, but Clay [5] believes that in these measurements some ions of smalle mobilities may have been included. But even so, it is clear that the conductivit of air over the oceans in locations sufficiently far from the continents is almos entirely due to the small ions.

It is a pleasure to acknowledge gratefully the cooperation of the officers of th United States Lines aboard the *America*, and to thank the Captain, Commodor Anderson, for his permission to carry out these measurements.

References

[1] V. F. Hess, Terr. Mag., **53**, 399–403 (1948).
[2] V. F. Hess and C. O'Brolchain, Beitr. Geophys., **37**, 386 (1932).
[3] H. Landsberg, Atmospheric condensation nuclei, Ergebn. Kosm. Physik, **3**, Akad. Ver lagsgesell., Leipzig (1938).
[4] J. Clay and M. Rutgers van der Loeff, Physica, **3**, 775 (1936).
[5] Private communication of Prof. Clay.

ON THE RATE OF ION FORMATION AT GROUND LEVEL AND AT ONE METER ABOVE GROUND

BY VICTOR F. HESS AND GEORGE A. O'DONNELL

Fordham University, New York 58, New York (1) and
Iona College, New Rochelle, New York (2)

(Received September 11, 1951)

ABSTRACT

Two identical flat ionization chambers were used to find the rate of ion formation (q) by beta, gamma, and cosmic rays at ground level and at one meter above ground. From the rate of ion formation, at one meter, due to alpha particles determined previously, the rate at the ground was calculated. The total ionizations at the ground and meter levels were found to be 11.48 I and 7.40 I, respectively. Observations were made on the lawn of the garden of the Fordham University Seismic Station.

Introduction

A variation of the ionization of the atmosphere within the first few meters from the ground can be expected as alpha and beta rays diminish in intensity from the surface of the earth upward. This phenomenon is not without importance, as it determines to some extent the behavior of the conduction current and the polar conductivities close to the surface of the earth. Chalmers [see 1 and 2 of "References" at end of paper] has shown that a suitable form for the rate of ionization variation with height can lend to a sort of ionization equilibrium, in which the total space charge is relatively small, so that there is not much alteration of field with height. According to recent measurements by O'Donnell, the positive polar conductivity at the surface is not equal to the sum of the positive and negative conductivities at the one meter level, as should be expected from Scrase's [3] survey of the field's distortion within the first meter above ground. Therefore, there is a discrepancy with Hogg's [4] results. This would indicate that equilibrium is perhaps not established in all cases and that further experimentation seems to be necessary.

Since to our knowledge, only Hogg [4] has measured the variation with height of ionization near the surface of the earth, it seemed worth while to make more extensive tests. As it will be seen, our results confirm expectations and lead to a revised evaluation of the rôle of the beta radiation in the ionization of the lowest part of the atmosphere. These experiments will be continued with improved

equipment. They form part of the program of project AF 19(122)-409 of the United States Air Force Geophysical Research Laboratory.

Apparatus and method of observation

For this research, two identical ionization chambers were constructed. Strips of aluminum, 8.1 cm wide and 0.08 cm thick, were bent into square frames 30 × 30 cm. The collecting electrodes, aluminum rods 0.24 cm in diameter and bent into frames 16 × 16 cm, were centered in the chambers. External connection was made through the usual guard-ring by an aluminum rod 0.48 cm, in diameter, which was terminated by a small metal cup. A very light spring, fastened directly to the electrometer terminal, fitted into this cup. In preliminary experiments, polystyrene was used for insulation between the inner electrode and the grounded guard-ring. It was observed that this plastic picked up a static charge which was difficult to remove, and that it was also easily polarized. Because of these defects, amber was substituted. Two Lindemann-Ryerson electrometers were used. One was a slightly larger model (No. 1) and had a smaller capacity than the other (No. 2).

Preliminary experiments over a period of two months were made to determine a suitable covering for the chambers. Aluminum foil (2.5×10^{-3} cm thick) was finally adopted. The chambers were found to be slightly sensitive to changing wind velocities, but this defect was eliminated by using a low sensitivity and placing an aluminum plate (0.31 cm thick) on top of each chamber. Thus, the final form of the chambers was that of a rigid aluminum box having for the bottom an aluminum "window" 30 × 30 cm and a thickness of 2.5×10^{-3} cm. The form of the chambers made it impossible to seal them hermetically. When standing overnight, some air seeped in. To overcome this difficulty, aged air which had been stored in steel cylinders for over a month was allowed to flow slowly through the chambers during observations. The rate of flow was approximately 3 liters per minute. Forty-five volts applied between the chamber and the inner electrode gave practically saturation current. The capacity of chamber and electrometer No. 1 was 17.25 cm and No. 2 was 19.31 cm. The volume (w) of each chamber was 7,290 cm^3. For computation of the rate of ion production, the following equation was used;

$$q = \frac{C}{300we} \times \frac{\mathrm{d}V}{\mathrm{d}t}$$

Before any formal records of observations were made, the two sets of equipment were alternated between the one meter and ground levels for several series of observations. When it was found that the chambers gave corresponding results at each level, equipment No. 1 was fixed at one meter and No. 2 at ground level. Observations were made on the lawn of the enclosure of the Seismic Station of Fordham University.

Observations and discussion

The results of observations are given in Table 1. The number of observations from which the daily mean was obtained is given in parentheses. The values have

been corrected for the residual ionization of the chambers. This residual ionization was obtained by taking a series of readings with the chambers in an "iron house" having walls 10 cm thick.

TABLE 1—*Rates of ion formation at one meter (q_1) and near the ground (q_0)*

Date	q_1	q_0	$q_0 - q_1$
1950	*100 cm*	*15 cm*	
7–14	5.73 *I* (22)	7.78 *I* (18)	
7–17	5.59 *I* (16)	7.77 *I* (17)	
7–31	5.77 *I* (14)	7.92 *I* (13)	
8–4	5.45 *I* (17)	7.57 *I* (16)	
Mean	5.64 *I*	7.76 *I*	2.12
	100 cm	*3 cm*	
8–9	5.69 *I* (22)	7.97 *I* (22)	
9–6	5.59 *I* (15)	7.93 *I* (15)	
9–13	5.60 *I* (4)	7.86 *I* (4)	
9–15	5.66 *I* (13)	7.94 *I* (11)	
9–18	5.63 *I* (14)	7.78 *I* (13)	
9–21	5.75 *I* (20)	7.97 *I* (20)	
9–28	5.59 *I* (16)	7.86 *I* (11)	
9–29	5.60 *I* (15)	7.91 *I* (17)	
10–19	5.67 *I* (11)	7.87 *I* (13)	
Mean	5.64 *I*	7.90 *I*	2.26

For the same location, Hess [5] has found the value of q for cosmic rays to be 1.96 *I*. Subtracting this from the above means, the following values of q due to beta and gamma rays are obtained:

At 100 cm..................3.68 *I*
At 15 cm..................5.80 *I*
At 3 cm..................5.94 *I*

Table 2 gives the results obtained at the meter and ground levels by taking readings alternately with and without an aluminum plate (thickness, 0.31 cm) on the bottom of each chamber. This thickness of aluminum is sufficient to stop all beta rays. The last column gives the same readings after subtracting 1.96 for cosmic rays. Correction has been made for residual ionization.

In order to obtain a value of q, at 100 cm, with the aluminum plate on the bottom of the chamber, which can be compared with the mean of all values (3.68 *I*) without the plate, the ratio of the values of q at one meter with and without the plate (3.29/3.79) is multiplied by 3.68. This gives 3.19 *I*. Then,

$$3.68 - 3.19 = 0.49\ I \text{ for beta rays at one meter}$$

Similarly, for the ground (3 cm) values after obtaining the averages of the two sets in Table 2, we obtain

$$5.94 - 3.67 = 2.27\ I \text{ for beta rays at ground level}$$

Taking the mean absorption coefficient for gamma rays (hard component) in aluminum to be 0.126 cm^{-1}, we find that the intensity of these rays on passing through 0.31 cm of aluminum is reduced to 0.96 of their original values. Therefore

Table 2—*Separation of beta and gamma components*

No. 1 at 100 cm	5.75 I	(12)	3.79 I	
With an Al-plate on the bottom	5.25 I	(15)	3.29 I	
q due to beta rays			0.50 I	
No. 2 at 3 cm	9.21 I	(10)	7.25 I	(Soil very dry)
With an Al-plate on the bottom	6.69 I	(11)	4.73 I	
q due to beta rays			2.52 I	
No. 1 at 3 cm	8.65 I	(14)	6.69 I	
With an Al-plate on the bottom	5.71 I	(13)	3.75 I	
q due to beta rays			2.94 I	

4 per cent of the reduced values given above are due to gamma rays and the true rates of ionization for beta rays alone are

$$0.49 \times 0.96 = 0.47\ I \quad \text{at one meter}$$
$$2.27 \times 0.96 = 2.18\ I \quad \text{at ground}$$

If we add these decreases, 0.02 and 0.09, to 3.19 and 3.67, respectively, we obtain

3.21 I for gamma rays at one meter
3.76 I for gamma rays at ground level

At this location it has been found that the average rate of ion formation at one meter due to the alpha particles of radon and its products amounts to 0.72 I, and for thoron and its products to 1.04 I, giving for q at one meter 1.76 I [6]. From these values it is possible to make an approximate estimate of the rate of ion formation due to alpha particles at ground level.

Priebsch [7] has shown theoretically from the coefficient of turbulence and the half-lives of the radioactive matter in the air that, taking the relative amounts of radon, thoron, and thorium B at ground level as 100 per cent each, there would be 95, 27, and 76 per cent, respectively, of the ground-level concentrations present at one meter. Because of the very short life of ThA, the ratio of this element at ground to the amount at one meter should be the same as for Tn (100/27). As the number of ions produced by each alpha particle of

Tn is 1.23×10^5
ThA is 1.92×10^5
ThC is 1.71×10^5 (0.35 to ThC″)
ThC′ is 2.54×10^5 (0.65 to ThD)

and assuming the ratios for ThC and ThC′ to be the same as for ThB (100/76) the following would give the ratio of the rate of ion formation for alpha particles at ground level to the rate at one meter:

$$\frac{q \text{ at ground level}}{q \text{ at one meter}} = \frac{(1.23 + 1.92)100/27 + (1.71 \times 0.35 + 2.54 \times 0.65)100/76}{(1.23 + 1.92) + (1.71 \times 0.35 + 2.54 \times 0.65)} = 2.71$$

Because of the relatively long life of radon, the amounts present at ground vel and at one meter do not differ greatly (100/95). Therefore, the ratio of the oncentration of its products at ground level to their concentration at one meter ould be the same as for radon itself. From the above is obtained

q for thoron and its products at ground level, . . .	$1.04 \times 2.71 = 2.82\ I$
q for radon and its products at ground level, . . .	$0.72 \times 100/95 = 0.76\ I$
Total rate of ion formation at ground level, by alpha particles . .	$= 3.58\ I$

Table 3 is a summary of the rates of ion formation at ground level and at one eter above ground at the place of observation. In the third column are the results otained at the same location by Hess [5] using a different kind of ionization amber.

TABLE 3—*Summary of the rates of ion formation*

	3 cm	*100 cm*	*100 cm*
Alpha rays	3.58 *I*	1.76 *I*	1.76 *I*
Beta rays	2.18 *I*	0.47 *I*	0.40 *I*
Gamma rays	3.76 *I*	3.21 *I*	3.15 *I*
Cosmic rays	1.96 *I*	1.96 *I*	1.96 *I*
Total	11.48 *I*	7.40 *I*	7.27 *I*

The difference in total ionization at ground level (3 cm) and one meter, there- re, is 4.08 I.

The total nuclei (Z) found at this location has the mean value 40,000 per cm^3]. The mean concentration of small positive ions in the daytime according to e measurements of one of the authors [5] is 161 cm^3. If we reduce Schweidler's uation

$$q = \alpha n_1 n_2 + 2\eta_2 n_1 N_2$$

the form $q = \omega Z n_1$ by using the relations for equilibrium, $N_0/N_2 = 2.2$ and $= N_0 + 2N_{\pm}$, and using Scrase's value $\eta_2 = 2.35 \times 10^{-6}$ as being the more rrect value for a location having a high concentration of nuclei and a low con- ntration of small ions, the value of ω becomes 1.12×10^{-6} for this location.

Substituting the values of Z, n_1, and ω in $q = \omega Z n_1$, $q = 7.17\ I$. This is in od agreement with the above experimental value (7.40).

The decrease in the rate of ion formation between 3 cm and 15 cm was found be very small (0.14 I for beta and gamma rays). This is smaller than should expected if the decrease with height were due only to the air absorption of the ta and gamma radiations from the soil. But, as we have seen above, near the ound there is a considerable higher concentration of radioactive matter in the , particularly of thoron and some of its products, than at one meter above

ground. This would account for the small decrease in the rate of ion formatio
up to 15 cm.

References

[1] J. A. Chalmers, Q. J. R. Met. Soc., **72**, 199–205 (1946).
[2] J. A. Chalmers, Atmospheric electricity, Oxford, Clarendon Press, p. 81 (1949).
[3] F. J. Scrase, London, Met. Office, Geophys. Mem., No. 58 (1933).
[4] A. R. Hogg, Mem. Solar Obs., Mt. Stromlo, Canberra, No. 7 (1939).
[5] V. F. Hess, Arch. Met. Geophys. Biokl., A, **3**, 56–63 (1950).
[6] R. P. Vancour, Thesis, Fordham University, New York (1950).
[7] J. Priebsch, Physik. Zs., **16**, 622–629 (1931).
[8] M. Donnelly, Thesis, Fordham University, New York (1949).

AN AID FOR COMPUTING THE DENSITY OF THE UPPER ATMOSPHERE*

BY EDWARD V. ASHBURN

Naval Ordnance Test Station, Inyokern,
China Lake, California

(Received September 4, 1951)

ABSTRACT

A graph is given that will aid in the rapid calculation of the density distribution of the upper atmosphere when the scale height and the scale height change with altitude are given.

Warfield [see 1 of "References" at end of paper] and Grimminger [2] have ublished tables of the density of the upper atmosphere. Each of these sets of ables was computed for only one specified vertical distribution of temperature. The temperatures and temperature gradients that have been computed from in-irect methods vary between relatively wide limits for any given altitude in the tmosphere. In addition, it appears probable that there are periodic and aperiodic emperature changes at all elevations. The extension of the previously published tmospheric density tables to cover a wider range of temperature distributions vould therefore be useful.

Marcel Nicolet [3] has suggested that the author compute the densities ac-ording to the following method. The gas law may be expressed as

$$P = kTn \quad \text{.............................(1)}$$

here P = pressure, k = Boltzman constant, T = absolute temperature, and = number of molecules per cubic centimeter. The hydrostatic equation is

$$\mathrm{d}P = nmg\mathrm{d}h \quad \text{.............................(2)}$$

here m = molecular weight, g = acceleration of gravity, and h = height.

Combination of equation (1) with equation (2) gives

$$\frac{\mathrm{d}n}{n} = \frac{\mathrm{d}h}{H_1 + \beta h} - \frac{\mathrm{d}H}{H} - \frac{\mathrm{d}g}{g} - \frac{\mathrm{d}m}{m}$$

here $H_1 = kT_1/mg$ is the scale height at h_1 and β is a constant. Integration of quation (3) between limits corresponding to h_1 and h_2 yields

*Work done under Project NR-082-045 of the Office of Naval Research.

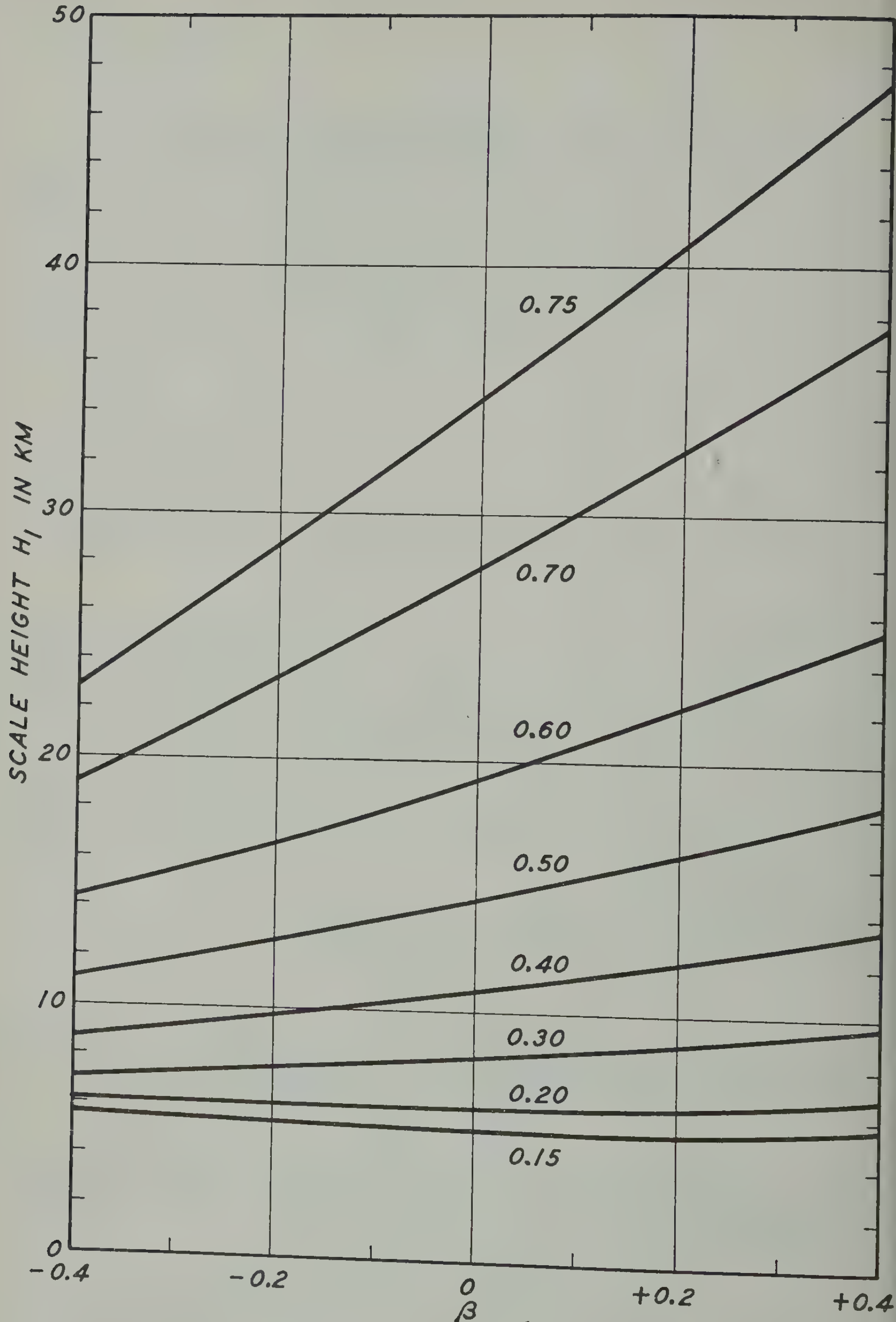

FIG. 1—ISOLINES OF $(H_1/H_2)^{(1+\beta)/\beta}$ FOR $h=10$ KM

$$n_2 = \frac{n_1 g_1 m_1}{g_2 m_2} \left(\frac{H_1}{H_2}\right)^{\frac{1+\beta}{\beta}} \qquad (4)$$

$_2 = H_1 + \beta h_2$ is the scale height at h_2 .

Figure 1 gives the values of

$$\left(\frac{H_1}{H_2}\right)^{\frac{1+\beta}{\beta}}$$

significant factor in equation (4), as a function of H_1 and β for $h = 10$ km.

References

[1] C. N. Warfield, Tentative tables for the properties of the upper atmosphere, National Advisory Committee for Aeronautics, Technical Note 1200 (1947).

[2] G. Grimminger, Analysis of temperature, pressure, and density of the atmosphere extending to extreme altitudes, Rand Report R-105 (1948).

[3] M. Nicolet, Conversation.

VARIATION OF [*OI*] EMISSION (5577) ON THE NIGHT OF 5/6 JANUARY 1951

By Dorothy N. Davis

United States Naval Ordnance Test Station,
Pasadena and China Lake, California

(Received September 14, 1951)

ABSTRACT

Photoelectric observations of the nightglow on 5/6 January 1951 are analyzed and compared with similar observations made on the following night. The height of the oxygen layer, as deduced from the variation of I_Z/I_O with zenith distance, is 200 ± 25 km. Comparison of observations in the east and west with an isophote map based on the remainder of the sky provides semi-quantitative support for the Roach-Pettit hypothesis that there is an apparent westward diurnal motion of a stable excitation pattern. A height of 300 km is indicated by the time required for a given emission area to progress from east to west.

I—INTRODUCTION

The data which are analyzed in this paper were obtained at Cactus Peak (near the Mojave Desert) with the photoelectric photometer described recently by F. E. Roach and Helen Pettit [see 1 of "References" at end of paper].

Instrumentation, calibration, and the method of treating data were identical for both nights. In order to show that the night of 6/7 January 1951 was not anomalous and that the Roach-Pettit hypothesis of a semi-fixed intensity pattern provides an even more fruitful basis for analyzing nightglow data, the observations of the preceding night (5/6 January 1951) are discussed in some detail.

II—HEIGHT OF EMITTING LAYER

The method of estimating height from the variation of $\overline{I_Z/I_O}$ with zenith distance has been described before [2]. Figure 1, where $\overline{I_Z}/\overline{I_O}$ (arithmetic mean of average I_Z/I_O for all surveys) is plotted *versus* Z, shows that the oxygen layer was about 50 km lower on 5/6 January 1951 than on the following night. The absolute value of the height depends on the choice of absorption and scattering coefficients, both of which were assumed equal to 0.125 for the theoretical curves*

*I am indebted to Miss Pettit for allowing me to use her computations of theoretical intensity ratios.

in Figure 1. The results are summarized in Table 1, which shows that over a rang covering the most reasonable values of τ the oxygen layer was at a height o 200 ± 25 km, depending upon the choice of extinction coefficients.

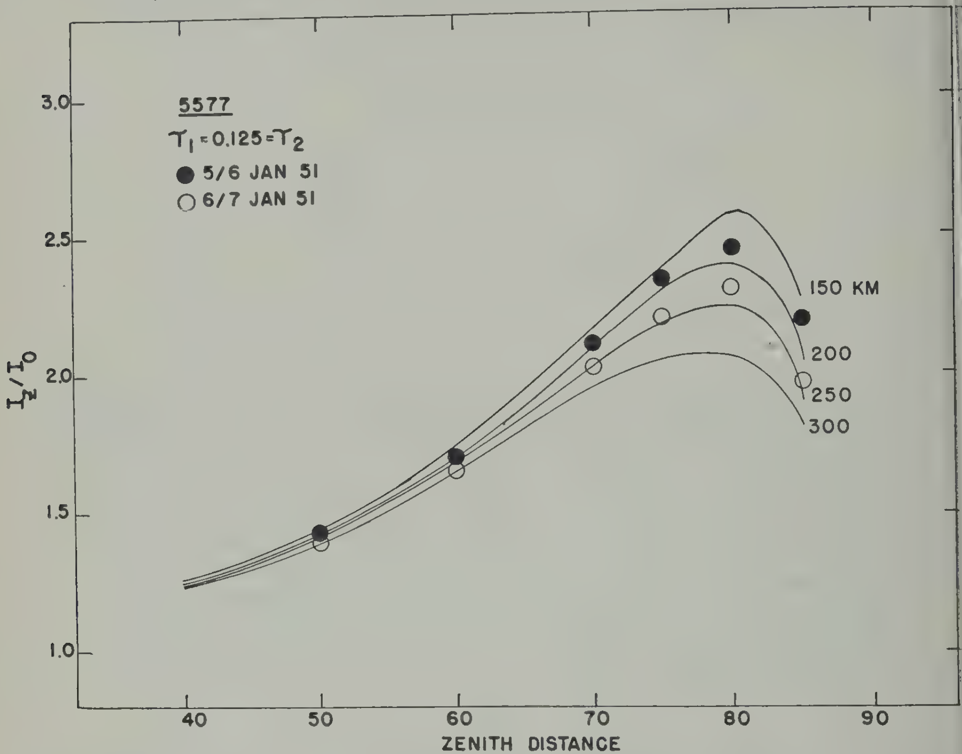

Fig. 1—$\bar{I}_Z/\bar{I}_O$ *versus* Z for 5577. Theoretical curves are based on computations for $\tau_1 = \tau_2 = 0.125$

III—COMPARISON OF ISOPHOTE MAPS BASED ON SWEEPS 1, 2, 3, 7, AND 8

In their study of the observations on the night of 6/7 January 1951, Roach and Pettit concluded that the data were best represented by an east-west alignment of observations from successive surveys. The resulting panoramic isophote

Table 1—*Dependence of deduced height on extinction coefficients*

τ_1 (Absorption)	τ_2 (Scattering)	Deduced height of oxygen layer, 5/6 January 1951
		km
0.10	0.10	225
0.10	0.05	200
0.125	0.125	180

map showed that the observed phenomena may be most easily interpreted by supposing that the observer, while being carried eastward by the earth's rotation views successive portions of a semi-fixed intensity pattern.

In addition to using the north-south data of Sweep 1 for an isophote map, we have plotted also the data from Sweeps 2, 3, 7, and 8. The sequence of sweeps of the observing program is shown in Figure 2. Panoramic space-time maps are

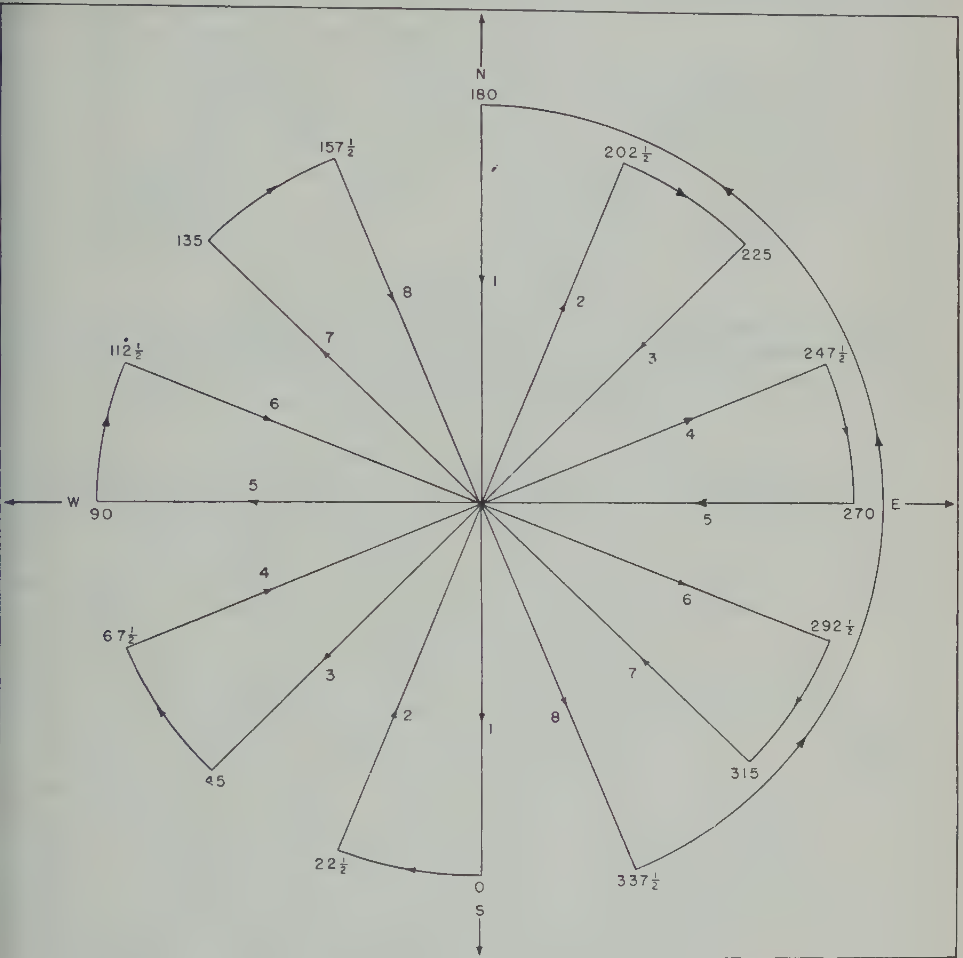

FIG. 2—Sequence of sweeps in observing program

constructed by entering successively for each sweep the local zenith intensities in the proper geographical positions, the scale depending on the assumed height. Isophotes are then drawn for every 50×10^6 quanta.

The isophote maps resulting from the data of Sweeps 1, 2, and 3 are remarkably similar. While the Sweep 7 map appears to differ most from the Sweep 1 map, the relationship may be clearly traced through the Sweep 8 map, which resembles both the Sweep 1 and Sweep 7 maps. Although the agreement is close, it is not feasible to construct an average isophote map by entering the data for all five sweeps on a single map. In addition to instrumental errors, there exist small scale time and/or space variations in intensity. In practice, the data from four sweeps

were combined by superimposing tracings of the different maps and drawin generalized isophotes for a single representative isophote map, which will b referred to hereafter as the Sweep 1238 map (see Fig. 3).

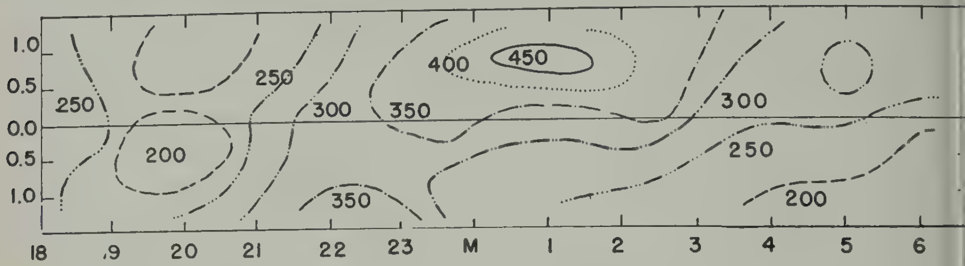

Fig. 3—Space-time isophote map for 5577 on 5/6 January 1951. The ordinate scale has been explained in a paper by Roach and Pettit [3]. For a layer height of 250 km, unity corresponds to 964 km, the distance along the earth's surface to the point directly beneath the intersection of the line of sight for $Z = 80°$ and the emitting layer.

When the Sweep 1238 map was compared with each of the five separate maps, the maximum deviations observable for the six isophotes were determined by inspection. Table 2 shows that although the Sweep 7 map least resembles the others,

Table 2—*Maximum deviation of isophotes on Sweep 1238 map from isophotes on single sweep maps*

	Maximum deviation in quanta $\times 10^6$						Average
Isophote	200	250	300	350	400	450	
Map							
Sweep 1	20	30	25	25	35	30	28
2	10	15	20	20	30	50	24
3	25	40	35	20	25	50	36
7	50	50	65	50	20	10	41
8	50	30	50	35	50	25	40
	Average maximum deviation for all isophotes						34

the average maximum deviation from the Sweep 1238 map is nearly the same a for the Sweep 8 map. Perhaps the main reason why the Sweep 7 and Sweep 8 maps differ more from the average map than the other maps is due to the fac that the Milky Way coincided for the longest time with Sweeps 7 and 8. Ou method of subtracting the intensity observed at 5300 Å may not correct perfectl for background light in the Milky Way.

IV—DEDUCTIONS FROM DATA OF SWEEPS 4, 5, AND 6

If the local zenith intensities from Sweep 5 are plotted in the same manne as those from Sweeps 1, 2, 3, 7, and 8, the values fall along the time axis. Since i

impossible to construct space-time isophote maps from such data, some other anner of utilizing the data of Sweep 5 as well as Sweeps 4 and 6 was sought. It ill be shown not only that the latter may be compared significantly with the her data, but also that the resulting comparison provides semi-quantitative

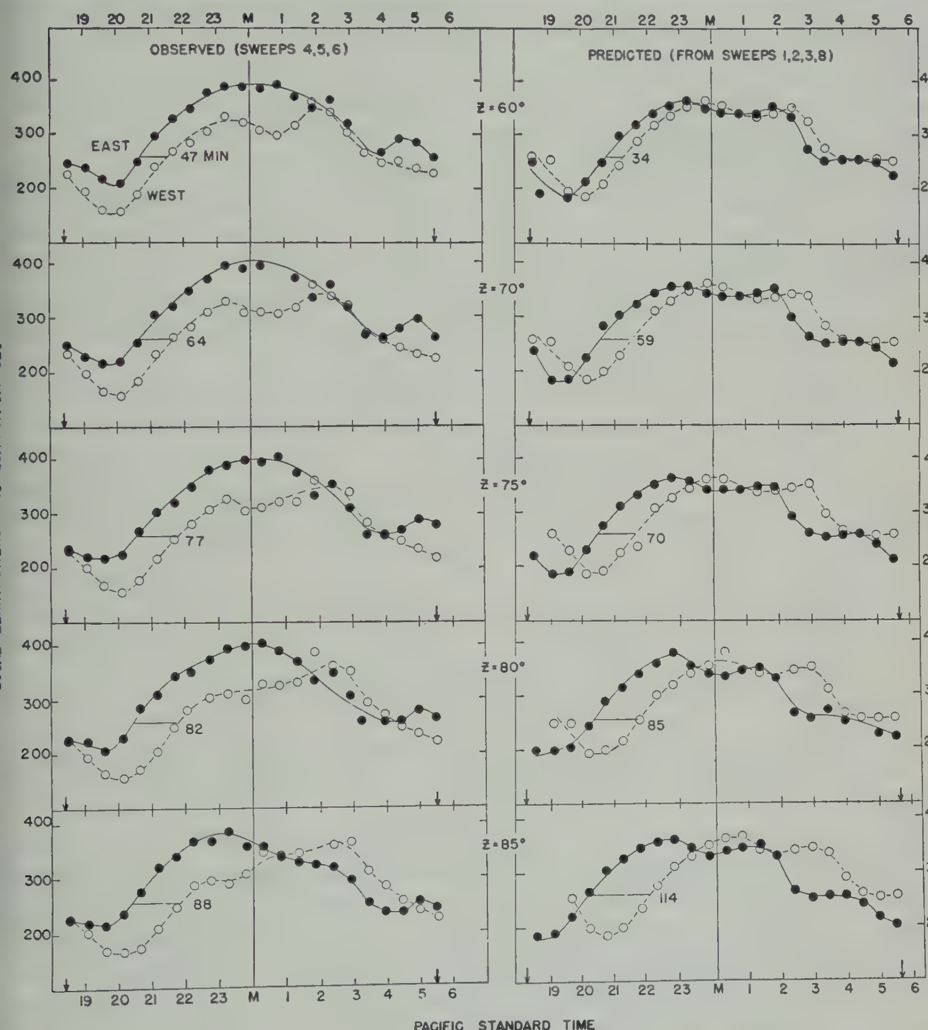

IG. 4—Intensities in east (filled circles) and west (open circles). *Observed* intensities are averages f observations in Sweeps 4, 5, and 6; *predicted* intensities were deduced from Sweep 1238 isophote ap; arrows on the time axis indicate the end of astronomical twilight and the beginning of dawn. Measured values of $2\Delta t$ are shown near the center of each section.

upport of the Roach-Pettit hypothesis. According to this hypothesis, when looking ast one would observe the intensity which will be observed overhead after an inerval Δt, where Δt depends on the height of the emitting layer and the zenith istance. Similarly, if looking west, one would obseve the intensity which was bserved overhead Δt minutes earlier.

The value of Δt may either be computed as a function of height and zenit distance, or it may be deduced from the Sweep 1238 map (Fig. 3) by laying zenith distance scale (for a plausible height such as 250 km) along the time axi centering it each time at the position corresponding to the middle of each surve and interpolating by inspection for the intensity which corresponds to each zenit distance. When the east and west intensities thus derived are plotted against tim the curves in the right half of Figure 4 are the result. It will be seen that th predicted curves correspond closely to the observed curves in the left half Figure 4 in at least one important respect; namely, when the portion of the pattern where the isophotes are perpendicular to the time axis, passes across the field view, the east and west curves are nearly parallel and separated by an interva $2\Delta t$, which is close to the correct value for a height of 250 km. It should be note that the value deduced for $2\Delta t$ does not depend upon the use of local zenith in tensities. The results would have been the same if slant intensities had been plotted

The results are summarized in Table 3, where computed values of $2\Delta t$ fo

TABLE 3—*Time interval, $2\Delta t$, between east and west positions of equal intensity*

Z	Observed time lag, 5/6 January 1951	Predicted time lag*	
		h = 250 km	h = 300 km
degrees	*minutes*	*minutes*	*minutes*
85	88	115	128
80	82	86	98
75	77	66	76
70	64	52	61
60	47	33	42

*Computed for apparent pattern velocity equal to earth's rotational velocity, latitude = 36°.

heights of both 300 and 250 km are given. Although the numerical agreement not perfect, the trend is in the right direction for an apparent east-west motion Little weight should be given to the 85° curves because the true intensities ar especially difficult to determine at such low altitudes. Furthermore, the volum of the earth's atmosphere which is included in the field of view is far greater a 85° than at any lesser zenith distance. The observed intensity at 85° is thus boun to be an average of considerably different intensities. In addition, the Sierra occulted part of the western field of view at 85°.

If the numerical differences between the observed and predicted curves i Figure 4 are plotted *versus* time, the resulting plots (Fig. 5) show that there we three main periods when the deviations were greatest; namely, when the maximu shown in Figure 3 was passing, and when conditions were evidently disturbe after twilight and just before dawn. Instead of concluding that the Roach-Pett hypothesis is not applicable at these times, it seems more reasonable to conclu that another force is operating simultaneously to disturb the intensity patte which on the average is well represented by the Sweep 1238 map. It may ve

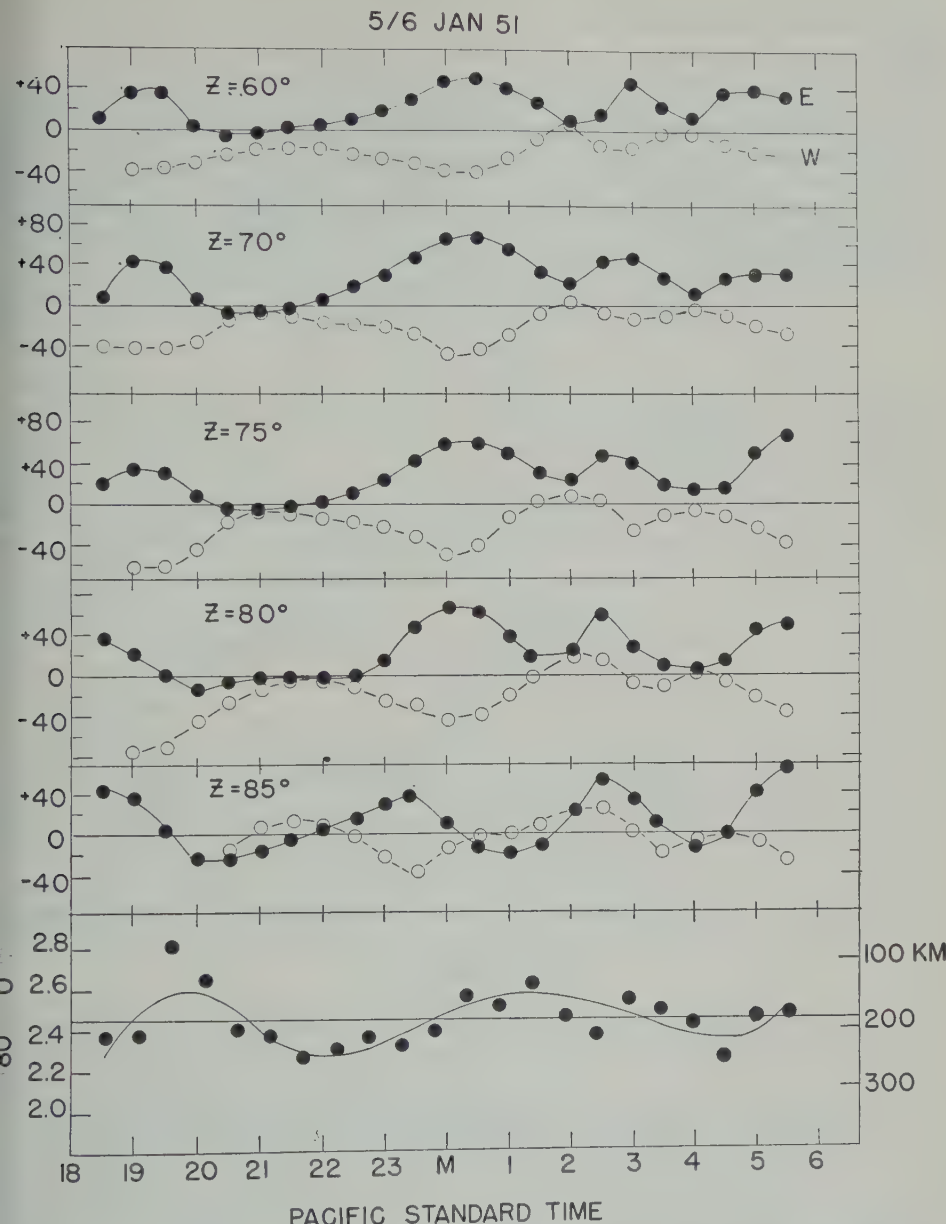

G. 5—Differences (observed minus predicted in Fig. 4) between intensities in east and west

ell be that the formation of a maximum is attended by some vortex motion of e emitting material, which is sufficient to maintain the eastern intensity on a gher level than the western. The curves in Figure 5 show that random, short-eriod fluctuations are probably ruled out, in favor of systematic fluctuations hich require more than an hour to develop. It should be pointed out, of course,

that our method of analysis smoothes out fluctuations taking place in less than 3 minutes.

Another factor which might be operating simultaneously is change of height of the whole emitting layer or even large portions of the layer. The average height of the layer may alter during the night, possibly in a manner similar to that observed for the ionospheric layers. In addition, winds exist. Curves plotted in the manner of Figure 4 would be affected by height changes in at least two ways. The lower the layer, the smaller Δt would be. If we may take the ratio I_Z/I_O as measure of height, a plot of $\bar{I}_{80}/\bar{I}_0$ (see bottom of Fig. 5) shows that the layer

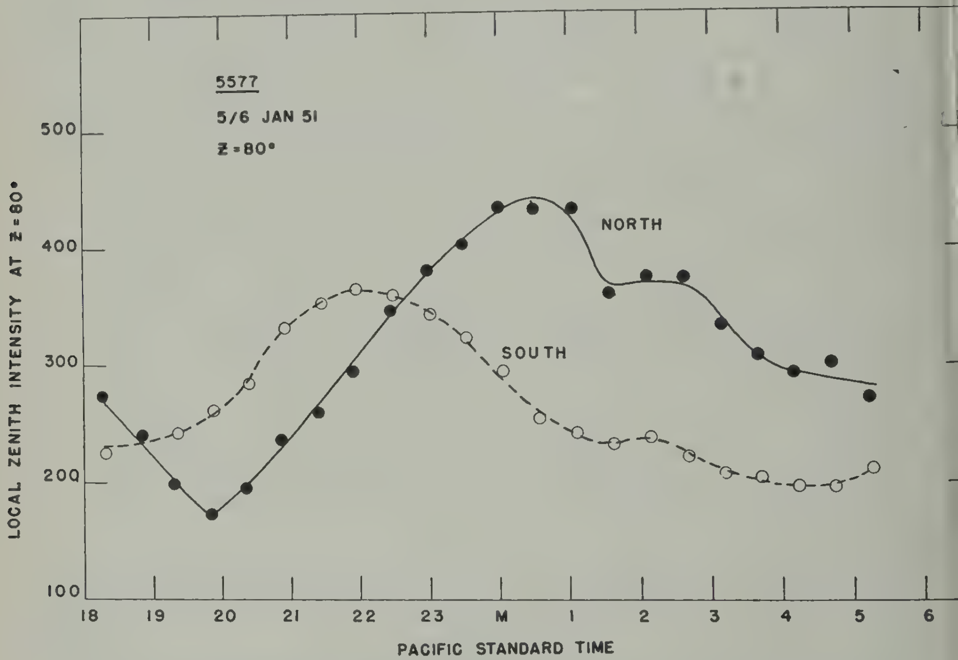

Fig. 6—Local zenith intensities (in quanta/cm² sec) at $Z = 80°$ in north and south

emitting 5577 Å was, indeed, lower when Δt was smaller; that is, between 02^h 00 and 04^h 00^m (PST). Furthermore, $\bar{I}_{80}/\bar{I}_0$ was smaller than the average value fro 21^h 30^m (PST) until midnight, when the conditions were most favorable for determining $2\Delta t$. As a result, a greater height should logically be deduced from th $2\Delta t$ values than from the $\bar{I}_Z/\bar{I}_O$ values, the latter being averages for the whole night.

Another way in which height change may produce deviations is by causin the division of q (number of quanta) by the all-night average of $\bar{\bar{I}}_Z/\bar{\bar{I}}_O$ to produ relatively incorrect local zenith intensities when the instantaneous height is f from the average height. For example, if the layer is 75 km higher than the averag I_{80}/I_0 is 9 per cent smaller. Hence, the calculated local zenith intensity would 9 per cent too large.

V—INTERPRETATION OF NORTH AND SOUTH INTENSITY CURVES

When intensities are plotted *versus* time for zenith distances of 80° north and 0° south (see Fig. 6), each curve has a single maximum separated by an interval f $2^h\ 28^m$. Contrary to the behavior noted for the following night,* the maximum ı the south preceded the maximum in the north on 5/6 January 1951. This result ıight have been anticipated from a study of the Sweep 1238 isophote map (Fig. 4). f the order of reaching a maximum is regarded as indicating a north-south comonent of motion, it could be concluded that the maximum was travelling in pposite directions on the two nights with different velocities.

VI—CONCLUSIONS

(1) The variation of $\overline{\overline{I_Z/I_0}}$ with Z shows that the oxygen layer is at a height f 200 ± 25 km. On the other hand, the time lag data from Sweeps 4, 5, and 6 ıdicate a greater height, close to 300 km. If a diurnal change of height can be dmitted, these seemingly discordant conclusions may be reconciled (see above).

(2) The fact that observations made exclusively in the east and west (Sweeps , 5, and 6) agree so well, quantitatively as well as qualitatively, with deductions rom observations which were made only in the remaining three-fourths of the ky is a strong point in favor of the Roach-Pettit hypothesis.

ACKNOWLEDGMENT

For the privilege of analyzing these interesting observations, I am indebted to Dr. F. E. Roach and the other observers, P. St. Amand and H. Pettit. J. Heppner, f the Geophysical Institute of the University of Alaska, gave computing assistance, nd H. Pettit prepared the illustrations. Discussions with F. E. Roach, E. V. shburn, P. St. Amand, and D. R. Williams were valuable.

The project was supported in part by a research grant from the Office of Naval Research, Project NR-082-045.

References

[1] F. E. Roach and H. Pettit, On the diurnal variation of [OI] 5577 in the nightglow, J. Geophys. Res., **56**, 325–353 (1951).

[2] F. E. Roach and D. Barbier, The height of emission layers in the upper atmosphere, Trans. Amer. Geophys. Union, **31**, 7–12 (1950).

[3] F. E. Roach and H. Pettit, Ann. d'Astrophys., in press (1951).

*Roach and Pettit, Figure 10.

UR DES OBSERVATIONS À LA LIMITE ULTRAVIOLETTE DU SPECTRE DU CIEL NOCTURNE

By F. W. Paul Götz et M. Nicolet

Lichtklimatisches Observatorium, Arosa, Suisse (1) et Service du Rayonnement, Institut Royal Météorologique, Uccle, Belgique (2)

(Received October 3, 1951)

ABSTRACT

An analysis of the ultraviolet limit of the airglow spectrum is given. Indications on the presence of the electronic system of OH are compared with the results obtained by identification of Herzberg's bands.

(1) Au cours des années 1936 à 1940, des observations spectrales du ciel nocturne nt été effectuées à la Station du Tchuggen (altitude 2,000 m) du Lichtklimatisches bservatorium à Arosa. Le but de ces observations était l'analyse du spectre du el nocturne ultraviolet avec un spectrographe ouvert à $F/1$ à prisme de quartz [1] ont la dispersion moyenne était de 400 Å entre λ3000 Å et λ4000 Å.

Parmi les spectres obtenus, nous avons retenu

1936	—Zénith et horizon	—fente normale	—Durée de la pose: 45 heures
1938–1939	—Horizon	—fente fine	—Durée de la pose: 75 heures
1939–1940	—Horizon	—fente normale	—Durée de la pose: 120 heures
1940	—Horizon	—fente normale	—Durée de la pose: 45 heures

Les spectres ne purent être analysés complètement au cours des années 1940–945. Entretemps, les publications successives de Elvey, Swings, et Linke [2], e Barbier [3] et de Déjardin et Dufay [4] ont fourni les données essentielles pour le ectre ultraviolet. Nos résultats sont essentiellement les mêmes pour toutes les diations intenses mesurées par ces auteurs. Comparés aux spectres de Barbier, os spectres ne présentent pas les mêmes qualités générales. Peut-être y a-t-il rtaine structure dans le spectre de 1938–39 pris avec une fente très fine, mais ous ne sommes pas certains que les détails sont tous réels. En conséquence, il ne ous apparaît pas utile de reproduire les résultats obtenus.

(2) Cependant, le spectre dont la durée de pose fut de 120 heures permet analyser l'extrémité ultraviolette jusqu'aux plus courtes longueurs d'onde. 'ailleurs, cette longue durée de pose fut à l'époque envisagée pour une étude rticulière du domaine spectral de longueurs d'onde inférieures à 3100 Å.

Le spectre est sur-exposé jusqu'à 3145 Å. Un dessin d'un enregistrement micro-otométrique de 3600 à 3213 est donné à la Figure 1. En utilisant diverses sensi-

bilités avec le microphotomètre Zeiss de l'Observatoire Royal de Belgique, il a é possible d'analyser le domaine spectral de longueurs d'onde inférieures à 3145 Å La Figure 2 permet de se rendre compte de la variation d'intensité en allant d λ2950 Å à λ3213 Å.

On note les radiations 2996 – 3004 – 3018 – 3029 – 3051 ? – 3062 ? – 3067 ? e 3078 – 3087 – 3095.

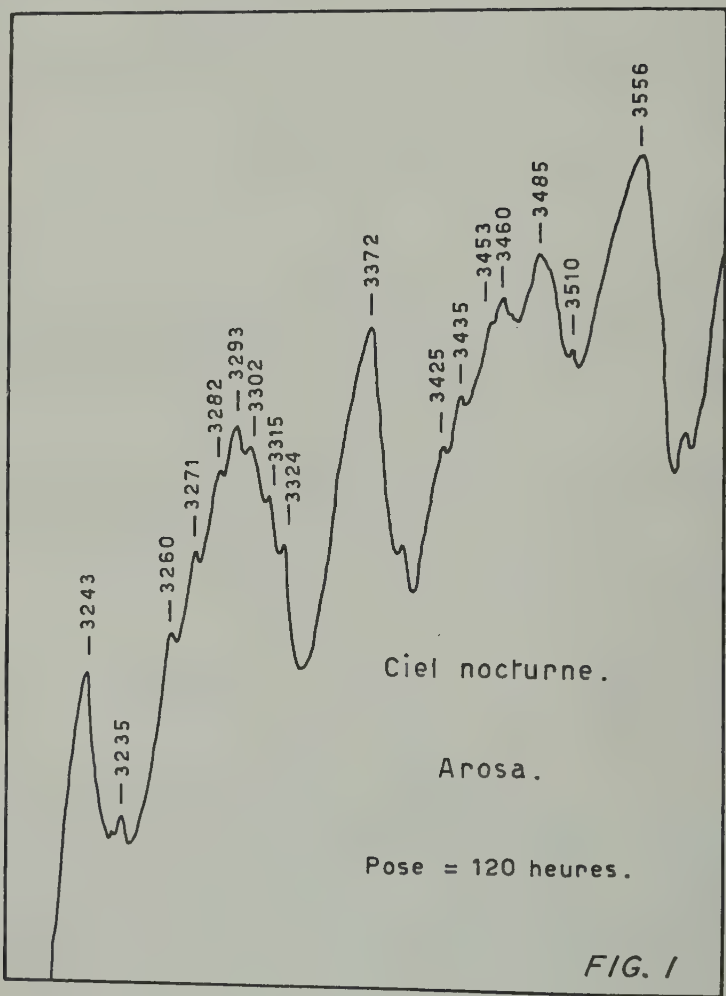

FIG. I

En confrontant cette liste avec celle de Déjardin et Dufay [4] on voit que, dans la liste I, les radiations 3096 – 3085 et 3029 sont indiquées. Dans leur liste II apparaissent 3074 – 3067 – 3052 (3041) – 3019 (3012) – 3004 – 2996.

La liste de Dufay et Déjardin [4] est limitée à 3029 Å et Barbier [3] n'a observé aucune raie de $\lambda < 3083$ Å. Il est donc certain que c'est par suite de la longue durée de pose (120 *h*) avec un spectrographe ouvert à $F/1$ que l'observation* a pu être

*Voir, par exemple, reference [5].

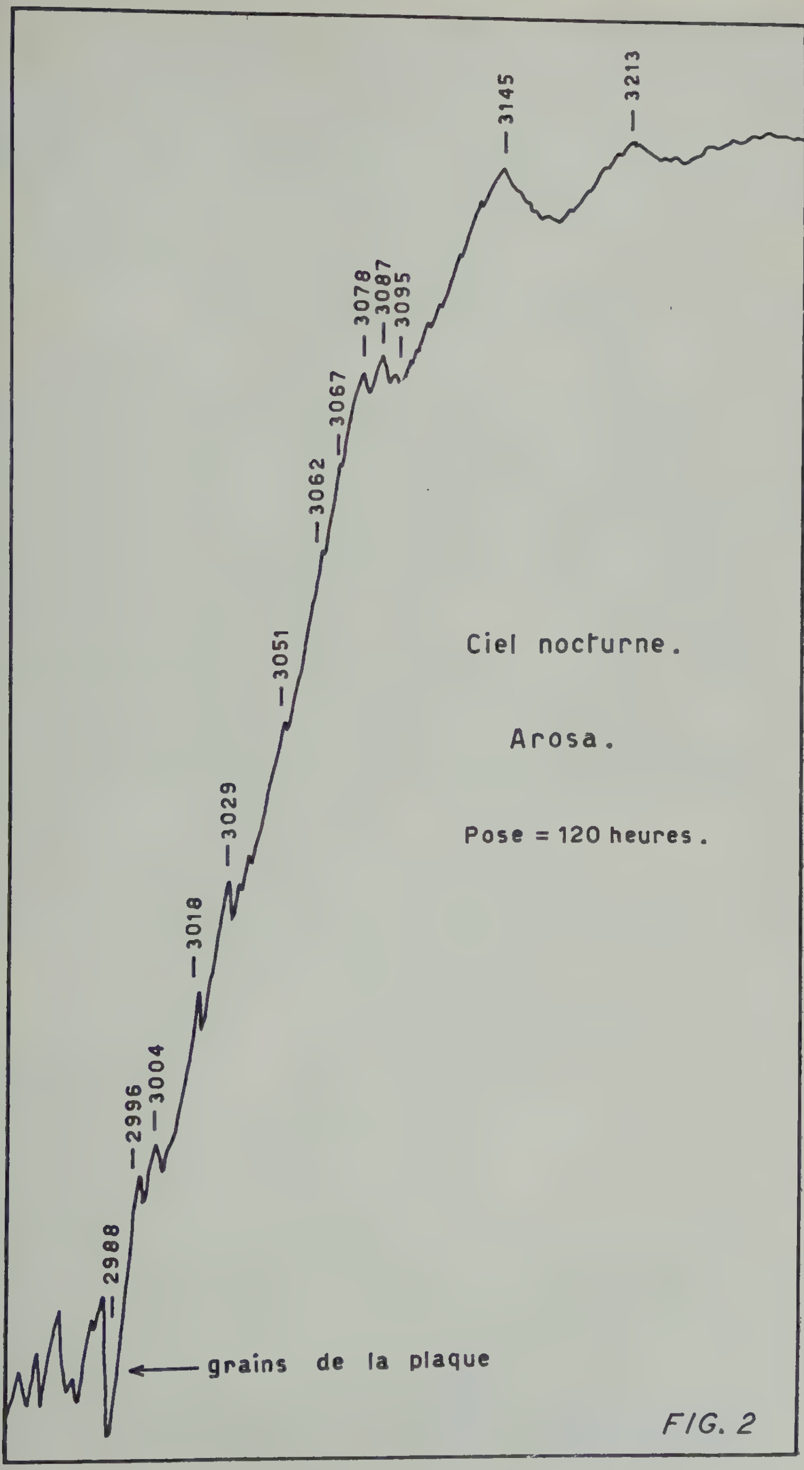
3213
3145
3078
3087
3095
3067
3062
3051
3029
3018
2996
3004
2988
Ciel nocturne.
Arosa.
Pose = 120 heures.
grains de la plaque

FIG. 2

effectuée jusqu'à 3000 Å malgré l'absorption de l'ozone atmosphérique. De plu aucune radiation n'apparaît à des longueurs d'onde plus courtes.

(3) *Essai d'interprétation*—D. Barbier [3] a interprété les deux bandes à λ3213 et λ3144 Å respectivement par les deux bandes de Herzberg (2–4) et (3–4) et deux bandes à λ3164 Å et λ3084 par les bandes (5–5) et (4–4). On peut donc prendre, dans les mêmes notations, les autres bandes de Herzberg de $\lambda < 3080$ Å. On [4]

$$(1\text{–}2),\ \lambda 2993;\ (2\text{–}3),\ \lambda 3064;\ (3\text{–}3),\ \lambda 3002;\ (5\text{–}4),\ \lambda 3025\ \text{Å}$$

qui devraient correspondre aux radiations du ciel nocturne

$$2996 \qquad 3067 \qquad 3004 \qquad 3029$$

Néanmoins, avant d'être assuré d'une identification certaine, il faut attend une nouvelle détermination basée sur la structure de vibration et de rotation fai par Herzberg [6]. D'après son étude, la numérotation des nombres de vibration doit être augmentée de 3 unités, c'est-à-dire $v' = 0 + 3$. D'après notre enregistr ment, la structure vers λ3085 n'apparaît pas simple. Il semble y avoir des band situées grosso-modo à $\lambda\lambda$3078 – 3087 et 3095 Å. Il n'est pas possible de dire si u telle structure fine du système $^3\Sigma_u^+ \rightarrow {}^3\Sigma_g^-$. C'est pourquoi il est utile d'attir l'attention sur la concordance qui apparaît avec la bande (0–0) du systèm $^2\Sigma - {}^2\Pi$ de OH. On retrouve d'ailleurs dans les publications diverses discussio sur le sujet; mais, les procédés de comparaison utilisés permettent difficilement tirer des conclusions affirmatives sur la présence des bandes de OH. Au contrai les observations les plus récentes indiquaient plutôt leur absence [7].

En tenant compte de la possibilité de l'excitation [8] par collision triple

$$\mathrm{H + O + M \rightarrow OH\ (^2\Sigma) + M}$$

les niveaux $v' = 0$ et $v' = 1$ pourraient être peuplés. Des transitions de probabilit à partir de $v' = 0$ et $v' = 1$,* on devrait avoir en émission [9]

	Transition	*Probabilité*	*λ moyen*
$v' = 0 \rightarrow$	$v'' = 0$	1	3087
	$v'' = 1$	0.004	3470
$v'' = 1 \rightarrow$	$v'' = 0$	0.3	2826
	$v'' = 1$	0.6	3145
	$v'' = 2$	0.003	3522

On voit immédiatement qu'à partir de $v' = 0$ seule la bande (0–0) est à reten Pour les transitions à partir de $v' = 1$, seule la bande (1–1) peut être observab Nous retiendrons donc la bande (0–0) pour une analyse plus detaillée.

La structure dans le spectre du ciel nocturne d'une bande telle que celles de C dépend de la largeur effective de la fente sur la plaque photographique et du *pa mètre* de température qu'il convient d'adopter pour la répartition sur les niveaux rotation.

*Pour $v' = 1$, tout dépend de la valeur exacte de la châleur de dissociation OH: 4.40 ± 0.05 eV.

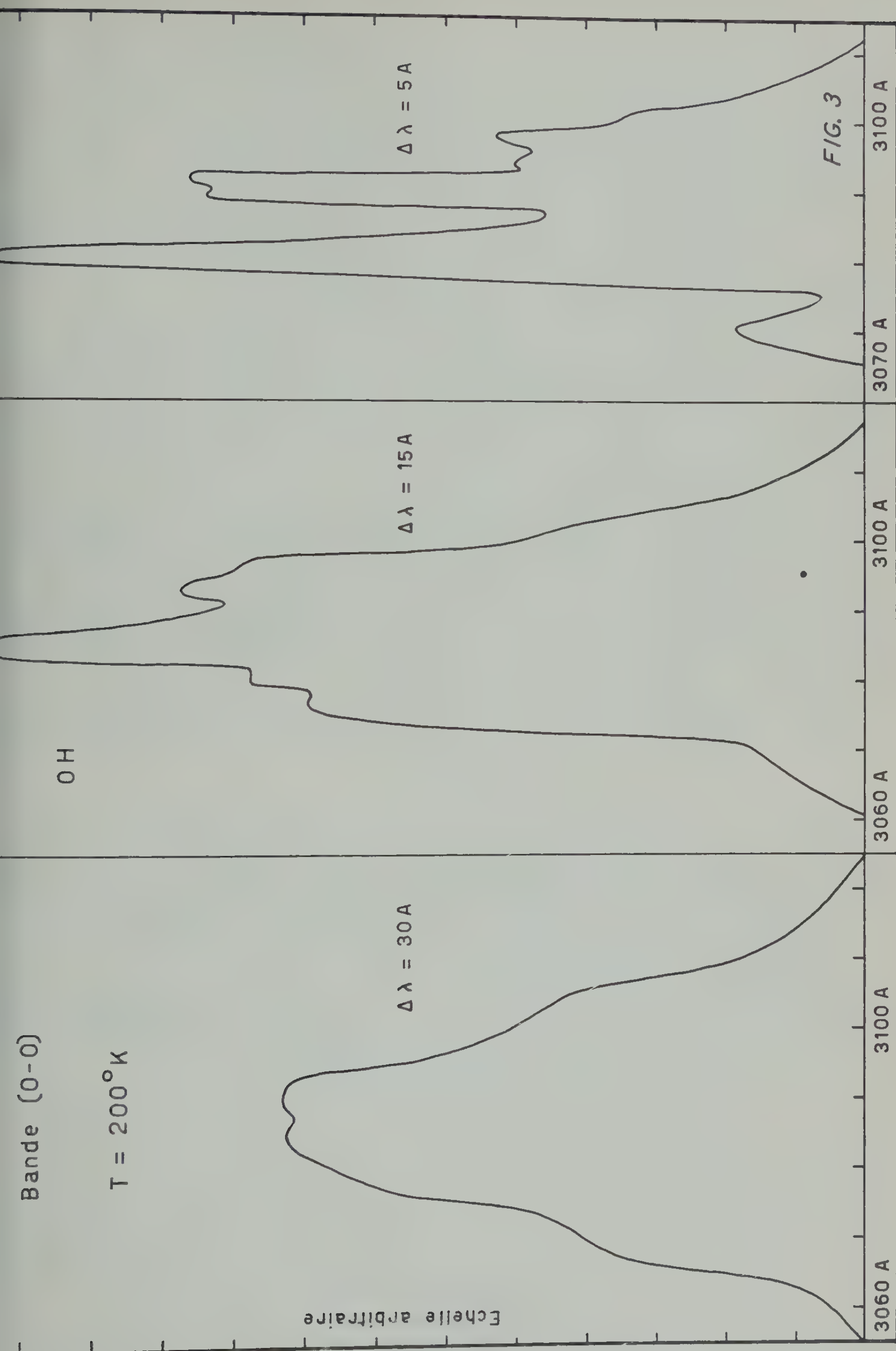
Bande (0-0)
T = 200°K
OH
Echelle arbitraire
Δλ = 30 A
Δλ = 15 A
Δλ = 5 A
3060 A
3100 A
3060 A
3100 A
3070 A
3100 A

FIG. 3

Nous avons choisi 200°K comme paramètre de répartition boltzmannienne e des largeurs effectives de fente de 30, 15, et 5 Å. La Figure 3 donne les résultats sou forme d'une bande simple ou à structure suivant la largeur de la fente.

Avec une largeur de fente de 30 Å, on obtient une bande unique pratiquemen non degradée dont le maximum d'intensité est situé vers λ3087 Å.

La fente ayant une largeur de 15 Å, une structure apparaît avec un maximum net vers λ3085 Å et degradée vers le rouge. La largeur de 5 Å pour la fente perme de voir apparaître une structure assez nette. Le premier maximum, qui se présent après une croissance tres rapide, est situé à λ3085 Å tandis que le second apparaî vers λ3090 Å. Une aile marquée est à noter vers 3095 – 97 Å.

Cette dernière structure est à rapprocher de celle que nous obtenons par notr enregistrement photométrique dans ce domaine de longueurs d'onde. Nous ob tenons, en effet, 3 maxima vers 3078 – 3087 et 3095 Å. Rappelons que Barbier [3 donne la longueur d'onde 3084 et Déjardin et Dufay [4] signalaient des radiation à 3096 et 3085. Les conditions optima se présentent donc pour relier l'émission du spectre du ciel nocturne à celle de OH.

Avec le pouvoir de résolution des spectrographes utilisés, il n'est pas possible de tirer des conclusions définitives sur le spectre ultraviolet du ciel nocturne, en particulier à sa limite extrême. Néanmoins, on retiendra que la limite extrême observée atteint 2995 Å et que l'effet des bandes de Herzberg, qui semble encore s'y manifester doit être soumis à une nouvelle investigation. Enfin, la présence de la bande (0–0) du système $^2\Sigma \rightarrow {}^2\Pi$ de OH ne peut être exclue actuellement d'après les résultats théoriques et d'observation.

Un des auteurs (M.N.) remercie la Fondation Universitaire de Belgique pour le subside qu'il lui fut accordé.

References

[1] F. W. P. Götz, Handbuch der Geophysik, 8, Rap. 7, 418 (1943).
[2] C. T. Elvey, P. Swings, and Linke, Astroph. J., **93**, 337 (1941).
[3] D. Barbier, Ann. Géophys., **1**, 224 (1945); Ann. Astrophys., **10**, 47 (1947).
[4] G. Déjardin et J. Dufay, Cahiers de Physique, **3**, 12 (1942); Ann. Géophys., **2**, 249 (1946)
[5] A. Arnulf, Paris, C.-R. Acad. sci., **202**, 1412 (1936).
[6] G. Herzberg, communication privée.
[7] P. Swings, The atmospheres of the earth and planets, Chicago, University of Chicago Pres (1949).
[8] D. R. Bates and M. Nicolet, J. Geophys. Res., **55**, 301 (1950).
[9] K. E. Schuler, J. Chem. Phys., **18**, 1221 (1950).

MEASUREMENTS OF THE VERTICAL DISTRIBUTION OF ATMOSPHERIC OZONE FROM ROCKETS

By F. S. Johnson, J. D. Purcell, and R. Tousey

United States Naval Research Laboratory, Washington 25, D. C.

(Received August 28, 1951)

ABSTRACT

The vertical distribution of ozone above White Sands Proving Ground, New Mexico, was calculated for October 10, 1946, and April 2, 1948. The data were obtained by photographing the ultra-violet spectrum of the sun with small automatic spectrographs installed in V-2 rockets. No ozone could be detected above an altitude of about 45 km, with a maximum possible error of 0.004 mm. The maximum concentration occurred at 23.5 km on October 10, 1946, and at 18.5 km on April 2, 1948. On both occasions, the maximum concentration relative to air was at about 28 km.

INTRODUCTION

Since its discovery in 1920 by Fabry and Buisson [see 1 of "References" at nd of paper], there has been considerable interest in the ozonosphere, in the hotochemistry by which it is produced, and in its effect upon life on the earth. lthough the total ozone can be determined fairly easily from the ground, the ertical distribution is difficult to measure. Balloon-carried experiments have suceeded in reaching only to about 32 km, through the region where the ozone is ontrolled largely by meteorological factors, but hardly to altitudes where the zone production is in photochemical equilibrium. Measurements of the vertical stribution of ozone from ground by means of the Umkehr effect [2] give data overing rather wide ranges in altitude, and not of great accuracy.

In 1946, United States Army Ordnance made available space in V-2 rockets r upper atmosphere experimentation. We undertook to photograph the ultraolet spectrum of the sun by means of rocket-borne spectrographs. One of the urposes was to measure directly the vertical distribution of ozone to altitudes gher than could be reached by balloons, and so to study the top edge of the one layer where photochemical equilibrium is believed to prevail.

INSTRUMENTATION

The rocket spectrographs were designed to make possible, during ascent through e ozone layer, the recording of a series of spectra suitable for determining the

change in ozone absorption by means of photographic photometry. At the sam time the spectrographs were required both to produce high-resolution spectra, i order to show the Fraunhofer lines, and also to be capable of recording wavelength

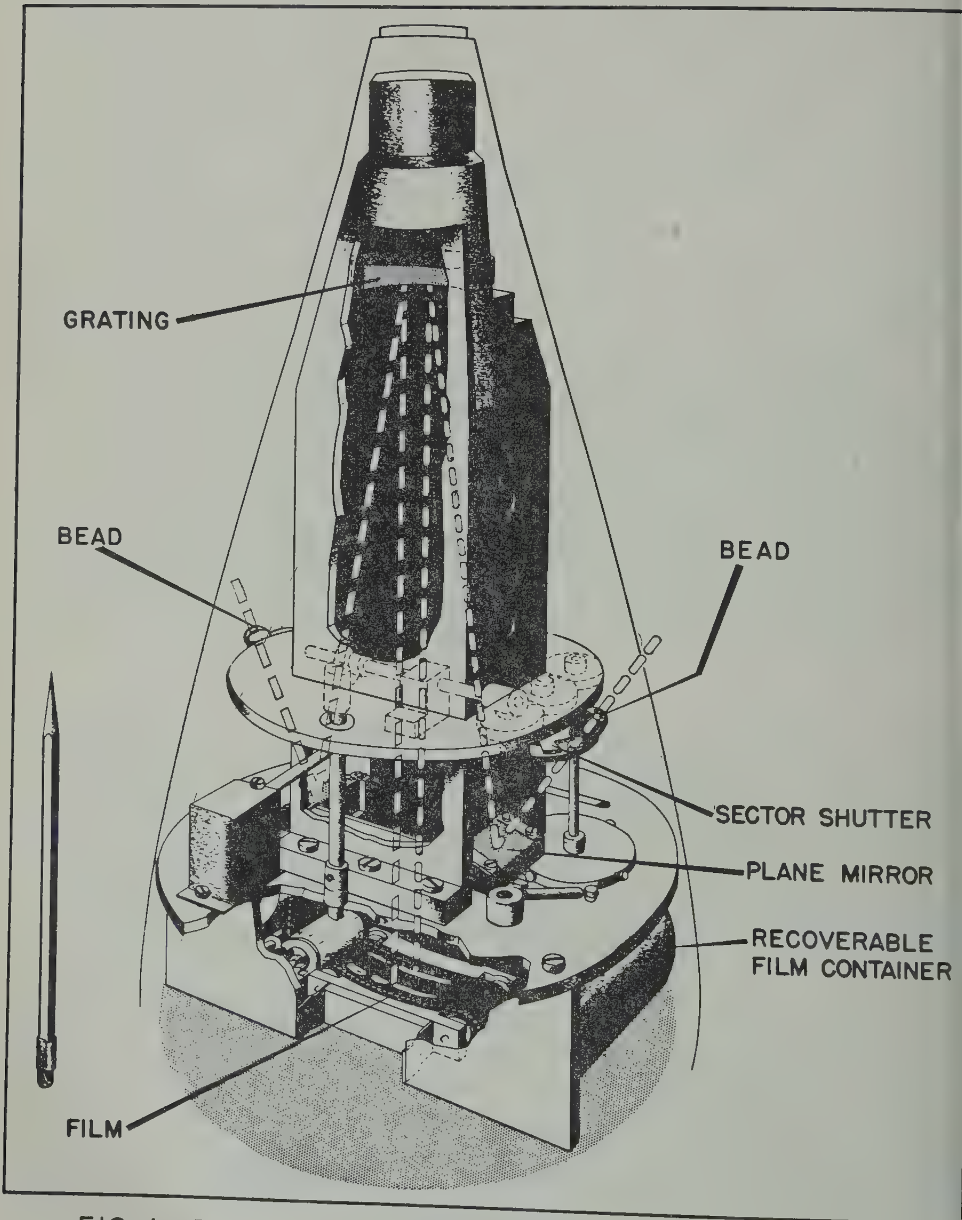

FIG. 1—DIAGRAM OF THE ROCKET SPECTROGRAPH

as short as 1216 Å or lower. The several requirements were incompatible and the spectrograph design represented a compromise.

A cut-away drawing of the spectrograph is shown in Figure 1. Dispersion was

rovided by a 40-cm radius, 15,000 lines per inch, concave diffraction grating, uled on aluminum, used in a normal incidence mounting. The wavelength coverage vas from 3400 to 1100 Å, in the first order. Sunlight entered the spectrograph hrough either of two apertures or "beads," and was reflected from a plane mirror o the grating. The two identical entrance paths on opposite sides of the grating ormal were provided to double the chance that sunlight would enter the spectro-raph. The optical paths were folded by the plane mirrors to make the form of he spectrograph fit the rocket. By turning the mirrors and changing the bead ositions to correspond, it was possible to adjust the center of the field of view of he spectrograph to an angle from the rocket axis which was optimum for the ltitude of the sun at the time it was planned to fire the rocket. In the spectrograph lown on October 10, 1946, the angle was 45° from the rocket axis, and on the april 2, 1948, spectrograph it was 90°.

The spectra were photographed on 35-mm film, conformed to the Rowland ircle by means of a template, and with the centers of the spectra near the grating ormal. A 25-foot length of film was carried and was exposed frame by frame. On he first flight, three exposure times—3.6, 0.66 and 0.12 seconds—were employed n rotation, while on the second a continuous sequence of one second exposures vas made.

The problem of providing a wide field of view for the spectrograph, together vith high intensity and good resolution, was solved by the use of lenses in the orm of small spheres or "beads" in place of slits. The spheres were made of lithium luoride so as to be transparent to the ultraviolet down to 1100 Å. Each sphere vas 2 mm in diameter, and acted as a short-focus wide-angle lens, collecting unlight within a large solid angle and forming a small solar image from which ight diverged to fill the grating. Since the solar image, serving in place of the lit, was very bright, the speed of the spectrograph was of the order of 100 times reater than that of a spectrograph producing the same resolution but equipped vith a slit and diffuser. The useful field of view was a cone of 140° diameter. Though the speed was reduced as the sun's direction departed from the optical xis, the reduction was less rapid than with the conventional slit and diffuser. If he rocket rolled and yawed during an exposure, the definition of the spectra was mpaired somewhat, because the position of the solar image, and thus of the spec-rum, depended on the angle between the sun and the optical axis. This effect vas of no consequence in the determination of ozone.

The type of film used was Eastman 103-0, ultraviolet sensitized by overcoating vith a fluorescent lacquer. This was the fastest available film for the region 3400 o 1100 Å. In order to prevent static fogging due to rolling the film in vacuum, the ack was coated with rim-jet black, which is an electrically conducting anti-alation coating. The film transport was governed by a timing motor, and, each ime the film moved forward, an impulse was transmitted to earth through the elemetering system. Thus, the altitudes at which the individual exposures were nade were obtained from the telemetering record and the rocket trajectory.

The spectrographs were mounted in a tail-fin, with one entrance aperture ooking out on each side, and were usually recovered with little damage, provided he nose of the rocket was blown off on the descent.

THE FLIGHTS

Ten spectographs were flown in V-2 rockets during 1946-1948, and four flight were successful. Series of spectra, from which ozone could be determined, wer obtained on two of the flights. On October 10, 1946, a rocket was fired to an altitud of 170 km at 11:03 a.m. MST, the solar elevation being 49°. A series of 35 spectr extending through the ozone layer and on to 88 km was obtained. Several of th spectra made with three-second exposures are reproduced in Figure 2. From 2 t

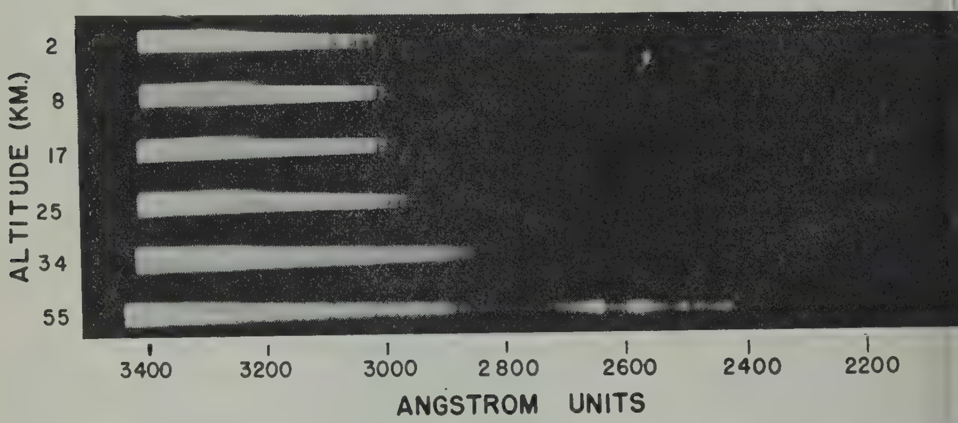

FIG. 2—SPECTRA OF THE SUN SELECTED FROM THE RESULTS OF THE ROCKET FLIGHT OF OCTOBER 10, 1946

25 km, the spectra became gradually extended to shorter wavelengths, partl because of decreased Rayleigh attenuation and partly because of passage throug the ozone. At 34 km, however, most of the ozone lay below the rocket and th spectrum was greatly extended. At this altitude, a weak spectrum was recorde from 2100 to 2250 Å, through the window between oxygen and ozone absorptio though this may be lost in reproduction. Fuel burn-out occurred at 40 km, an thereafter the rocket was unstable. At 55 km, the spectrum was not weakened b ozone, but the exposure was less intense, because of the less favorable aspect the rocket. No records at altitudes above 88 km were obtained because of e haustion of the film supply due to a mechanical defect in the escapement mecha nism.

The second successful ozone firing took place on April 2, 1948. The rocket w to be flown near dawn in order to increase the slant air mass and so to measu ozone to higher altitudes than was possible on the first firing with a high su Technical difficulties delayed the rocket firing until 6:47 a.m. MST, when the sol altitude angle was 11°. Flight and recovery were successful, with a peak altitu of 145 km. However, the results were disappointing, since the rocket became u usually stable after burn-out and assumed a position for the remainder of t flight such that neither side of the spectrograph was able to receive sunligh Good spectra to an altitude of 35 km were obtained.

PHOTOMETRY

The determination of ozone required that the spectra be reduced to relative itensities and that the photographic photometry involved be carried out with ie greatest possible care. After recovery, the films were returned to the Naval esearch Laboratory and developed with especial attention to uniformity. The ctober 10, 1946, film was developed in the large continuous processing machine t the Naval Photographic Center. The temperature of the developer was adısted to reproduce closely a development of 4 minutes in D-19. The ultraviolet ensitizer was first removed with several baths of cyclohexane. The development eemed to be uniform, but there was appreciable directional development which esulted in a lower background density behind the trailing edges of the spectra. n order to avoid this, the April 2, 1948, film was developed by the brush method a tray 28 feet long, constructed especially for this purpose. The results were niform and free from directional effects.

For measurements of the densities of the spectra, a Knorr-Albers micropho-ometer manufactured by the Leeds and Northrup Company was used. Several odifications were necessary because of the special nature of the spectra. A ribbon-lament, 6-volt, 18-ampere lamp was used as the light source; the filament was naged on the film and the spectrum was imaged on the defining slit, located irectly in front of the photocell. The area of spectrum measured was usually .05 to 0.2 mm high by 0.05 to 0.1 mm wide. The dimensions were dictated by the ature of the particular spectrum. The spectra were non-uniform in density per-endicular to the dispersion, and the slit height was reduced to include only a egion over which the density was uniform. To extend the density range covered y the instrument, a neutral filter of density 0.6 was inserted in the beam in front f the lamp. With this, it was possible to measure densities as high as 3.0. Care 'as taken to avoid errors produced by stray light and those connected with the ick of linearity of the gas-filled photocell.

Perhaps the most difficult feature of the densitometry lay in securing exact lignment of the spectra and the direction of travel of the microphotometer stage. rotary stage attachment was constructed, and the spectra were rotated until a ransverse adjustment for maximum density made at one wavelength was main-ained at all positions in the spectrum. A dial indicator gage for measuring ransverse motion was attached to the stage and was of assistance in making this djustment.

A special holder was constructed to keep the spectra flat without the use of lass plates. Apochromatic microscope objectives were installed in place of the chromatic objectives in order to avoid having to correct the visual focus to obtain he optimum photoelectric focus.

The calibration exposures required to reduce the densities to relative intensities 'ere made with a carbon-arc anode crater as light source. A few exposures were laced on the actual flight roll, and a more extensive set of exposures was placed n a second strip of film. Sector disks, rotating sufficiently rapidly to produce no itermittency error, were employed to reduce the intensity. *H* and *D* curves of ensity *versus* log intensity were prepared from the spectra for 28 wavelengths rom 3400 to 2100 Å.

Three series of calibration exposures were made, using exposure times of 3, 0.6 and 0.1 seconds, which were approximately the same as for the rocket spectra. The arc distance was adjusted so that the spectra were approximately of the same density as the rocket spectra for equal exposure times. It turned out that the characteristic curves for these three times were all parallel and therefore one set of curves was sufficient. This meant that, for this particular emulsion and exposure range, the reciprocity failure followed the Scharzschild law, $D = f(It^p)$, where D is the density, I the intensity, t the exposure time, and p a constant.

By means of the H and D curves and data on the intensity distribution in the carbon-arc crater, the density traces were converted to curves of intensity *versus* wavelength, the intensity being on a relative basis for each spectrum. As far as the determination of ozone was concerned, it was not necessary to derive relative intensity curves at all, because intensity comparisons between spectra were required at single wavelengths only, and not between different wavelengths. A corollary is that errors affecting the shape of all the relative intensity curves, such as incorrect data for the carbon-arc distribution, had no effect on the ozone determination.

It was a part of our program, however, to determine the relative intensity curves of sunlight outside the earth's atmosphere, and it was convenient to use the intensity curves in the ozone determination. The complete curves will be described in another paper, and they are included here only in so far as they were used in the ozone determination.

The ozone between the spectrograph and the sun at a particular altitude was determined by correcting the spectral intensity curve determined at that altitude for absorption by ozone, and comparing it with the average intensity curve made up from all spectra taken well above the ozone layer. The ozone absorption coefficients used were those of Ny and Choong [3]. The correct quantity of ozone was that which brought the two curves into agreement at all wavelengths, except for a factor depending on exposure conditions.

The advantage of using the whole intensity curve, rather than selected points, was that it made use of all the data and gave results of greater accuracy. Each spectrum extended from 3400 Å to a short wavelength limit determined by the ozone and exposure. In the curve matching process, in general, the short wavelength end of the spectrum where the absorption coefficient was highest gave the best value for ozone. However, the last few angstroms where the density was less than 0.1 were not useful, because the densities were on the toe of the H and D curves. The long wavelengths were usually of little value because of overexposure and low coefficients of absorption of ozone.

Figure 3 illustrates how the ozone was determined by curve matching for two cases. The upper solid curves are portions of the relative intensity distribution plotted on a logarithmic scale, for a 3-second exposure above all measurable ozone and were determined by averaging the spectra exposed at altitudes above 45 km. The lower curves are the intensity distributions obtained from the 3-second exposures at 30 km and 2 km; their short and long wavelength limits were determined, respectively, by the low and high extremes of density that could be reduced to intensity.

Taking first the case of 30-km altitude, there is shown in Figure 3 the optical ensity of 0.16 mm of ozone. The use of a logarithmic plot makes it easy to correct e observed intensity curve for ozone absorption. This is done simply by adding the observed intensity curve the optical density of 0.16 mm of ozone, and the pper broken curve is the result. The curve so obtained agrees very well with the lar curve outside the atmosphere, when 0.16 mm ozone is selected as the correcon. Therefore, 0.16 mm was accepted as the amount of ozone between the ectrograph and the sun at 30 km.

The case for 2-km altitude is similar, but here it is necessary to take into acount also the attenuation by Rayleigh scattering. The optical density due to attering by 0.85 atmosphere is shown in Figure 3, as well as that due to ab-

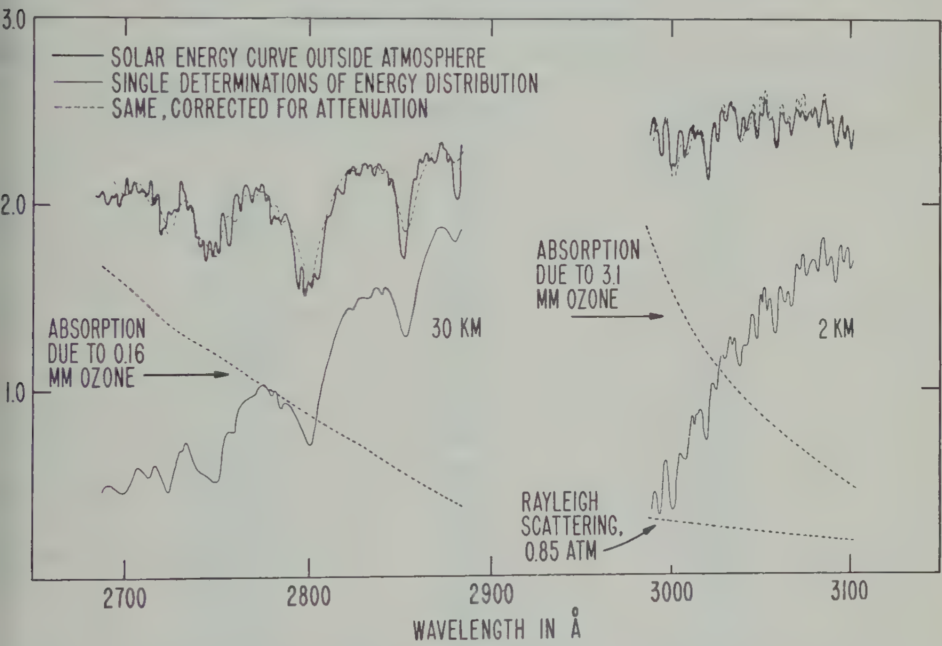

FIG. 3—RELATIVE SOLAR INTENSITY DISTRIBUTION CURVES DETERMINED ABOVE AND BELOW THE OZONE; THESE ILLUSTRATE THE METHOD OF DETERMINING THE OZONE QUANTITY BY CORRECTING THE SPECTRUM FOR ABSORPTION BY OZONE AND RAYLEIGH SCATTERING

rption by 3.1 mm of ozone. The upper dotted curve is the resulting intensity rve, corrected for all absorption by adding these two optical densities, and it rees well with the curve outside the atmosphere. Therefore, 3.1 mm was accepted the amount of ozone between the spectrograph and the sun at 2 km.

In most cases, it was possible to produce at all wavelengths a close fit between e reference and corrected curves by proper choice of the quantity of ozone. The one quantity was determined quite critically in this way. There was always esent the possibility, however, that the sensitivity was not uniform over the otographic film and, if it varied from one end of a spectrum to the other, an

error would be introduced. On a few spectra, such an error was suspected. It w impossible to measure this error explicitly. It was decided that the maximu possible error in log intensity between the ends of the spectra was ±0.05 and th probable error in ozone was taken as the change in ozone required to make th two intensity curves fail to match by 0.05.

It may be noted from Figure 3 that the detail on the corrected curves is le than on the curve outside the atmosphere. The various spectra differed greatly i resolution, because of roll and yaw, and also because of vibration during th burning period. This did not reduce the accuracy of the ozone determination.

In practice, the curve matching process was carried out by superimposing o

Table 1—*Vertical distribution of ozone above New Mexico, October 10, 1946, 11:03 a.m. MST*

Mean altitude above sea level	Vertical O_3	Estimate of accuracy
km	*mm(STP)*	*mm*
1.33	2.34	0.15
2.12	2.42	0.15
3.78	2.34	0.15
6.49	2.34	0.15
10.34	2.34	0.11
12.2	2.15	0.15
13.2	2.12	0.11
15.5	2.12	0.08
17.9	1.96	0.11
19.3	1.85	0.08
22.3	1.25	0.08
25.4	0.83	0.08
27.2	0.55	0.015
31.3	0.12	0.006
35.5	0.038	0.009
37.9	0.019	0.003
47.9	<0.004	0.002
50.4	0	0.002
55.4	0	0.002
60.0	0	0.002
62.4	0	0.002
67.1	0	0.002

a light table the particular curve, corrected for ozone absorption, and the referen curve above all ozone. Small trial changes in ozone could be introduced simp by rotating one curve relative to the other.

VERTICAL DISTRIBUTION OF OZONE

The reduction of the spectra gave the total ozone over the slant path betwe the spectrograph and the sun. The total ozone vertically above the spectrogra was derived from the slant ozone by multiplying by the geometrical factor corr sponding to the particular solar altitude. For the first flight, the altitude was 4

nd the factor was sine 49°, or 0.755. For the second flight, the altitude was 10° 56′ nd it was necessary to consider the curvature of the earth and the mean altitude f the ozone layer. The factor varied from 0.198 at 12 km to 0.190 at 21 km and bove.

The final values of the total vertical ozone are presented in Tables 1 and 2. 'he first column gives in kilometers the mean altitude above sea level at which he spectrum exposure took place; the second column is the total quantity of ozone ertically overhead in millimeters at STP. The third column is an estimate of the ccuracy of the measurement, made as described earlier, and represents the extreme rror that might be introduced through the photographic photometry.

TABLE 2—*Vertical distribution of ozone above New Mexico, April 2, 1948, 6:47 a.m. MST*

Mean altitude above sea level	Vertical O_3	Estimate of accuracy
km	*mm(STP)*	*mm*
11.3	1.73	0.06
12.0	1.76	0.06
12.8	1.70	0.06
13.5	1.71	0.06
14.3	1.71	0.05
15.2	1.64	0.05
16.1	1.52	0.05
17.0	1.42	0.05
17.9	1.30	0.04
19.0	1.15	0.04
20.0	1.03	0.03
21.1	0.89	0.03
22.3	0.77	0.025
23.5	0.68	0.02
24.7	0.54	0.016
26.1	0.415	0.012
27.5	0.33	0.01
28.9	0.225	0.006
30.3	0.15	0.005
32.0	0.10	0.004
33.6	0.72	0.004
35.3	0.055	0.004

The vertical ozone overhead is shown for the two flights in Figure 4, and is otted logarithmically against altitude. The smooth curves pass through the xperimental points within the limits of accuracy given in Tables 1 and 2. Limits re shown for the high-altitude end of the curve for October 10, in accordance ith the upper limit of 0.004 mm of ozone determined from the spectra.

The best value of the total vertical ozone above the earth was 2.38 mm on ctober 10, 1946. The data for April 2, 1948, extend down to only 11 km, and it not possible to extrapolate with assurance to ground level. The value appears be in the neighborhood of 2 mm, however.

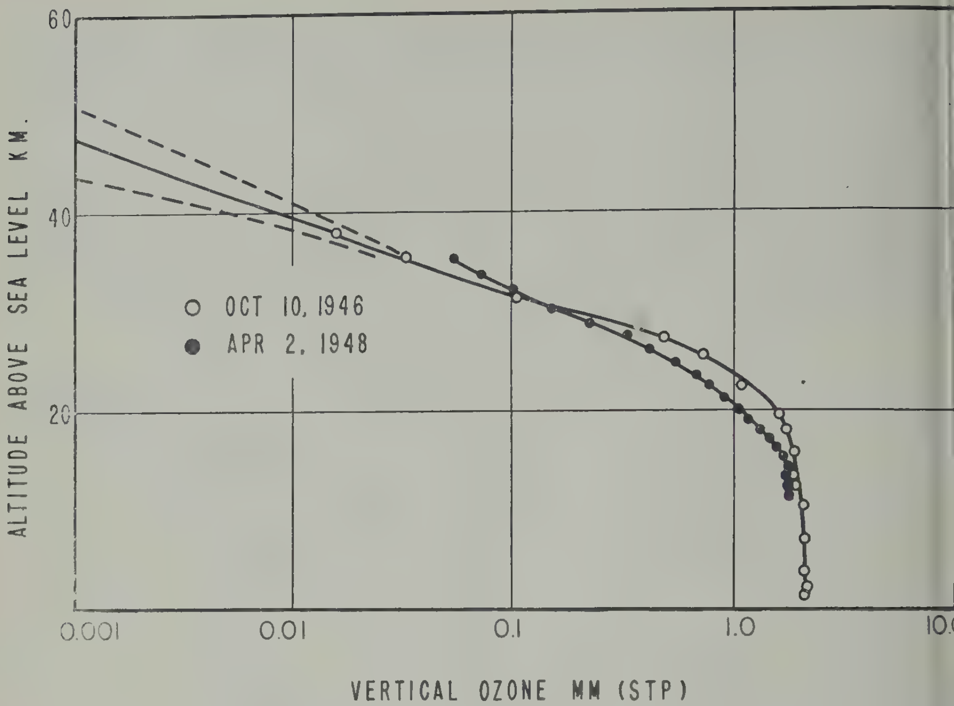

FIG. 4—TOTAL VERTICAL OZONE ABOVE NEW MEXICO

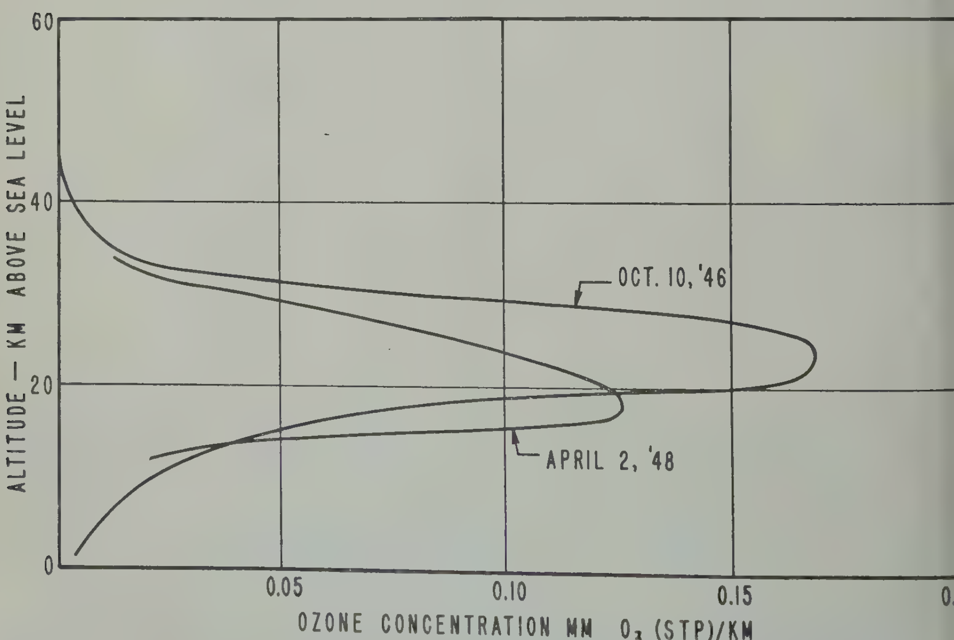

FIG. 5—THE CONCENTRATION OF OZONE ABOVE NEW MEXICO

The concentration of ozone as a function of altitude was given by the slope the tangent to the curves of Figure 4. Concentration curves for the two dates e presented in Figure 5. On October 10, 1946, the maximum concentration lay about 23.5 km, while on April 2, 1948, its altitude was 18.5 km.

The shapes of the concentration curves are extremely sensitive to the way in iich the smoothed curves of Figure 4 are drawn through the experimental points. e have chosen to smooth the data as much as possible, consistent with our allowed obable error, and in such a way as to produce distribution curves showing no ecial features other than the expected broad maximum. If the curves are made pass closer to or through the most probable positions of the experimental points,

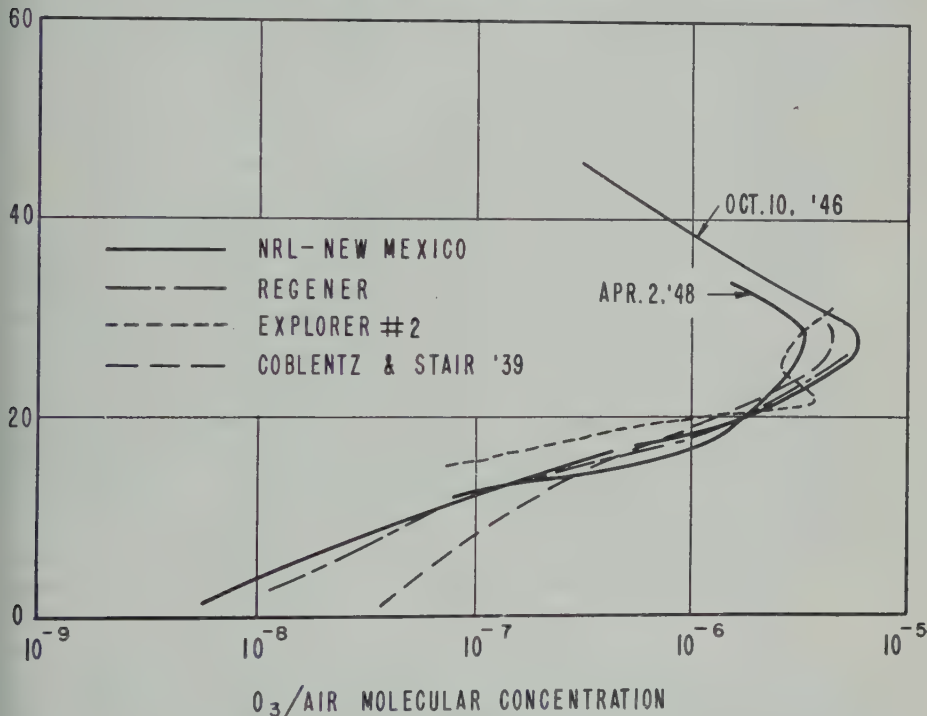

FIG. 6—THE MOLECULAR CONCENTRATION OF OZONE RELATIVE TO AIR AS MEASURED OVER NEW MEXICO; SIMILAR DATA OBTAINED BY BALLOON FLIGHTS ARE SHOWN FOR COMPARISON

is possible to obtain concentration curves that have other features, such as axima, minima, and shoulders. Although such features may indeed be real, they ay be produced by a patchy geographical distribution of ozone, or they may ginate in the errors of photographic photometry. Therefore, we have chosen to aw the curves so as not to produce them.

The ozone distribution for October 10, 1946, has appeared in several survey pers [4] in a preliminary form showing two maxima. Remeasurements of the ectra indicated that the double maximum was produced largely by difficulties the preliminary densitometry. A single smooth curve, as shown in Figure 5, is that the final data support with certainty.

The molecular concentration ratio of ozone to air was calculated using the a density data obtained by Havens, Koll, and LaGow [5] during several rock flights. The curves for New Mexico on our two dates are shown in Figure 6. Th maximum of concentration relative to air lies at approximately 28 km on bot dates. The portion of the curve for October 10, 1946, at low altitudes is qui arbitrary, because it depends critically on the way the smoothed total ozone cur is drawn.

The data for October 10, 1946, extend to higher altitudes than have been reache hitherto, and to a lesser extent this is true of April 2, 1948. Both curves show continuously decreasing concentration above the maximum, which is consiste with the photochemical theories of ozone formation. Also plotted in Figure 6 a the concentration curves resulting from three balloon flights. The curve obtaine by E. Regener and V. H. Regener [6] over Germany in 1934 agrees well with o data of October 10, 1946. The curve shown for Coblentz and Stair [7] is one three obtained over Washington and again is in reasonable agreement with our The data from the *Explorer II* [8], however, show a second rise in concentratio above 25 km which is not found in any other results.

V. H. Regener [9], in four balloon flights in 1950, has measured the vertic distribution of ozone to 30-32 km above New Mexico, using a spectrograph an photographic photometry. His curves, which are not reproduced here, differ fro ours in exhibiting more detail, in showing somewhat lower positions of the maxim and in indicating higher concentrations of ozone at low altitudes. The total ozo value found on his flights ranged from 3.3 to 4.0 mm. These values are high than any found by us and are unusually high for the latitude of New Mexic Measurements from the ground at New Mexico made by Stair [10] in the mont of December, January, June, and July indicate values between 2.0 and 2.4 m in agreement with the rocket data and with the average data for this latitu published by Götz [11].

References

[1] C. Fabry and H. Buisson, J. Phys. et Le Radium, **2**, 197 (1921).

[2] F. W. P. Götz, Beitr. Geophysik, **31**, 119 (1931); F. W. P. Götz, A. R. Meetham, a G. M. B. Dobson, Proc. R. Soc. (London), A, **145**, 416 (1934).

[3] Ny Tsi-Ze and Choong Shin-Piaw, Chinese J. Phys., **1**, 1 (1933).

[4] E. Durand, "Rocket sonde research at the Naval Research Laboratory," The atmosphe of the earth and the planets, G. P. Kuiper, Chicago, University of Chicago Press (194 E. H. Krause, Proc. Amer. Phil. Soc., **91**, 430 (1947); Durand, Johnson, Oberly, Purc and Tousey, Naval Research Laboratory Report R-3171, 74 (1947).

[5] R. J. Havens, R. T. Koll, and H. E. LaGow, The pressure, density, and temperature the earth's atmosphere to 160 kilometers, to appear in the March, 1952, issue of t Journal.

[6] E. Regener and V. H. Regener, Physik. Zs., **35**, 788 (1934).

[7] W. W. Coblentz and R. Stair, J. Res., Nation. Bur. Stan., **22**, 573 (1939) and **26**, (1941).

[8] B. O'Brien, F. L. Mohler, and H. S. Stewart, Jr., Nation. Geog. Soc., Contrib. Te Papers, Stratosphere Ser., No. 2, 71 (1936).

[9] V. H. Regener, Nature, **167**, 276 (1951).

[10] R. Stair, J. Res., Nation. Bur. Stan., **40**, 9 (1948) and **42**, 145 (1949).

[11] F. W. P. Götz, Vierteljahrsch. Natf. Ges., **89**, 250 (1944).

RNAL OF GEOPHYSICAL RESEARCH VOLUME 56, No. 4 DECEMBER, 1951

ISANOMALEN DER $F2$-IONISATION

VON OTTO BURKARD

Institut für Meteorologie und Geophysik, Universität Graz, Austria

(Received November 21, 1951)

ABSTRACT

Lines of isonomalies give new insight into wide changes of the ionospheric $F2$-layer. Some maps of isonomalies show that hourly observations indicate an east wind, but often they do not suffice to explain the changes from one hour to the next. On the other hand, isonomalies should be a splendid means for the study of ionospheric changes at a solar eclipse.

Ausgehend von der bekannten Tatsache, dass die kritischen Frequenzen und nso auch die scheinbaren Höhen der $F2$-Schicht meist recht beträchtlichen wankungen unterliegen, sodass erst Monatsmittel einen glatten Kurvenverlauf ben, hat schon vor längerer Zeit J. O. Brand [1] den gleichzeitigen Zustand der Schicht an verschiedenen Orten untersucht. Die beiden Stationen, deren Be-chtungen er verglich, lagen auf ungefähr gleicher geographischer Länge rund km von einander entfernt und das Ergebnis der damaligen Untersuchung war, s sich für die beiden Stationen auch im einzelnen eine weitgehende Überein-nmung findet.

Nun hat sich in der letzten Zeit auch in Europa das Netz der Ionosphären-ionen soweit verdichtet, dass es aussichtsreich erschien, die Schwankungen der Schicht über einen grösseren Raum hinweg zu untersuchen. Für diesen Zweck sich eine Darstellung in Form von Isanomalen als recht vorteilhaft erwiesen. habe mich zunächst auf die Untersuchung der Ionisationsschwankungen hränkt, da mir die scheinbaren Höhen wegen der schon oft erwähnten Schwie-eiten in der Auswertung der $(h' - f)$-Kurven als zu wenig gesichert erscheinen. vorliegenden Kärtchen beziehen sich somit stets auf die maximale Elektronen-entration in der $F2$-Schicht, wobei allerdings auf die Umrechnung in die ahl der Elektronen pro ccm verzichtet und überall nur mit den Quadraten der schen Frequenzen gerechnet wurde. Werden letztere in $(\mathrm{Mc/s})^2$ gemessen, so lt man ja die Elektronenkonzentration durch einfache Multiplikation mit dem or 1.24×10^4. Die Schwankungen der Elektronenkonzentration wurden auf jeweiligen Monatsmittelwert bezogen, sodass also die Isanomalenkurven Orte her Differenz $(f_0F_2)^2$ minus $\overline{(f_0F_2)}^2$ miteinander verbinden. Die zu den Kurven

hinzugeschriebenen Zahlen geben die Grösse dieser Differenz in (Mc/s)^2 an, wob eine Elektronenkonzentration, die kleiner als der Mittelwert ist, strichliert g zeichnet wurde, während über dem Mittelwert liegende Elektronenkonzentratione voll ausgezogen erscheinen.

Aus der geradezu verblüffenden Mannigfaltigkeit der so entstehenden Isan malenkärtchen wurden für diesen Bericht nur einige charakteristische Fälle au gewählt, um einen wenigstens ungefähren Überblick zu gewinnen. Die Abb. zeigt auf einer Skizze von Europa den Ausschnitt an, über den sich die Isanomal der folgenden Abbildungen erstrecken.

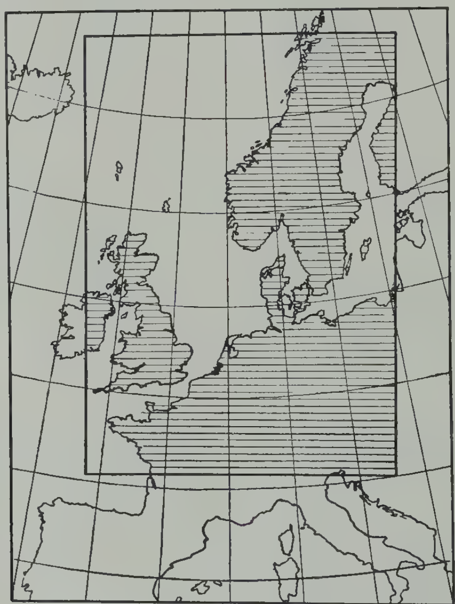

FIG. 1—DER VON DEN ISANOMALEN ERFASSTE RAUM IN EUROPA

Die erste Reihe der Isanomalenkärtchen (Abb. 2) stellt die Verhältnisse für d vier aufeinanderfolgenden Beobachtungstermine von 09^h GMT bis 12^h GM am 7. Februar 1951 dar. Es war dies ein Tag, der auf einen Ionosphärenstur folgte. Zwar machte sich dieser bis in die frühen Morgenstunden bei den meist Stationen noch bemerkbar, dann aber kehrten rasch wieder normale Verhältnis zurück. Geomagnetisch fiel dieser Tag noch in die Reihe der zehn ruhigsten Tag die (vorläufige) internationale Charakterzahl war $C = 0.5$. Die Isanomalen zeig zu allen vier Terminen einen annähernd gleichen Verlauf, nämlich eine etwa v NW nach SE abnehmende Elektronenkonzentration, die im Norden wesentli über, im Süden dagegen etwa um den gleichen Betrag unter dem Normalw (Monatsmittel)liegt. Die Änderungen von Stunde zu Stunde sind dabei nur gerin fügig.

Einen hierzu gewissermassen spiegelbildlichen Charakter weisen die Isanomal am 20.2.1951 auf (Abb. 3). Denn jetzt liegt eine ausgeprägte Überkonzentrati im SW, dagegen findet sich eine unter dem Durchschnitt liegende Elektrone

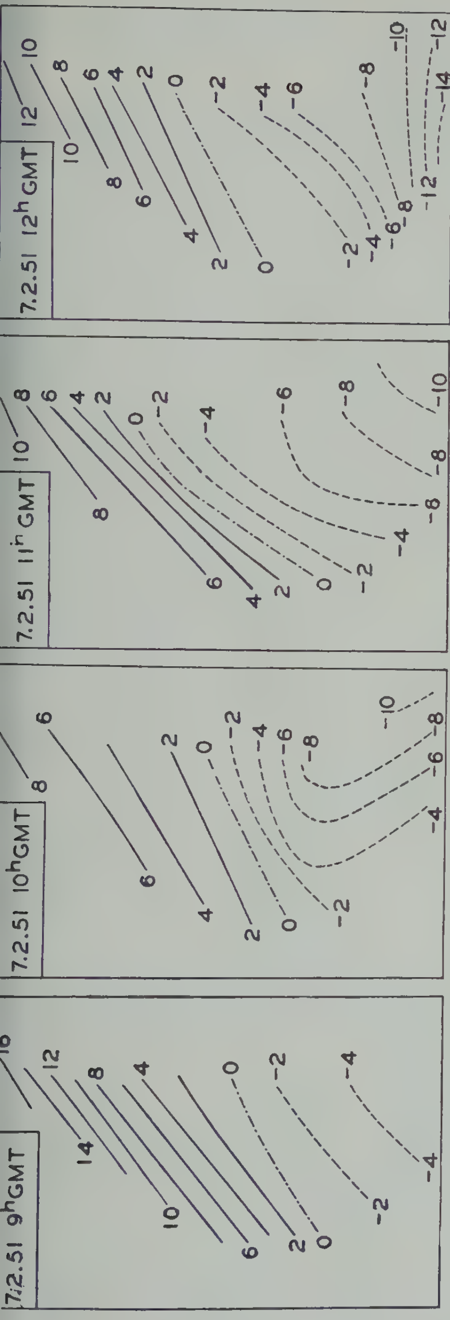

FIG. 2—ISANOMALEN VOM 7.2.1951

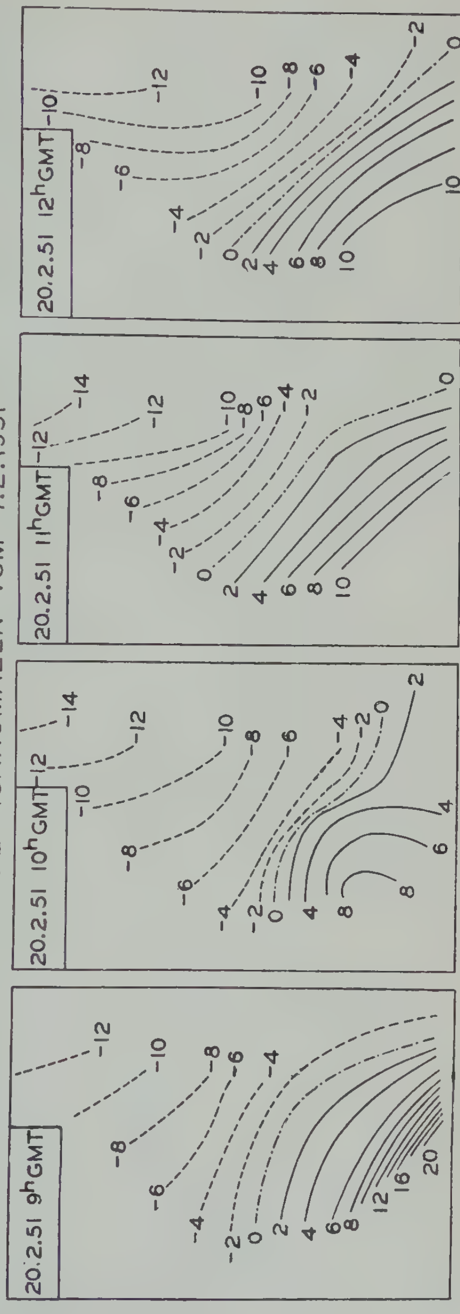

FIG. 3—ISANOMALEN VOM 20.2.1951

konzentration im NE. Aber auch hier wieder sind die Veränderungen innerhalb de gezeigten Zeitraumes nur unwesentlich, sie bleiben es allerdings nicht im weitere Verlauf des Tages. Geomagnetisch war dieser Tag gekennzeichnet durch $C = 0.2$ auch er fiel unter die fünf ruhigsten Tage des Monats.

Zum Beweis aber dafür, dass solche verhältnismässig ruhigen Verhältnisse in der $F2$-Schicht keineswegs die Regel bilden und gleichsam als Gegenstück zu diesen beiden eben gezeigten Fällen seien zum Schluss noch die Isanomalen vom 16.2.195 (Abb. 4) gezeigt. Auch dieser Tag war geomagnetisch einer der fünf ruhigsten seine (vorläufige) Charakterzahl ist sogar $C = 0.0$ und dennoch findet man in de $F2$-Schicht eine ganz unerwartet starke Turbulenz. Verfolgt man die Isanomalen von Stunde zu Stunde, so fällt zunächst in den beiden ersten Fällen (08^h bzw. 09^h) die selten geringe Dichte der Isanomalen im Norden auf. Die Abweichung der Elektronenkonzentration vom Monatsdurchschnitt macht sich dort also kaum bemerkbar, während allerdings im SW ein Gebiet mit Überkonzentration liegt. Dieses "Hoch" schiebt sich nun um 09^h GMT keilförmig nach Norden vor und liegt eine Stunde später mit seinem Kern bereits über dem Ärmelkanal, gleichzeitig verschiebt sich die Null-Isanomale allmählich weiter gegen Norden, wo ebenso wie im SE eine Abnahme der Elektronendichte beginnt. Um 11^h ist das Bild nicht allzu stark gegenüber dem vorhergehenden verändert, aber diese Stabilisierung ist nicht von langer Dauer, denn um 12^h verlaufen die Kurven plötzlich ganz anders und es sieht so aus, als ob im Osten eine Verlagerung der Isanomalen nach Norden stattgefunden hätte, während sie im Westen eine weitere Verschiebung westwärts erfahren hätten Aber auch dieser Zustand, einmal in Bewegung gekommen, bleibt nicht erhalten denn eine weitere Stunde später (13^h) ist das "Tief" von Osten nach SW gewandert und ein anscheinend neues Hoch tritt über Südskandinavien auf. Insgesamt ergibt sich auch hier der Eindruck, als ob eine Ost-West-Strömung (Ostwind) mit einer gleichzeitigen leichten Drehung im entgegengesetzten Uhrzeigersinn vorherrschen würde. Obwohl das Beobachtungsmaterial keineswegs für einen sicheren Nachweis der Richtigkeit dieser Vermutung ausreicht, wird die genannte Strömung aber doch auch durch die beiden folgenden Isanomalenkärtchen nahegelegt.

Ohne einer abschliessenden Stellungnahme vorgreifen zu wollen, kann doch bereits jetzt schon gesagt werden, dass die hier gezeigte Isanomalendarstellung einen weitaus tieferen Einblick in die oft turbulenten Vorgänge in der obersten Ionosphäre gestattet als es bisher bei der Betrachtung der Verhältnisse an nur einer Station möglich war. Man darf dabei allerdings nicht vergessen, dass uns durch die kritischen Frequenzen nur die maximale Elektronenkonzentration zugänglich wird und dass zunächst die vertikalen Änderungen auf diese Weise nicht miterfasst werden können. Auch ersieht man schon aus dem letzten Beispiel, dass die bisher üblichen stündlichen Beobachtungen häufig nicht genügen, die raschen Veränderungen in der $F2$-Schicht vollständig verfolgen zu können. Für derart rasch vor sich gehende Turbulenzerscheinungen wird es also wohl notwendig sein, die zeitliche Aufeinanderfolge der Messungen zu verdichten, sodass etwa von 10 zu 10 Minuten je ein Momentbild des jeweiligen Zustandes aufgenommen wird. In dieser Hinsicht kann man auf die Ergebnisse gespannt sein, die die Ionosphärenbeobachtungen anlässlich der totalen Sonnenfinsternis am 25.Februar 1952 ergeben werden Durch zehn Tage hindurch sollen ja nach einem Vorschlag der U.R.S.I. die beteilig

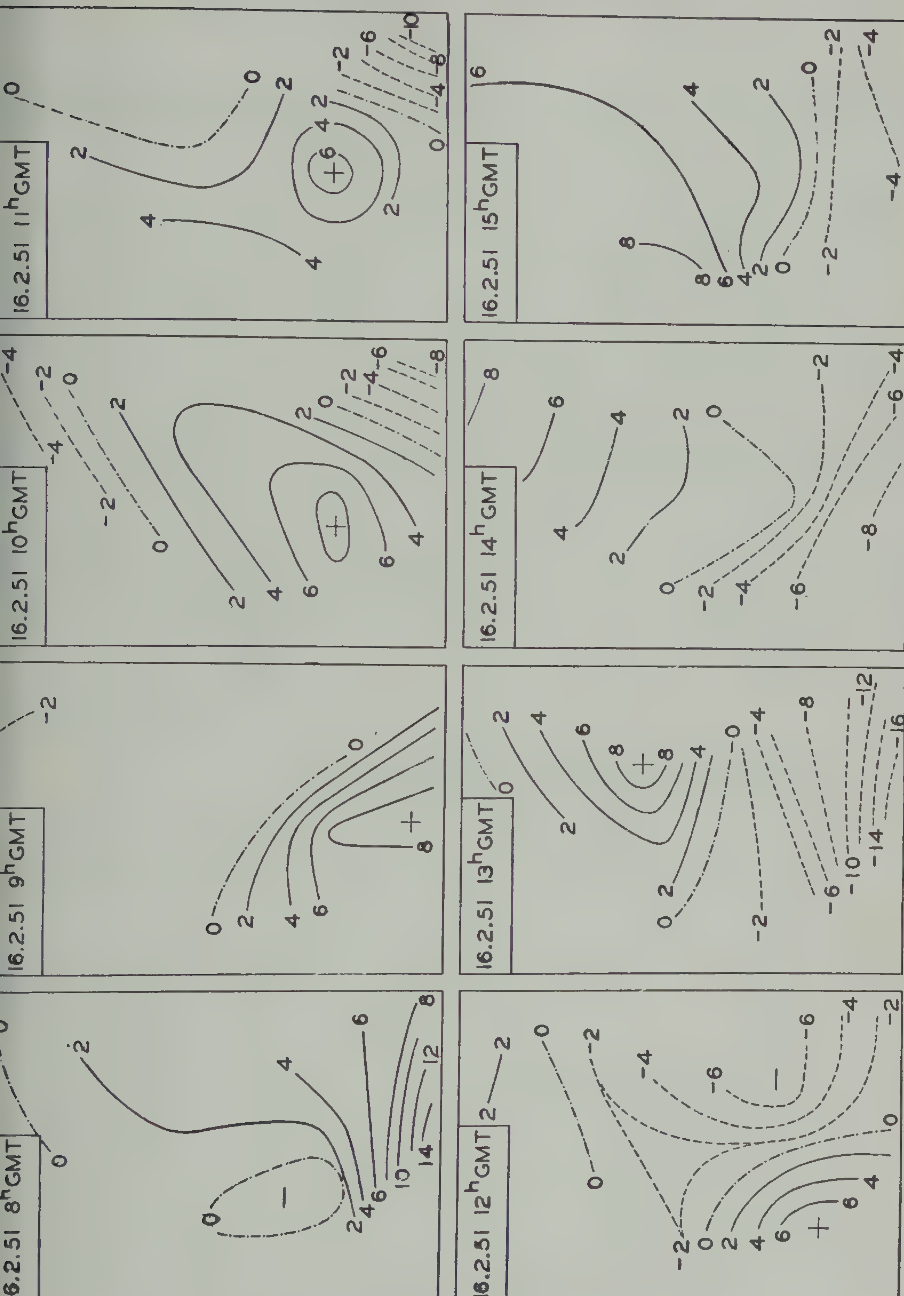

FIG. 4—ISANOMALEN VOM 16.2.1951

ten Ionosphärenstationen von 5 zu 5 Minuten Beobachtungen anstellen. Andrerseits beweisen allerdings schon die wenigen hier gezeigten Fälle die fast dauernde Unruhe im Zustand der $F2$-Schicht, die mitunter so stark wird, dass möglicherweise auftretende Verfinsterungseffekte ganz oder zu mindest zum Grossteil verdeckt bleiben. Wahrscheinlich ist diese Turbulenz auch die Ursache dafür, dass die bisherigen Untersuchungen über den Einfluss von Sonnenfinsternissen auf die $F2$-Schicht so durchaus unklare Ergebnisse erbrachten.

Völlig offen bleibt auch durch die vorliegenden Untersuchungen die Frage, ob die Änderungen in der Elektronenkonzentration auf eigentliche Wirbelströmungen zurückzuführen sind, bei denen die ganze Materie an der Bewegung beteiligt ist, oder ob die Massenverteilung zwar mehr oder weniger unverändert bleibt und nur der elektrische Zustand raschen Änderungen unterworfen ist. Letzteres könnte etwa dadurch veranlasst sein, dass ein die Schicht ionisierender Energiestrahl räumlich und zeitlich stark schwankt. Auf Grund der ersteren Anschauung hat bereits vor längerer Zeit D. Martyn [2] eine Theorie entwickelt, während J. Krautkrämer [3] in seinem Bericht (hier auch zahlreiche Literaturhinweise) über die Windmessungen in den Ionosphärenschichten keine Stellung zu dieser Frage nimmt.

Zum Schluss sei die Aufmerksamkeit auch noch darauf gelenkt, dass die Turbulenzerscheinungen auch an magnetisch vollkommen ruhigen Tagen in beachtlichem Ausmass auftreten, was insofern überrascht, als ja bekanntlich die grossen Ionosphärenstürme immer von magnetischen Stürmen begleitet sind.

Schrifttum

[1] J. O. Brand, Schr. D. Akad. Luftfahrtforsch, 7, 11-16 (1943).
[2] D. F. Martyn, Proc. R. Soc., A, **201**, 216-234 (1949).
[3] J. Krautkrämer, Arch. Elektr. Übertragung, 4, 133-138 (1950).

GEOMAGNETIC AND SOLAR DATA

INTERNATIONAL DATA ON MAGNETIC DISTURBANCES, SECOND QUARTER, 1951

Preliminary Report on Sudden Commencements

S.c.'s given by five or more stations are in italics. Times given are mean values, with special weight on data from quick-run records.

Sudden commencements followed by a magnetic storm or a period of storminess (s.s.c.)

1951 April 10d 06h 19m: Tl.—10d 18h05: Fu.—11d 01h08: Pi.—*12d 21h55:* six.—12d 22h31: Te. Ap.—13d 11h23: Ma.—14d 10h12: Te.—18d 05h25: Do.—*18d 06h52:* thirty-three.—19d 02h45: Le.—20d 00h51: To.—25d 10h48: Wn Fu.

1951 May 01d 00h 20m: Do –01d 04h51: Te.—02d 08h20: El.—*09d 17h50:* nine.—13d 18h25: Te.—15d 08h43: Sw El.—18d 11h35: Tl.—23d 20h20: Do.—*25d 18h48:* twenty-four.—*30d 08h53:* five.

1951 June 01d 04h 31m: Hu.—01d 08h03: El.—01d 08h43: El.—06d 04h15: Do Sw CF.—10d 13h15: El.—*14d 17h51:* thirty-two.—*17d 17h02:* thirty-two.—*18d 23h14:* nineteen.—22d 12h47: Le.—*25d 04h28:* twenty-seven.—26d 20h08: Le.—28d 05h52: Al.

Sudden commencements of polar or pulsational disturbances (p.s.c.)

1951 April 01d 00h 52m: Wn Fu.—01d 20h50: Tr Wn Fu.—01d 21h01: So.—04d 16h12: Fu.—04d 23h43: Wn Fu.—*06d 18h10:* five.—06d 23h23: Wn Fu Tl.—07d 23h35: Wn Fu CF.—08d 22h04: Wn Fu CF Tl.—09d 18h07: So.—*10d 01h14:* five.—10d 19h33: So.—10d 21h00: Wn.—11d 23h07: Wn Fu SF.—16d 21h22: Wn Fu.—18d 19h22: So.—18d 23h25: Wn.—20d 22h24: Wn Fu.—21d 23h30: Wn Fu.—22d 19h24: So.—23d 21h50: So.—26d 00h24: Fu.

1951 May *01d 20h 59m:* eight.—03d 17h12: Fu.—04d 19h38: Wn Fu.—*05d 03h23:* five.—06d 19h02: Tr So Wn Fu.—07d 03h06: Wn Fu Tl.—07d 19h04: So.—07d 19h23: Wn Fu.—08d 19h34: So Wn Fu.—09d 19h58: Do Wn Fu.—*09d 22h42:* nine.—12d 00h02: El.—12d 16h50: Fu.—14d 21h08: Wn Fu.—16d 02h32: CF.—16d 22h55: Wn.—17d 01h35: Wn CF El.—18d 23h22: Wn Fu.—20d 20h45: Wn Fu.—21d 23h18: Wn Fu.—23d 00h55: CF.—23d 19h42: Te.—24d 21h42: So.—26d 21h35: El.—*28d 05h33:* nine.—*29d 22h35:* seven.—30d 21h08: Wn Fu.—31d 09h25: Te El Va.

1951 June 03d 00h 07m: Wn Fu El Hr.—04d 19h57: So.—08d 03h25: Do.—11d 19h40: Do.—12d 00h19: CF.—12d 20h27: Wn Fu CF.—*13d 21h35:* five.—16d 00h18: CF Hr.—17d 23h50: Tl El Hr.—19d 15h29: Fu.—20d 01h19: Hr.—*20d 22h55:* six.—21d 23h20: CF.—22d 20h48: Wn Fu Hr.—23d 01h11: Wn Fu CF.—29d 23h25: CF.—*30d 19h33:* six.

Geomagnetic planetary three-hour-range indices Kp, preliminary magnetic character-figures, C, an
final selected days, April to June, 1951

	April 1951									May 1951								
E	1	2	3	4	5	6	7	8	Sum	1	2	3	4	5	6	7	8	Sum
1	2 +	1 +	1 +	2 +	0 +	1o	2 −	3o	13 +	4 −	5 −	5 +	6 −	3o	5 −	7 −	7 +	41o
2	4 −	4 −	4 −	2 +	4o	5o	5o	5o	32 +	7 +	2 +	4 +	5 +	6o	5 +	6o	6o	43 −
3	5 +	5o	4 +	5 −	5 −	6o	6 −	5o	41 −	5 −	2 +	4 −	3 +	4 −	5 −	5o	5 +	33 −
4	5 −	5 +	5 +	4o	5o	6o	3 +	5o	39 −	5 +	4 −	3 +	4 +	4 +	4o	4o	3 −	32 −
5	6 −	6 +	5 −	5o	5 +	4o	4 +	4 +	40 −	1o	3 −	2 +	2o	1o	1 +	2o	3 +	16 −
6	4o	5 +	5o	4o	5 −	5o	5 +	6o	39 +	3 +	3 +	4o	1 +	2 +	2 +	3o	2o	22 −
7	5o	6 −	4 −	4 −	4o	4 +	4 +	4 +	35o	2o	2 +	2 +	2 −	3 −	2o	2 −	2o	17 −
8	5 −	4 +	4 +	3o	3o	3o	4 −	4 +	30 +	1o	1 −	0 +	1o	2 −	1 +	2o	1o	9o
9	3 +	4o	4o	4 −	4o	3 +	4 −	3 −	29 −	2 −	2o	3 +	3 +	3o	4 −	5 −	7 +	29o
10	5o	3o	4 −	3 +	4 −	2o	3 +	3o	27o	3 +	5o	5 +	5o	7 −	5 +	4o	2 +	37o
11	3 +	3 +	3o	2o	3 −	2o	1o	4 +	22 −	3o	3 −	4 −	4 +	5 −	3o	3 +	4o	29 −
12	4o	3o	3 −	2o	2 +	3o	3 −	5 +	25o	4o	3 +	3o	2o	2o	4 +	4o	1 +	24o
13	6 −	5o	3o	5o	6o	4o	3 +	5o	37o	1 +	1o	2 −	2 −	0 +	1 −	1o	2o	10 −
14	5 −	4 −	4 −	4o	3o	3 −	2 +	3 −	27 −	3o	4 −	3 −	3 −	1 −	3 −	4 −	4 +	23 +
15	2 +	2o	1 +	2 +	3o	3 −	2 +	2 −	18 −	5 −	3 +	3 −	2 +	3o	3o	3 +	3 +	26 −
16	2 +	1 +	1 −	0 +	1 −	1 +	1o	4 −	11 +	4 +	4 +	3o	3 +	2 +	3 −	3 −	3o	26 −
17	4 −	3 −	3 −	2 +	3 −	2 −	2o	1 −	18 +	4o	5 −	4 +	4 +	4o	4o	4 −	4o	33o
18	1o	1o	4 +	7o	8 −	6o	5o	5o	37o	5 −	4 +	2 +	3o	2 −	2o	2 +	3 −	23o
19	5o	3 −	3 −	3 +	2o	2o	2 −	4o	23 +	3 −	3 −	2 +	2 −	3 −	1 +	2 −	2 +	17 +
20	3o	4 −	3o	3 −	3 +	5 +	6 +	6 +	34 −	2o	2o	2 −	1 +	2o	1 −	2 −	1 +	13 −
21	6 −	5 +	4 +	5 +	5 −	4o	2 +	4 +	36o	1o	1o	1o	1 −	1o	1 −	1 +	1 +	8o
22	5 +	5 +	5 −	5 −	5o	4 +	5o	3 +	38 −	3 −	2 −	1 −	1o	2 +	2 +	1 +	1 +	13 +
23	4 −	5o	3 +	2 −	3 −	2o	1 −	3 −	22 −	2 +	2 +	2o	4o	4o	3 +	6o	5 −	29 −
24	2 −	4o	5o	4 +	6o	5o	5 +	4 +	36 −	4 +	3o	2 +	3 −	3o	4o	3 −	3 −	25 −
25	6 −	6 −	5 −	4 +	4 −	5o	5 −	4o	38 −	2 −	2o	3o	2o	2o	1 +	3 +	4 −	19o
26	6 −	3 −	2o	2 −	1 +	3 −	2 −	0o	18 −	3 +	2o	2o	3o	4 −	6 −	6 −	7o	32 +
27	1 −	1 +	2 +	2 −	3o	3 +	3o	3o	18 +	5 +	5 +	3 −	3 +	2 −	1o	1 −	2 −	22 −
28	3 +	2 −	2 −	2 +	1 +	2 +	2o	2 −	16 +	2o	3 −	2o	2 −	2 −	1 +	1 −	0 +	12 +
29	4o	4 −	2 +	2 +	3 +	3 +	2o	1o	22o	1 −	1 +	4o	3 −	4 −	2 +	2 −	3 +	20 −
30	1 −	1o	1 +	1o	1 +	1 −	1 −	2 −	8 +	1 +	1 −	3o	5o	4 +	2o	2 −	2 +	20 +
31										2 +	3 −	2 −	3 −	2 −	1 −	3 −	3o	17 +

	June 1951									Preliminary C, 1951		
E	1	2	3	4	5	6	7	8	Sum	Apr.	May	June
1	2 +	3 +	3o	3 −	4 −	4 +	4o	3o	26 +	0.4	1.6	1.0
2	2o	4 −	4 −	3o	4 −	4 −	4 +	4 −	28 −	1.3	1.6	1.0
3	4 +	2 +	2 +	2o	3 +	1 −	1o	2 −	18 −	1.5	1.2	0.8
4	1 +	2 −	2 +	2 −	3 −	3 −	2o	3o	17 +	1.5	1.1	0.6
5	3o	2 +	2 +	1o	2o	3 −	2 +	3 −	18 +	1.3	0.5	0.6
6	2 +	3o	6 −	5o	4 +	3o	2 +	2 −	27 +	1.4	0.6	1.1
7	3 −	4 −	3o	2 −	4 −	2 −	2o	2 +	21 −	1.2	0.4	0.6
8	3 +	4 +	3o	2o	3 +	4 +	3o	3o	26 +	1.0	0.2	1.0
9	4o	3o	2o	3 −	3 +	3 +	0 +	1o	20 −	1.0	1.4	0.7
10	1 −	0 +	0 +	2 +	3 +	2 +	2o	1 +	13 −	1.0	1.4	0.5
11	2o	3 −	2o	3 −	2 +	4 −	3 +	3o	22 −	0.7	1.0	0.7
12	4o	3 −	3 +	3o	3 −	2o	3o	3 −	23 +	1.0	1.0	0.7
13	3 −	2o	3o	3 +	4o	2 −	2 −	2 +	21 −	1.4	0.2	0.7
14	1o	1 +	0o	1 +	1o	4o	6 −	6 −	20o	0.8	0.8	1.3
15	4o	4 −	4o	3 +	5 −	4 +	4o	4 −	32 −	0.5	0.9	1.1
16	4o	2o	3o	3o	3 +	3o	3 +	3 −	24 +	0.3	0.9	0.8
17	2 +	1 +	2 −	1o	1 −	5 −	4 +	8o	24o	0.5	1.1	1.4
18	7 +	7 −	6 −	4 +	3o	4 −	2 +	4 −	37 −	1.7	0.9	1.6
19	3 +	6o	5o	5 +	3o	5 +	3 −	2 +	33o	1.0	0.4	1.3
20	3 +	1 +	1o	2 −	1 +	1 −	1 −	4 −	14 −	1.4	0.2	0.4
21	2o	3 −	4o	2 +	3 −	3o	1 +	2o	20o	1.4	0.1	0.6
22	2 +	2 −	2 −	3 −	3o	2 +	2 +	2 +	18 +	1.3	0.3	0.3
23	3o	2 −	2o	1 −	1 −	1 +	1 +	2o	13 −	0.7	1.2	0.2
24	2 −	1 +	1 +	3 −	2 +	1o	2 +	3 −	15 +	1.3	0.8	0.2
25	3o	4o	4 +	4 +	6 −	5 +	5 −	4o	35 +	1.3	0.6	1.4
26	3o	4 −	4 −	3 −	2 +	2 −	3o	2o	22o	0.8	1.5	0.6
27	2o	3 −	4o	2 −	2 +	4 +	3 −	3o	23 −	0.7	1.2	0.8
28	3 −	3o	3o	3 −	3o	2o	2o	3 +	22 −	0.5	0.3	0.8
29	3 −	2 +	1 +	1 +	3 +	3 −	3 +	3 −	20 −	0.7	0.7	0.7
30	3 −	3o	3o	3 −	2 +	2o	3o	1 +	20o	0.1	0.8	0.6
31											0.6	

Final selected days		
Apr.	May	June
Five quiet		
1	8	10
15	13	20
16	20	22
28	21	23
30	22	24
Five disturbed		
3	1	6
4	2	17
6	9	18
13	10	19
18	26	25
Ten quiet		
1	5	4
11	7	5
15	8	10
16	13	20
17	19	21
23	20	22
27	21	23
28	22	24
29	28	29
30	31	30

Other impulses found in the magnetograms

1951 April 05d 16h 13m: Tl.—16d 20h50: Te.—18d 10h27: Do Te.—18d 17h54: Te.—24d 04h37: Te.

1951 May 11d 14h 18m:Tl.—18d 02h30: El.—19d 18h51: Te.—26d 11h19: Sw El.—29d 06h21: Ch.

1951 June 06d 00h 48m: El.—13d 00h45: El.—18d 06h31: Tl.—18d 15h15: Tl Va.—18d 18h15: Ch.—24d 21h24: Te.—27d 16h06: Fu CF Va.

Ionospheric or solar disturbances without clear geomagnetic effect

1951 April 02d 17h 11-22m: CF.—10d 14h39-46: CF.—15d 09h03-12: CF.—5d 12h43-50: CF.—17d 12h10-29: CF.—17d 14h20-29: CF.—19d 14h25-30: CF.—9d 15h05-20: CF.—25d 06h50-57: CF.—25d 09h00-10h00: Hr.—27d 10h08-18: CF.—27d 11h35-45: CF.—27d 13h36-40: CF.

1951 May 15d 11h 20m-12h 20m: Wi CF Hr.—16d 11h29-33: CF.—17d 07h09-5: CF.—17d 09h44-50: CF.—17d 12h36-43: CF.—17d 14h42-50: CF.—17d 15h30-7: CF.—18d 10h20-40: Wi CF.—18d 11h36-45: CF Eb.—18d 10h40-13h00: Hr.—8d 13h03: CF.—19d 12h15-25: Wi CF.—19d 13h45-52: Wi CF.—19d 14h48-56: CF.—20d 08h00-20: Hr.—21d 12h15-25: CF.—21d 16h15-28: CF.—22d 12h00-05: CF.

1951 June 06d 07h 20m: CF.—16d 16h22-17h00: CF.—19d 09h45-50: CF.—9d 10h15-25: CF.—19d 12h59-13h14: CF.—19d 16h22-27: CF.—24d 14h00-22: CF.—25d 15h20-25: CF.—26d 15h59-16h16: CF.

Preliminary Report on Solar-Flare Effects

Effects confirmed by ionospheric or solar observations are in italics.

1951 April 01d 17h 30m: Hu.—10d 13h54-14h21: Do Tl Hu.—12d 17h30: Hu i.—17d 18h42-19h03: Ho.—*18d 23h50-19d 01h00:* Am.—*19d 08h54-09h05:* CF.—*0d 00h50-01h20:* Ka Tu Ap Am.—20d 01h50-57: Ho.—*20d 22h26-21d00h 02:* Am.—*3d 13h48-14h00:* CF.—25d 01h49-57: Ap.—*25d 08h45-09h00:* Wi.—30d 06h40: Al. —*30d 14h20-30:* CF.—30d 15h43-56: Tl.—*30d 17h20-30:* CF Hu.

1951 May 05d 18h 03m-24h 00m: Tu.—*06d 07h15-08h51:* Ka.—*08d 15h05-45:* Vn Wi CF Eb Tl Hu Va Pi Hr.—*10d 09h54-10h15:* Wi(ion) CF(ion) Eb Hr.—*4d 11h30-50:* Sw Wn Wi CF Eb Pi Hr.—18d 20h00-21h00: Ch Hu.—19d 19h53-0h00: Tu.—*20d 19h55-21d 02h00:* Tu Ho.—*21d 01h50-02h40:* Ka Ap Am.—1d 23h05: Tu.—*22d 00h36-45:* Ka.—*22d 00h55-03h00:* Ap Am.—*22d 09h10-40:* Vi(ion) CF Hr(ion).—*22d 13h37-14h15:* Wi CF(ion).—*23d 10h40-11h10:* Wi CF(ion) r(ion).—23d 19h41-51: Va.

1951 June 01d 13h 27-35m: Va.—09d 21h30-10d 01h52: Tu.—*13d 05h47:* Al.—*3d 07h10-22:* Wi CF.—*16d 15h44-52:* Al.—18d 14h48-15h30: Ch Sw.—*20d 14h10-5:* CF.—*20d 17h16-25:* CF.—*21d 09h10-20:* CF.—*22d 08h51-09h03:* CF.—*2d 11h40-52:* CF—*26d 17h10-50:* CF.—27d 16h06-50: Ch Tl Hu Va.

COMMITTEE ON CHARACTERIZATION OF MAGNETIC DISTURBANCES

BARTELS, *Chairman*
University
öttingen, Germany

J. VELDKAMP
Kon. Nederlandsch Meteorologisch Instituut
De Bilt, Holland

PROVISIONAL SUNSPOT-NUMBERS FOR JULY TO SEPTEMBER, 1951

(Dependent on observations at Zurich Observatory and its stations at Locarno and Orosa)

Day	July	Aug.	Sep.
1	17	64	46
2	16	71	47
3	36	55	48
4	50	57	55
5	32	73	64
6	56	74	84
7	69	83	77
8	86	102	91
9	105	121	108
10	109	132	118
11	112	121	129
12	96	112	123
13	95	82	114
14	92	66	107
15	90	62	100
16	40	58	89
17	45	54	93
18	48	49	98
19	40	66	89
20	33	67	91
21	26	54	104
22	28	62	109
23	70	38	104
24	78	42	80
25	61	24	76
26	52	8	70
27	60	6	63
28	79	8	58
29	61	24	23
30	66	15	31
31	58	40	
Means.......	61.5	61.0	83.0
No. days.....	31	31	30

Mean for quarter: 68.3 (92 days)

M. Waldmeier

Swiss Federal Observatory
Zurich, Switzerland

CHELTENHAM THREE-HOUR-RANGE INDICES K FOR JULY TO SEPTEMBER 1951

[$K9 = 500\ \gamma$; scale-values of variometer in γ/mm: $D = 5.4$, $H = 2.6$; $Z = 4.0$]

Gr. day	July 1951		August 1951		September 195	
	Values K	Sum	Values K	Sum	Values K	Sum
1	4212 2336	23	3322 2554	26	3111 2113	13
2	7765 3435	40	5444 2333	28	3111 1122	12
3	4443 5445	33	3222 2223	18	3332 2123	19
4	4442 2434	27	4311 3444	24	2311 2122	14
5	3332 2313	20	4221 2233	19	3322 1155	22
6	2332 2233	20	3021 3424	19	4243 3244	26
7	2221 1334	18	2323 2233	20	3212 1122	14
8	3311 1234	18	2321 1123	15	2321 2211	14
9	4422 3343	25	1233 3233	20	3303 4233	21
10	3232 1232	18	1232 3233	19	5464 4122	28
11	1122 2232	15	3344 3335	28	3252 3356	29
12	2212 2224	17	4434 3233	26	5433 4236	30
13	3212 1123	15	3554 4343	31	6432 4446	33
14	2122 1133	15	1112 2233	15	5442 3223	25
15	2132 2336	22	4242 3354	27	4554 4443	33
16	3423 3333	24	2456 2334	29	5655 5456	41
17	4334 3344	28	4231 3333	22	6545 4335	35
18	3353 3443	28	3331 1112	15	5523 2333	26
19	3244 2333	24	1233 3223	19	3343 4654	32
20	3332 2223	20	5553 3234	30	5666 5456	43
21	4343 1121	19	6444 4336	34	6555 4445	38
22	1464 3435	30	5454 4223	29	6665 4456	42
23	6344 2233	27	3332 3325	24	6653 4354	36
24	2342 3112	18	4544 3233	28	5544 5333	32
25	1242 2333	20	3654 2433	30	4445 6567	41
26	3453 3434	29	5554 3245	33	8742 1233	30
27	4445 1324	27	3553 3334	29	5554 3343	32
28	5654 3344	34	3333 2333	23	6121 1113	16
29	3444 2223	24	4443 3322	25	4231 4333	23
30	2223 3233	20	2211 2233	16	3332 2210	16
31	4554 3454	34	2242 3334	23		

Ralph R. Bodle
Observer-in-Charge

Cheltenham Magnetic Observatory
Cheltenham, Maryland, U.S.A.

PRINCIPAL MAGNETIC STORMS

dvance knowledge of the character of the records at some observatories as regards disturbances)

vatory erver- arge) (1)	Green-wich date (2)	Storm-time: GMT of begin. (3)	Storm-time: GMT of ending[1] (4)	Sudden commencement: Type[2] (5)	Amplitudes[3]: D (6)	Amplitudes[3]: H (7)	Amplitudes[3]: Z (8)	C-figure, degree of activity[4] (9)	Maximal activity on K-scale 0 to 9: Gr. day (10)	Gr. 3-hr. period (11)	K-index (12)	Ranges: D (13)	Ranges: H (14)	Ranges: Z (15)
	1951	h m	d h		′	γ	γ					′	γ	γ
	July 1	11 15	3 24	.....	....	....	....	ms	2	4	7	280	1530	1600
Cleven)	July 26	04 00	26 17	.....	....	....	....	ms	26	6	7	250	1680	800
	July 31	01 00	31 21	.....	....	....	....	ms	31	6	7	320	2070	1760
	Aug. 12	06 00	13 20	.....	....	....	....	ms	13	4, 5	6	200	1290	980
	Aug. 19	08 00	22 18	.....	....	....	....	ms	21	4	7	280	1600	1530
									22	3, 5	7			
	Sep. 9	09 00	10 19	.....	....	....	....	ms	10	3, 4	7	280	1400	980
	Sep. 11	12 00	14 14	.....	....	....	....	ms	12	6	6	140	1200	930
									13	6	6			
									14	3	6			
	Sep. 15	07 30	17 18	.....	....	....	....	s	16	4	8	400	2650	1680
	Sep. 19	15 00	26 05	.....	....	....	....	s	25	7	8	530	2430	1720
	July 1	11 00	4 13	.....	....	....	....	s	2	2, 4	8	155	1325	830
killman)	July 26	03 27	27 11	.....	....	....	....	ms	26	4	7	63	574	377
	July 27	22 20	29 15	.....	....	....	....	ms	28	4	7	49	485	518
	July 31	00 59	1 12	.....	....	....	....	ms	31	4	7	78	847	605
	Aug. 11	06 15	14 00	.....	....	....	....	ms	13	3, 5, 6	7	117	931	653
	Aug. 15	20 11	17 09	s.c.	+13	−14	+17	s	16	4	8	175	1307	751
	Aug. 19	07 58	22 16	s.c.	+2	+13	+6	s	22	3	8	104	985	704
	Aug. 23	07 30	24 16	.....	....	....	....	ms	24	2	6	55	440	443
	Aug. 25	02 00	30 00	.....	....	....	....	ms	26	3	7	79	559	410
	Sep. 5	20 47	6 21	s.c.*	+9	+9	+6	ms	6	4	6	34	308	139
	Sep. 9	02 07	10 20	.....	....	....	....	ms	10	3, 4	7	102	821	546
	Sep. 11	07 34	14 22	.....	....	....	....	ms	12	3, 5	6	60	565	543
	Sep. 15	07 30	17 18	.....	....	....	....	s	16	4	8	197	1100	967
	Sep. 19	05 58	24 16	.....	....	....	....	s	20	3, 4	9	161	2077	1042
	Sep. 25	04 15	26 07	.....	....	....	....	s	25	5	9	239	2546	1080
	Sep. 27	00 04	28 04	s.c.*	+6	+91	−8	ms	27	3	6	39	254	257
en	Apr. 2	12 00	8 24	.....	....	....	....	ms	3	6, 7	6	40	205	130
Sabben)									4	6	6			
									6	8	6			
	Apr. 12	19 00	14 14	.....	....	....	....	ms	12	8	6	45	245	85
									13	1, 8	6			
	Apr. 18	06 53	19 03	s.c.	+9	+12	+2	ms	18	4, 5	7	40	340	85
	Apr. 20	12 00	22 24	.....	....	....	....	ms	20	7, 8	6	45	215	125
	Apr. 24	05 00	26 02	.....	....	....	....	m	24	3, 5, 6. 7	5	35	165	125
									25	1, 6	5			
									26	1	5			
	May 1	00 00	4 21	.....	....	....	....	ms	1	8	7	60	280	180
									2	1	7			
	May 9	17 50	11 17	s.c.	−3	+16	0	ms	9	8	7	20	405	85
	May 23	07 00	24 21	.....	....	....	....	ms	23	7	6	35	160	65
	May 25	18 48	27 12	s.c.	−2	+38	−1	ms	26	6	6	45	210	100
									27	1	6			
	May 30	08 53	30 16	s.c.	+2	+6	+1	m	30	5	5	15	85	30
	June 6	04 00	6 19	.....	....	....	....	m	6	3, 4, 5	5	20	145	45
	June 14	17 52	15 22	s.c.	−4	+81	−3	m	14	6, 7, 8	5	30	175	65
									15	5	5			
	June 17	17 02	18 19	s.c.	−4	+104	−3	ms	17	8	7	45	345	200
									18	1	7			
	June 18	23 14	19 18	s.c.	−1	+50	−1	ms	19	6	6	15	185	90
	June 25	04 28	25 24	s.c.	−6	+19	−1	ms	25	5	6	25	160	90

oximate time of ending of storm construed as the time of cessation of reasonably marked disturbance movements in the re specifically, when the K-index measure diminished to 2 or less for a reasonable period.

= sudden commencement; s.c.* = small initial impulse followed by main impulse (the amplitude in this case is that of the lse only, neglecting the initial brief pulse); ... = gradual commencement.

of amplitudes of D and Z taken algebraically; D reckoned positive if towards the east and Z reckoned positive if ver-nwards.

n described by three degrees of activity: *m* for moderate (when K-index as great as 5); *ms* for moderately severe (when 7); *s* for severe (when K = 8 or 9).

PRINCIPAL MAGNETIC STORMS—Continued

Observatory (Observer-in-Charge) (1)	Greenwich date (2)	Storm-time: GMT of begin. (3)	Storm-time: GMT of ending[1] (4)	Sudden commencement: Type[2] (5)	Sudden commencement: Amplitudes[3] D (6)	Amplitudes[3] H (7)	Amplitudes[3] Z (8)	C-figure, degree of activity[4] (9)	Maximal activity on K-scale 0 to 9: Gr. day (10)	Gr. 3-hr. period (11)	K-index (12)	Ran… D (13)
	1951	h m	d h		′	γ	γ					′
Witteveen *Continued* (D. van Sabben)	July 1	22 26	4 18	s.c.	+1	+86	−3	ms	2	2	7	50
	July 15	15 30	18 24	.....	....	....	....	m	15	8	5	30
									16	5, 6	5	
									17	4	5	
									18	5, 6	5	
	July 22	04 00	23 12	.....	....	....	....	m	22	3, 6	5	20
									23	1	5	
	July 26	03 00	27 03	.....	....	....	....	m	26	2, 6	5	20
									27	1	5	
	July 28	01 00	28 24	.....	....	....	....	m	28	2, 4, 6, 7	5	25
	July 31	00 59	31 24	s.c.	−2	+33	0	m	31	5, 6, 7, 8	5	25
	Aug. 1	15 42	2 09	s.c.	−2	+29	−3	ms	1	6, 7, 8	6	25
	Aug. 13	03 36	13 21	s.c.	−1	+23	−1	ms	13	7	6	30
	Aug. 15	20 10	16 17	s.c.	−5	100	−4	ms	16	3	6	20
	Aug. 16	21 59	17 24	s.c.	−2	+29	−1	m	17	6	5	15
	Aug. 20	01 00	22 24	.....	....	....	....	ms	21	1, 6	6	35
	Aug. 25	01 00	26 24	.....	....	....	....	ms	25	3, 7	6	30
	Sep. 5	20 46	6 24	s.c.	−3	+66	−4	m	5	7	5	20
									6	1	5	
	Sep. 11	10 00	18 24	.....	....	....	....	ms	11	8	7	50
	Sep. 19	08 43	24 24	s.c.	+2	−10	0	s	19	6	8	70
	Sep. 25	10 00	26 12	.....	....	....	....	s	25	8	9	120
	Sep. 27	00 05	27 15	s.c.	−4	+47	−2	m	27	1, 2, 3, 4	5	30
Cheltenham (R. R. Bodle)	July 1	22 27	5 07	s.c.	4	101	6	ms	2	1, 2	7	62
	July 17	09 ..	19 10	.....	....	....	....	m	8	3	5	10
	July 22	03 ..	23 23	.....	....	....	....	ms	23	1	6	22
	July 26	04 ..	29 10	.....	....	....	....	ms	28	2	6	22
	July 31	05 ..	3 03	.....	....	....	....	m	31	2, 3	5	24
	Aug. 11	03 15	13 22	s.c.	1	1	5	m	13	2, 3	5	28
	Aug. 15	20 10	17 09	s.c.	1	72	3	ms	16	4	6	28
	Aug. 20	01 ..	22 14	.....	....	....	....	ms	21	1	6	32
	Aug. 23	21 42	28 09	s.c.	1	24	6	ms	25	2	6	25
	Sep. 5	20 40	6 02	s.c.	1	8	4	m	5	8	5	7
	Sep. 6	06 12	7 01	s.c.	1	33	4	m	6	3	4	1
	Sep. 10	02 ..	10 14	.....	....	....	....	ms	6	3	6	30
	Sep. 11	08 ..	14 09	.....	....	....	....	ms	12	8	6	38
									13	1	6	
	Sep. 15	01 ..	18 06	.....	....	....	....	ms	16	2	6	38
	Sep. 19	11 57	26 07	s.c.	2	20	2	s	26	1, 2	8	58
	Sep. 27	00 06	28 03	s.c.	2	43	1	ms	28	1	6	30
Tucson (J. B. Campbell)	July 1	22 26	4 08	s.c.	−1	+30	....	ms	2	2	7	28
	July 22	03 ..	23 12	.....	....	....	....	ms	22	3	6	13
	July 30	21 ..	1 06	.....	....	....	....	ms	31	2	6	19
	Aug. 1	15 ..	2 12	.....	....	....	....	m	1	6, 8	5	9
									2	1, 2, 3	5	
	Aug. 11	22 ..	13 23	.....	....	....	....	ms	13	3	6	16
	Aug. 15	20 11	? ?	s.c.	−1	+38	+1	....	....	....	...	....
		(*Note*: Magnetograph record lost between 06^h 08^m, Aug. 16, and 16^h 18^m, Aug. 17, because of damage to equipment by a severe electrical storm)										
	Aug. 20	01 ..	29 24	.....	....	....	....	ms	20	1	6	22
									21	1	6	
									23	8	6	
	Sep. 5	20 45	6 23	s.c.	−2	+31	+2	m	6	3	5	14
	Sep. 9	02 ..	28 03	.....	....	....	....	ms	26	1, 2	7	32
San Juan (P. G. Ledig)	July 1	22 27	2 11	s.c.	+1	+22	−9	ms	1	8	6	13
									2	1, 2	6	
	Sep. 19	08 41	21 12	s.c.	0	+13	−2	ms	19	6	6	13
		(Followed by a very disturbed period of about two days)										
	Sep. 25	04 ..	26 06	.....	....	....	....	ms	26	1	7	11
	Sep. 27	00 05	28 02	s.c.	0	+17	−5	m	27	1, 3	5	6
									28	1	5	

PRINCIPAL MAGNETIC STORMS—Continued

vatory	Green-wich date	Storm-time		Sudden commencement				C-figure, degree of ac-tivity[4]	Maximal activity on *K*-scale 0 to 9			Ranges		
erver-harge)		GMT of begin.	GMT of ending[1]	Type[3]	Amplitudes[3]				Gr. day	Gr. 3-hr. period	*K*-index	*D*	*H*	*Z*
					D	*H*	*Z*							
1)	(2)	(3)	(4)	(5)	(6)	(7)	(8)	(9)	(10)	(11)	(12)	(13)	(14)	(15)
	1951	h m	d h		′	γ	γ					′	γ	γ
lu	July 1	22 25	4 12	s.c.	0	5	4	ms	2	3	6	16	242	77
White)	Aug. 1	03 40	2 09	.....	....	....	....	m	1	6	5	16	250	78
	Aug. 15	20 09	17 09	s.c.	2	31	22	m	16	4	5	11	119	61
	Sep. 11	18 00	18 17	.....	....	....	....	m	17	8	5	11	97	59
	Sep. 19	08 40	28 08	.....	....	....	....	ms	25	7	6	12	253	48
to Geo-	July 1	22 26	3 05	s.c.	0	+41	+6	ms	1	8	6	9	292	45
e									2	2	6			
ayo	July 31	01 00	2 20	s.c.	0	+17	+3	ms	1	6, 7	6	6	334	41
Giesecke)	Aug. 15	20 18	17 18	s.c.	+1	+78	+10	m	15	7	5	5	188	46
	Sep. 9	01 40	14 08	.....	....	....	....	m	13	5, 6	5	9	271	55
	Sep. 15	04 30	18 05	.....	....	....	....	ms	16	6	6	8	339	53
	Sep. 19	08 42	23 04	s.c.	+1	+41	+4	ms	19	5, 6	7	11	409	54
	Sep. 25	04 12	26 05	.....	....	....	....	ms	25	6, 7	6	9	450	51
									26	1, 2	6			
	Sep. 27	00 06	28 02	s c.	0	+31	+4	m	27	3, 4, 5	5	5	253	29
thville	Apr. 2	04 57	10 02	s.c.*	+1	−13	−1	m	2	6	...	8	159	31
xandre)	Apr. 12	07 20	13 24	.....	....	....	....	m	13	4, 5	...	11	140	39
	Apr. 18	06 55	19 04	s.c.	−3	+46	+4	ms	18	4, 5	...	10	250	39
	Apr. 20	13 00	21 05	.....	....	....	....	m	20	7	...	8	81	22
	Apr. 21	11 45	23 06	.....	....	....	....	m	21	5	...	8	118	27
	Apr. 24	06 35	21 05	s.c.*	−1	−6	−1	m	24	6	...	9	85	35
	May 1	05 00	3 24	s.c.*	−4	145	+8	m	1	8	...	8	190	23
	May 1	21 01	.. ..	s.c.	....	....	....	....	....	....	...	....	....	....
	May 9	22 45	10 24	s.c.*	+3	120	+8	m	10	6	...	10	161	35
	May 25	18 48	27 04	s.c.	−1	+14	+1	m	26	8	...	9	173	25
	June 17	17 00	19 24	s.c.	−1	+32	+2	ms	17	8	...	10	149	23
	June 25	04 30	26 01	s.c.	−1	+13	−1	m	25	4, 7	...	9	142	27
	July 1	22 27	4 12	s.c.	0	+5	−3	ms	2	1, 3	6	6	281	32
M. King)	July 24	04 30	27 10	.....	....	....	....	m	26	2	5	4	94	19
	July 31	01 00	2 10	s.c.?	0	+7	−2	m	1	6, 8	5	5	127	30
	Aug. 12	19 55	13 16	.....	....	....	....	m	13	2, 3	5	4	108	19
	Aug. 15	20 09	17 09	s.c.	0	+29	−12	m	16	4	5	5	138	26
	Aug. 18	23 ..	22 14	.....	....	....	....	m	20	1	5	5	142	35
	Aug. 24	23 ..	26 12	.....	....	....	....	m	25	3, 4	5	5	100	22
	Sep. 5	20 44	6 15?	s.c.	0	+19	−7	m	6	3	5	4	109	26
	Sep. 9	09 ..	10 15	.....	....	....	....	m	10	3, 4	5	4	112	21
	Sep. 11	08 ..	18 12	.....	....	....	....	m	11	7	5	6	124	36
									12	8	5			
									14	3	5			
									16	2, 4	5			
									17	8	5			
	Sep. 19	07 ..	24 13	.....	....	....	....	m	19	6	5	6	126	32
									20	2, 3, 4	5			
									21	1, 3	5			
									22	3	5			
	Sep. 25	05 ..	26 12	.....	....	....	....	ms	25	7, 8	6	5	202	31
									26	2	6			
	Sep. 27	00 07	28 03	s.c.	0	+18	−4	m	27	2, 3, 4, 5	5	4	95	25
nus	July 1	22 27	4 16	s.c.	+1	+28	+21	m	1	8	5	26	90	77
									2	1, 2, 3, 4	5			
jk)									4	2	5			
	July 15	19 ..	16 01	—— Large bay ——				m	15	8	5	....	....	....
	July 22	02 ..	23 12	.....	....	....	....	m	22	4	5	15	53	61
									23	1	5			
	July 27	22 ..	29 18	.....	....	....	....	m	28	6, 7	5	13	90	70
	July 31	00 59	1 06	s.c.?	+1	+10	+9	ms	31	8	6	14	120	95
		(Possibility of earlier start, p.s.c., July 30, 18^h 30^m)												
	Aug. 1	15 ..	2 09	.....	....	....	....	m	1	6	5	14	72	82
									2	1, 2	5			

PRINCIPAL MAGNETIC STORMS—Concluded

Observatory (Observer-in-Charge) (1)	Greenwich date (2)	Storm-time: GMT of begin. (3)	Storm-time: GMT of ending[1] (4)	Sudden commencement: Type[2] (5)	Sudden commencement: Amplitudes[3] D (6)	Amplitudes[3] H (7)	Amplitudes[3] Z (8)	C-figure, degree of activity[4] (9)	Maximal activity on K-scale 0 to 9: Gr. day (10)	Gr. 3-hr. period (11)	K-index (12)	Ran D (13)	H (14
	1951	h m	d h		′	γ	γ					′	γ
Hermanus—*Continued* (A. M. van Wijk)	Aug. 13	03 36	13 22	s.c.?	+2	+11	+10	m	13	5, 7	5	14	11
	Aug. 15	20 11	16 16	s.c.	+2	+16	+9	m	16	3, 4	5	10	10
	Aug. 20	00 56	30 00	p.s.c.	....	....	....	m	20	3	5	19	10
									21	1, 6, 8	5		
									23	8	5		
									25	4, 6	5		
									26	8	5		
	Sep. 6	06 10	7 02	s.c.	−1	+9	+8	m	6	4	5	10	8
		(Earlier abrupt change at $20^h\ 46^m$, Sep. 5)											
	Sep. 11	00 ..	19 01	.....	....	....	....	ms	11	8	6	33	14
	Sep. 19	08 41	25 01	s.c.	....	....	....	ms	19	6	7	33	20
		(Amplitudes of s.c. uncertain)											
	Sep. 25	04 ..	26 12	.....	....	....	....	ms	25	8	7	33	20
		(Abrupt changes, Sep. 25, $09^h\ 45^m$; suspected s.f.e , $09^h\ 35–50^m$)											
	Sep. 27	00 05	28 03	s.c.	+2	+21	+18	ms	27	3, 4	6	25	13
		(Amplitudes of s.c. uncertain)											
	Sep. 28	21 ..	30 14	.....	....	....	....	m	29	6	5	18	8.
Watheroo (L. S. Prior)	July 1	22 26	2 19	s.c.*	+5	+10	+22	m	1	8	5	13	13
									2	1, 2, 3, 4	5		
	July 31	12 00	2 08	.....	....	....	....	m	31	5, 8	5	17	11
									1	8	5		
									2	2	5		
	Aug. 13	03 37	13 21	s.c.	+1	+3	−1	m	13	3	5	17	8
	Aug. 15	20 12	17 09	s.c.	+3	+12	+20	m	16	3, 4	5	10	12
	Aug. 17	07 07	.. ..	s.c.	−2	+24	−12	(No appreciable disturbance followed)					
	Aug. 20	23 36	22 20	s.c.	−2	+12	−13	m	21	4, 5, 6	5	14	9
	Aug. 25	07 00	26 15	.....	....	....	....	m	25	3, 4, 6, 7	5	12	12
									26	4	5		
	Sep. 5	20 46	.. ..	s.c.*	+3	+14	+18	....	....	....	...	....	...
	Sep. 6	06 11	.. ..	s.c.	−1	+16	−1	....	....	....	...	....	...
	Sep. 10	04 00	10 20	.....	....	....	....	ms	10	5	6	17	7
		N.B. Movements from $20^h\ 46^m$ GMT, Sep. 5, to $10^h\ 20^m$ GMT, Sep. 10, were considered as one storm)											
	Sep. 11	16 00	17 20	.....	....	....	....	ms	16	5	7	24	14
	Sep. 19	12 00	24 18	.....	....	....	....	ms	21	4	7	24	21
	Sep. 25	11 00	27 16	.....	....	....	....	ms	25	8	7	30	17
Amberley J. W. Beagley)	July 1	22 26	4 13	s.c.*	−2	−43	+7	ms	2	3, 4	6	46	18
	July 17	07 34	18 22	s.c.?	−1	+8	+2	m	17	4	5	12	8
	July 22	00 18	23 12	.....	....	....	....	ms	22	3	6	21	13
	July 25	04 42	27 12	.....	....	....	....	m	26	3, 4	5	13	12
	July 31	01 00	2 09	s.c.*	0	+13	+2	m	31	4, 5, 6	5	22	11
	Aug. 11	01 12	14 01	.....	....	....	....	m	13	2, 3	5	17	10
	Aug. 15	20 12	17 09	s.c.?	−1	+26	+2	m	16	3, 4	5	25	9
	Aug. 19	04 00	22 16	.....	....	....	....	ms	22	3	6	20	14
	Aug. 23	21 43	29 14	.....	....	....	....	m	25	3, 4	5	25	14
									26	3	5		
	Sep. 5	20 46	.. ..	s.c.*	−3	−13	+15	m	6	3, 4	5	15	8
	Sep. 6	06 12	7 03	s.c.*	−2	+36	+6	....	....	....	...	....	...
	Sep. 10	02 19	14 14	s.c.*	+2	+23	−7	m	10	3, 4	5	18	11
									11	7	5		
									14	3	5		
	Sep. 15	02 42	18 13	s.c.*?	+1	+14	−6	ms	16	4, 5	6	27	22
	Sep. 19	06 30	26 13	.....	....	....	....	ms	19	6	6	47	33
									20	4	6		
									22	2	6		
									25	7	6		
									26	1, 2	6		
	Sep. 27	00 05	28 08	s.c.*	−2	+31	+8	ms	27	3	6	14	19
	Sep. 29	07 04	30 09	.....	....	....	....	m	29	6	5	9	11

REVIEWS AND ABSTRACTS

V. UYTENBOGAARDT: *Tables for microscopic identification of ore minerals.* Princeton, Princeton University Press, vii + 242 (1951). 25 cm.

This is an analytic key to the determination of the opaque ore minerals, by xamination of polished surfaces in reflected light, both ordinary and polarized. n adequate discussion is given of the properties employed in the systematic lassification for determinative purposes, such as polishing hardness, Talmadge ardness, reflectivity percentages, color, anisotropy, structural features, and paraenesis. Practically every known ore mineral is listed, and there is a bibliography f 421 titles which, together with the earlier one of Schneiderhohn-Ramdohr (1931), ffords a fairly complete bibliography of this branch of mineralogical science.

The beginner will find no better book to guide his efforts, and the expert will nd an invaluable systematization of a vast volume of data.

CHARLES MILTON

. BOCK: *Atlas of magnetic declination of Europe for epoch 1944.5.* Washington, D. C., Army Map Service, Corps of Engineers, Department of the Army, iii + 9 pp. + 69 isogonic charts + 8 figs. + 75 app. (1951). 66 cm.

The most comprehensive compilation of charts, mainly for magnetic declinaon, of Europe and North Africa is included. The results are based on extensive rveys made by parties of the German Military during World War II, as well as all available published material and non-published manuscripts.

The publication is divided into five sections. Part 1 discusses origin of the atlas; art 2, embracing the period since 1845, cites all sources that have been used in e compilation; and Part 3 gives complete and detailed notes on survey data d 69 isogonic charts of Europe for epoch 1944.5, on scale 1:1,000,000, in sections, combinations of sections, of the International Map of the World. In the apndices are shown the density of magnetic declination observations for Europe, cations of magnetic stations, and various isogonic charts for Europe. Magnetic omalies, which normally cannot be shown on small-scale sheets, appear clearly these more-open-scale charts. An admirable printing job has been done by the my Map Service on this project.

The charts will be invaluable for various engineering needs of surveying, in vigation, and no doubt will be utilized in problems of European crustal geology.

E. H. VESTINE

PHOTOELECTRIC OBSERVATIONS OF LIGHTNING

Oscillographic records of the output of a photomultiplier exposed to the sky during a thunderstorm can provide data for the study of the intensity and fre- quency distributions of the components of lightning flashes. Records of this kind have been made at the United States Naval Observatory as a by-product of another photometric investigation. I am not aware of previous observations of this kind.

The accompanying photograph shows a half-second glimpse of a thunderstorm as seen by a photomultiplier. The photoelectric photometer was viewing a patch of sky on the meridian, some 45° above the south point. The output of the photo- multiplier was connected to an oscilloscope and the time axis was produced by photographing the moving cathode-ray spot on a continuously moving film, so that the illustration is really a plot of sky brightness against time. The pips were

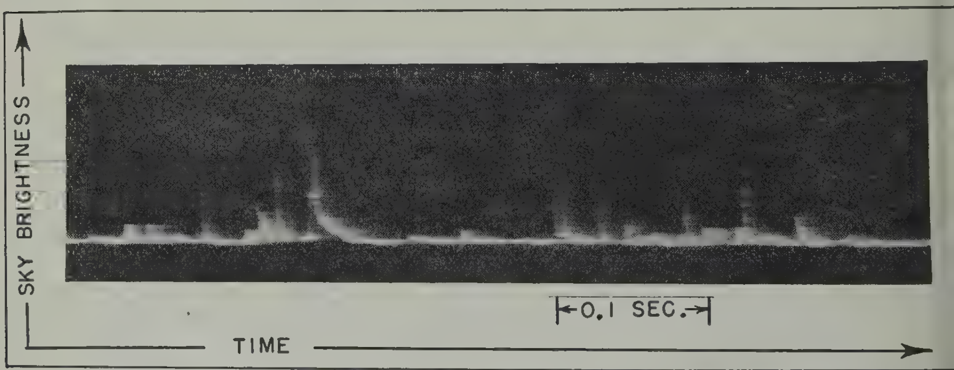

FIG. 1—SECTION OF AN OSCILLOGRAPH RECORD SHOWING LIGHT- NING AS OBSERVED BY A PHOTOMULTIPLIER

produced by lightning in a storm some five or ten miles NNW of the Observatory The sky at the time was clear though hazy, except for 0.2 cloud cover to the NW The blurring of the features is caused by the persistence of the oscilloscope screen and the dark horizontal lines are those of a superimposed grid. Two flashes are shown resolved into components. Most of the discharges persisted for about a thousandth of a second; but for one, in the first flash, the light lasted for almost thirty thousandths of a second.

The photoelectric method is ideal for the measurement of the rapid light changes produced by lightning, as the response time of a photomultiplier is about 10^{-8} second.[1] Changes in light intensity over intervals as short as a fraction of a microsecond can be recorded. In addition, an accurate quantitative record of ligh

[1]R. W. Engstrom, J. Optical Soc. Amer., 37, 420 (1947).

tensity is obtained. Simultaneous visual observations must be made in order to void confusing separate flashes with the components of an individual flash.

ARTHUR A. HOAG

NITED STATES NAVAL OBSERVATORY,
Washington, D. C., July 12, 1951

GEOMETRIC INTERPRETATION OF THE Π-WAVE AND COUPLING FACTOR IN IONOSPHERIC LONG-WAVE THEORY

The continuous-wave solution to the Appleton-Hartree equations leads to two ormal modes of propagation such that

$$\frac{E_y^{(1)}}{E_x^{(1)}} = u_1 \; ; \qquad \frac{E_y^{(2)}}{E_x^{(2)}} = u_2 \; ; \qquad u_1 u_2 = 1 \ldots\ldots\ldots\ldots\ldots (1)$$

nere u_1 and u_2 are the polarizations of ordinary and extraordinary waves, re- ectively. If we construct the complex plane of the Figure, we have

$$\tan \theta = \frac{jE_y}{E_x} = ju \ldots\ldots\ldots\ldots\ldots\ldots\ldots\ldots (2)$$

that in this representation the normal modes appear linearly polarized in the rection given by the complex angle θ. Furthermore, since

$$\tan \theta_1 \tan \theta_2 = (ju_1)(ju_2) = -1$$

e two modes represent orthogonal directions in this space. This property suggests e use of these directions as a set of axes for a coordinate system. We then have

$$\Pi_1 = \frac{E_x}{\sqrt{1 - u^2}} = \frac{E_x}{\sqrt{1 + \tan^2 \theta}} = E_x \cos \theta$$

$$\Pi_2 = \frac{E_y}{\sqrt{1 - u^2}} = \frac{E_y}{\sqrt{1 + \tan^2 \theta}} = E_y \cos \theta$$

us the Π-waves are simply components along the principal axes. A vector E ving polarization u has as unique ordinary and extraordinary components:

$$(E)_0 = \frac{E_x + juE_y}{\sqrt{1 - u^2}} \; ; \qquad (E)_x = \frac{E_y - juE_x}{\sqrt{1 - u^2}}$$

Coupling takes place between the two modes due to the space-variation of the gle θ. Differentiation of the relation (2) gives

$$\sec^2 \theta \frac{d\theta}{dz} = j \frac{du}{dz}$$

$$\frac{d\theta}{dz} = j\left(\frac{du/dz}{1 - u^2}\right) = j\psi$$

where ψ is the coupling factor as defined in the magneto-ionic theory.[1] Thus *represents the space rate-of-twist of the polarization axes* (usually in radians per km

One should regard the ordinary and extraordinary waves, not as being endowe

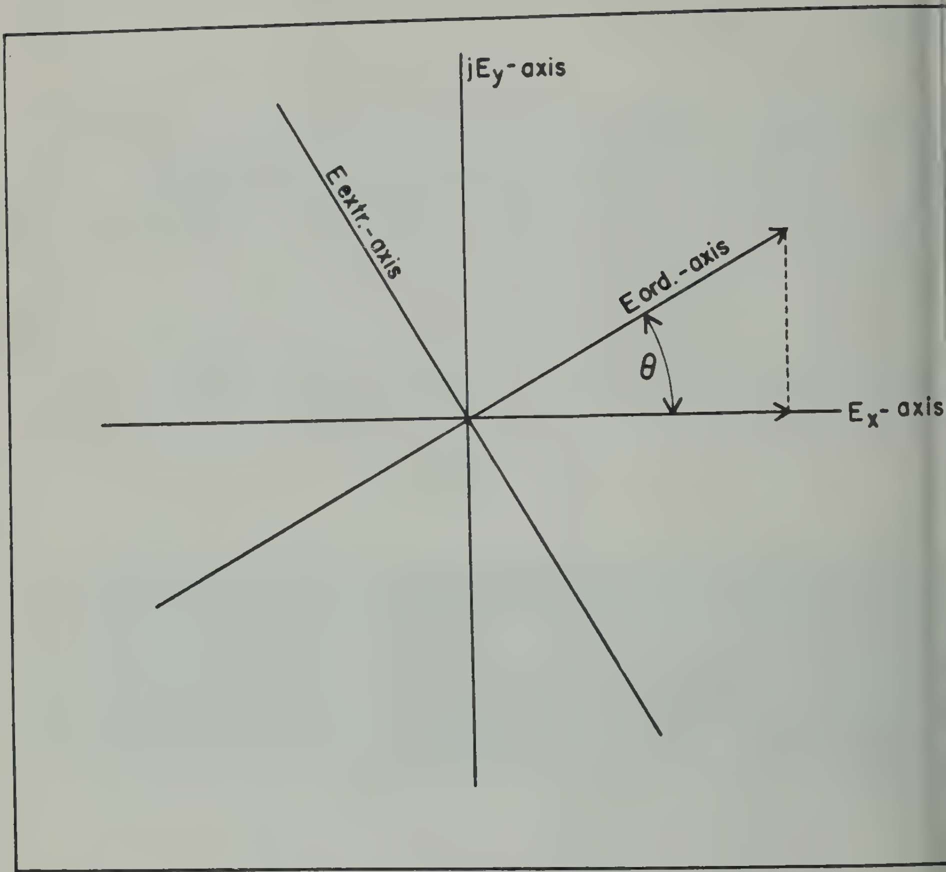

PRINCIPAL POLARIZATIONS AS REFERENCE AXES

with any special physical significance, but simply as components in a movi Cartesian coordinate system.

The research reported in this paper has been sponsored by the Geophysi Research Division of the Air Force Cambridge Research Center under Contr No. AF19(122)-44.

Norman David

Ionosphere Research Laboratory,
The Pennsylvania State College,
State College, Pennsylvania, October 11, 1951

[1] O. E. Rydbeck, On the propagation of radio waves, Trans. Chalmers Univ., Gotheb No. 34 (1944).

)T-FREQUENCY IONOSPHERIC RECORDING—A COMBINATION OF SWEEP- AND FIXED-FREQUENCY TECHNIQUES

'he panoramic high-speed ionospheric recorders which have been used by the artment of Terrestrial Magnetism, Carnegie Institution of Washington, in e-station experiments for studies of ionospheric irregularities, traveling dis- ances, and special eclipse observations, sweep through the useful frequency trum in a few seconds and record vertical heights. The motion-picture technique ribed by Wells, Watts, and George* provides a valuable tool for the observation ynamic characteristics of the ionosphere. However, quantitative analysis of spheric events requires careful scanning or scaling of the individual records. never a research project involves the continuous operation of one or more -speed ionospheric recorders, the problem of data analysis becomes immense. example, a ten-hour period of continuous recording at a sweep rate of 10 sec- s produces 3,600 individual records (approximately 100 feet of 16 mm film).

'he advantages as well as the limitations of fixed-frequency ionospheric record- $(h' - t)$ have been apparent since the original pulse experiments of Breit and e. The problem of data assimilation posed by the motion-picture type of oramic recording has led to the trial of a method which appears to combine the bility of the sweep-frequency instrument with the simplicity of the fixed- uency recorder. The sweep-frequency instrument is keyed to emit pulse trains fferent frequencies which are selected at will. The number of selected frequencies nited only by the desired amount of definition. Tests have been conducted with o ten individual channels. The film motion is changed from intermittent to a continuous movement and the horizontal deflecting voltage is removed from ecording oscilloscope.

'he result is equivalent to taking a series of cross-sections of the $h' - f$ structure lected frequencies, which are repeated every few seconds, depending upon the ating speed of the panoramic recorder. The slight advance of film during each ating sequence is adequate to identify the echo pattern at successive frequencies if the heights are similar. Consequently, a running log of ionospheric character tained simultaneously at a number of selected frequencies.

'he principle is illustrated in Figure 1 (*A* and *B*), which shows a normal sweep and the record obtained from two successive sweeps (*B*) through recording uencies of 9.5, 7.5, and 5.0 Mc/sec.

'igure 2 is a record made during an interval of approximately ten minutes on fternoon of December 17, 1951. The recording frequencies are 9.5, 7.5, and Mc/sec, as sketched in Figure 1. The recording film motion was 12 inches per , and the sweep interval was 25 seconds. At 9.5 Mc/sec, the "O" and "X" -components are fully resolved. A merging trend may be observed; at 7.5 he separate wave-components are merged and a multiple echo is present. The points are near the minimum height of *F* region and are appreciably weaker. ht markers at intervals of 50 km are identified by the horizontal rows of "dots" site the scale at left of Figure.

Phys. Rev., **69**, 540–541 (1946).

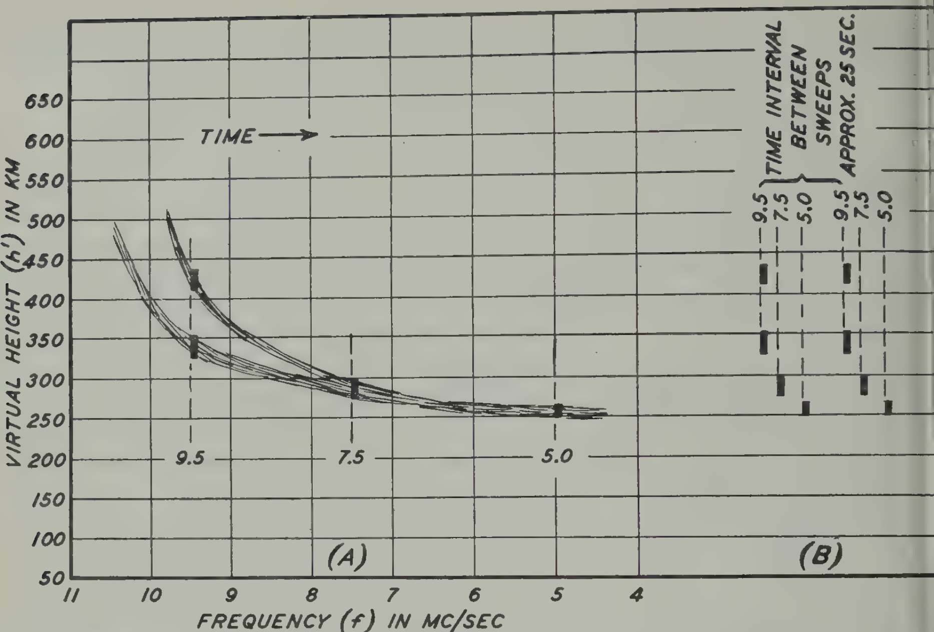

FIG. 1—h'-f RECORD, 15^h40^m, 75° WMT, DECEMBER 17, 195[1]
DERWOOD EXPERIMENTAL LABORATORY, DTM CIW

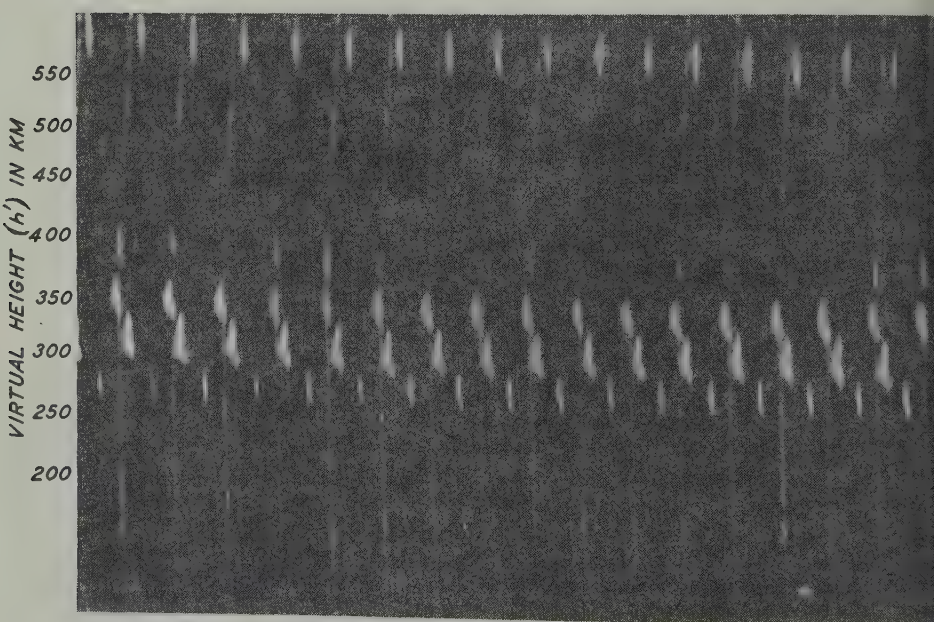

FIG. 2—SPOT-FREQUENCY RECORD AT 9.5, 7.5, AND 5.0 MC, 15^h40^m–15^h50^m, DECEMBER 17, 1951, DERWOOD EXPERIMENT[AL] LABORATORY, DTM CIW

The record of Figure 2 demonstrates the recording principle. It does not illus-
e any ionospheric event of unusual interest. The fact that a complete tabulation
onospheric heights may be readily obtained at each of the sampling frequencies
pparent from the Figure. Dynamic effects in the ionosphere, such as winds,
ds, turbulence, and traveling disturbances, are subject to positive identification
description without the laborious scaling of a large number of individual $h' - f$
ords as obtained in the normal operation of a high-speed panoramic instrument.
les or graphs of ionospheric heights at each frequency channel are obtained
a minimum of scaling effort. Another apparent advantage is the virtual elimi-
ion of interference to other services by an instrument of this type.

This method of spot-frequency recording is being subjected to further tests to
ss its over-all utility, and is being seriously considered for field testing in a
e-station network observing dynamic effects and measuring apparent velocity
direction of traveling disturbances.

H. W. Wells

artment of Terrestrial Magnetism,
arnegie Institution of Washington,
Washington 15, D. C., December 20, 1951.

NOTES

(36) *Geomagnetic data on solar wave radiation*—Dr. J. Bartels (Göttingen)
computed daily values of δW_2 in continuation of those published in *Terr. Mag.*,
190-205 (1946), based on magnetic observations of the Huancayo Observato
for 1938 to 1947. Copies of these tables are available on application to Dr. Jo
W. Mauchly, Remington Rand Inc., 1624 Locust Street, Philadelphia 3, Pa., U.S

(37) *Changes at the magnetic station of Dombås*—Dr. K. F. Wasserfall, of M
netiske Byrå, Bergen, Norway, reports some modifications at the Dombås magne
station. A new set of D, H, and Z variometers (de Copenhague) have been p
cured, and, at about 1.5 km from the old station, a new variation-house has be
constructed. The geographical coordinates of this new observatory are 62° 04
north and 9° 07′.0 east (about 660 meters above sea-level). The building is hea
during the winter, and the instruments are compensated for change in temperatu
Comparison during three months of parallel registration showed that the p
turbations for the D and H curves are the same for both stations, while the
instrument showed the relation "Old/New = 1.467." Eschenhagen variomet
were previously in use at Dombås. A new absolute house is expected to be erec
sometime in the future. In addition to the regular absolute instruments, a compl
set of the la Cour type has been acquired.

(38) *Progress report, Danish deep-sea expedition, 1950-52*—This Journal p
viously contained notes (see issues of December, 1949, page 407, and of Decemb
1950, page 497) concerning the *Galathea* on its two-year round-the-world cru
The expedition left Copenhagen on October 15, 1950. One of its purposes is
measure the magnetic forces at the surface and at very great depths of the ocea
Dr. Niels Arley, who is carrying out these magnetic researches, reported on Aug
8, 1951, that a single non-magnetic sphere had succeeded in withstanding
pressure at a depth of 10,000 meters in the Philippines. The sphere came up int
and contained only 1.4 liters of water in an internal volume of 65 liters, the sli
leakage resulting where the two halves of the sphere are fastened together.
Arley now plans to place the instruments for measuring the magnetic field of
earth at great depths in a closed container, to protect the instruments agai
the small amount of water leakage. The spheres being used by the expedition w
made by the kind help of two Danish firms, Messrs. Paul Bergsøe and Son, wh
created the new special non-magnetic alloy, and Messrs. Burmeister and W
which constructed the spheres of this alloy. Dr. Arley has recently solved
important problem of damping the rotations and other movements of the sph
below the critical rotation period of the instrument during deep dives. When
Galathea returns home sometime in 1952, Dr. Arley plans to continue laborat
work with these instruments in a special magnetic building to be constructe
Rude Skov Observatory.

(39) *Seismic reflection-quality map of the United States*—A reflection-qua
map of the United States has been prepared by a subcommittee of the Prog

d Arrangements Committee for 1950-51, Society of Exploration Geophysicists. ıe map designates as good, fair, or poor to NG all sedimentary areas of the iited States in respect to reflection quality in seismic explorations. The map may used in the planning of seismograph operations. Reflection quality is a function many factors.

(40) *New Argentine journal "Meteoros"*—The scientific and technical personnel the National Meteorological Service, Buenos Aires, Argentina, will publish a arterly review or expression of its organization's activities in meteorology and ophysics. The first issue of January, 1951, contained 120 pages. The articles are in Spanish with summaries in Spanish and either English or French.

(41) *Kodaikanal Magnetic Observatory*—Final value of the azimuth of the mark ed in absolute observation of declination has now been determined from a series pole-star observations. The value of D appearing for Kd on page 436 of this URNAL, September 1951 issue, should be replaced by 3° 43′.0 Wa.

(42) *Geomagnetic activities of the United States Coast and Geodetic Survey*—Two ter-American Geodetic Survey observers continued on magnetic surveys in South nerica under the technical direction of the United States Coast and Geodetic rvey.

A report containing reproductions of Tucson magnetograms for the first half of 49 was issued. "Magnetic hourly values, Sitka, Alaska, 1948" was also issued.

A Ruska observatory magnetometer for the National Geophysical Institute, of me, Italy, has been received at Cheltenham for standardization and determina- n of the constants.

Commander W. M. Gibson attended the International Union of Geodesy and ophysics meeting at Brussels, representing the Geomagnetism Branch, Division Geophysics, of the Survey.

Mr. J. H. Nelson was transferred from the Sitka Magnetic Observatory to the ashington office in August 1951 and assumed the duties of Assistant Chief, omagnetism Branch, of the United States Coast and Geodetic Survey.

Mr. Thomas L. Skillman was transferred from the Washington office to the ka Magnetic Observatory, where he became Observer-in-Charge in August 1951.

(43) *Personalia*—Dr. *Takesi Nagata*, of the Geophysical Institute, Tokyo Uni- rsity, was recently awarded the 1950 prize by the Science Academy of Japan his physical and geophysical studies of the magnetic properties of rocks and k-forming minerals. Dr. Nagata and his colleagues are now investigating the ssibility of a definite relation between composition and magnetic properties of romagnetic minerals in rocks, in order to arrive at a clearer understanding of magnetic behavior of the earth's crust and mantle.

Dr. *Beno Gutenberg*, of the Seismological Laboratory, California Institute of chnology, was elected first president of the International Association of Seismo- y and Physics of the Earth's Interior, to serve a three-year term. Dr. Gutenberg been president of the International Committee on Physics of the Earth's erior, which was merged with the new association at the recent Brussels meeting.

Dr. *Edward U. Condon* resigned as Director of the National Bureau of Standards September 30, 1951, and has accepted a position as director of research and velopment at the Corning Glass Works, at Corning, New York.

DANIEL LYMAN HAZARD, 1865—1951

Daniel Lyman Hazard, retired Chief Magnetician of the United States Co and Geodetic Survey, died suddenly at his home at Narragansett, Rhode Islan on September 21, 1951, and was buried in the family plot at Island Cemete Newport. His death came as a shock to his associates at the Survey, for he had be vigorous and active despite his advanced years, and his occasional visits to Wa ington were always stimulating and helpful.

Mr. Hazard was born at South Kingston, Rhode Island, on August 26, 18 the son of Thomas G. and Mary K. (Brooks) Hazard. He was educated at Rog High School in Newport, and at Brown and Harvard Universities, receiving B.A. degree at Harvard in 1885. In this Journal for March 1936 (vol. 41, p. 9 there was a sketch (accompanied by a portrait as frontispiece) detailing his lo career, which extended from 1892 to 1936. During a part of this period, he w Chief of the Division of Terrestrial Magnetism (now the Division of Geophysic He leaves the warm regard of his many friends and colleagues, and an enduri monument represented by the success of the magnetic survey of the United Sta during an extended period, coupled with the achievement of efficient and effecti procedures for conducting and processing magnetic observations, and surmounti the countless difficulties that arise in this work.

Mr. Hazard was never married, and the nearest surviving relative is a cous Mr. Peyton R. Hazard, of Newport, Rhode Island.

LIST OF RECENT PUBLICATIONS

By W. E. Scott

Department of Terrestrial Magnetism,
Carnegie Institution of Washington,
Washington 15, D. C.

(Received October 15, 1951)

A—*Terrestrial Magnetism*

A OBSERVATORY. Magnetic and meteorological results for 1948. Issued under the authority of the Hon. K. J. Holyoake, Minister of Scientific and Industrial Research. Wellington, R. E. Owen, Govt. Printer, 154 pp. (1950).

RTELS, J., AND J. VELDKAMP. Geomagnetic indices *K* and *C*, 1950. Washington, D. C., Internat. Union Geod. Geophys., Assoc. Terr. Mag. Electr., Bull. No. 12e, 138 pp. (1951).

APMAN, S. Notes on aurorae and magnetic storms. J. Atmos. Terr. Phys., **1**, No. 3, 189–199 (1951).

APMAN, S. The theory of magnetic storms and auroras. Nature, **168**, 86 (July 14, 1951). [Letter to Editor.]

UTSCHES HYDROGRAPHISCHES INSTITUT. Jahresbericht 1950. Hamburg, No. 5, 72 pp. with 11 pls. (1951). [Contains report on terrestrial magnetism.]

BAR PUERTAS, R. La variación secular de la intensidad geomagnética y su influjo en la distribución geográfica de la imantación terrestre. Urania, Madrid, **36**, Núm. 226, 65–95 (1951).

RGI, M., E. MEDI, E C. MORELLI. Rilievo magnetico regionale nell Marche per la istituzione di un Osservatorio Magnetico Centrale. Ann. Geofis., Roma, **3**, No. 2, 143–171 (1950).

RNÁNDEZ, R. P. J. Proceso de reducción de observaciones de campañas magnéticas. Buenos Aires, Meteoros, **1**, Nos. 2–3, 198–205 (1951).

MITI, S. One of the universal variations of geomagnetic field. Mem., Kakioka Magnetic Observatory, **6**, No. 1, 18–23 (1951). [In Japanese with English summary.]

KIOKA MAGNETIC OBSERVATORY. Annual report of the Kakioka Magnetic Observatory for the year 1935. Kakioka, No. 13, 96 with 10 pls. (1951). 30 cm. [Contains hourly values of the magnetic elements, atmospheric electric potential gradient, and earth-current potential, observed at the Kakioka Magnetic Observatory, Japan, during 1935.]

O, Y. Investigation of the magnetic disturbance by the induction magnetograph. Sci. Rep. Tôhoku Univ., Ser. 5, Geophysics, **3**, No. 1, 40–44 (1951).

O, Y. On the magnetic moment of the residual magnetism of the rock. Sci. Rep. Tôhoku Univ., Ser. 5, Geophysics, **3**, No. 1, 45–47 (1951).

ES, F. J., AND S. K. RUNCORN. The analysis of the geomagnetic secular variation. Phil. Trans. R. Soc., A, **243**, No. 871, 525–546 (1951).

HT, H. G. The representation of the main geomagnetic field and of its secular variation by means of two eccentric dipoles. Trans. Amer. Geophys. Union, **32**, No. 4, 555–562 (1951).

ER, O. Über eine besondere Art von erdmagnetischen Bay-Störungen. D. Hydrogr. Zs., **4**, Heft 1/2, 61–65 (1951).

RINIAK, N. Magnetic studies of the proposed dam sites at Atiamuri. N.Z. J. Sci. Tech., B, **32**, No. 4, 15–27 (1951). [Investigations by vertical magnetic intensities and magnetic susceptibility values.]

ELLI, C. Nuovi criteri per la sistematica magnetica. Ann. Geofis., Roma, **3**, No. 3, 7 pp. (1950).

EA, P. L., AND H. H. HOWE. Six additional years of spontaneous increase in magnetic moment. Trans. Amer. Geophys. Union, **32**, No. 4, 563–564 (1951).

Parkinson, W. C., F. W. Wood, W. E. Scott, and E. Balsam. Magnetic results from Wather[illegible] Observatory, Western Australia (Department of Terrestrial Magnetism, Carnegie Instituti[illegible] of Washington, January 1945–June 1947. Australian Commonwealth Bureau of Geology, G[illegible] physics, and Mineral Resources, July–December 1947). Washington, D. C., Carnegie In[illegible] Wash. Pub. 175, vol. 7-C, v + 127 pp., 120 tables (1951). 28 cm.

Princep Curto, J. M^{a}. Bahías geomagnéticas. Mem. Observatorio del Ebro, No. 10, 119 [illegible] (1949).

Rikitake, T. A miniature earth-inductor. Bull. Earthquake Res. Inst., Tokyo Univ., **29**, Pt.[illegible] 147–152 (1951).

Rikitake, T. The distribution of magnetic dip in Ooshima (Oo-sima) Island and its change th[illegible] accompanied the eruption of volcano Mihara, 1950. Bull. Earthquake Res. Inst., Tok[illegible] Univ., **29**, Pt. 1, 161–181 (1951).

Slichter, L. B. An electromagnetic interpretation problem in geophysics. Geophysics, **16**, No.[illegible] 431–449 (1951).

Stoyko, N. Sur les variations du champ magnétique et de la rotation de la Terre. Paris, C.[illegible] Acad. sci., **233**, No. 1, 80–82 (1951).

Trigonometrical Survey Office. The secular variation of the earth's magnetic field in Sou[illegible] Africa, 1939–1948. Results of observations at the secular variation field stations of the ma[illegible] netic observatory, Hermanus. Govt. Printer, Pretoria, 85 pp. with 5 charts (1950). 33 cm.

Tromsö, Auroral Observatory. Results of magnetic observations for the year 1949. By [illegible] Tönsberg and S. Berger. Bergen, Pub. Inst. Kosmisk Fysikk, No. 32, 31 pp. (1951).

United States Coast and Geodetic Survey. Magnetograms, Tuscon, Arizona, January–Ju[illegible] 1949. Washington, D. C., U. S. Coast Geod. Surv., No. MG-T49.1, 53 pp. (1951). 25 cm.

United States Coast and Geodetic Survey. Magnetic hourly values, Sitka, Alaska, 19[illegible] Washington, D. C., U. S. Coast Geod. Surv., No. HV-Si48, 46 pp. (1951). 25 cm.

Weber, E. K., F. Gassmann, E. Niggli, and H. Röthlisberger. Die magnetische Anoma[illegible] westlich von Locarno. Mitt. Inst. Geoph., Zürich, No. 15, 18 pp., 2 pls. (May 1950).

Witteveen Magnetic Observatory. Yearbook 1947. B—Geomagnetism (K. Nederlands M[illegible] Inst. No. 98). 's-Gravenhage, iii + 28 (1950). 34 cm.

Yumura, T. On the "three-hour-range indices" K at Kakioka. Mem., Kakioka Magnetic Obser[illegible] tory, **6**, No. 1, 1–17 (1951). [In Japanese with English summary.]

Zietz, I., and R. G. Henderson. Magnetic anomalies at high altitudes. Trans. Amer. Geoph[illegible] Union, **32**, No. 3, 397–404 (1951).

B—*Terrestrial Electricity*

Garner, D. M. Preliminary investigation of Aurora Australis activity from 1931 to 1949. N.Z[illegible] Sci. Tech., B, **33**, No. 1, 11–14 (1951).

Israël, H., und H. W. Kasemir. Ueber die Schirmwirkung von Gebäuden auf die Schwankun[illegible] des atmosphärisch-elektrischen Feldes. Ann. Géophys., **7**, No. 1, 63–68 (1951).

Jones, F. L. Physics of electrical discharge. Nature, **168**, 140–142 (July 28, 1951). [General the[illegible] of a symposium, Physical Society, University College of Swansea, March 29–31, 1951.]

Meinel, A. B. The auroral spectrum from 6200 to 8900 A. Astroph. J., **113**, No. 3, 583–588 (19[illegible]

Misaki, M. On the antenna-earth current during thunderstorm. Mem., Kakioka Magne[illegible] Observatory, **6**, No. 1, 24–30 (1951). [In Japanese with English summary.]

Mühleisen, R. Blitzentladungen von Gewitterwolken nach oben. Naturwiss., **38**, No. 6, [illegible] (1951).

C—*Cosmic Rays*

Beiser, A. New light on the origin of cosmic rays. Physics Today, **4**, No. 7, 14–16 (1951).

Caro, D. E., J. K. Parry, and H. D. Rathgeber. The momentum spectrum and positive ex[illegible] of cosmic ray mesons at sea-level. Aust. J. Sci. Res., **4**, No. 1, 16–35 (1951).

Dolbear, D. W. N., H. Elliot, and D. I. Dawton. The cosmic ray intensity and radio fade-o[illegible] J. Atmos. Terr. Phys., **1**, No. 3, 187–188 (1951).

AHY, E. F. Investigations on large cosmic-ray bursts. Phys. Rev., **83**, No. 2, 413–421 (1951).
AO, A. S., V. K. BALASUBRAHMANYAM, G. S. GOKHALE, AND A. W. PEREIRA. High altitude measurements of the penetrating component intensity of cosmic radiation near the geomagnetic equator. Phys. Rev., **83**, No. 1, 173 (1951).
TINCHCOMB, T. G. Experiments on large cosmic-ray bursts under thick absorbers at 11,500-feet elevation. Phys. Rev., **83**, No. 2, 422–431 (1951).

D—*Upper Air Research*

AILEY, V. A. The relativistic theory of electro-magneto-ionic waves. Phys. Rev., **83**, No. 2, 439–454 (1951).
ANERJEE, S. S., AND V. D. RAJAN. Long distance scattering of radio signals. J. Sci. Industr. Res., New Delhi, **10B**, No. 7, 161–164 (1951).
ATES, D. R. The temperature of the upper atmosphere. Proc. Phys. Soc., B, **64**, No. 381, 805–821 (1951).
RAMLEY, E. N., AND W. ROSS. Measurement of the direction of arrival of short radio waves reflected at the ionosphere. Proc. R. Soc., A, **207**, 251–267 (1951).
UDDEN, K. G. The reflection of very low frequency radio waves at the surface of a sharply bounded ionosphere with superimposed magnetic field. Phil. Mag., **42**, No. 331, 833–850 (1951).
ARBENAY, F. L'action statistique des atmosphériques sur un récepteur accordé sur 27 kc/sec. Paris, C.-R. Acad. sci., **232**, No. 10, 949–950 (1951).
HRISTIANSEN, W. N., J. V. HINDMAN, A. G. LITTLE, R. PAYNE-SCOTT, D. E. YABSLEY, AND C. W. ALLEN. Radio observations of two large solar disturbances. Aust. J. Sci. Res., **4**, No. 1, 51–61 (1951).
OMMONWEALTH OF AUSTRALIA. Second annual report of the Commonwealth Scientific and Industrial Research Organization for the year ending 30th June, 1950. Canberra, L. F. Johnston, Commonwealth Govt. Printer, 157 pp. (1950). 33 cm. [Contains sections on radiophysics and extraterrestrial physics.]
UFAY, J. Bandes d'émission des molécules OH et O_2 dans le spectre du ciel nocturne, entre 9000 et 1100 Å. Ann. Géophys., **7**, No. 1, 1–8 (1951).
UFAY, M. Une nouvelle bande de vibration-rotation de la molécule OH dans le spectre du ciel nocturne. Paris, C.-R. Acad. sci., **232**, No. 25, 2344–2346 (1951).
UNGEY, J. W. Derivation of the dispersion equation for Alfvén's magneto-hydrodynamic waves from Bailey's electromagneto-ionic theory. Nature, **167**, 1029–1030 (June 23, 1951).
LLISON, M. A. Source points of radio noise bursts associated with solar flares. Nature, **167**, 941–942 (June 9, 1951).
EINSTEIN, J., AND H. K. SEN. Radio wave generation by multistream charge interaction. Phys. Rev., **83**, No. 2, 405–412 (1951).
LAMBARD, A. Les radars terrestres. Onde Électrique, **31**, No. 292, 320–328 (1951).
ORSGREN, S. K. H. Some calculations of ray paths in the ionosphere. Göteborg, Chalmers Tekn. Högsk. Handl., No. 104 (Avd. Elektroteknik 20), 22 pp. (1951).
RIEDMAN, H., S. W. LICHTMAN, AND E. T. BYRAM. Photon counter measurements of solar X-rays and extreme untraviolet light. Phys. Rev., **83**, No. 5, 1025–1030 (1951).
EOPHYSICAL RESEARCH DIVISION, AIR FORCE CAMBRIDGE RESEARCH CENTER. Proceedings of the colloquium on mesospheric physics (edited by N. C. Gerson). Geophysical Research Papers No. 8, 100 pp. (July 1951). 27 cm. [Colloquium held at Cambridge, Mass., July 31 and August 1, 1950.]
ERZBERG, G. The atmospheres of the planets. J. R. Astr. Soc. Can., **45**, No. 3, 100–123 (1951).
EY, J. S. Radio astronomy. Science Progress, **39**, No. 155, 427–448 (1951).
ORNBECK, G. A., AND R. C. HERMAN. The vibration-rotation bands of OH in the photographic infrared. J. Chem. Phys., **19**, No. 4, 512 (1951).
STITUTO GEOFÍSICO DE HUANCAYO. Boletin de radio propagacion. Min. Fomento y Obras Publicas, Peru, edicion de enero 1951, 17 pp. (1951). [Published monthly in mimeograph form; contains hourly values of ionospheric characteristics.]
ES, H. E. Revisions of the Lorentz transformations. Amer. Phil. Soc., **95**, No. 2, 125–131 (1951).

Kelso, J. M. The ionospheric polarization of low frequency radio waves. J. Sci. Industr. Re New Delhi, **10B**, No. 6, 123–133 (1951).

Lejay, P., J.-M. Ardillon, and G. Bertaux. Relation entre le magnétisme terrestre et la prop gation des ondes radioélectriques entre Washington et Bagneux. Paris, C.-R. Acad. sci., 23 No. 22, 1975–1976 (1951).

Lejay, P., and D. Lepechinsky. Formation des couches ionisées. Influence de la températur Paris, C.-R. Acad. sci., **232**, No. 23, 2058–2061 (1951).

Lindquist, R. Polar blackouts recorded at the Kiruna Observatory. Göteborg, Chalmers Tek Högsk. Handl., No. 103 (Avd. Elektroteknik 19), 24 pp. (1951).

Lindquist, R. A survey of recent ionospheric measurements at the ionospheric and radio wa propagation observatory at Kiruna. Ark. Geofysik, **1**, No. 11, 247–266 (1951).

Lindquist, R. A 16 kw panoramic ionospheric recorder. Göteborg, Chalmers Tekn. Högsk. Hand No. 109 (Avd. Elektroteknik 25), 40 pp. (1951).

Mao-Lin, T. Mesures de la quantité d'ozone contenue dans l'atmosphère par spectrophotométr photographique du ciel bleu au zénith. Ann. Géophys., **7**, No. 1, 45–58 (1951).

Moses, H. E., and Ta-You Wu. A self-consistent treatment of the oxygen dissociation region i the upper atmosphere. Phys. Rev., **83**, No. 1, 109–121 (1951).

Nicolet, M. Effects of the atmospheric scale height gradient on the variation of ionization an short wave absorption. J. Atmos. Terr. Phys., **1**, No. 3, 141–146 (1951).

Pennsylvania State College. Proceedings of the Conference on Ionospheric Physics, Sta College, Pennsylvania, July 24, 25, 26, 27, 1950. Edited by C. H. Grace, Vol. II, 500 p approx. with illus. (1951). 28 cm.

Ross, W., E. N. Bramley, and G. E. Ashwell. A phase-comparison method of measuring t direction of arrival of ionospheric radio waves. Proc. Inst. Elec. Eng., **98**, Pt. 3, No. 54, 29 302 (1951).

Rydbeck, O. E. H. The theory of magneto ionic triple splitting. Göteborg, Chalmers Tekn. Högs Handl., No. 101 (Ave. Elektroteknik 17), 38 pp. (1951).

Shannon, C. E., and W. Weaver. The mathematical theory of communication. Urbana, Un versity of Illinois Press, 117 pp. (1949). 23 cm.

Smerd, S. F. A radio-frequency representation of the solar atmosphere. Proc. Inst. Elec. Eng., 9 Pt. 3, No. 50, 447–452 (1950).

Veldkamp, J. On the propagation of sound over great distances. J. Atmos. Terr. Phys., **1**, No. 147–151 (1951).

Westfold, K. C. The interpretation of the magneto-ionic theory. J. Atmos. Terr. Phys., **1**, No. 152–186 (1951).

Wild, J. P. Observations of the spectrum of high-intensity solar radiation at metre wavelength IV—Enhanced radiation. Aust. J. Sci. Res., **4**, No. 1, 16–35 (1951).

Yerg, D. G. Ionospheric wind systems and electron concentrations of the *F* layer. J. Met., No. 4, 244–250 (1951)

E—*Earth's Crust and Interior*

Bateman, A. M. The formation of mineral deposits. New York, John Wiley and Sons, Inc., 371 p (1951).

Cotton, C. A. Redeposition theory of sedimentation. N.Z. J. Sci. Tech., B, **32**, No. 5, 19–25 (195

Dyk, K., and J. D. Eisler. A study of the influence of background noise on reflection pickin Geophysics, **16**, No. 3, 450–455 (1951).

Geologischen Landesanstalten der Bundesrepublik Deutschland. Geologisches Ja buch für die Jahre 1943–1948. Hannover/Celle, **64**, 646 pp. with illus. (1950).

Geologischen Landesanstalten der Bundesrepublik Deutschland. Geologisches Jahrbu für das Jahr 1949. Hannover, **65**, 789 pp. with illus. (1951).

Gutenberg, B. *PKKP*, *P'P'*, and the earth's core. Trans. Amer. Geophys. Union, **32**, No. 373–390 (1951).

Gutenberg, B. (Chairman, Special Editorial Committee). Summary of colloquium on plas flow and deformation within the earth. Trans. Amer. Geophys. Union, **32**, No. 4, 539–5

(1951). [Colloquium sponsored jointly by the International Union of Geodesy and Geophysics and the International Union of Theoretical and Applied Mechanics; held at Hershey, Pennsylvania, September 12–14, 1950.]

IALE, A. L.; P. L. WILLMORE. Crustal layers of the earth. Nature, **168**, 163–164 (July 28, 1951).

IALES, A. L., AND D. I. GOUGH. Measurements of gravity in Southern Africa. Govt. Printer, Pretoria, 58 pp. with appendix (1950). 25 cm.

IEISKANEN, W. On the world geodetic system. Helsinki, Veröff. Finn. Geod. Inst., No. 39, 25 pp. (1951). [Pub. No. 26 of Isostatic Inst.]

UNGER, A. Deep basement reflections in Big Horn County, Montana. Geophysics, **16**, No. 3, 499–505 (1951).

ING, P. B. The tectonics of middle North America (Middle North America east of the Cordilleran System). Princeton, Princeton University Press, xix + 203 with illus. (1951). 26 cm.

YONS, P. L. A seismic reflection quality map of the United States. Geophysics, **16**, No. 3, 506–510 (1951).

IORELLI, C. Collegamento gravimetrico Padova-Trieste e rilievo gravimetrico regionale del Veneto centro-orientale. Riv. Geof. appl., Milano, **11**, No. 2, 20 pp. (1950).

IORELLI, C. Rilievo gravimetrico e riduzione isostatica nell'Italia nord-orientale. Tecnica Italiana, Trieste, N.S., **6**, Nos. 3 and 4, 47 pp. (1951). [Pub. Osservatorio Geofisico, No. 20.]

IORELLI, C. Studio del gravimetro Worden n. 50 e sua applicazione per un rilievo geofisico di dettaglio alle foci del Timavo. Ann. Geofis., Roma, **4**, No. 2, 247–271 (1951).

VEY, C. D. International co-operation in the analyses of the deep-sea cores collected by the Swedish deep-sea expedition 1947–48. Nature, **168**, 148–149 (July 28, 1951).

RESS, F., AND M. EWING. Ground roll coupling to atmospheric compressional waves. Geophysics, **16**, No. 3, 416–430 (1951).

IDGE, J. D. Water in primordial and derivative magma and its relation to the ore-forming fluid. Amer. J. Sci., **249**, No. 7, 512–532 (1951).

IKITAKE, T. Electromagnetic induction within the earth and its relation to the electrical state of the earth's interior. Bull. Earthquake Res. Inst., Tokyo Univ., **29**, Pt. 1, 61–69 (1951).

IKITAKE, T. Diffraction of electromagnetic waves around the crater of volcano Mihara. Bull. Earthquake Inst., Tokyo Univ., **29**, Pt. 1, 153–159 (1951).

OTHE, J. P. The structure of the bed of the Atlantic Ocean. Trans. Amer. Geophys. Union, **32**, No. 3, 457–461 (1951).

NITED STATES COAST AND GEODETIC SURVEY. Seismological bulletin, January, February, March, 1949. Washington, D. C., U. S. Coast Geod. Surv., MSI-137, 87 pp. (1951).

ANAGIHARA, K. Earth-resistivity near the Kakioka Magnetic Observatory. Mem., Kakioka Magnetic Observatory, **6**, No. 1, 36–41 (1951). [In Japanese with English summary.]

F—*Miscellaneous*

NANTHAKRISHNAN, R. Intensity variation in sunspots. Nature, **168**, 291–292 (Aug. 18, 1951).

EYNON, W. J. G., AND G. M. BROWN. Geophysical and meteorological changes in the period January-April 1949. Nature, **167**, 1012–1014 (June 23, 1951). [Unusual correspondence between certain solar and terrestrial phenomena.]

ENISSE, J.-F., J. L. STEINBERG, ET S. ZISLER. Contrôle de l'activité géomagnétique par les centres d'activité solaires distingués par leurs propriétés radioélectriques. Paris, C.-R. Acad. sci., **232**, No. 25, 2290–2292 (1951).

ODSON, H. W., AND R. W. DONSELMAN. The eruptive prominence of August 7, 1950. Astroph. J., **113**, No. 3, 519–524 (1951).

AMOW, G. The origin and evolution of the universe. Amer. Scientist, **39**, No. 3, 393–411 (1951).

ASSMANN, F. Recent geophysical research-work. Mitt. Inst. Geoph., Zürich, No. 16, 10 pp., 1 pl. (June 1951).

LEISSBERG, W., UND A. KIRAL. Prognose für das kommende Sonnenfleckenminimum. Zs. Astroph., Berlin, **28**, Heft 1, 17–27 (1950).

AGEN, J. P. Temperature gradient in the sun's atmosphere measured at radio frequencies. Astroph. J., **113**, No. 3, 547–566 (1951).

Jeffreys, H. The relations between astronomy and geophysics. Amer. Scientist, **39**, No. 3, 407-411 (1951).

Jones, H. S. The origin of the solar system. Endeavour, **10**, No. 39, 119–125 (1951).

McIntosh, D. H. Geomagnetic effects of solar flares. Nature, **167**, 985 (June 16, 1951).

Sedra, R. N. Intensity of ultraviolet radiation from solar flares. Phys. Rev., **83**, No. 1, 190 (1951).

Waldmeier, M. Die Sonnenkorona: Beobachtungen der Korona 1939–1949. Vol. I. Verlag Birkhäuser, Basel, 270 pp. (1951).

Wegener, K. Verification experimental de la constante solar. Buenos Aires, Meteoros, **1**, Nos. 2–3, 171–182 (1951).

NOTICE

When available, single unbound volumes can be supplied at $3.50 each and single numbers $1 each, postpaid.

Charges for reprints and covers

Reprints can be supplied, but prices have increased considerably and costs depend on the mber of articles per issue for which reprints are requested. It is no longer possible to publish a edule of reprint charges, but if reprints are requested approximate estimates will be given when ley proofs are sent to authors. Reprints without covers are least expensive; standard covers th title and author) can be supplied at an additional charge. Special printing on covers can also supplied at further additional charge.

Fifty reprints, without covers, will be given to institutions paying the publication charge of 00 per page.

Alterations

Major alterations made by authors in proof will be charged at cost. Authors are requested, refore, to make final revisions on their typewritten manuscripts.

rders for back issues and reprints should be sent to Editorial Office, 5241 Broad Branch Road, V., Washington 15, D.C., U.S.A.

Subscriptions only are handled by The Johns Hopkins Press, Baltimore 18, Maryland, U.S.A.

CONTENTS—Concluded

INDEX OF AUTHORS

VOLUME 56, 1951